UNIVERSITÀ DEGLI STUDI DI TRIESTE

XXV CICLO DEL DOTTORATO DI RICERCA IN

INGEGNERIA DELL'INFORMAZIONE

CROSS-LAYER DESIGN AND ANALYSIS OF COOPERATIVE WIRELESS NETWORKS RELYING ON EFFICIENT CODING TECHNIQUES

Settore scientifico-disciplinare **ING-INF/03 TELECOMUNICAZIONI**

DOCTORAL STUDENT
ALESSANDRO CRISMANI

DOCTORAL PROGRAM COORDINATOR
PROF. WALTER UKOVICH

THESIS SUPERVISOR
PROF. FULVIO BABICH

ACADEMIC YEAR 2011/2012

SUMMARY

This thesis work aims at analysing the performance of efficient cooperative techniques and of smart antenna aided solutions in the context of wireless networks. Particularly, original contributions include a performance analysis of distributed coding techniques for the physical layer of communication systems, the design of practical efficient coding schemes that approach the analytic limiting bound, the cross-layer design of cooperative medium access control systems that incorporate and benefit from advanced physical layer techniques, the study of the performance of such solutions under realistic network assumptions, and, finally the design of access protocols where nodes are equipped with smart antenna systems. The contributions presented in this dissertation are the result of a three-year study period as a Ph.D. student in information engineering at the Telecommunication Group of the Department of Engineering and Architecture at the University of Trieste and of a visiting period at the Communications Research Group of the University of Southampton.

Mobile communications have recently experienced a rapid growth, due to the increasing users' request to provide real time information independently by their position. Nowadays, smartphones and personal digital assistants are able to connect to both 3G networks and 802.11 compliant wireless networks. New devices, such as tablets, ``netbooks'' and ``ultrabooks'' have seen a wide diffusion as they provide applications, usually available on more powerful desktop computers, on smaller terminals, characterized by a low weight and a long battery life, and hence ``mobility'' oriented.

Despite this recent interest in cable-free communications, wireless links were always characterized by a lower bandwidth compared to the one offered by their wired counterparts. This fact limited the quantity of information that could be reliably delivered to a mobile user.

A solution to increase the ``quality'' of wireless links was given by the introduction of multiple-Input multiple-output techniques. Multiple-input multiple-output systems provide a way to achieve a higher throughput in a mobile communication, however this enhancement comes at the cost of multiple radio frequency frontends at both the transmitter and the receiver. The main drawback of multiple-input multiple-output is that accommodating more antennas on a single device is not always possible, as the small size of some mobile equipment could not allow it.

Recent studies on cooperative communications addressed the problem of squeezing multiple antennas on tiny handheld devices with a new design approach.

In a cooperative scenario, nodes equipped with a single antenna share their information to form a virtual antenna array, achieving the same spatial diversity provided by the standard co-located multiple-input multiple-output design, without employing multiple radio frequency frontends in every device.

Another approach for increasing the capacity of a wireless network is to host multiple communications at a single time, hence reducing the mutual interference among communicating nodes using beamforming techniques. Particularly, smart antenna systems, which are composed by an antenna array that contains multiple radiating elements and by signal processing algorithms for feeding such elements, allow mitigating the interference from undesired sources and hence may be equipped on wireless stations for enabling concurrent transmissions with the end result of improving the user experience.

This thesis provides novel results and insights on the physical and medium access control layers of a cooperative system. Particularly, the thesis shows analytic results for the performance of a distributed coding system adopting retransmissions, and proposes a design approach for contriving practical coding schemes that perform close to the bounding performance. Such efficient coding schemes are later amalgamated with cooperative medium access schemes in a cross-layer design fashion. Furthermore, the performance of cooperative medium access control protocols are evaluated under realistic assumptions for the network environment, and novel schemes are proposed for mitigating the impairments incurred when nodes rely on imperfect knowledge of the scenario where they operate in. Finally, the thesis proposes practical medium access control systems where a higher network performance is obtained by hosting multiple communications at a single time. Such novel systems are designed to be backward compatible with the legacy IEEE 802.11 standard, and hence are a practical solution for improving the network performance without modifying the network infrastructure. The performance of such systems is simulated for many network scenarios, demonstrating the actual throughput increase over the legacy IEEE 802.11 standard.

This thesis is composed of two parts. The first part summarises literature works that are relevant as background for the main contributions of the dissertation. The second part presents the novel results obtained during the Ph.D. studies in a coherent fashion and contains the main contributions of this work. Both parts are divided into chapters, and the whole work is organised as follows.

The background part is divided into three chapter.

- The first chapter summarises the main properties of a wireless channel, with a particular focus on the fading phenomenon. The chapter also reviews the techniques that are used for mitigating the impairments imposed by the time varying channel, such as adaptive systems and diversity. Among the different approaches to diversity, a particular interest is given to multiple-input

multiple-output techniques, which motivate the cooperative approach. Cooperative physical layer techniques are discussed in detail in the rest of the chapter, which also contains an overview of literature works that studied distributed channel coding solutions.

- The second chapter reviews the IEEE 802.11 standard for wireless networks, focusing on the medium access scheme aspect. The chapter then analyses literature works that extended the IEEE 802.11 access scheme by introducing a cooperative approach. Particularly, the chapter details the design choices and problems that are encountered when allowing IEEE 802.11 stations to cooperate. Finally, the chapter briefly reviews the most popular cooperative medium access control schemes found in the literature.

- The third chapter concludes the background section by presenting the main limitations of literature works that target cooperation. These limitations motivate further research on cooperative communications. Particularly, the chapter outlines the research lines followed in this work and finally summarises the main contributions of the thesis.

The following four chapters present novel results.

- Chapter four introduces an analytic framework for determining the limiting performance of cooperative coding schemes. The novel framework is based on the sphere-packing bound and hence does not rely on the adoption of a specific encoder, rather it considers generic characteristic of the code scheme. The framework is shown to be an accurate benchmark tool for existing coding techniques. Furthermore the chapter shows that the analysis may be used for deriving the throughput and delay performance of an adaptive cooperative system.

- The fifth chapter addresses the design problem of finding efficient distributed codes that are capable of approaching the limiting performance derived in the previous chapter. Particularly, the chapter presents a design strategy, based on a genetic algorithm aided optimisation technique, for contriving distributed turbo code schemes showing a satisfactory performance over a wide range of channel conditions. The chapter also addresses the problem of determining the performance in the low signal to noise ratio region of a turbo code that is punctured in a periodic way by introducing a novel tridimensional extrinsic information transfer chart technique.

- Chapter six considers the design of cooperative access protocols for wireless networks. Particularly, the chapter adopts a cross-layer design approach

for amalgamating advanced physical layer techniques with medium layer aspects. The chapter than derives the performance of the designed cross-layer access schemes, and discusses the impact of distributed physical layer coding on the medium access control layer performance.

- The seventh chapter analyses the performance of cooperative medium access control schemes that rely on imperfect knowledge of the network characteristics. Furthermore, the chapter proposes novel protocols, that are based on Markov prediction techniques, which mitigate the performance downgrade experienced when the relay selection algorithm does not have access to perfect channel estimates.

- Chapter eight addresses the design of high throughput wireless networks that rely on smart antenna equipped stations for hosting multiple communications at a single time. The chapter presents some guidelines for contriving schemes for wireless networks composed by smart antenna aided nodes. Such guidelines are used as a base for designing two novel access schemes that are backward compatible with the IEEE 802.11 standard and are shown to provide a throughput increase by obtaining spatial reuse.

Finally, chapter nine contains a discussion of the results presented in this thesis, along with a description of future possible improvements of the topics covered in this work.

TABLE OF CONTENTS

List of acronyms

ACK	ACKnoledgement
APSK	Amplitude Phase Shift Keying
ARQ	Automatic Repeat and reQuest
AWGN	Addittive White Gaussian Noise
BCJR	Bahl-Cocke-Jelinek-Raviv
BER	Bit Error Ratio
BLER	BLock Error Ratio
BPSK	Binary Phase Shift Keying
CC	Common Channel
CLDC	Cooperative Linear Dispersion Code
CMAC	Cooperative communication Medium Access Control
CPU	Central Processing Unit
CSI	Channel State Information
CSMA	Carrier Sensing Multiple Access
CTR	Clear-To-Receive
CTS	Clear-To-Send
DCF	Distributed Coordination Function
DIFS	Distributed InterFrame Space
DOA	Direction Of Arrival
EXIT	EXtrinsic Information Transfer
FEC	Forward Error Correction
FSMC	Finite State Markov Chain
GA	Genetic Algorithm
HARQ	Hybrid Automatic Repeat and reQuest
HI	Helper Indication
HTS	Helper ready-To-Send
IOC	Information Outage Criterion
IRCC	IRregular Convolutional Code
LAN	Local Area Network
LDC	Linear Dispersion Code
LDPC	Low Density Parity Check
LLR	Log-Likelihood Ratio
LMS	Least Mean Square
MAC	Medium Access Control
MCC	Multiple Communications Channel

MDP	Markov Decision Process
MIMO	Multiple-Input Multiple-Output
MPC	Multi-Packet Communication
MPR	Multi-Packet Reception
MRC	Maximal Ratio Combining
MUSIC	
NACK	Negative ACKnoledgement
NAV	Network Allocatin Vector
NCSW	Node Cooperative Stop and Wait
NCT	Neighbouring Characteristic Table
OC-MAC	Opportunistic Cooperative Medium Access Control
OFDM	Orthogonal Frequency Division Multiplexing
PHY	PHYsical
POMDP	Partially Observable Markov Decision Process
PSK	Phase Shift Keying
QAM	Quadrature Amplitude Modulation
QPSK	Quadrature Phase Shift Keying
RC	Relay Confirmation
RCTS	Relay Cleat-To-Send
RRTS	Relay Ready-To-Send
RSC	Recursive Systematic Convolutional
RTH	Ready-To-Help
RTS	Ready-To-Send
SAMPC	Signal-to-interference ratio Access Multi-Packet Communication
SAS	Smart Antenna System
SECCC	SElf-Concatenated Convolutional Code
SIC	Successive Interference Cancellation
SIFS	Short InterFrame Space
SINR	Signal to Interference plus Noise Ratio
SIR	Signal to Interference Ratio
SISO	Soft-Input Soft-Output
SNR	Signal to Noise Ratio
SPB	Sphere-Packing Bound
STBC	Space-Time Block Code
TAMPC	Threshold Access Multi-Packet Communication
WLAN	Wireless Local Area Network

List of symbols

$\mathbf{a}$	Systematic bits produced by a turbo encoder
$\mathbf{a}^{p}$	Systematic bits produced by a turbo encoder that are punctured
$\tilde{\mathbf{a}}_{\mathrm{a}}$	A-priori LLR values of systematic bits
$\tilde{\mathbf{a}}_{\mathrm{c}}$	Channel LLR values of systematic bits
$\tilde{\mathbf{a}}_{\mathrm{e}}$	Extrinsic LLR values of systematic bits
$\tilde{\mathbf{a}}_{\mathrm{e}}^{\mathrm{p}}$	Extrinsic LLR values of punctured systematic bits
$\tilde{\mathbf{a}}_{\mathrm{e}}^{\mathrm{u}}$	Extrinsic LLR values of unpunctured systematic bits
$\tilde{\mathbf{a}}_{\mathrm{p}}$	A-posteriori LLR Ratio values of systematic bits
$\mathbf{a}^{u}$	Systematic bits produced by a turbo encoder that remain unpunctured
$\mathbf{b}$	Interleaved version of the systematic bits produced by a turbo encoder
$\mathbf{b}(\mathbf{s})$	Believes of possible states
$\tilde{\mathbf{b}}_{\mathrm{a}}$	A-priori LLR values of interleaved systematic bits
$\tilde{\mathbf{b}}_{\mathrm{c}}$	Channel LLR values of interleaved systematic bits
$\tilde{\mathbf{b}}_{\mathrm{e}}$	Extrinsic LLR values of interleaved systematic bits
$\tilde{\mathbf{b}}(\mathbf{s})$	Updated believes of possible states
$b(s)$	belief of a state s
$\tilde{b}(s)$	Updated belief of state s
B	Number of coded bits
$\mathbf{c}$	Upper parity bits produced by a turbo encoder
$\tilde{\mathbf{c}}_{\mathrm{a}}$	A-priori LLR values of upper parity bits
$\tilde{\mathbf{c}}_{\mathrm{c}}$	Channel LLR values of upper parity bits
$\tilde{\mathbf{c}}_{\mathrm{e}}$	Extrinsic LLR values of upper parity bits
c_i	i-th discretised SNR value
C	Code scheme representation for the GA
$\mathbf{C}$	List of codes populating a generation of the GA
C_i	Puncturer for the i-th attempt of code C
$\mathbf{d}$	Lower parity bits produced by a turbo encoder
$\tilde{\mathbf{d}}_{\mathrm{a}}$	A-priori LLR values of lower parity bits
$\tilde{\mathbf{d}}_{\mathrm{c}}$	Channel LLR values of lower parity bits
$\tilde{\mathbf{d}}_{\mathrm{e}}$	Extrinsic LLR values of lower parity bits
$\mathcal{D}$	Delay value
F	Number of segments in successive relaying schemes
G_i^{av}	Average gain of station i
G_i^{null}	Null gain of station i
$G(\phi)$	Radiation pattern

$G_i(\phi)$	Radiation pattern of station i
G_{RD}	Power gain on the link between the i-th relay and the destination stations
G_{SD}	Power gain on the link between the source and the destination stations
G_{SR}	Power gain on the link between the source and the i-th relay stations
$h(t)$	Fading envelope at time t
$h_I(t)$	Fading in-phase component at time t
$h_Q(t)$	Fading quadrature component at time t
$\mathcal{H}$	Set containing relay stations in the wireless network
$\tilde{\mathcal{H}}$	Set containing candidate helpers
I_A	Mutual information conveyed by a-priori LLRs
$\mathcal{I}_{A,B}^{0}$	Ordered set containing active interferers of the A, B node pair
$\mathcal{I}_{A,B}^{0^{\text{av}}}$	Ordered set containing active interferers of the A, B node pair that are not nulled
$\mathcal{I}_{A,B}^{0^{\text{null}}}$	Ordered set containing active interferers of the A, B node pair that are nulled
I_E	Mutual information conveyed by extrinsic LLRs
I_E^p	Mutual information conveyed by punctured extrinsic LLRs
I_E^u	Mutual information conveyed by unpunctured extrinsic LLRs
$I(\mathbf{x}; \tilde{\mathbf{x}})$	Mutual Information between the bit sequence $\mathbf{x}$ and the LLR sequence $\tilde{\mathbf{x}}$
J_{MAX}	Maximum number of attempts
$\lambda(i)$	Average number of bits carried in a symbol in the i-th attempt
$\lambda_{RD}(i)$	Number of bits carried by a symbol transmitted from the relay to the destination in the i-th attempt
$\lambda_{SD}(i)$	Number of bits carried by a symbol transmitted from the source to the destination in the i-th attempt
$\mathcal{L}$	Maximum number of communications sustained in the network
$\Lambda(i)$	Average number of bits carried in a symbol after i attempts
L_{t_i}	Access threshold of TAMPC node i
m	maximum retry limit
m'	maximum backoff stage
$\mathcal{M}^i$	i-th Modulation mode
$\mathcal{M}_{RD}$	Modulation mode used on the relay-destination link
$\mathcal{M}_{RD}^*$	Optimal modulation mode on the relay-destination link
$\mathcal{M}_{SD}$	Modulation mode used on the source-destination link
$\mathcal{M}_{SD}^*$	Optimal modulation mode on the source-destination link
$\mathcal{M}_{SR}$	Modulation mode used on the source-relay link
$\mathcal{M}_{SR}^*$	Optimal modulation mode on the source-relay link
$\mathcal{N}$	Set containing stations composing the wireless network

$\mathcal{N}^{\mathrm{l}}$	Set containing legacy stations composing the wireless network
$\mathcal{N}^{\mathrm{nl}}$	Set containing non-legacy stations composing the wireless network
$\mathcal{N}^{\mathrm{dst}}$	Set containing destination stations in the wireless network
$\mathcal{N}^{\mathrm{src}}$	Set containing source stations in the wireless network
N_{codes}	Number of candidate codes
$o_i(t)$	Observation i-th is obtained at time t
O	Set containing possible observations
p_c	Probability of collision in a slot
p_D	Probability of dropping a packet
p_F	Probability of failure of a communication in a slot
$p_f(i)$	Error probability after i attempts
$p_f^R(i)$	Error probability after i attempts at the relay
p_S	Probability of successfully transmitting
$p_s(i)$	Success probability after i attempts
$p_s^{i,j}$	Success probability at stage (i,j)
p_S^r	Probability of successfully transmitting to the relay
$p_s^R(i)$	Success probability after i attempts at the relay
p_{tr}	Probability that at least one station transmits in a slot
P	Packet length
P_{a}	Puncturer for systematic bits
$\mathrm{P}_{\mathrm{a}}^{-1}$	Puncturer for systematic bits
$P_{A,B}^r$	Power received by station A from station B
P_B	Block error ratio
P_{c}	Puncturer for upper parities bits
$\mathrm{P}_{\mathrm{c}}^{-1}$	Puncturer for upper parities bits
$\mathcal{P}_a^i$	Positions of punctured systematic bits at the i-th attempt
$\mathcal{P}_c^i$	Positions of punctured upper parities bits at the i-th attempt
$\mathcal{P}_d^i$	Positions of punctured lower parities bits at the i-th attempt
P_{d}	Puncturer for lower parities bits
$\mathrm{P}_{\mathrm{d}}^{-1}$	Puncturer for lower parities bits
P_e	Bit error rate ratio
$\mathcal{Q}_i$	i-th quantising threshold
$r_{\mathrm{eq}}^{A,B}$	Equivalent rate of the transmission between stations A and B
r_{sus}	Sustainable rate
$r_{\mathrm{sus}}^{A,B}$	Sustainable rate of the transmission between stations A and B
R	Radius of the network
R_c	Code rate
$\mathcal{R}_c$	Set of available code rates
R_c^i	Coding rate used by station i
$\mathcal{R}^i$	i-th transmission mode

R_{c_i}	Code rate of the i-th attempt of an retransmission scheme
$\mathcal{R}^j(U^i)$	Positions of bits in the set $\mathcal{U}^i$ that have been transmitted j times within the first i attempts
$\mathcal{R}^*_{H_iD}$	Optimum transmission rate on the link between the i-th relay and the destination stations
$\mathcal{R}^*_{SD}$	Optimum transmission rate on the source-destination link
$R_{c_s}^{D}$	Code rate at the destination performing a joint decoding procedure at the s-th stage
$\mathcal{R}^*_{SH_i}$	Optimum transmission rate on the link between the source and the i-th relay stations
s	Modulated symbol
s_i^t	Link is in state i at time t
$\mathbf{s}$	Modulated symbol sequence
S	Number of modulated symbols
$\mathcal{S}$	Throughput value
$\overline{T_S}$	Average transmission duration
$\mathcal{T}_a^i$	Positions of systematic bits transmitted within the i-th attempt
$\mathcal{T}_c^i$	Positions of upper parity bits transmitted within the i-th attempt
$\mathcal{T}_d^i$	Positions of lower parity bits transmitted within the i-th attempt
T_{coll}	Time wasted when colliding
T^{dir}	Duration of the fastest available direct communication
T_i^{dir}	Time duration of a direct communication using the i-th modulation mode
T^{r_h}	Duration of the fastest available cooperative communication through the h-th relay
$T_{i,j}^{r_h}$	Time duration of a cooperative communication through the h-th relay using the (i,j)-th modulation mode pair
T^{r_i,r_j}	Time duration of a successive relayed communication through the (i,j) relays
U	Number of information bits
$\mathcal{U}_a^i$	Positions of punctured systematic bits at the i-th attempt
$\mathcal{U}_c^i$	Positions of unpunctured upper parities bits at the i-th attempt
$\mathcal{U}_d^i$	Positions of unpunctured lower parities bits at the i-th attempt
$\mathbf{x}$	Encoded symbol sequence
$\mathbf{y}$	Received symbol sequence
η^*_{coop}	Maximum efficiency on the source-relay-destination cooperative link
$\eta_{\text{coop}}(i,j)$	Efficiency of the cooperative modulation mode pair (i,j)
η^*_{dir}	Maximum efficiency on the source-destination link
$\eta(i)$	Efficiency pf the i-th modulation mode
γ	SNR value

$\gamma(t)$	SNR value at time t
γ_{AB}	SNR value on the link between stations A and B
γ_{AB}^{t}	SNR value between stations A and B at the time slot t
$\hat{\gamma}_{AB}^{t}$	Quantised SNR value between stations A and B at the time slot t
$\hat{\gamma}_{R_iD}^{t}$	Quantised SNR between the i-th relay and the destination stations at the time slot t
$\hat{\gamma}_{SD}^{t}$	Quantised SNR between the source and the destination stations at the time slot t
$\hat{\gamma}_{SR_i}^{t}$	Quantised SNR between the source and the i-th relay stations at the time slot t
$\gamma_l(t)$	SNR value of replica l at time t
γ_{RD}	SNR value on the link between the relay and the destination
γ_{RD}^{n}	SNR value of the n-th segment received from the relay station and accumulated over all replicas
$\gamma_{RD}^{n,i}$	SNR value of the i-th replica n-th segment received from the relay station
$\gamma_{R_iD}^{t}$	SNR between the i-th relay and the destination stations at the time slot t
γ_{SD}	SNR value on the link between the source and the destination
γ_{SD}^{n}	SNR value of the n-th segment received from the source station and accumulated over all replicas
$\gamma_{SD}^{n,i}$	SNR value of the i-th replica n-th segment received from the source station
γ_{SD}^{t}	SNR between the source and the destination stations at the time slot t
γ_{SR}	SNR value on the link between the source and the relay
$\gamma_{SR_i}^{t}$	SNR between the source and the i-th relay stations at the time slot t
$\tilde{\gamma}_{AB}^{t}$	Corrupted SNR between stations A and B at the time slot t
γ_t^i	Switching threshold of modulation mode i
$\gamma_{t_R}^{\ i}$	Switching threshold of modulation mode i at the relay station
$\tilde{\gamma}_{R_iD}^{t}$	Corrupted SNR between the i-th relay and the destination stations at the time slot t
$\gamma_{t_{RD}}$	Switching threshold on the relay-destination link
$\gamma_{t_{RD}}^{i,\gamma_{SD}}$	Switching threshold on the relay-destination link at the attempt i
$\tilde{\gamma}_{SD}^{t}$	Corrupted SNR between the source and the destination stations at the time slot t
$\gamma_{t_{SD}}$	Switching threshold on the source-destination link
$\gamma_{t_{SD}}^{i}$	Switching threshold on the source-destination link at the attempt i
$\tilde{\gamma}_{SR_i}^{t}$	Corrupted SNR between the source and the i-th relay stations at the time slot t
$\gamma_{t_{SR}}^{i}$	Switching threshold on the source-relay link at the attempt i

Γ	Average SNR value
Γ_{AB}	Average SNR value on the link between stations A and B
Γ_c	SNR yielding a channel capacity equal to a target code rate
Γ_{EXIT}	Decoding threshold
Γ_{RD}	Average SNR value on the link between the relay and the destination stations
Γ_{R_iD}	Average SNR between the i-th relay and the destination stations
Γ_{SD}	Average SNR value on the link between the source and the destination stations
Γ_{SR_i}	Average SNR between the source and the i-th relay stations
Γ_{SR}	Average SNR value on the link between the source and the relay stations
λ_{RD}	Number of modulated symbols of the transmission between the relay and destination stations
λ_{SD}	Number of modulated symbols of the transmission between the source and destination stations
$\Omega(i)$	Cost function value of a channel code candidate C
T	Puncturing period
ψ	Offset for the switching threshold
σ_1	SNR under-estimation probability
σ_2	SNR over-estimation probability
$\sigma_{\tilde{x}}$	Standard deviation of LLR sequence $\tilde{x}$
$\sigma_{\tilde{x}}^2$	Variance of LLR sequence $\tilde{x}$
ξ	Additional offset for the switching threshold on the source-relay link

PART I

BACKGROUND

1

COMMUNICATIONS ON A WIRELESS CHANNEL

This chapter reviews the characteristics that define a wireless communication channel and presents techniques that are used for mitigating the impairments incurred when transmitting on a radio channel. Particularly, adaptive strategies and the cooperative approach are reviewed, since they are the main area of interest of the thesis.

1.1 THE WIRELESS CHANNEL

In a wireless channel a transmitter and a receiver exchange information over a radio interface. A wireless communication is characterised by reflections, refractions, diffractions and scattering. The ultimate result of these propagation characteristics is that the received signal is composed by the superposition of different replicas of the transmitted signal. Such phenomenon is referred to as multipath. Furthermore, the propagation is also influenced by mobility, which causes short term fluctuations (fading) and long term fluctuations (shadowing) of the received signal power.

1.1.1 FADING

As previously introduced, the signal received in a wireless channel is composed of many replicas of the same transmitted signal, that are shifted in phase and attenuated because of reflections, refractions, diffractions and scattering. Such phenomena, and the additional influence of mobility, determine a fast fluctuation of the power of the received signal. This behaviour is referred to as multipath fading, and is detrimental for the performance of the wireless system. Particularly, the effect of fading may be modelled by multiplying the received signal by a complex quantity

$h(t)$ that represents the signal variation in amplitude and phase incurred because of fading itself.

The fading properties are characterised by its statistic at a given time instant, and by the correlation over two different time instants. Many statistics may be used for modelling the fading behaviour, such as the Rice statistic, the Nakagami statistic and the Rayleigh one. This work considers Rayleigh fading, which indicates the particular situation where the direct path between the transmitter and the receiver is absent, and hence the entire signal is received through multipath propagation.

For characterising the instantaneous time property of Rayleigh fading, denote the fading value at a time t by $h(t)$, and its in-phase and quadrature components by $h_I(t)$ and $h_Q(t)$, respectively. When considering Rayleigh fading, the in-phase and quadrature components of fading may be modelled as independent Gaussian random variables having a mean equal to zero and variance equal to $\frac{1}{2}$. Hence, the probability density functions of $h_I(t)$ and $h_Q(t)$ may be written as:

$$p_{h_I(t)}(z) = \frac{1}{\sqrt{\pi}} e^{-(z-1)^2}, \tag{1.1}$$

$$p_{h_Q(t)}(z) = \frac{1}{\sqrt{\pi}} e^{-(z-1)^2}. \tag{1.2}$$

Such probability distribution for the in-phase and quadrature components translates to a variation of the received power due to the fading that is exponentially distributed, and follows the law:

$$p_{|h(t)|^2}(z) = e^{-z}. \tag{1.3}$$

The Rayleigh fading model accounts for the distribution of the received signal envelop during a particular time instant. The temporal characteristic of the fading process is instead influenced by the Doppler effect, which accounts for the relative velocity between the transmitter and the receiver. The Clark model [1] is usually considered as the classic approach for accounting for the time variation of the fading process. Particularly, the Clarke model assumes that received signals are uniformly distributed over the whole azimuth domain. Under such assumption, the correlation between the in-phase components, and similarly between the quadrature components of the fading values at two different time instants may be expressed as:

$$\mathcal{E}(h_I(t), h_I(t+\tau)) = J_0(2\pi f_d \tau), \tag{1.4}$$

$$\mathcal{E}(h_Q(t), h_Q(t+\tau)) = J_0(2\pi f_d \tau), \tag{1.5}$$

where J_0 is the zero-order unmodified Bessel function of the first kind and f_d is the Doppler frequency. The in-phase and quadrature components of fading values are

independent. Such correlation property between in-phase and quadrature signal components translates to a correlation law between the power gains received in different time instants that may be written as:

$$\mathcal{E}(|h(t)|^2, |h(t+\tau)|^2) = J_0^2(2\pi f_d \tau). \tag{1.6}$$

The time characteristics of the fading process depend on the value $f_d\tau$. In the case where $f_d\tau << 0.1$ the fading is referred to as slow fading, being the fading values highly correlated over time. The opposite case is referred to as fast fading, where fading values are less correlated over time.

1.1.2 The effects of fading on the system performance

Fading has a detrimental influence on the system performance. Particularly, it increases the error ratio of digital transmissions over the channel. Consider, for example, an uncoded transmission using the Binary Phase Shift Keying (BPSK) mode. The Bit Error Ratio (BER) $P_e(\gamma)$ of such system over an Additive White Gaussian Noise (AWGN) channel, where the transmission is affected by noise, but the signal does not experience fading and hence is received at a constant Signal to Noise Ratio (SNR) γ, is given by:

$$P_e(\gamma) = Q\left(\sqrt{2\gamma}\right). \tag{1.7}$$

When the signal is affected by Rayleigh fading, the SNR value γ fluctuates over time, and may be written as $\gamma = |h|^2\Gamma$, with Γ being its expected value. The average BER of such system may be obtained as:

$$\overline{P_e(\Gamma)} = \mathcal{E}[P_e(\gamma)] = \int_0^{+\infty} Q\left(\sqrt{2s\Gamma}\right) p_{|h|^2}(s)\mathrm{d}s. \tag{1.8}$$

For a Rayleigh fading scenario, after some manipulations, one obtains:

$$\overline{P_e(\Gamma)} = \frac{1}{2}\left(1 - \sqrt{\frac{\Gamma}{1+\Gamma}}\right). \tag{1.9}$$

Figure 1.1 compares the BER performance of the uncoded BPSK system over the AWGN channel and over the Rayleigh faded channel. It can be seen that the BER performance is much worse in the faded scenario. Such observation is more general, and it applies to both uncoded and coded scenarios [1].

The next section reviews techniques that allow mitigating the negative effects of fading on the system performance. Particularly, adaptive and cooperative systems are reviewed, since they are the main topics covered in the rest of this thesis work. A complete review of the characteristic of the fading channel and techniques used to overcome its negative effects may be found in [2].

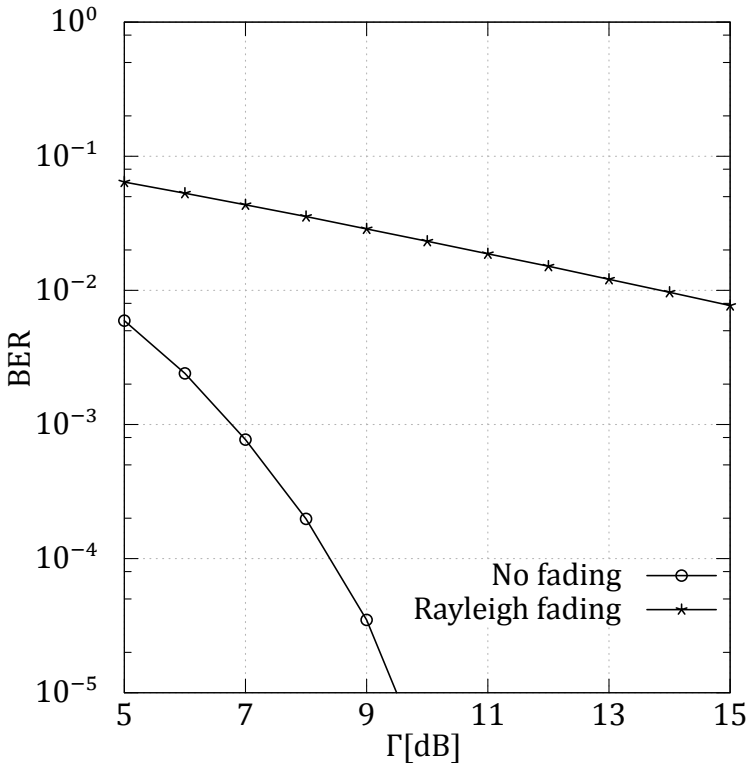

Figure 1.1: Comparison between the performance of an uncoded system using the BPSK modulation mode in non-faded and faded environments.

1.2 Adaptive techniques

As detailed in the previous section, the fading phenomenon translates to a SNR value that varies over time. Such variation of the channel quality is detrimental for the system performance, and it ultimately may result in a failed transmission, when the channel quality does not support the particular selected transmission mode.

Adaptive techniques, as the name suggests, try to adapt the transmission mode to the instantaneous channel condition. In particular, they aim at selecting the transmission mode (e.g. the modulation mode, the coding rate) that provides the most prompt transmission and has a success rate higher than a target threshold given the instantaneous channel conditions.

Many research works considered the problem of selecting the transmission mode when knowing the instantaneous channel quality. These papers share the base idea that using a higher modulation mode or a lower coding rate when the channel condition is high, and reducing the modulation order or increasing the code rate when the channel condition is low, provides an increased bandwidth efficiency than using the same transmission technique independently from the channel state.

Particularly, reference [3] considers an uncoded system operating on a fading channel. This work shows using both theoretical and experimental means that selecting the transmission characteristics according to an instantaneous channel prediction allows the system designer to achieve an increased performance in terms of error probability.

A different point of view is considered in [4], where the characteristics defining the transmission of a user, including the transmission power and the bit rate, are adapted to the particular service level that the user requires.

References [5, 6] consider instead a coded system, where the adaptive regime matches the selected modulation mode and code rate to the instantaneous channel quality. Again, the papers confirm that adaptive strategies are an efficient solution for mitigating the negative effects experienced in time varying channels.

The introduction of turbo codes [7] and the rediscovery of Low Density Parity Check (LDPC) codes motivated additional research on adaptive algorithms for exploiting the near capacity performance achieved by such coding techniques. Particularly, the works of [8, 9, 10] study adaptive techniques when turbo codes are used for transmitting information on a time varying channel. LDPC codes are instead taken into account in references [11, 12, 13, 14, 15]. Again, the above mentioned works show that adaptive techniques, where the coding rate and other characteristics of the encoding technique are adapted to the channel quality, are an efficient and practical solution for addressing the variance over time of a faded channel.

1.3 Diversity techniques

The previous section shown that the time varying nature of the wireless channel may be tackled by using transmission schemes that adapt their characteristics to the instantaneous channel quality. However, such schemes typically require a feedback channel or either rely on estimation mechanisms for obtaining information on the actual channel state.

Another approach for mitigating the negative effects of fading is diversity. Diversity techniques overcome the impairments imposed by the fluctuation of the received signal by providing different replicas of the same information to the receiver in a way such that the replicas experience independent fading. The idea behind diversity is that at least one among such replicas will be received with a sufficient quality for supporting the communication.

1.3.1 The effects of adopting diversity techniques

Diversity techniques typically combine the different replicas, and the optimal combining strategy is the Maximal Ratio Combining (MRC), where the replicas are re-

phased and weighted according to the fading that they experienced during transmission. The end result of adopting MRC is that the recombined signal is characterised by a SNR value that is the sum of the SNR values of the single replicas. Particularly, denote the SNR of the l-th replica at a time t by $\gamma_l(t)$. The SNR of the signal obtained by using the MRC combination is:

$$\gamma(t) = \sum_{l=1}^{L} \gamma_l(t). \tag{1.10}$$

By calculating the probability density function of the SNR of the signal obtained after the MRC combiner for a given fading statistic, one may observe that the ultimate effect of such a combination technique is to reduce the variance of the SNR. For exemplifying the effects of diversity and MRC combining on the received signal quality, Figure 1.2 compares the probability of receiving a signal characterised by a particular SNR value both for diversity aided scenarios and for the case where no diversity techniques are used under Rayleigh fading. For the sake of having a fair comparison, a transmit power that is L times less than the one used for the single transmission without diversity is given to each replica of a scenario where diversity with L replicas is considered. It can be seen that using diversity increases the probability of receiving a signal with quality closer to the average SNR value, while the most likely SNR value when no diversity technique is adopted is the zero value. Figure 1.2 is obtained using Monte-carlo simulations, though analytic results may be found in [1].

The effect of MRC on the SNR distribution influences the system performance. In particular, having a higher probability of receiving a signal characterised by a better quality translates to an improved BER performance. Figure 1.3 shows the BER performance averaged over fading realisations of an uncoded transmission using the BPSK modulation mode for the case where no diversity is provided and for the case where L independently faded replicas are combined by the receiver. It can be seen that diversity techniques significantly improve the BER performance of the system, and hence are an effective way for mitigating the impairments of fading.

1.3.2 Diversity using multiple-input multiple-output solutions

Many approaches may be adopted for providing L independent replicas at the receiver for activating the benefits offered by diversity. The most common ones are summarised in the following.

- Frequency diversity: The transmitter sends the same message on L different frequencies, separated by a frequency value that must be equal or higher

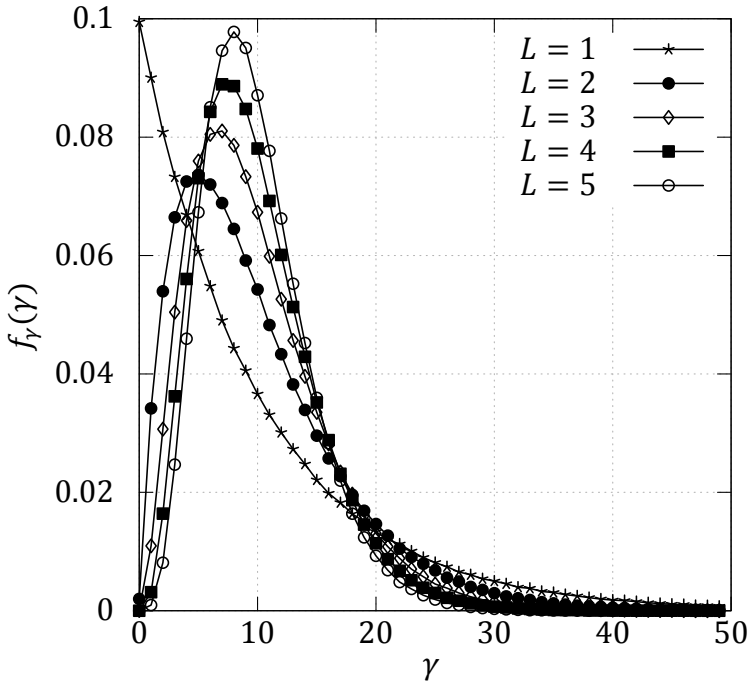

Figure 1.2: Probability density function of the received SNR after MRC combining, for $\Gamma = 10$ dB.

than the coherence band value characterising the channel. The main disadvantages of frequency diversity are its high bandwidth requirement and the fact that the coherence band value is typically unknown a priori.

- Time diversity: The transmitter sends L replicas at different times, separated by at least $0.1/f_d$ seconds, where f_d is the normalised Doppler frequency. The main drawbacks of time diversity are a throughput decrease and the correlation between f_d and the users' mobility: particularly, if the transmitter and the receiver are not in motion, time diversity may suffer from high correlation between replicas.

- Polarisation diversity: The signal is sent using both vertical and horizontal polarisations, or with right and left circular polarisations. In order to employ polarisation diversity the transmitter has to collaborate. Furthermore, for polarisation diversity, L may only assume the value of $L = 2$.

- Antenna diversity: The receiver is equipped with L antennas, separated by a distance equal at least to $\lambda/2$, being λ the wavelength value. The main disadvantage of antenna diversity is that it increases the receiver complexity.

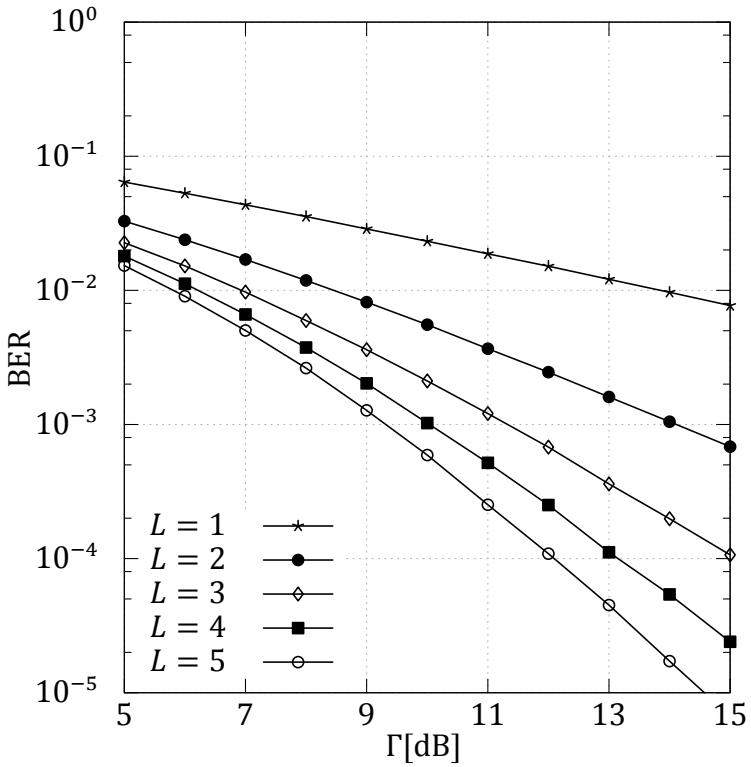

Figure 1.3: Comparison between the performance of an uncoded system using the BPSK modulation mode and receiving a different number of independently faded replicas.

A modern way to interpret antenna diversity was proposed by Alamouti [16] and refined by Tarokh *et al.* [17] with the introduction of Space-Time Block Codes (STBCs). The diversity schemes proposed by Alamouti and Tarokh *et al.* target Multiple-Input Multiple-Output (MIMO) channels. A MIMO channel is a network scenario where both the transmitter and the receiver are equipped with multiple antennas. The key idea of Alamouti's work was to spread the symbols at the transmitter over successive time instants and map them in a particular way to transmit antennas. Such mapping over the temporal and spatial domains, which in Alamouti's work was limited to two antennas at the transmitter, was shown to obtain the same degree of diversity of the classic two-antenna receiver diversity [16]. Tarokh *et al.* extended Alamouti's findings by providing schemes for different values of transmit antennas [17]. These mapping schemes over time and antennas are referred to as space-time block codes. The work of Tarokh *et al.* further proved that a STBC aided transmission system operating on a MIMO scenario where the transmitter is equipped with N_T transmit antennas and the receiver is equipped with N_R receive antennas achieves a diversity gain equal to $N_T \times N_R$ [17].

The main advantage of diversity MIMO systems is that they move the complexity required for activating diversity from the receiver to the transmitter. Particularly, in many scenarios the receiver suffers from limited spatial characteristics and computational capabilities, such as when dealing with handsets in downlink transmissions in mobile networks. In such scenarios, shifting the complexity to the transmitter is beneficial, since it allows resource limited receivers to benefit from a diversity gain and hence to experience an improved decoding performance. One may also note that MIMO diversity systems may allow achieving a higher diversity gain in the case where both the transmitter and the receiver are equipped with multiple antennas, compared to the traditional receiver based antenna diversity.

Despite being a practical way for achieving diversity, STBC and MIMO diversity based solutions suffer from a major disadvantage. Particularly, they require accommodating multiple antennas on a single device, with the additional constraint of adequately separating such antennas for providing independently faded paths between the transmit and receive radiating elements. Such constraint may be very limiting when tiny devices are considered, such for example for mobile phones.

1.4 The cooperative approach

The previous section shown that diversity techniques mitigate the BER downgrade experienced in fading channel. Furthermore, among diversity solutions, STBCs were introduced as a practical way for providing independently faded replicas at the receiver. However, MIMO solutions require accommodating multiple antenna elements both at the transmitter and at the receiver. Hence STBC aided solutions are limited by space constraints on tiny devices.

Recent studies on cooperative communications overcame the problem of accommodating multiple antennas on a tiny device by letting nodes equipped with a single antenna to share their information in order to form a virtual antenna array, achieving the same spatial diversity provided by a standard co-located MIMO design, without employing multiple radio frequency frontends in every device.

In a cooperative communication the signal transmitted from the source station is received and forwarded by one or more relays. Since the direct and the relayed signals typically arrive via completely different paths, the correlation between these signals is small, hence a diversity gain is provided. A cooperative scenario is shown in Figure 1.4.

As one can see, cooperation is typically divided into two phases. During the initial phase, represented using dashed lines, the source station transmits its information to potential helpers. Such transmission is also received by the destination station, which stores the signal and later combines it with the information gleaned from relays. After potential relays received the signal transmitted from the source

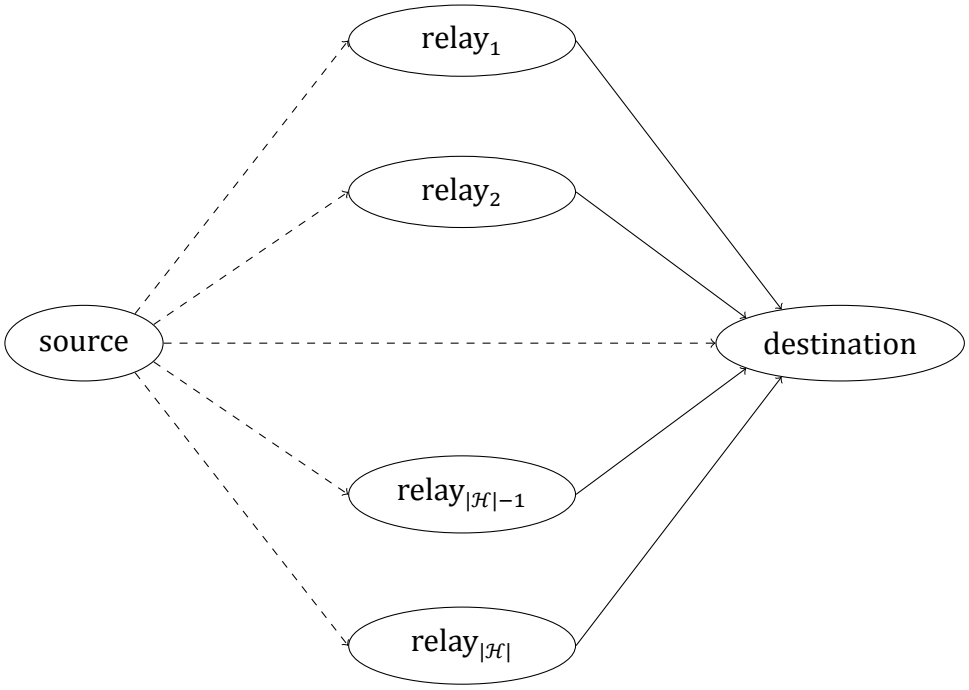

Figure 1.4: Data transmission in a cooperative scenario including $|\mathcal{H}|$ available relay stations.

station, they initiate a second phase, represented using solid lines, where they forward information to the destination station. Finally, the destination combines signals received by relays with the information gleaned from the source station and performs its decoding algorithm.

1.4.1 Possible relaying strategies

Cooperation techniques differ in the way information is forwarded by relay stations. Particularly, a potential relay can forward data in three different ways, namely amplify-and-forward, decode-and-forward and coded cooperation [18]. These forwarding schemes are summarised in the following:

- amplify-and-forward: each relay receives a noisy version of the signal transmitted from the source to the destination, amplifies it and finally forwards it to the destination. The drawback of using amplify-and-forward techniques is that by amplifying the signal transmitted by the source station, relay stations also amplify noise;
- decode-and-forward: each relay receives a noisy version of the signal transmitted from the source to the destination, decodes it and then retransmits

a new noise-free replica; decode-and-forward achieves better performance than amplify-and-forward schemes as noise is not amplified, however it assumes that each relay is able to decode the received information (i.e. decode-and-forward requires having a high SNR source-relay link) and forward it on time;

- coded cooperation: each relay receives a noisy version of the signal transmitted from the source to the destination, decodes it and then retransmits an re-encoded message that contains different information than the one previously transmitted by the source station, i.e. coded cooperation integrates channel coding into cooperation.

  Among these forwarding solution, Hunter *et al.* [19, 20] shown that coded cooperation provides efficiency improvements over amplify-and-forward and decode-and-forward schemes as it benefits from advanced coding techniques and hence attains a higher throughput together with a lower BER at the destination.

1.4.2 Distributed cooperative coding techniques

The findings of Hunter *et al.* [19, 20] fostered research on distributed channel coding techniques, where cooperation among the encoders used at the source and relay stations allows increasing the decoding performance at the destination. Particularly, noting that the optimal performance in cooperative scenarios is attained if new information is forwarded by the relay, instead of simply retransmitting the information gleaned from the source station, researchers studied efficient distributed coding schemes where relays add new information or invoke an additional coding layer for improving the performance of the overall cooperative link. A brief review of distributed coding techniques proposed in the literature is presented in the following paragraphs.

1.4.2.1 Cooperative space-time block codes and linear dispersion codes

As shown in the previous section, STBCs were proven to be a promising coding technique in a co-located scenario. Distributed space-time block codes [21] extend STBCs to a cooperative scenario, where the joint transmissions of the source and relay stations form a space-time block coding technique, providing a diversity gain at the destination.

Distributed STBC schemes are a subset of Cooperative Linear Dispersion Codes (CLDCs) [22], which provide a general framework comprehending a wide variety of cooperative coding schemes. The co-located version of CLDCs, namely Linear

Dispersion Codes (LDCs), use a matrix-based linear modulation, where the space-time transmission matrix is obtained by a linear combination of so-called dispersion matrices [23]. The performance of LDCs and CLDCs over a channel affected by Rayleigh fading was summarised by Hanzo *et al.* in [22], assuming that the source-destination Channel State Information (CSI) was perfectly known at the receiver. Particularly, Hanzo *et al.* shown that LDCs outperform their cooperative counterpart in a Rayleigh fading channel, due to the time used in the latter to spread the original signal to all the relays. However, when the channel is affected by shadow fading, the achievable throughput severely downgrades and CLDCs obtain better results as they use multiple relays which experience different shadow fading.

1.4.2.2 Distributed turbo codes

Aiming to benefit from the performance increase using coded cooperation promised by Hunter *et al.* [19, 20], Valenti and Zhao proposed an efficient distributed coding scheme in [24]. The technique proposed by Valenti and Zhao mimics the behaviour of turbo codes [7] by adapting Berrou *et al.* codes to a cooperative scenario, and hence is referred to as a distributed turbo code.

Valenti and Zhao divide the transmission sequence into two phases. During the initial phase, the source station transmits a signal that was previously encoded using a Recursive Systematic Convolutional (RSC) code. This signal is received and decoded by the designated relay. During the second phase, the relay interleaves the bits obtained by decoding the signal gleaned from the source station during the first phase and re-encodes their interleaved version using again an RSC. The destination obtains both the non-interleaved and the interleaved encoded bit sequences by receiving the signals transmitted by the source and the relay stations during the two successive phases, and hence may activate the iterative algorithm that is typically employed for decoding co-located turbo codes. The BER and outage performance of distributed turbo codes were shown to be close to the capacity of a relay-aided link, with the provision of having an error-free decoding at the relay of the signal transmitted by the source station during the initial phase.

1.4.2.3 Capacity approaching distributed coding techniques

The limit of the distributed turbo code scheme proposed in [24] by Valenti and Zhao and of the CLDC of [22] was to adopt the simplifying assumption of having a perfect source-relay link. However, in a realistic scenario, the signal decoded by the relay may potentially contain errors, which are then propagated to the destination. Furthermore, the CLDCs of [22] were designed with the aim of eliminating the effects of antenna-element correlation typically imposed on co-located antenna elements of space-time codes, where the virtual array antenna elements were constituted by

the mobiles' single antennas; however no attempt was made to jointly decode the source's and relay's transmissions at the destination. These issues are addressed in recent papers, where an imperfect source-relay communication is considered and an efficient joint decoding strategies for the source's and relay's signals are proposed.

In [25] Uddin Butt *et al.* adopt an Iteratively-Decoded SElf-Concatenated Convolutional Code (SECCC-ID) [26] at the source station and an additional RSC encoder at the relay. An EXtrinsic Information Transfer (EXIT) chart analysis is performed for guaranteeing the possibility of decoding the signal with an infinitesimally low BER at the relay. Finally, a novel decoder architecture is adopted at the destination and its design is aided by an EXIT chart analysis. The new decoding architecture jointly decodes the SECCC encoded signal transmitted by the source station and the RSC encoded signal forwarded by the relay. The scheme of Uddin Butt *et al.* is shown to attain a remarkable decoding performance at very low SNR values.

A similar approach is considered by Kong *et al.* in [27], where again an additional layer of coding is introduced at the relay, and the whole scheme amalgamates STBC codes for additionally obtaining a diversity gain. More particularly, the distributed coding scheme of Kong *et al.* adopts a combination of an IRregular Convolutional Code (IRCC) and a STBC at the source station and at the relay. The irregular code at the source station is designed for attaining an infinitesimally BER at the relay during the initial phase, for mitigating the propagation of errors. In turn, the encoder used at the relay station is optimised using an EXIT chart matching technique for guaranteeing a vanishingly BER performance at the destination when performing a joint decoding of the signals gleaned during the two successive transmission phases. A novel three-stage iterative decoder is used at the destination, which allows performing an efficient joint decoding of the received signals.

The previous schemes are provided as examples of physical layer systems where cooperative communications are carefully considered, taking into account both the performance at the relay and at the destination stations. Many schemes following the design guidelines of the above-mentioned works have been presented in the literature. An overview of distributed iterative systems for MIMO channels may be found in [22].

The previous presented schemes adopt concatenations of convolutional encoders at the source and relay stations. However, other solutions have been proposed for cooperative links. Particularly, given the promising performance of LDPC codes in the single-link scenario, many research efforts were devoted at extending such coding technique to the cooperative channel.

A parallel concatenation of rate-compatible punctured LDPC codes is used in [28] for transmitting information with the aid of a relay. The authors show that the proposed scheme provides significant performance gains for a wide variety of

channel conditions while simultaneously offering a high degree of flexibility.

The work of [29] considers the design of LDPC codes that achieve optimal performance both over the Gaussian and the faded channels. Codes are proposed for cooperative communications, and the paper shows that the universal design outperforms previous solutions.

Hybrid automatic repeat and request systems are considered in [30], where the authors propose a novel retransmit strategy that relies on LDPC codes. It is shown that the novel strategy outperforms previous cooperative solutions, even in the case when it is artificially limited to activating a single rely, while classic cooperative systems are allowed invoking multiple helpers.

An overview of distributed techniques adopting LDPC codes is presented in [31], together with a discussion of different design strategies an their resulting performance. The paper shows that distributed techniques that rely on puncturing solutions outperform schemes that adopt an additional layer of coding at the relay, when the relay station is located in the proximity of the destination station. An opposed result is found for scenarios where the relay station is instead closer to the source stations.

Two-way relaying scenarios are considered in [32], which derives the optimal degree distribution for an LDPC code adopted in such systems. Particularly, the degree distribution is optimised for situations where the different segments within the distributed codeword have been transmitted through different channels and experience different SNRs. The paper relies on density evolution techniques and on a multi-edge type LDPC design for contriving codes which provide the lowest decoding threshold as possible.

Finally, LDPC are amalgamated with STBCs for contriving high performance solutions for cooperative systems operating on MIMO links [33]. The authors adopt a soft-relay solution and include a low-complexity decoding algorithm, showing that the proposed scheme outperforms previously published solutions.

2

The IEEE 802.11 standard for wireless networks and its cooperative extensions

This chapter presents a brief review of the IEEE 802.11 standard family, which is a widely popular solution for supporting wireless communications between networked stations. The chapter focuses on the medium access control layer aspects of the standard, and in particular it summarises literature works trying to enhance the performance of an IEEE 802.11 based network by adopting a cooperative approach. The chapter also briefly pictures the main limitations of cooperative medium access control solutions that have been proposed by the research community.

2.1 Wireless Local Area Networks

Recent years have seen a significant demand of communication technologies that provide an increased users' mobility. Particularly, users want to be able to communicate without location constraints imposed by wired solutions. This trend affected Local Area Networks (LAN), where wireless solutions extended and in many situations replaced cabled networks. Today, Wireless Local Area Networks (WLANs) are widespread in people's homes, in business environments and in public places, since they are a practical way of allowing users to communicate without sacrificing mobility and without requiring a cabled architecture.

Among different solutions for creating a WLAN infrastructure, the most popular one is represented by the IEEE 802.11 standard [34]. The IEEE 802.11 standard allows defining both centralised and distributed WLANs, and devices that mount IEEE 802.11 compliant modules include laptop computers, smartphones, tablets and more recently even home appliances. The ubiquitous diffusion of IEEE 802.11 networks attracted a wide research effort aimed at analysing the performance of

such networks and at contriving enhanced schemes which may provide an increased user experience. Among the diverse ideas proposed for extending IEEE 802.11, cooperation has been shown lately to provide a throughput and outage performance increase. Particularly, extending the IEEE 802.11 by introducing cooperation is one of the core contributions of this thesis work. This chapter briefly reviews the IEEE 802.11 standard and its cooperative extensions presented in literature works, for providing a background to later chapters which address the design of cross-layer cooperative medium access control solutions based on this standard.

2.2 The IEEE 802.11 standard for wireless networks

The IEEE 802.11 is the most diffused standard for wireless networks. The IEEE 802.11 was originally proposed in 1997 [34], and later extended by diverse task groups that provided a set of enhanced standards, that are typically referred to as 802.11x and aim at increasing the network performance in terms of throughput [34, 35, 36], Quality of Service (QoS) [37] and security [38]. The 802.11 standard specifies both PHYsical (PHY) layer and Medium Access Control (MAC) layer aspects that define the behaviour of the WLAN. The 802.11 standard family may operate on the 2.4 GHz and 5.8 GHz frequency bands, and supports multiple nominal bit rates, that vary between 1 Mbits/s and 11 Mbits/s in the IEEE 802.11b amendment, between 6 Mbits/s and 54 Mbits/s in the IEEE 802.11a and IEEE 802.11g amendments and between 6.5 Mbits/s and 600 Mbits/s in the IEEE 802.11n amendment. These different transmission rates are obtained by varying the combination of modulation mode and code rate adopted for the channel encoder, as well as using advanced transmission techniques such as MIMO schemes and Orthogonal Frequency Division Multiplexing (OFDM) solutions.

2.2.1 The IEEE 802.11 medium access control scheme

The IEEE 802.11 MAC scheme for distributed scenarios, where there is not a central controller, is the Distributed Coordination Function (DCF). The DCF algorithm is based on the CSMA scheme, where sensing is performed by stations before they send their own data frames. More explicitly, when a packet is ready for transmission, a station senses the channel for assessing if other stations are currently transmitting information. In the case where there are not other ongoing communications, the station waits for a Distributed InterFrame Space (DIFS) time and checks the channel again. If the medium is still free the station transmits its information using a DATA frame. Finally, if the destination station correctly receives the

information transmitted by the source station, it confirms the success of the data exchange with an acknowledgement (ACK) frame after waiting a Short InterFrame Space (SIFS) time. In the opposite case, that is when the station senses ongoing communications, it waits a random time, referred to as the backoff time, for reducing the likelihood of colliding with other active transmissions. The backoff time is regulated by a random process, which sets a backoff counter to a random number that is selected uniformly between zero and an integer value referred to as the station's contention window. At the beginning of the following slot, the station senses the channel again. If the medium is free for a DIFS duration, that is if the station does not sense communications from other nodes during a DIFS time, the node decreases its backoff counter, otherwise it waits until the beginning of the next slot. When the counter reaches the zero value the station transmits its packet.

If the destination cannot decode the signal transmitted by the source station (either because data is corrupted due to impairments imposed by the communication channel or because a collision occurred), or if the source station does not receive the ACK frame, a retransmission is scheduled and a backoff procedure is initiated after doubling the value of the station's contention window and increasing the retransmission counter.

Particularly, the value of the contention window varies from a minimum value, referred to as the minimum contention window, to a maximum value, referred to as the maximum contention window, which is obtained by multiplying the minimum contention window value times the value of two to the power of the maximum backoff stage. The contention window update is regulated by the following rules:

- every time a packet is successfully transmitted a station resets its contention window to the minimum contention window value;
- when a transmission is unsuccessful or when the medium is found busy trying to transmit, the contention window is doubled, until it reaches the maximum value.

The access scheme described in the previous paragraph is referred to as the basic access scheme of the DCF. The problem of the basic access is that in congested situations there might be a high number of collisions, resulting in a significant time waste, since collided DATA frames may be very long. The DCF algorithm offers a way for mitigating the probability of collisions that is based on collision avoidance techniques.

2.2.2 The DCF collision avoidance mechanism

The collision avoidance solution adopted by the DCF consists of a four-way handshake mechanism for transmitting DATA frames. This four-way handshake relies

on exchanging additional frames before the actual DATA frame transmission takes place. Particularly, when a station wants to transmit a DATA frame, it initiates the communication by sending a small Ready-To-Send (RTS) frame. If this frame is successfully received (i.e. no collision occurs), the destination replies with a Clear-To-Send (CTS) frame. Both the RTS and the CTS frames contain a field which indicates the duration of the future DATA/ACK exchange. Every other station which receives the RTS frame or the CTS frame knows that a DATA transmission is being initiated and hence defers its transmission to a later time, for avoiding collisions. Particularly, the station records the DATA/ACK exchange duration by setting its Network Allocation Vector (NAV) to a value that matches the transmission duration indicated in the RTS and CTS frames. While the NAV is set, the station waits before sending its packet, in order to avoid colliding with the ongoing transmission. Figure 2.1 shows the data exchange when adopting the RTS/CTS frames exchange aided access solution.

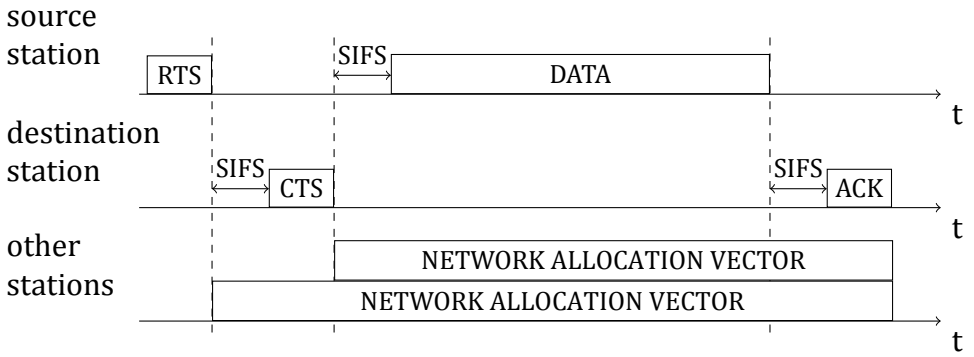

Figure 2.1: Data exchange when adopting the RTS/CTS frames exchange aided access solution.

The RTS/CTS mechanism is very effective in terms of system performance when large packets are considered. Particularly, as previously noted, when adopting the basic access for large DATA frames a collision leads to a considerable waste of time. By contrast, when employing the RTS/CTS mechanism the collision only involves the shorter RTS/CTS frames and hence less time is wasted.

2.3 Cooperative MAC schemes for IEEE 802.11 WLANs

The previous chapter introduced the cooperative approach for mitigating the performance downgrade incurred in faded scenarios and reviewed distributed coding techniques proposed for the PHY layer in the literature. However, cooperative solu-

tions are not limited to the PHY layer, and may be adopted at the MAC layer for increasing the performance of wireless networks in terms of throughput and outage.

Particularly, the works of [39, 40] shown that a performance downgrade is incurred in IEEE 802.11 networks because of slow stations, which occupy the channel for long periods of time and hence prevent faster nodes from transmitting their DATA frames, ultimately limiting the network throughput. These works also shown that a cooperative approach may be beneficial for reducing such performance downgrade by allowing multi-hop communications through faster relays when the direct link may only operate at a slow speed because of a low channel quality. The outage performance may be also improved by noting that, when channel impairments reduce the link quality to the point that a direct communication may not take place, the source station can still transmit its DATA frame to the destination by invoking the aid of an appropriate partner.

The following parts review the cooperative solutions for IEEE 802.11 networks proposed in the literature, with a particular emphasis on the requirements and the issues that characterise the design of a cooperative MAC protocol for WLANs.

2.3.1 Cooperative MAC protocols overview and design issues

Cooperative MAC control protocols based on the IEEE 802.11 standard modify the access scheme of station and the following frame exchange by intrinsically allowing multi-hop transmissions where data is transmitted to the destination with the aid of a relay station. Diverse proposed solutions differ in the particular way in which they enable cooperation, in the algorithm adopted for selecting the relay and in the actual frame exchange strategy. Despite showing significant differences in stations' behaviours, all the cooperative MAC protocols proposed in the literature address some of the following design questions, which may be seen as fundamental issues characterising the design process of a cooperative MAC scheme [41]. Such questions are:

- whether to cooperate or not to cooperate;
- if cooperation is invoked, how should the helper be identified and selected;
- how to address hidden and exposed terminal problems in a cooperative scenario;
- whether cooperation should be used for improving throughput, for minimising the number of retransmissions (obtained achieving a better BER at the destination) or for reducing interference.

The following paragraphs provide more literature background on the first two design issues.

2.3.1.1 To cooperate or not to cooperate

A design choice that is of paramount importance for defining the behaviour of a cooperative MAC is to decide whether cooperation should be invoked for the upcoming transmission or if a direct communication is to be preferred, and in the case where a cooperative approach is adopted how the particular transmission sequence should develop. Particularly, cooperative MAC protocols are divided into two categories based on how they interpret cooperation, namely proactive and reactive schemes.

In proactive schemes, the decision if cooperation should be invoked is taken before transmitting, while in reactive schemes cooperation is adopted only when the transmission on the direct link fails. In particular, proactive schemes aim at maximising the throughput by selecting the most prompt transmission before it actually takes place. Such systems may in fact select to transmit to a relay with a high order modulation mode, which is not supported on the source-destination link, and let the relay forward the information to the destination, if such transmission sequence requires less time than the one using the modulation mode supported on the direct link. Conversely, reactive schemes aim at reducing the error probability at the destination by providing an additional transmission that experiences independent fading and shadowing characteristics than the one from the source to the destination, in the case that the latter was unsuccessful.

These two design strategies are the common base for a wide range of cooperative solutions that are found in the literature. Particularly, the works of [41, 42, 43, 44, 45, 46, 47] take a proactive approach, while the schemes proposed in [48, 49, 50] base their transmission strategy on reactive cooperative solutions.

2.3.1.2 Relay selection mechanism

Another design choice which differentiates cooperate MAC protocols is the relay selection mechanism. Particularly, the relay selection mechanism defines the metric that is used for selecting the adopted relaying partner, the mechanism that performs the actual selection and also the particular strategy that is used for informing the stations involved in the communication about the identity of the chosen relay.

The typical metric that is used for selecting the adopted relay station relies on channel qualities [41, 43, 44], which are in most case identified with SNR values on the source-relay and relay-destination links. Such metric choice is motivated by noting that channel qualities determine whether the relay may understand the transmission made by the source station and later the success of the relay to destination transmission. Hence, selecting a relay with satisfactory channel quality characteristics translates to selecting a relay which will successfully receive and forward information to the destination. Furthermore, higher channel qualities also

support higher data rates. Hence, selecting relays having high channel qualities towards the source and the destination may provide more prompt transmissions due to the adoption of higher order modulation modes. Many works were motivated by the above-mentioned considerations, and relay selection schemes based on channel qualities for achieving faster transmission rates may be found in [42, 45, 46].

Even though SNR is the metric that is typically used for selecting the communication partner, other metrics were considered in the literature. Particularly, another metric that was adopted for discriminating between possible relay stations is energy. The work of [51, 52] provide relay selection schemes that takes into account the amount of energy that is used for performing a cooperative transmission for identifying the most appropriate partner. A further metric considered for the relay selection problem is spatial reuse. Particularly, the works of [53, 54] select the relay which provides a better spatial reuse, in the sense that it allows minimising the number of nodes that may not transmit because their are in the collision avoidance range of the adopted partner.

Cooperative protocols also differ in the practical way of selecting the relay and notifying its identity to other stations involved in the communication. Particularly, some cooperative protocols rely on a contention mechanism between possible relay stations [41, 44, 50, 52] for determining the actual partner. A contending relay typically transmits an additional frame for informing the source and destination stations about its identity, its willingness to cooperate and its network characteristics. Some protocols also introduce busy tones [41, 44], that are transmitted by contending relays for reserving a time window where they send the additional identifying frame. Busy tones are typically very short, and are detected by stations located farther away, since decoding a busy tone is simply achieved by noting that there is power on the channel, while decoding a frame requires understanding the bit sequence that it contains and hence is only supported by higher channel qualities [41].

A different set of cooperative protocols assumes that the adopted partner is decided by the source station before initiating the frame exchange procedure [42, 43, 46]. In such scenario, the source station typically addresses the relay station using a modified RTS frame, and the relay station replies using an additional frame for confirming its willingness to cooperate.

One may note that when the relay is chosen by the source station, other stations do not need to pay attention to the frame exchange. By contrast, when contention between relays that successfully decoded the signal transmitted from the source is chosen as the strategy for selecting the partner, every station that may serve as a potential relay has to decode the source station's transmission. Hence, adopting a mechanism where the identity of the adopted relay station is decided at the source station may help reducing the energy usage in the network. However, such choice

comes with some drawbacks. Particularly, the source station may only decide to rely on a particular relay station based on information about past communications. Such information may be outdated, particularly in scenarios where channel qualities vary quickly. By contrast, schemes where relay stations contend to be the active partner typically rely on more accurate channel state information. This is because relays stations receive the RTS and CTS frames, and in some cases even the DATA frame transmitted by the source station, before they are asked to contend for advertising their willingness to cooperate. Hence, potential relay stations may obtain information of their current channel state towards both the source and destination stations from these frames, and ultimately make a more informed guess at their ability to serve as a good relay for the upcoming transmission sequence.

2.3.2 Review of cooperative medium access protocols proposed for wireless networks

This section reviews some of the most popular cooperative MAC schemes presented in the literature. Between these schemes, the CoopMAC protocol is of particular interest, since it will be used as a base for designing cross-layer cooperative MAC schemes in the following of these works.

2.3.2.1 The CoopMAC protocol

CoopMAC [42, 45] is a proactive cooperative MAC protocol, in which high data rate stations assist low data rate nodes in their transmissions by forwarding their traffic. CoopMAC provides both a higher throughput and a lower interference level in a wireless network than the IEEE 802.11 DCF scheme.

For enabling cooperation between 802.11 stations, the CoopMAC protocol modifies the access scheme. Particularly, when a source node has a new packet ready to send, it decides if cooperation is needed and which will be the helping relay. If cooperation is invoked and a relay is available, a modified RTS message is used by the source node to inform the chosen helper. Besides the standard DCF control packets, CoopMAC introduces a new message, called Helper ready-To-Send (HTS), which is used by the selected relay to confirm its willingness to cooperate after it receives the RTS message from the source. If the destination hears the HTS, it sends a CTS message to reserve the channel for the source-relay and the relay-destination transmissions. When the source station receives both the HTS and the CTS, it transmits the packet to the relay, which will then forward it to the destination. If the source node does not receive an HTS, a direct transmission takes place. A normal ACK is used by the destination station to confirm a successful reception, regardless of whether the packet was forwarded by the relay or was directly transmitted by

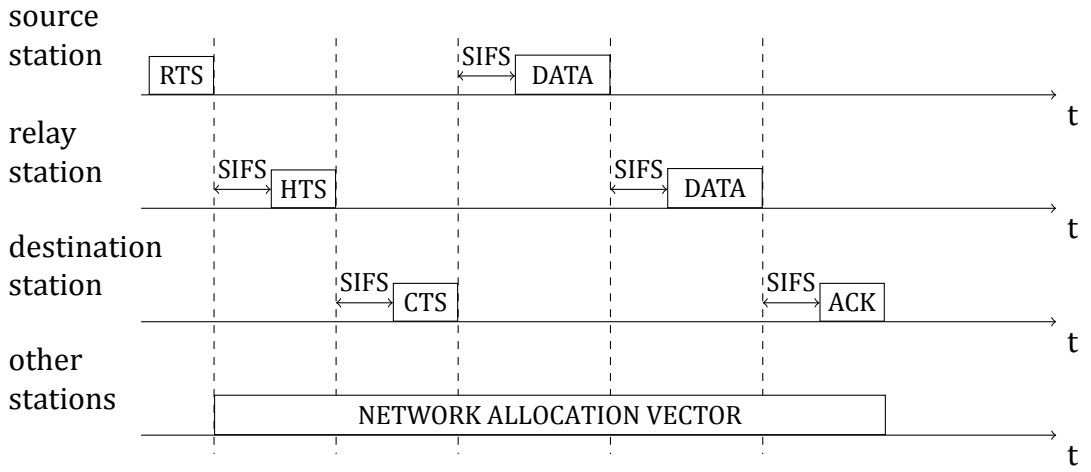

Figure 2.2: Frame exchange in a network based on the CoopMAC protocol.

the source station. Figure 2.2 shows the data exchange in a network based on the CoopMAC protocol.

A major part of the CoopMAC protocol consists in obtaining information about possible helpers. Each station maintains a table for every destination, called `CoopTable`, where all possible helpers are listed. This table can be populated by passively listening to all ongoing transmissions. Every entry of the table corresponds to a possible relay and contains its MAC address, the latest time at which a packet from the relay is received by the station and the potential data rate between the relay and the destination and between the station and the relay. This information can be obtained listening to an RTS/CTS exchange between the particular relay and the destination.

When a station wants to transmit a packet, it searches for possible helpers in its `CoopTable`. If more helpers are available the helper selection criterion invokes the relay that provides the most prompt transmission.

2.3.2.2 The rDCF protocol

The relay-enabled Distributed Coordination Function (rDCF) scheme [43] is another popular proactive MAC scheme, which adopts an approach that is very close to the one used in the CoopMAC protocol.

In rDCF every station passively listens to RTS/CTS exchanges between other stations. By extracting the transmission rate from a CTS packet a station may know the channel condition between the sender and the receiver. The station may also measure the channel conditions between itself and both the CTS source, let it be node ``$A$'' and the CTS destination, let it be node ``B''. If the station finds out that a faster transmission would have been possible by invoking cooperation and propos-

ing itself as a partner, it adds the association $A \rightarrow B$ into its willing list. Periodically every station transmits its willing list to its neighbours. When a station receives a willing list, it searches for associations where it is listed as a frame source. If at least one association is found, then the station from which the willing list originates is inserted into a relay table.

When a node ``$A$'' has a packet ready to be transmitted to a destination ``B'', it first searches in its relay table an $A \rightarrow B$ row. If such row is not found the transmission continues using the legacy IEEE 802.11 DCF. Otherwise, A chooses the relay node ``r'' that corresponds to the match in the relay table and starts a cooperative transmission. More explicitly A sends a new frame, called Relay Ready-To-Send (RRTS1) to the relay. The relay replies with another RRTS2, directed to A. The destination node B overhears the both the RRTS1 and RRTS2 frames, obtaining information about the possible data rates between A and r, A and B and r and B. If the multi-hop transmission via the relay is faster, B sends a Relay Clear-To-Send (RCTS), which tells A to transmit the DATA frame to r, who will forward it. Otherwise B sends a standard CTS packet and a direct transmission from A to B takes place. Further enhancements are provided in rDCF concerning multi-rate use and rate calculation for the sake of attaining a better performance in particular scenarios [43].

2.3.2.3 OC-MAC, an opportunistic MAC protocol

The Opportunistic Cooperative MAC (OC-MAC) protocol proposed in [46] provides relay-aided transmissions with automatic relay selection. OC-MAC also allows to determine if cooperation should be used or not, basing this decision on a throughput maximisation criterion. In OC-MAC a novel idea of throughput is used, which takes into account the probability of successful reception at the receiver and not only the data rates available on the direct and on the relay-aided channels. A more detailed analysis on the throughput definition and maximisation in OC-MAC will be given in the next paragraphs.

The relay selection in OC-MAC is done by the source station. Each station in the network keeps a table listing all the possible relays it could use. The rows of this table contain the MAC addresses of the relays, the channel gains between the node and each relay, and the last time a packet is received from every relay. When a source station ``$A$'' has to transmit data to a node ``B'', it firstly checks if a relay is available in its relay table. If there are many, the best relay is chosen (i.e. the one which has the maximum channel gain). Then the station checks if the channel is idle and after completing its backoff it transmits a modified RTS frame that contains the MAC address of the chosen relay. The relay addressed by the modified RTS decides whether he wants to cooperate or not. In the first case, after waiting a SIFS time, it sends a Relay Confirmation (RC) frame to A. The destination node receives both the

RTS and the RC frames, and decides if the relay should be used, as further detailed in the following. When a relay aided transmission is invoked, B sends a CTS frame specifying that the station listed in the modified RTS should be used for relaying data, otherwise a standard CTS with no confirmation is sent to A, which begins a direct communication.

In OC-MAC the decision on whether to cooperate or not is made by the destination and is based on a throughput maximisation criterion. This is achieved not only using the fastest channel among all the possible relays, but also taking into account the probability of a successful reception at the receiver. More explicitly, the throughput for the direct link is defined as:

$$\mathcal{S}_{\text{dir}} = \frac{p_S}{T^{\text{dir}}},$$

where T^{dir} is the communication duration using the direct link and p_S represents the probability of having a successful direct transmission. By contrast, when a cooperative communication is invoked, the throughput is defined as:

$$\mathcal{S}_{\text{coop}} = \frac{p_S}{T^{\text{dir}}} + \frac{(1-p_S)p_S^r}{T_{,}^r},$$

where T^{dir} is again the transmission duration when the direct transmission is successful, $T_{,}^r$ is the transmission duration using the relay aided multi-hop link and p_S^r is the probability of having a successful cooperative communication. The destination node invokes cooperation sending a modified CTS only if $\mathcal{S}_{\text{coop}} > \mathcal{S}_{\text{dir}}$.

2.3.2.4 A reactive medium access control protocol proposed by Li Yi and Ji Hong

A reactive MAC protocol is proposed by Yi and Hong in [50]. This protocol further improves both the Cooperative communication MAC (CMAC) [48] protocol and the Node Cooperative Stop and Wait (NCSW) [49] Automatic Repeat and reQuest (ARQ) protocol.

In the scheme proposed by Yi and Hong each neighbour of both the source node and the destination node can help relaying the message. The basic algorithm develops as follows. At first, the source station tries to transmit its data to the destination. If the direct communication fails, the relay accesses the channel and retransmits the information. In order to select the actual relay, potential partners undergo through a contention phase. The contention mechanism is priority driven, where relays having higher channel conditions are given a higher change of being selected as the actual partner.

Finally, the scheme improves previous solutions by introducing both frame numbering and traffic categories:

- frame numbering is used to distinguish between original frames and relay retransmitted frames. In this way multiple-cooperation is avoided (multiple-cooperation consists in retransmitting already relayed packets) as only source originated data could be forwarded.
- traffic categories are introduced in order to prioritize transmissions of own data or retransmissions of other stations' data.

2.3.2.5 A distributed Cooperative MAC protocol by Shan *et al.*

In [41] Shan *et al.* proposed a new MAC protocol for multi-hop wireless networks. The protocol is based on a proactive approach, however a reactive one can be integrated when retransmissions are considered. Shan *et al.* address questions as *when to cooperate*, *whom to cooperate with* and provide an automatic relay selection rule which gives higher priority to the best relays.

The protocol adopts an helper selection method where each possible relay monitors the instantaneous channel conditions towards the source and the destination using as information RTS and CTS frames. Multiple rates are allowed, hence the helpers can provide a higher transmission rate than the one available on the source-destination link. A source initiates its transmission by sending a RTS frame, which is acknowledged by the destination with a CTS. Each of the common neighbours of the source and the destination stations hears both the RTS and the CTS frames and finds out the potential maximum cooperative data rate. Every neighbour who is able to provide a better rate than the one available on the direct link contends to be the helper as follows.

Firstly, the potential helper sends a Helper Indication (HI), which is similar to a busy tone and its purpose is to inform the source and the destination of the relay's willingness to cooperate. If there is no HI the source starts a direct transmission. After sending the HI each potential relay transmits a Ready-To-Help (RTH) frame after a backoff time that prioritises stations with higher maximum cooperative data rates. After receiving the RTH, the destination sends a Clear-To-Receive (CTR) frame to notify all helpers to stop contention and to inform the source node to send data. When two relays collide trying to access the channel the destination does not send any CTR, and the helpers will resend their RTH frame in a random selected minislot from M minislots, where a minislot duration is equal to the symbol duration.

When a Negative ACK (NACK) frame is received from the destination, indicating that the previous exchange was unsuccessful, data has to be retransmitted. Usually the helper has better channel conditions than the source, hence a retransmission by the helper should be chosen. However, when the helper is quickly moving, it is possible that its channel condition has become worse, thus sometimes a source

retransmission could be the best solution. To deal with this situation, the helper and the source station contend to retransmit as follows. The helper increases its contention window by steps within [1, 2), while the source node doubles it. In order to avoid multiple-helpers retransmissions, only the prearranged helper (i.e. the one who won the contention to become the chosen relay) can retransmit data. A reactive approach could be introduced by letting the helper to cooperate only when a NACK is received, and not before.

Finally, the protocol provides a way to automatically decide whether to cooperate or not. The choice is based on channel conditions and on payload length, and adopts a time minimisation criterion, similarly to solutions proposed for the CoopMAC and rDCF protocols [42, 43].

2.3.2.6 Studies that consider an imperfect knowledge of the network parameters

As previously mentioned, many cooperative schemes rely on the assumption that some stations have a perfect knowledge of some network characteristics, with the most typical example being channel qualities of links composing the network. Such assumption is very limiting in a wireless scenario, where mobility and multipath influence the received signal, which shows a time varying behaviour.

Research studies hence considered scenarios where the knowledge of network parameters is not ideal, but night be corrupted. However, the majority of such studies idealises either the cooperative protocol description, or dispenses with including a detailed physical layer into their analysis, and particularly did not account for multiple data rates or signal combining at the destination.

A cooperative system using realistic imperfect CSI knowledge is considered in [55], though the paper does not include multiple rates for transmissions or consider benefits from channel coding techniques. The temporal characteristics of reactive relaying are identified in [56], which also discusses the impact of the overhead involved in setting up a cooperative link on the network performance. The drawback of [56] is that its analysis again supports only single rate transmissions and a simple Gilbert-Elliot [57] channel model is adopted. The work of [58] analyses the performance of a cooperative sensor network, with the drawback of again dispensing with adaptive modulation systems and with a detailed cooperative MAC protocol description.

One may hence observe that research on cooperative systems for the medium access control layer is limited on the protocol side by assuming an unrealistic knowledge on physical layer quantities, such as SNR values, and on the physical layer side by dispensing with considering higher layer techniques, such as adaptive solutions and combining at the destination.

3

MOTIVATIONS AND CONTRIBUTION

This chapter summarises the major limitations of works presented in the literature that address cooperative transmissions, limitations which motivate the research efforts behind this thesis. The chapter also summarises the actual contribution of this work and outlines the novel results that are presented in the following chapters.

3.1 RESEARCH GOALS

From the overview of cooperative systems presented in the previous chapters one may identify some areas of potential research which could improve the results obtained in the reviewed literature papers.

A first interesting topic would be analysing the performance of efficient coding techniques over cooperative links for a wide set of retransmission schemes and channel qualities. Particularly, literature works are mainly focused on obtaining asymptotic results by determining the channel capacity of a distributed wireless system. These works tough are not suited for benchmarking cooperative schemes that adopt multiple retransmission solutions, both because they assume a potentially infinite frame length and because calculations involved in determining the capacity of complex relaying systems are typically challenging.

Secondly, distributed channel coding techniques proposed in the literature typically target a particular network scenario, where the relay is located at a specific point between the source station and the destination station. Hence, the code layer used at the relay and the decoder adopted by the destination are typically optimised for the fixed network situation; if such systems were to be used in other network environments the design strategy would have to be modified, or at least run again for adapting to the new network characteristics.

Cooperative MAC layer protocols may also be further enhanced. Particularly, it seems interesting to study the performance of cooperative access solutions relying on advanced physical layer techniques, since literature works typically assume that

the access scheme sits on the top of an ideal physical layer. Furthermore, the physical layer should consider a joint decoding at the destination of the signals gleaned from the source station and the relay station for the sake of enabling real cooperation. Finally, studies that analyse the behaviour of cooperative access schemes under imperfect knowledge of the system state might be enhanced for including rate adaptation and an appropriate relay selection scheme, for the sake of closely matching the behaviour of existing cooperative MAC protocols.

As a final note, it could be also interesting to evaluate other solutions for increasing the network performance of WLANs, which may be complementary to cooperation, or even be amalgamated with it in order to contrive MAC schemes that are capable of providing a better user experience when a high throughput is required.

3.2 Main contributions of this thesis

This thesis work is motivated by the considerations presented in the previous section, and presents novel results that aim both at analysing the performance of the cooperative PHY and MAC layers techniques and at developing novel solutions capable of outperforming existing ones.

Particularly, this thesis starts with proposing an estimator for the performance of cooperative retransmission systems relying on efficient codes. The proposed estimator does not target the asymptotic performance, but rather it aims at being a benchmark for practical coding schemes, and hence it considers quantities such as the block length and the modulation mode for an arbitrary retransmission sequence.

Once having obtained a benchmarking tool for evaluating the performance of distributed coding techniques, the thesis addresses the design problem of finding practical schemes that are capable of approaching such limiting performance for a wide range of network scenarios. Particularly, the thesis proposes a design strategy that may be used for contriving codes with arbitrary rate that perform close to the bounding performance for a large set of channel qualities.

The PHY layer contributions mentioned in the previous paragraphs are then included into a cross-layer designed MAC scheme. Such scheme removes ideal assumptions of literature solutions on the PHY layer, and it shows that relying on advanced distributed coding techniques may be of benefit for the network performance when a cross-layer design strategy and optimisation is taken into account.

The thesis also addresses the problem of estimating the performance of a cooperative access scheme that relies on imperfect channel knowledge. Furthermore, novel schemes that are capable of mitigating the performance downgrade caused by relying on outdated and corrupted channel estimates are also presented.

Finally, the thesis considers the design of MAC protocols that allow achieving

a better network performance by equipping single nodes with multiple antenna radiating elements. The work shows that a throughput and delay increase may be achieved when nodes may benefit from beamforming capable antenna systems and hence may be able to reduce interference allowing multiple communications at the same time. Along this line, the work also proposes guidelines for designing practical systems that extend the IEEE 802.11 DCF access scheme for enabling multiple simultaneous transmissions.

Part II

Original results

4

Performance evaluation of cooperative coding schemes

This chapter presents an analytic method for assessing the performance of efficient cooperative channel coding schemes. The method is based on the sphere-packing bound, and does not rely on the choice of a particular encoding scheme. This chapter details the analytic model, and shows preliminary results of actual code simulations for verifying the analysis. Further discussions on the choice of efficient codes and on the influence of the code design on the performance will be shown in the following chapters.[1]

4.1 Introduction

From the literature overview presented in previous chapters, one may see that cooperation may be used for enhancing the decoding performance in wireless networks. Cooperation may be improved in faded scenarios by using a combination of ARQ and Forward Error Correction (FEC) techniques. Furthermore, an additional performance increase may be guaranteed by incremental redundancy and adaptive modulation systems [20, 59].

Despite the recent interest in cooperation, only few papers aimed at theoretically assessing the performance coded cooperation schemes. The analysis of references [60, 61, 62] is based on capacity considerations which do not consider adaptive or incremental redundancy systems. An evaluation of the Bit Error Rate (BER) performance of a decode-and-forward system is presented in [63] considering the mutual information of bits received from the source and the relay. The drawback of [63] is that the analysis relies on simulations of a particular code to relate the mu-

[1] The content of this chapter is based on F. Babich and A. Crismani, ``Cooperative coding schemes: design and performance evaluation'', IEEE Transactions on Wireless Communications, vol. 11, pp. 222–235, Jan. 2012.

tual information to the BER. This chapter presents a novel estimator for assessing the limiting performance of coded cooperation schemes in wireless scenarios. The analytic framework is based on the Sphere-Packing Bound (SPB) [64] and allows one to estimate the limiting performance of cooperative incremental redundancy systems over a fading channel. The approach is not limited to a specific code structure, instead it relies on some general characteristics of the transmission, such as the block-length, the modulation mode and the coding rate.

The chapter considers a general cooperative scenario, that involves transmitting with different modulation modes at the source and relay stations and accounts for multiple retransmissions, as proposed for Hybrid ARQ (HARQ) systems. The chapter shows that the limiting performance is closely approached by the actual performance obtained by simulations, provided that efficient coding schemes are used both at the source and at the relay stations. Hence, the theoretical analysis may be seen as a benchmark for the adopted channel code.

4.2 The sphere-packing bound

The SPB is an analytic method that allows assessing the limiting performance of an encoding technique over a communication channel, for a finite length of the encoded bit sequence. More particularly, the SPB relies on general characteristics of the transmission scheme, such as the coding rate, the modulation mode adopted, the length of the encoded sequence and the channel quality, rather than focusing on a particular channel encoding technique, for determining the probability that the received sequence contains corrupted information [65].

Such a general approach has the advantage of dispensing with ad-hoc and time consuming simulations of specific encoding schemes for obtaining their BLock Error Ratio (BLER) performance. The SPB analysis is briefly reviewed in the following of the section.

Consider a digital transmission system, where a sequence of U information bits is encoded into a sequence of B encoded bits using a channel encoder having a rate of $R_c = U/B$. These encoded bits are modulated into λ complex symbols using a linear modulation mode $\mathcal{M}$ and are then transmitted over the communication channel. Consider the case of an AWGN channel characterised by a SNR value of γ. The SPB formulates a relation between the coding rate R_c, the SNR γ, the modulation mode $\mathcal{M}$, the length of the symbol sequence λ and the block error ratio P_B. The SPB relation may be expressed as [66]:

$$P_B > 2^{-\lambda\left[E_{\mathrm{sp}}(R_c)+o(\lambda)\right]}, \tag{4.1}$$

where the sphere-packing exponent E_{sp} is [67] is obtained as:

$$E_{\text{sp}}(R_c) = \max_{\rho \geq 0} \left[E_0(\rho) - R_c^{\rho} \right], \tag{4.2}$$

with ρ being an optimisation parameter and the value $E_0(\rho)$ calculated for a D dimensional modulation mode consisting of M input symbols $\mathbf{s}_m$ by a D-fold integration as follows:

$$E_0(\rho) = -\log_2 \int_{-\infty}^{\infty} \dots \int_{-\infty}^{\infty} \left[\sum_{i=1}^{M} p_i \left(f(\mathbf{y}|\mathbf{s}_m) \right)^{\frac{1}{1+\rho}} \right]^{1+\rho} \mathrm{d}\mathbf{y}, \tag{4.3}$$

where p_m is the probability of the m-th symbol, and, for an AWGN channel, the probability that the received signal is $\mathbf{y}$ given that s_m was transmitted is:

$$f(\mathbf{y}|\mathbf{s_i}) = \prod_{j=1}^{D} \frac{1}{\sqrt{\pi N_0}} e^{-\frac{\left(y_j - s_{ij}\right)^2}{N_0}}. \tag{4.4}$$

An upper bound to the error probability is given by:

$$P_B < 2^{-\lambda E(R_c)}, \tag{4.5}$$

where

$$E(R_c) = \max_{0 \leq \rho \leq 1} \left[E_0(\rho) - R_c^{\rho} \right]. \tag{4.6}$$

One can observe that, as long as the optimising value of ρ is between 0 and 1, the two bounds are asymptotically equivalents. In the following of this chapter, for an improved clarity of exposition, the value of (4.1), when neglecting the effect of the term $o(\lambda)$, and of (4.5) will be denoted as:

$$P_B = P_B(\gamma, R_c, \mathcal{M}, \lambda). \tag{4.7}$$

One may note that any of the parameters contained in (4.7) may be calculated once a value is assigned to the others. In particular, Equation (4.7) allows one to analytically determine the BLER versus SNR curve $P_B = P_B(\gamma)$ for a fixed coding rate-modulation pair and length of the symbol sequence. This analytic curve is a steep function, as shown in Figure 4.1. A similar steep shaped curve is characteristic of efficient channel encoding techniques, such as turbo codes [7] and LDPC codes [68, 69], that are capable of performing within 1 dB from the curve obtained using the SPB. Hence, one can assess the system performance by approximating the BLER curve of efficient coding techniques for different values of SNR using a step function [65]. More explicitly, one can define a success threshold γ_t, that represents the SNR value that guarantees achieving a target BLER performance. The success

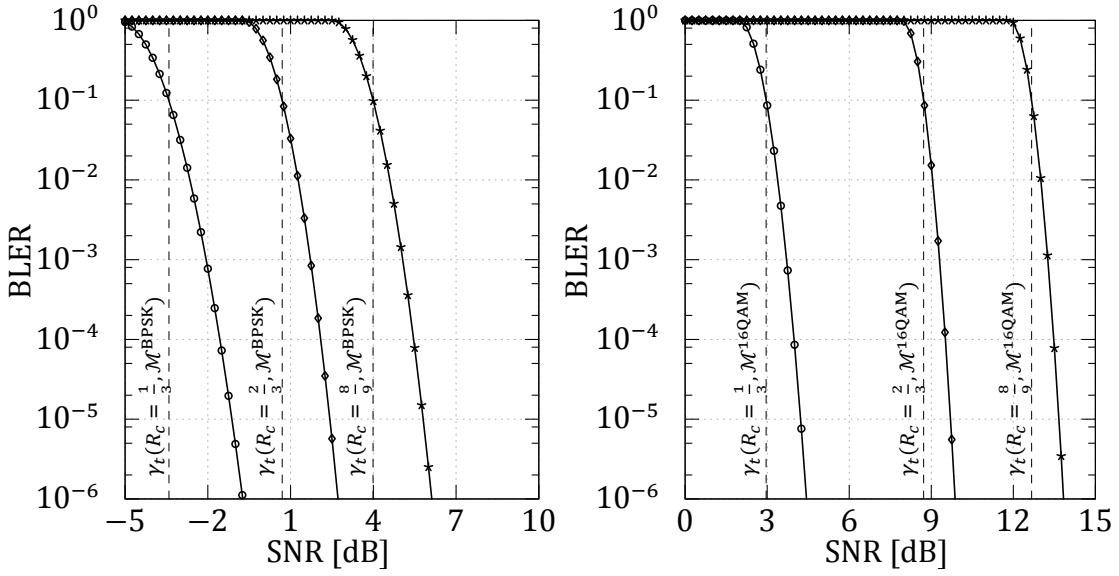

(a) BPSK (b) 16QAM

Figure 4.1: Block error ratio versus SNR curve as obtained using the SPB for the BPSK and 16QAM modulation modes and codes having rates of $R_c = \frac{1}{3}$ ($\circ$), $R_c = \frac{2}{3}$ and ($\diamond$) $R_c = \frac{8}{9}$ ($\star$)

threshold may be used for determining whether a transmission is successful or not. Particularly, a transmission is considered successful if the SNR satisfies the inequality $\gamma > \gamma_t$, while it is considered unsuccessful otherwise. The threshold γ_t may be evaluated using the SPB and is calculated as the SNR yielding:

$$P_B(\gamma_t) = 10^{-1}, \tag{4.8}$$

as proposed in [70].

Another system parameter may be determined by considering a given SNR instead of a given code rate. Particularly, consider a transmission at a fixed SNR value of γ, using a modulation mode $\mathcal{M}$ and transmitting a number of symbols equal to λ. The relation of Equation (4.7) allows obtaining the maximum code rate that guarantees a target BLER. This code rate is referred to as the equivalent rate of the system, and will be used in the following sections for assessing the performance of cooperative scenarios.

4.3 The performance of cooperative coding schemes

The previous section briefly summarised the sphere-packing bound theory, showing that the performance of a coding scheme over an AWGN channel having a channel quality that does not vary over time may be obtained using an analytic expression. However, a cooperative scenario involves multiple communications over channels having different qualities that may vary because of fading.

Particularly, a cooperative communication consists of a sequence of many single transmission attempts, carried out either by the source station or by the chosen relay, that ends when the destination successfully recovers the transmitted information or the maximum number of attempts is reached. The transmission attempts occur at different times, and hence they may experience different channel conditions. Finally, the different attempts may or may not contain the same coded bits, and in the more general case a coded bit may be transmitted only in a single attempt, in a subset of all the transmission attempts, in every attempt, or may not even be transmitted at all.

Given the significant difference between the single transmissions composing a cooperative communication, the simple relation between the block error ratio and the channel code characteristic of (4.7), which assumes having a single encoded sequence where every bit is transmitted once and experiences the same channel quality as other bits, may not be used in a straightforward fashion for determining the performance of a cooperative scheme, whose evaluation requires a more general approach.

The following subsections present a general framework, that is again based on the SPB, for evaluating whether a cooperative communication is successfully received at the destination. The analysis is divided into two parts. Firstly, the SPB theory is extended to account for a repetition cooperative scenario, where the destination receives two versions of the same encoded sequence, being one version gleaned from the source station and the other from the relay. Secondly, the analysis is extended to account for cooperative schemes composed of many attempts and relying on incremental encoding techniques, where different bits are transmitted in each attempt.

4.3.1 Repetition cooperative schemes

Consider a repetition decode-and-forward cooperative scheme, where the destination station receives two copies of the same B bits encoded with a rate R_c. The two copies are transmitted by the source station and by the relay, using possibly different modulation schemes $\mathcal{M}_{SD}$ and $\mathcal{M}_{RD}$ and hence obtaining sequences con-

taining λ_{SD} and λ_{RD} symbols, respectively. Furthermore, note that the qualities of the two copies may be significantly different, given that they are received from different sources, and that in a typical cooperative scenario the quality of the relay-destination link is higher than the one of the source-destination link, otherwise cooperation would not be helpful. Particularly, denote the instantaneous SNR values on the source-destination, source-relay and relay-destination links by γ_{SD}, γ_{SR} and γ_{RD}, respectively.

The reader may recall that the purpose of this section is to assess the performance of a cooperative scheme. Hence it is assumed that the relay can successfully decode the signal transmitted by the source station, i.e. the value γ_{SR} is chosen to support an error-free decoding. A more detailed HARQ system, where the relay station might not be able to decode the signal broadcasted by the source station, is thoroughly analysed in Section 4.3.4. Furthermore, the modulation modes $\mathcal{M}_{SD}$ and $\mathcal{M}_{RD}$ are chosen independently by the source station and by the relay, and this section dispenses with an in-depth analysis of the adaptive modulation scheme. A simple adaptive scheme that maximises the throughput of a cooperative communication scheme is presented and analysed in Section 4.3.3. A more detailed discussion on adaptive schemes for cooperative communications may be found in Chapters 6 and 7, which analyse the adaptive scheme from a MAC layer perspective and account for the relay selection algorithm and for the case where the channel information may be corrupted or outdated.

The performance of the repetition scheme may be defined in terms of the success thresholds of the source-destination and relay-destination links. Particularly, one may note that the single transmission on the source-destination link sees a channel quality that does not vary over time. Hence, one can use the SPB for determining the SNR value that guarantees the target BLER performance of 10^{-1}. Such SNR value is referred to as the success threshold $\gamma_{t_{SD}}$ for the selected coding rate-modulation mode pair on the source-destination link. That is, the success threshold $\gamma_{t_{SD}}$ is the SNR value obtained using the SPB that satisfies:

$$10^{-1} = P_B(\gamma_{t_{SD}}, R_c, \mathcal{M}_{SD}, \lambda_{SD}). \tag{4.9}$$

Similarly, considering the relay-destination link where the transmission is carried out over a channel of constant quality γ_{RD}, one can define the success threshold $\gamma_{t_{RD}}$ for the selected coding rate-modulation mode pair as the SNR that satisfies:

$$10^{-1} = P_B(\gamma_{t_{RD}}, R_c, \mathcal{M}_{RD}, \lambda_{RD}). \tag{4.10}$$

The two success thresholds may be combined for determining whether the whole cooperative communication may be correctly decoded at the destination station.

Assume at first that the same modulation is used for both the copies transmitted by the source and the relay stations. In such a scenario, the success thresholds for the source-destination transmission and for the relay-destination transmission are the same, i.e. $\gamma_{t_{SD}} = \gamma_{t_{RD}} = \gamma_t$, given that the two transmissions are characterised by the same coding rate, encoded bits, modulation mode, and target BLER of 10^{-1}.

When the same modulation mode is used for the copies, the cooperative communication may be seen as a single transmission using the same coding rate and modulation mode of the two cooperative attempts that takes place over a channel characterised by an SNR value of $\gamma_{SD} + \gamma_{RD}$. Hence, one can compare the SNR value of the equivalent system with the success threshold γ_t that characterises the decoding behaviour of such a transmission scheme, and the combined transmission is considered successful if the value of $\gamma_{SD} + \gamma_{RD}$ satisfies the inequality:

$$\gamma_{SD} + \gamma_{RD} > \gamma_t. \tag{4.11}$$

By recalling that γ_t represents the success threshold of both links, the above inequality may be also seen as a linear interpolation between the success thresholds of the two links. More explicitly, (4.11) may be rewritten as:

$$\gamma_{RD} > \gamma_t - \gamma_{SD} = \gamma_t \left(1 - \frac{\gamma_{SD}}{\gamma_t}\right). \tag{4.12}$$

The above linear expression may be extended to approximate the success performance of a combined transmission in a decode-and-forward scheme where the source and relay stations use different modulation modes. In particular, a combined transmission is assumed to be error-free if the following condition is met:

$$\gamma_{RD} > \gamma_{t_{RD}} \left(1 - \frac{\gamma_{SD}}{\gamma_{t_{SD}}}\right). \tag{4.13}$$

One can observe that the condition expressed by Equation (4.13) reduces to (4.11) if the same modulation modes are used on the source-destination and relay-destination links. Hence, in such situation, the bound of (4.13) is exact. Conversely, when different modulation modes are used, the inequality of (4.13) is an approximated expression for the limiting performance.

Such approximation is justified in the following paragraphs both by providing simulated results that confirm its accuracy and by comparing it with the Information Outage Criterion (IOC) proposed by Valenti in [71].

The information outage criterion is an analytic technique proposed by Valenti in [71] for determining whether a single transmission is successfully decoded or not. More particularly, the mutual information criterion considers a single transmission to be successful if the mutual information between the B received Log-Likelihood Ratio (LLR) values and the corresponding transmitted bits is higher that

the coding rate of that transmission. The mutual information $I(x;\tilde{x})$ between an LLR $\tilde{x}$ and its corresponding bit x, where x takes the values $+1, -1$ with the same probability of 0.5, is defined as:

$$I(x;\tilde{x}) = \frac{1}{2}\sum_{x=-1,1}\int_{\infty}^{\infty} f_{\tilde{x}}(\tilde{x}|x)\log_2\frac{2f_{\tilde{x}}(\tilde{x}|x)}{f_{\tilde{x}}(\tilde{x}|+1)+f_{\tilde{x}}(\tilde{x}|-1)}d\tilde{x}, \tag{4.14}$$

where $f_{\tilde{x}}$ is the probability that the real valued LLR is $\tilde{x}$ given that the bit x was transmitted. It can be shown that, if $f_{\tilde{x}}$ is a Gaussian distributed random variable having mean of $\sqrt{\frac{\sigma_{\tilde{x}}^2}{4}}$ and variance $\sigma_{\tilde{x}}^2$, the mutual information may be rewritten as:

$$I(x;\tilde{x}) = J(\sigma_{\tilde{x}}), \tag{4.15}$$

where the function J is a monotonic crescent function and is defined as:

$$J(\sigma) = 1 - \int_{\infty}^{\infty}\frac{e^{\left[-\frac{\left(\tilde{x}-\frac{\sigma}{2}\right)^2}{2\sigma^2}\right]}}{\sqrt{2\pi\sigma^2}}\log_2[1+e^{-\tilde{x}}]\mathrm{d}\tilde{x} \tag{4.16}$$

It can be shown that applying the mutual information criterion to a cooperative communication yields a linear formulation for the success threshold that parallels the SPB predicted threshold of Equation (4.13).

Particularly, consider at first a non-cooperative scenario using the BPSK mode for transmitting information. The received signal may be expressed as:

$$\mathbf{y} = \mathbf{x} + \mathbf{n}, \tag{4.17}$$

where $\mathbf{n}$ is the noise vector, whose elements n_i are distributed according to $n_i \sim \mathcal{N}(0, \frac{N_0}{2})$ and $N_0 = \frac{1}{\gamma_{SD}}$.

The LLRs that are produced by the soft demapper for the sequence of received BPSK encoded symbols $\mathbf{y}$ are:

$$\tilde{\mathbf{x}} = \frac{4}{N_0}\mathbf{y} = \frac{4}{N_0}(\mathbf{x}+\mathbf{n}) \tag{4.18}$$

One can note from (4.18) that the LLRs are Gaussian distributed with variance $\sigma_L^2 = \frac{8}{N_0}$, as further detailed in [72], and hence the mutual information $I(\mathbf{x};\tilde{\mathbf{x}})$ between the LLRs and the transmitted bits depends only on the noise power density N_0 and may be obtained as:

$$I(\mathbf{x};\tilde{\mathbf{x}}) = J\left(\sqrt{\sigma_L^2}\right) = J\left(\sqrt{\frac{8}{N_0}}\right) = J\left(\sqrt{8\gamma_{SD}}\right), \tag{4.19}$$

as shown previously.

The information outage criterion of [71] considers the non-cooperative transmission to be successful if:

$$R_c < I(\mathbf{x}; \tilde{\mathbf{x}}) = J(\sqrt{8\gamma_{SD}}). \tag{4.20}$$

The system's limiting performance may be then obtained by substituting the inequality with an equal operator, and the minimum SNR supporting an error free decoding is found to be $\gamma_{SD} = \frac{1}{8}[J^{-1}(R_c)]^2$. Note that the previous analysis's only assumption is that the LLRs $\tilde{\mathbf{x}}$ are Gaussian distributed.

Consider now the repetition cooperative system under study. Denote the LLRs pertaining to the bits received by the destination from the source station with $\tilde{\mathbf{x}}_{\mathrm{SD}}$ and, similarly, denote the LLRs pertaining to the bits received from the relay with $\tilde{\mathbf{x}}_{\mathrm{RD}}$. Considering again a BPSK modulated system, the LLR sequences $\tilde{\mathbf{x}}_{\mathrm{SD}}$ and $\tilde{\mathbf{x}}_{\mathrm{RD}}$ are Gaussian distributed, similarly to the non-cooperative scenario. Particularly, let the variance of the LLR sequence pertaining to bits received from the source station be $\sigma^2_{\tilde{\mathbf{x}}_{\mathrm{SD}}}$ and the variance of the LLR sequence pertaining to bits received from the relay be $\sigma^2_{\tilde{\mathbf{x}}_{\mathrm{RD}}}$. The MRC decoder operates using the sum of the LLRs pertaining to each encoded bit. Hence, the information outage criterion considers a decoded sequence to be error free if

$$R_c < I(\mathbf{x}; \tilde{\mathbf{x}}_{\mathrm{SD}} + \tilde{\mathbf{x}}_{\mathrm{RD}}). \tag{4.21}$$

It was shown in [73] that, for the case where $\tilde{\mathbf{x}}_{\mathrm{SD}}$ and $\tilde{\mathbf{x}}_{\mathrm{RD}}$ are Gaussian distributed, the mutual information $I(\mathbf{x}; \tilde{\mathbf{x}}_{\mathrm{SD}} + \tilde{\mathbf{x}}_{\mathrm{RD}})$ may be expressed as:

$$I(\mathbf{x}; \tilde{\mathbf{x}}_{\mathrm{SD}} + \tilde{\mathbf{x}}_{\mathrm{RD}}) = J\left(\sqrt{[J^{-1}(I(\mathbf{x}; \tilde{\mathbf{x}}_{\mathrm{SD}}))]^2 + [J^{-1}(I(\mathbf{x}; \tilde{\mathbf{x}}_{\mathrm{RD}}))]^2}\right). \tag{4.22}$$

Recalling that $I(\mathbf{x}; \tilde{\mathbf{x}}_{\mathrm{SD}}) = J\left(\sqrt{\sigma^2_{\tilde{\mathbf{x}}_{\mathrm{SD}}}}\right)$ and $I(\mathbf{x}; \tilde{\mathbf{x}}_{\mathrm{RD}}) = J\left(\sqrt{\sigma^2_{\tilde{\mathbf{x}}_{\mathrm{RD}}}}\right)$, Equation (4.22) can be rewritten as:

$$\begin{aligned} I(\mathbf{x}; \tilde{\mathbf{x}}_{\mathrm{SD}} + \tilde{\mathbf{x}}_{\mathrm{RD}}) &= J\left(\sqrt{\left[J^{-1}\left(J\left(\sqrt{\sigma^2_{\tilde{\mathbf{x}}_{\mathrm{SD}}}}\right)\right)\right]^2 + \left[J^{-1}\left(J\left(\sqrt{\sigma^2_{\tilde{\mathbf{x}}_{\mathrm{RD}}}}\right)\right)\right]^2}\right) \\ &= J\left(\sqrt{\left(\sqrt{\sigma^2_{\tilde{\mathbf{x}}_{\mathrm{SD}}}}\right)^2 + \left(\sqrt{\sigma^2_{\tilde{\mathbf{x}}_{\mathrm{RD}}}}\right)^2}\right) \\ &= J\left(\sqrt{\sigma^2_{\tilde{\mathbf{x}}_{\mathrm{SD}}} + \sigma^2_{\tilde{\mathbf{x}}_{\mathrm{RD}}}}\right). \end{aligned} \tag{4.23}$$

Hence, the information outage criterion bound formulates a linear relation between the quantities $\sigma^2_{\tilde{\mathbf{x}}_{\mathrm{SD}}}$ and $\sigma^2_{\tilde{\mathbf{x}}_{\mathrm{RD}}}$, provided that Gaussian distributed LLRs are fed to the decoder. It is known that using a BPSK or a QPSK modulation mode provides Gaussian distributed LLRs, while the LLRs of bits received using higher order QAM modulation modes are not Gaussian distributed [74]. Nonetheless, a Gaussian distribution has been used for approximating the probability density function of LLRs of higher order QAM modulation modes in order to analyse the performance of bit-interleaved coded systems [75]. The Gaussian approximation of [75] motivates the use of Equation (4.13) as an approximation of the bound for higher order QAM modulation sets.

Figure 4.2 compares the bound calculated using the SPB and the proposed linear interpolation with the bound based on the information outage criterion. Particularly, Figure 4.2 plots the SNR γ_{RD} required on the relay-destination link for achieving the target BLER at the destination for a given value of SNR γ_{SD} on the source-destination link. $B = \frac{U}{R_c} = 10^5$ bits are transmitted by the source station and then forwarded by the relay, and the bounds are plotted for different modulation mode couples and coding rates.

It can be seen that the cooperative bound based on the SPB and on the linear approximation is very close to the information outage criterion for the BPSK-QPSK modulation couple, when LLRs are Gaussian distributed. A good degree of agreement is also found using modulation mode couples that do not have Gaussian distributed LLRs. Finally, it has to be noted that the information outage criterion assumes an infinite block length, while the proposed SPB based bound correctly accounts for a finite length encoding.

For further verifying the accuracy of the SPB based estimator, Figure 4.3 compares the limiting value of γ_{RD} for a given SNR γ_{SD} obtained using Equation (4.13) with the actual performance of a systematic turbo code for a system adopting a code rate of $R_c = \frac{8}{9}$. It can be seen that the SPB accurately predicts the actual performance of the coded system, both in the case where the same modulation mode is used on the source-destination and on the relay-destination links and in the case where the modulation modes on the two links are different.

Finally, consider now a scenario where the channel qualities γ_{SD} and γ_{RD} on the source-destination and relay-destination links are fixed. Assume also that the modulation modes $\mathcal{M}_{SD}$ and $\mathcal{M}_{RD}$ and that the number of encoded bits B are given. In such case, the success thresholds $\gamma_{t_{SD}}$ and $\gamma_{t_{RD}}$ only depend on the code rate used by the source and by the relay stations for generating the encoded bit sequence. Hence, similarly to the non cooperative case, one can determine the maximum code rate that guarantees a target BLER at the destination by substituting the inequality in Equation (4.13) with an equal operator. The coding rate r_{eq} that yields success

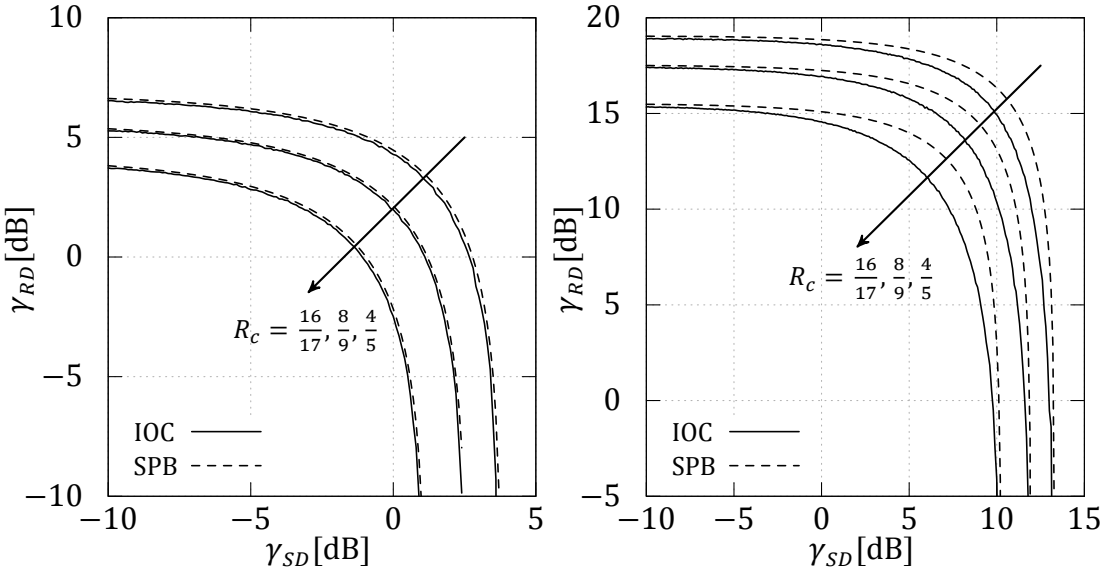

(a) BPSK-QPSK (b) 16QAM-64QAM

Figure 4.2: Comparison between the information outage criterion of [71] and the limiting performance obtained using Equation (4.13).

thresholds $\gamma_{t_{SD}}$ and $\gamma_{t_{RD}}$ that satisfy:

$$\gamma_{RD} = \gamma_{t_{RD}} \left(1 - \frac{\gamma_{SD}}{\gamma_{t_{SD}}} \right). \tag{4.24}$$

is defined as the equivalent rate of the repetition cooperative system.

4.3.2 Incremental cooperative scheme

The previous section shown that the SPB theory may be used for obtaining an estimator of the limiting performance of a cooperative coded system where the relay decodes and forwards the same bit sequence transmitted by the source station, albeit possibly using a different modulation mode.

This section extends the analysis to the general case where the source station and the relay station may transmit multiple times and each transmission may contain a different set of encoded bits. Particularly, this section considers an HARQ system [76, 77], where a transmission sequence consists of multiple attempts, that may be carried out either by the source station or by the relay. Each of these attempts may contain a different set of encoded bits, where the set is obtained by applying a particular puncturing scheme to a mother code. Again, since the purpose

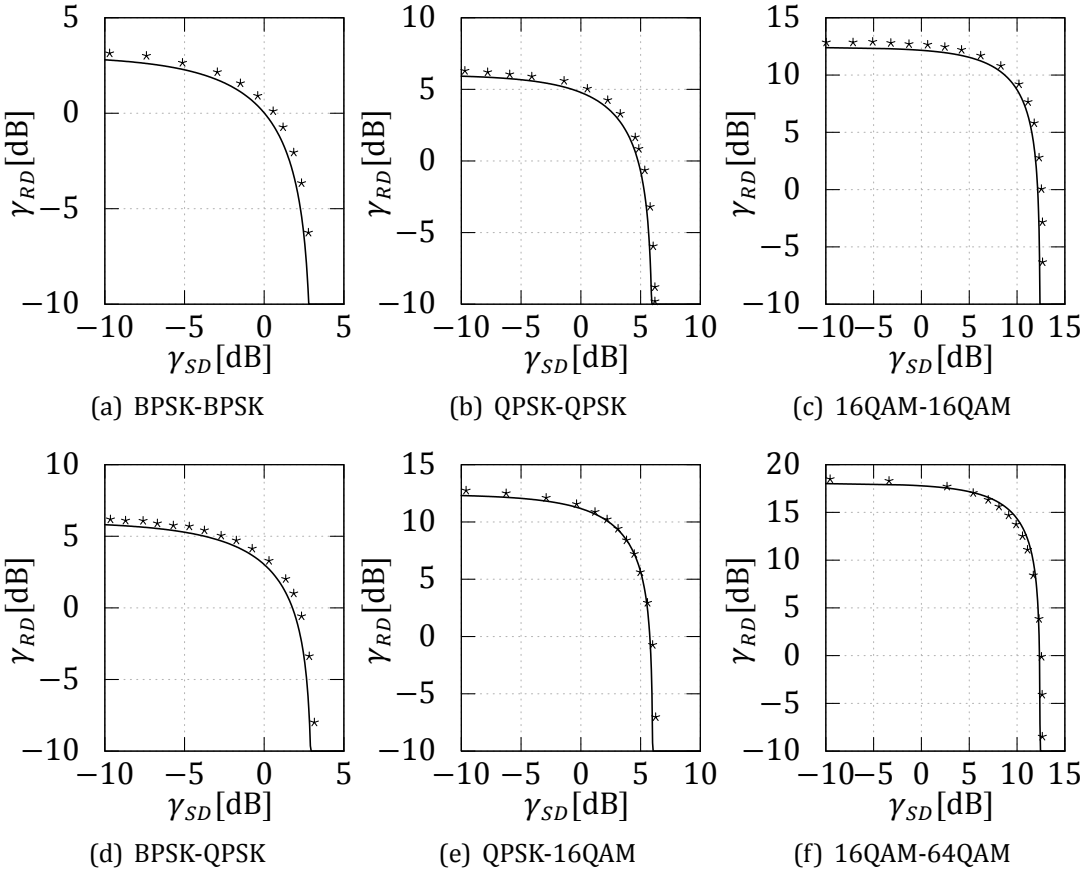

(a) BPSK-BPSK (b) QPSK-QPSK (c) 16QAM-16QAM

(d) BPSK-QPSK (e) QPSK-16QAM (f) 16QAM-64QAM

Figure 4.3: Comparison between the SPB limit (solid) and the actual simulated performance of a turbo coded system ($\star$) using different combinations of modulation modes for the source-destination and relay-destination links in a repetition cooperative scheme.

of the section is to evaluate the performance of a cooperative incremental transmission, it is assumed that the relay is able to perform an error-free decoding of the signal transmitted by the source station.

Consider the K-th step of an incremental forwarding scheme, consisting of I attempts transmitted by the source station and $J = K - I$ attempts transmitted by the relay. Denote the decoding rate obtained after receiving the joint transmission sequence composed by the K attempts by $R_{c_K}^{D}$.

The key idea for analysing the success of such step is to divide the L bits that have been transmitted within the first K attempts into groups containing bits that are received the same number of times and from the same paths. Particularly, Assume to divide the L bits transmitted within the first K attempts of the incremental process into N segments of respective lengths l_n ($1 \leq n \leq N, \sum_{n=1}^{N} l_n = L$). All the

bits contained in the n-th segment have been received a number i^* ($0 \leq i^* \leq I$) of times from the source station with the modulation mode $\mathcal{M}_{SD}$ and a number j^* ($0 \leq j^* \leq J$) of times by the relay station with the modulation mode $\mathcal{M}_{RD}$. The SNR of the i-th of the i^* attempts received from the source station is denoted by $\gamma_{SD}^{n,i}$ ($0 \leq i \leq i^*$). Similarly, the SNR of the j-th of the j^* attempts received from the relay is denoted by $\gamma_{RD}^{n,j}$ ($0 \leq j \leq j^*$).

Each of the N segments contributes to the success of the incremental scheme. Particularly, each segment may be characterised by two SNR values, namely γ_{SD}^{n} and γ_{RD}^{n}, that aggregate the qualities of the bits contained in the particular segment over the i^* different attempts transmitted on the source-destination link and over the j^* different attempts transmitted on the relay-destination link, respectively. These SNR quantities are obtained as:

$$\gamma_{SD}^{n} = \sum_{i=0}^{i^*} \gamma_{SD}^{n,i} \quad \text{and} \quad \gamma_{RD}^{n} = \sum_{j=0}^{j^*} \gamma_{RD}^{n,j}. \tag{4.25}$$

The two quantities γ_{SD}^{n} and γ_{RD}^{n}, together with the modulation modes $\mathcal{M}_{SD}$ and $\mathcal{M}_{RD}$, completely characterise the contribution of the n-th segment. Particularly, as shown in the previous section, γ_{SD}^{n} and γ_{RD}^{n} allow one to calculate the equivalent coding rate r_{eq}^{n} for the n-th segment. The equivalent rate r_{eq}^{n} represents the maximum coding rate that may be used by the source station and by the relay for the n-th segment.

The success of the whole incremental scheme may be determined by weighing the contribution of the single segments. In particular, one can obtain an estimate of the maximum code rate that the system supports by averaging the equivalent rate values of the single segments, after scaling such values according to the length of the segments. If the actual code rate is less than the maximum allowed rate, the incremental scheme is successful. Using a more formal notation, define as sustainable rate r_{sus} the maximum code rate for the whole transmission that provides an error-free decoding. The sustainable rate is obtained as the weighted average of the equivalent rates of the N segments:

$$r_{\text{sus}} = \sum_{n=1}^{N} w_n r_{\text{eq}}^{n}, \tag{4.26}$$

where $w_n = l_n/L$ is the weight factor for the n-th segment. Recalling that the used channel code has a rate equal to $R_{c_K}^{D}$, the transmission is successful if:

$$R_{c_K}^{D} < r_{\text{sus}}. \tag{4.27}$$

The analysis is validated by simulations in Figure 4.4, that shows the SNR required on the relay-destination link to achieve the target BLER of $P_B = 10^{-1}$ for

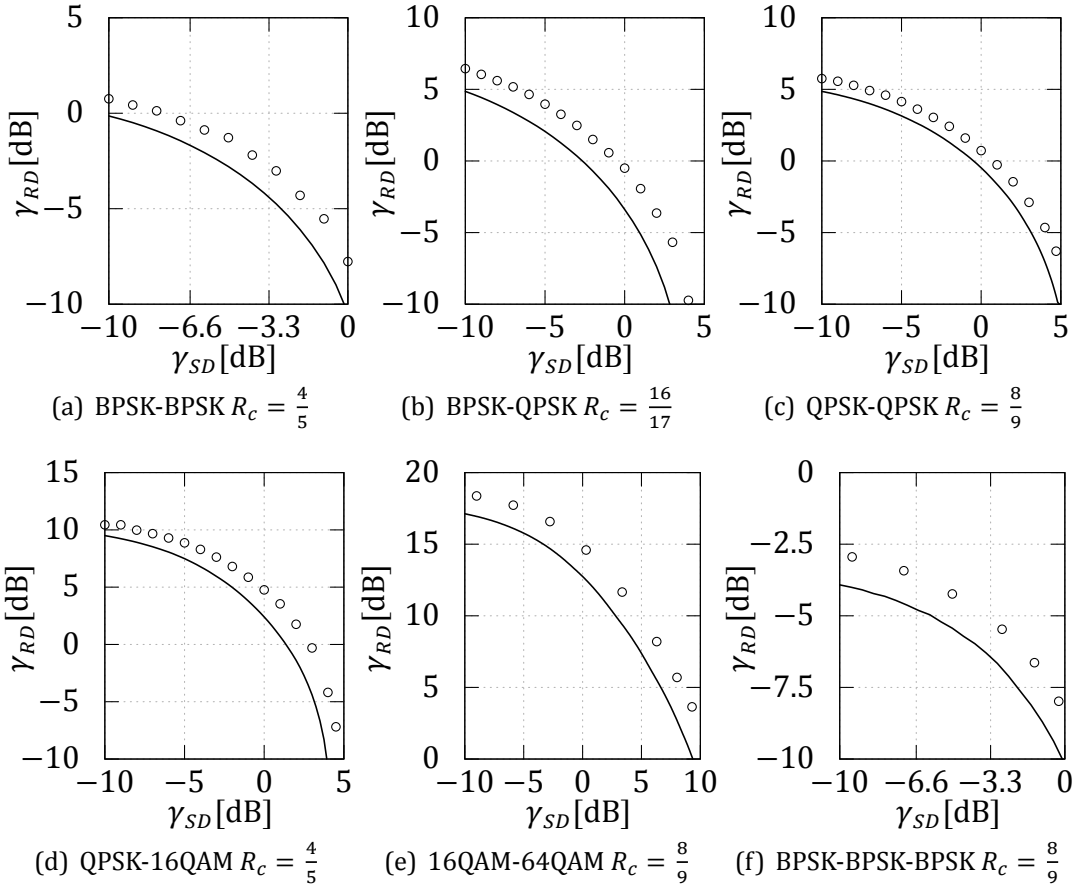

(a) BPSK-BPSK $R_c = \frac{4}{5}$ (b) BPSK-QPSK $R_c = \frac{16}{17}$ (c) QPSK-QPSK $R_c = \frac{8}{9}$

(d) QPSK-16QAM $R_c = \frac{4}{5}$ (e) 16QAM-64QAM $R_c = \frac{8}{9}$ (f) BPSK-BPSK-BPSK $R_c = \frac{8}{9}$

Figure 4.4: Comparison between the SPB limit (solid) and the actual simulated performance of a turbo coded system (◊) using different combinations of modulation modes for the source-destination and relay-destination links in an incremental cooperative scheme.

incremental systems that transmit two or three attempts and for different code rates used for the single attempts. A slow fading scenario is considered, where the channel quality values are constant over different attempts, i.e. $\gamma_{SD}^{n,i} = \gamma_{SD}$ and $\gamma_{RD}^{n,j} = \gamma_{RD}$ $\forall i, j, n$. Hence, in the slow fading scenario the qualities characterising each segment are given by $\gamma_{SD}^{n} = \gamma_{SD}$ and $\gamma_{RD}^{n} = \gamma_{RD}$. The incremental coding scheme used is a non-systematic distributed turbo code scheme, where each attempt contains both information and parity bits. Its design is further detailed in the following chapters, and in particular in Chapter 5, which addresses the design problem of finding schemes that are capable of approaching the limiting performance.

4.3.3 How to cooperate

The proposed analytic framework may be used for identifying the best pair of modulations to be adopted by the source and the relay stations in a cooperative communication. This subsection exemplifies how to use the SPB as a tool for determining the best cooperation mode for a system consisting of two transmission attempts.

Consider a scheme consisting of two attempts, the first transmitted by the source station and the second forwarded by the relay. The modulation modes $\mathcal{M}_{SD}$ and $\mathcal{M}_{RD}$, used respectively by the source and by the relay, are chosen between a set of modulation modes consisting of the Binary Phase Shift Keying (BPSK), the Quadrature Phase Shift Keying (QPSK), the Sixteen Quadrature Amplitude Modulation (16QAM) and the Sixty-Four Quadrature Amplitude Modulation (64QAM). Denote with $\eta(\mathcal{M})$ the number of bits mapped to each transmitted symbol by the modulation mode $\mathcal{M}$. Furthermore, assume to consider modulation modes couples consisting of the same modulation mode or of adjacent modulation modes for the source and the relay stations' transmissions, where the relay uses the higher order mode in the case of different modulations. This choice is justified by noting that a good quality on the relay-destination link allows one to use an high order modulation on the source-destination link and hence to transmit less symbols, achieving a faster communication, as can be seen later in Figure 4.6.

Since the purpose of this section is to evaluate the best way to cooperate, it is assumed that the quality of the source-relay link guarantees an error-free decoding at the relay of the signal transmitted by the source, independently of the chosen modulation mode $\mathcal{M}_{SD}$.

Name as available mode pair a couple of modulations satisfying (4.13) for repetition schemes or (4.27) for incremental schemes for a given sequence of SNRs on the source-destination and relay-destination links. The number of symbols transmitted by a cooperative scheme using a modulation mode couple $(\mathcal{M}_{SD}, \mathcal{M}_{RD})$ on the source-destination and relay-destination links may be calculated as:

$$\Lambda_{\text{coop}}(\mathcal{M}_{SD}, \mathcal{M}_{RD}) = \frac{B}{\eta(\mathcal{M}_{SD})} + \frac{B}{\eta(\mathcal{M}_{RD})}. \tag{4.28}$$

The best modulation mode couple $(\mathcal{M}^*_{SD}, \mathcal{M}^*_{RD})$ is the available pair of modulations that transmits the least number of symbols. Formally, the best modulation mode couple may be obtained as:

$$\begin{aligned} (\mathcal{M}^*_{SD}, \mathcal{M}^*_{RD}) = & \underset{(\mathcal{M}_{SD}, \mathcal{M}_{RD})}{\operatorname{argmin}} \left\{\Lambda_{\text{coop}}(\mathcal{M}_{SD}, \mathcal{M}_{RD})\right\}, \\ \text{subject to:} \quad & (\mathcal{M}_{SD}, \mathcal{M}_{RD}) \text{ satisfies (4.13) or (4.27).} \end{aligned} \tag{4.29}$$

Figures 4.5 and 4.6 show the available transmission mode couple providing the fastest communication for different SNRs on the source-destination and relay-

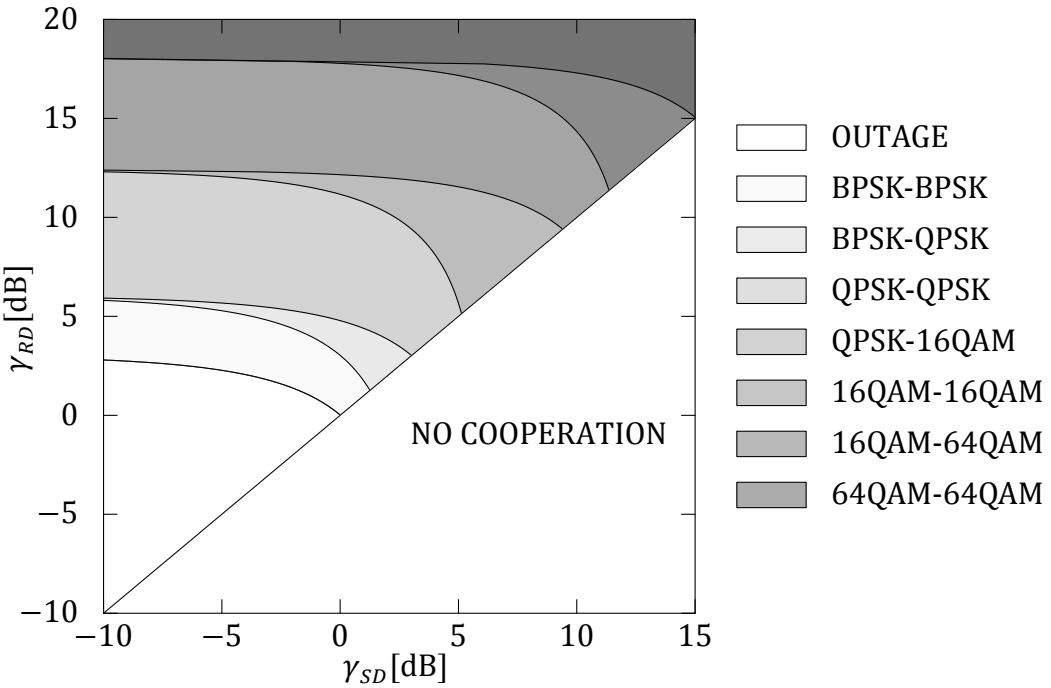

Figure 4.5: Best modulation mode couple for S's and R's transmissions of a two attempts cooperative scheme under repetition forwarding for different values of γ_{SD} and γ_{RD}.

destination links for repetition and incremental schemes consisting of two attempts, respectively. Only values $\gamma_{SD} < \gamma_{RD}$ are considered, since cooperation is only helpful when the quality of the relay-destination link is higher than the one of the source-destination link, while a direct transmission is to be preferred otherwise.

4.3.4 Performance of the cooperative HARQ system

The previous section presented how to assess the success of a cooperative system relying on HARQ techniques and how to select the best modulation modes to be used by the source and by the relay stations. This section uses these results for determining the limiting throughput, delay and outage performance of the cooperative scheme for diverse propagation conditions, including block and slow fading. The section also presents results for an adaptive system that maximises the throughput of the system.

Consider a scenario consisting of a source station, a destination and a relay located between them. Denote the average SNR on the source-destination link by Γ_{SD}, the average SNR on the source-relay link by Γ_{SR} and the average SNR on the

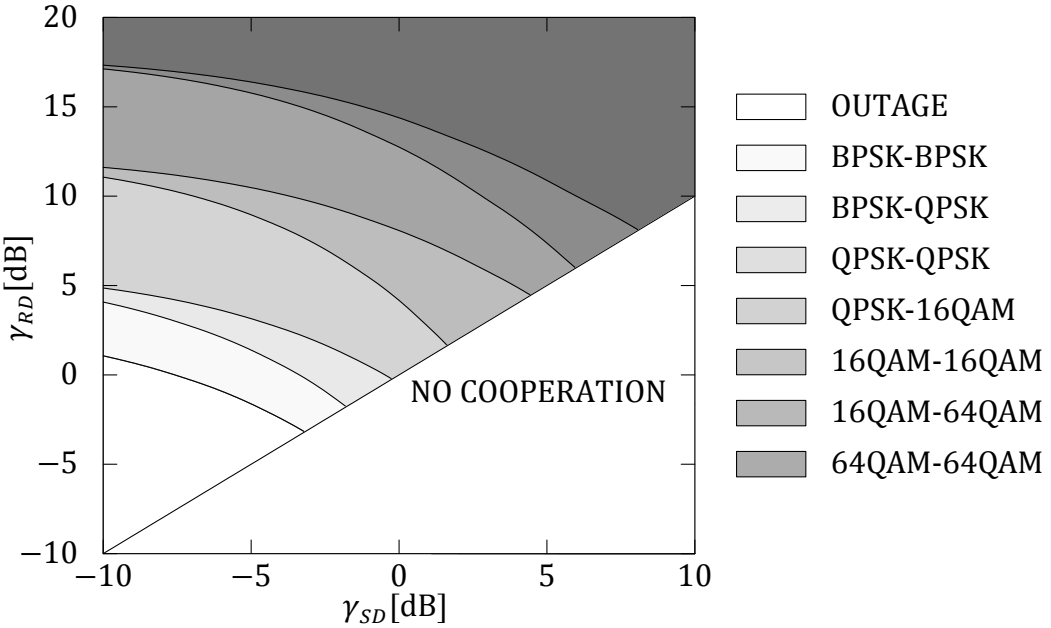

Figure 4.6: Best modulation mode couple for S's and R's transmissions of a two attempts cooperative scheme under incremental forwarding for different values of γ_{SD} and γ_{RD}.

relay-destination link by Γ_{RD}. The results provided consider average SNRs values of $\Gamma_{RD|\text{dB}} = \Gamma_{SR|\text{dB}} = \Gamma_{SD|\text{dB}} + 4.51$ dB. These values correspond to a network topology where the relay is located half-way between the source and the destination stations and the source-relay path forms an angle of value $\frac{\pi}{4}$ with the source-destination path, and to a propagation environment characterised by a path loss value of $\alpha = 3$.

The single transmissions are affected by fading. Particularly, name with $\gamma_{SD} = h_{SD}\,\Gamma_{SD}$, $\gamma_{SR} = h_{SR}\,\Gamma_{SR}$ and $\gamma_{RD} = h_{RD}\,\Gamma_{RD}$ the instantaneous SNR values on the source-destination, source-relay and relay-destination links, respectively. The quantity h represents the fading envelope. Results are provided for a Rayleigh faded scenario, hence h is exponentially distributed with mean and variance equal to unity.

Finally, this section considers the performance of schemes composed by codes having a rate of $R_c = \frac{8}{9}$. Similar results have been obtained using schemes formed by codes having rates of $R_c = \frac{4}{5}$ and $R_c = \frac{16}{17}$.

Consider a slow fading scenario, where the instantaneous link qualities remain constant over a transmission sequence, i.e. the values γ_{SD}, γ_{SR} and γ_{RD} are the same for all the transmission attempts. A number $B = 1800$ of encoded bits is transmitted in each attempt, where the encoded bit sequence is generated from $U = 1600$

information bits.

The transmission sequence develops as follows. The source station transmits the first group of bits, which is received both by the relay and by the destination. If the relay successfully decodes the received information it forwards the following group of bits, which is otherwise transmitted by the source station. The transmission sequence ends when the destination successfully decodes the received information or when the maximum number of attempts has been reached.

The transmission sequence may be modelled by using two indexes, namely s and t. The index s denotes the attempts transmitted by the source, while the index t denotes all the transmitted attempts. Hence, at the stage (s,t) the destination received the first s attempts from the source station with SNR γ_{SD} and the following $t-s$ attempts from the relay with SNR γ_{RD}.

Name with $\gamma_{t_{SD}}^{s}$ the SNR required on the source-destination link to correctly decode at the destination the information received in the first s attempts from the source station. Similarly, name with $\gamma_{t_{SR}}^{s}$ the SNR required on the source-relay link to correctly decode at the relay the information received from the source station after it transmitted the first s attempts. Finally, name with $\gamma_{t_{RD}}^{s,t}$ the minimum SNR on the relay-destination link supporting an error-free decoding at the destination at the stage (s,t).

The success thresholds $\gamma_{t_{SD}}^{s}$, $\gamma_{t_{SR}}^{s}$ and $\gamma_{t_{RD}}^{s,t}$ introduced before may be evaluated using the SPB, as shown in the previous subsection. Particularly, these threshold values may be obtained by considering the particular HARQ system obtained at the (s,t) stage and evaluating for such scheme the SNR values that satisfy (4.13) or (4.27) with an equal operator.

Note also that when bits are received from both the source station and the relay (i.e. $t > s$), the destination combines their LLRs and performs a joint decoding. Hence, the relay to destination threshold $\gamma_{t_{RD}}^{s,t}$ depends on γ_{SD}.

The probability that the destination successfully decodes the information at the (s,t) stage may be obtained by averaging over fading the probabilities that the instantaneous SNRs are higher than the thresholds $\gamma_{t_{SD}}^{s}$, $\gamma_{t_{SR}}^{s}$ and $\gamma_{t_{RD}}^{s,t}$. The mathematical formulation is presented in the following.

Denote the cumulative distribution function of an SNR value with $F_{\gamma}(\gamma) = \frac{1}{\Gamma}(1-e^{-\frac{\gamma}{\Gamma}})$ and assume $\gamma_{t_{SD}}^{0} = \gamma_{t_{SR}}^{0} = \gamma_{t_{RD}}^{s,s} = +\infty$. The probability $p_s^{s,t}$ of having a successful transmission at the stage (s,t) may be calculated as:

$$p_s^{s,t} = \begin{cases} 1 - F_{\gamma_{SD}}(\gamma_{t_{SD}}^{s}) & s = 1 \\ \left[F_{\gamma_{SD}}(\gamma_{t_{SD}}^{s-1}) - F_{\gamma_{SD}}(\gamma_{t_{SD}}^{s})\right] p_f^R(s-1) & t = s > 1 \\ \int_0^{\gamma_{t_{SD}}^{s}} \left[F_{\gamma_{RD}}(\gamma_{t_{RD}}^{s,t-1}) - F_{\gamma_{RD}}(\gamma_{t_{RD}}^{s,t})\right] p_s^R(s)\mathrm{d}\gamma_{SD} & t > 1 \end{cases}. \tag{4.30}$$

In (4.30), $p_s^R(s)$ is the probability that the relay successfully decodes the signal transmitted by the source station at the s-th stage and is equal to:

$$p_s^R(s) = F_{\gamma_{SR}}(\gamma_{t_{SR}}^{s-1}) - F_{\gamma_{SR}}(\gamma_{t_{SR}}^{s}), \tag{4.31}$$

while $p_f^R(s)$ is the probability that the relay could not decode the signal transmitted by the source station after receiving the first s attempts, which may be obtained as:

$$p_f^R(s) = 1 - \sum_{l=1}^{s} p_s^R(l). \tag{4.32}$$

Finally, the probability $p_s(t)$ that a transmission sequence successfully completes after t attempts may be calculated as:

$$p_s(t) = \sum_{s=1}^{t} p_s^{s,t}. \tag{4.33}$$

Conversely, the probability $p_f(t)$ that the information bits are not correctly decoded after receiving the first t attempts is obtained as:

$$p_f(t) = 1 - \sum_{s=1}^{t} p_s(s). \tag{4.34}$$

The outage probability P_{out} represents the probability that all the J_{MAX} attempts are unsuccessful and can be obtained as:

$$P_{\text{out}} = p_f(J_{\text{MAX}}). \tag{4.35}$$

For assessing the throughput and the delay performance of the system, one has to calculate the average number of bits that are transmitted by the HARQ scheme within the attempts that form a particular stage. The detailed procedure for obtaining such value is as follows.

Consider the t-th transmission attempt. Denote with $\lambda_{SD}(t) = B/\eta(\mathcal{M}_{SD})$ the number of symbols transmitted in the case where the B encoded bits are transmitted by the source station. Similarly, the value $\lambda_{RD}(t) = B/\eta(\mathcal{M}_{RD})$ denotes the number of symbols transmitted in the case where the attempt is sent by the relay.

The average number of symbols transmitted at the t^{th} attempt can be obtained as:

$$\lambda(t) = \begin{cases} \lambda_{SD}(t)p_f^R(t-1) + \lambda_{RD}(t)\left(1 - p_f^R(t-1)\right) & t > 1 \\ \lambda_{SD}(1) & t = 1 \end{cases}, \tag{4.36}$$

while the average number of bits transmitted within the first t attempts may be obtained as:

$$\Lambda(t) = \sum_{l=1}^{t} \lambda(l). \tag{4.37}$$

Finally, the throughput efficiency of the considered system is given by:

$$\mathcal{S} = \frac{(1 - P_{\text{out}})U}{\lambda(1) + \sum_{t=2}^{J_{\text{MAX}}} \lambda(t) p_f(t-1)}, \tag{4.38}$$

and the average normalised delay is given by:

$$\mathcal{D} = \frac{\sum_{t=1}^{J_{\text{MAX}}} p_s(t)\Lambda(t)}{(1 - P_{\text{out}})U}. \tag{4.39}$$

The analysis may be extended to correlated or block fading models by quantising the fading values. The interested reader is referred to [65], which fully covers the correlated and block fading regimes for non-cooperative systems and whose analysis may be extended to a cooperative system as shown in the previous sections for the slow fading scenario. The accuracy of the quantised model depends on the number of quantisation levels considered for the fading envelope variables, as detailed in [78].

Results for different fading regimes and an incremental system scenario consisting of two attempts (i.e. $J_{\text{MAX}} = 2$) are provided in Figures 4.7 and 4.8. The analysis is also validated comparing the theoretical evaluation with the actual performance of a HARQ system obtained using punctured turbo codes. Different modulation modes couples are considered for the source station's and the relay's transmissions, namely the BPSK-QPSK, QPSK-16QAM and 16QAM-64QAM couples. It can be seen that the theoretical estimator closely predicts the actual performance of the turbo coded system.

Note again that the purpose of this chapter is to assess the limiting performance of a cooperative system and to show that the analysis captures the performance of carefully designed schemes, and not to detail how to obtain practical systems that approach such limit. Further details on the code design algorithm and on how it influences the actual performance of a system will be given in the following chapters.

The proposed framework may also be used for quantifying the performance increase offered by cooperation and by incremental forwarding over a non-cooperative transmission scheme, as detailed in the following for a simple adaptive system. Particularly, the following results compare a non-cooperative scheme with a cooperative scheme. In the non-cooperative scheme, the source station may use a modulation mode chosen from a set containing the BPSK mode, the QPSK mode

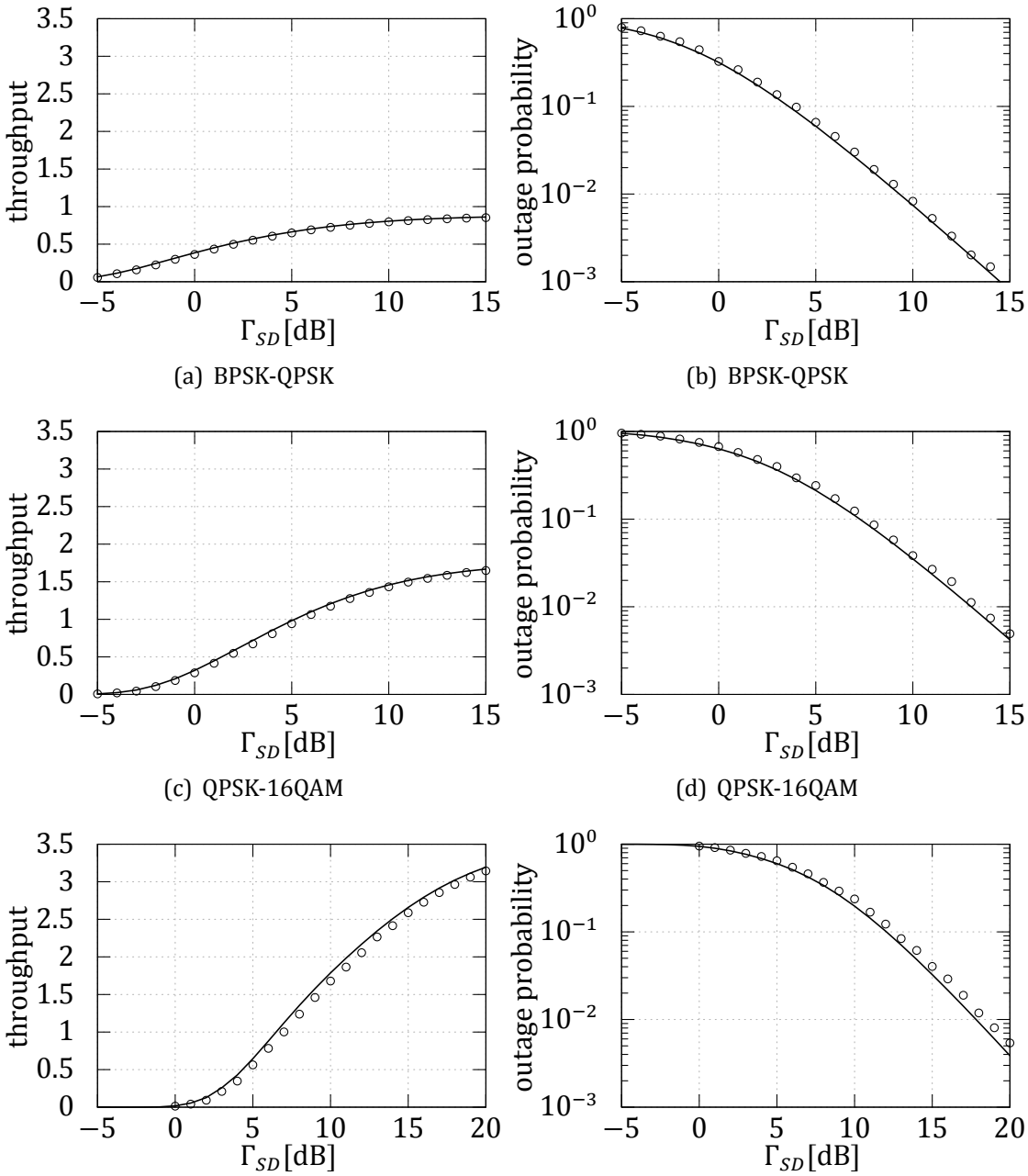

(a) BPSK-QPSK (b) BPSK-QPSK

(c) QPSK-16QAM (d) QPSK-16QAM

(e) 16QAM-64QAM (f) 16QAM-64QAM

Figure 4.7: Theoretical (solid) and simulated (○) outage probability and throughput performance of a coded cooperation system consisting of two attempts ($J_{\mathrm{MAX}} = 2$) using incremental encoding and different modulation couples over a slow fading channel.

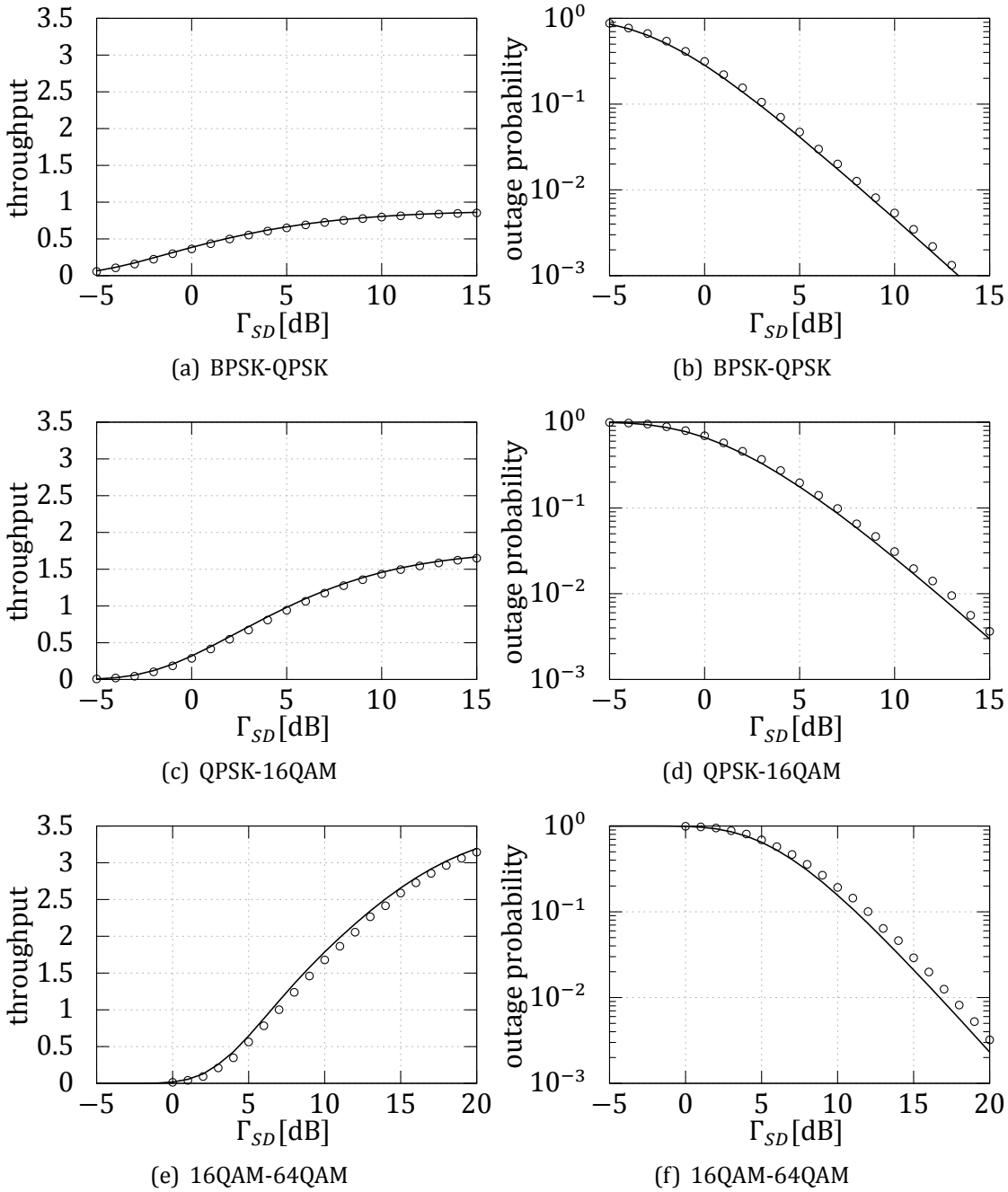

(a) BPSK-QPSK (b) BPSK-QPSK

(c) QPSK-16QAM (d) QPSK-16QAM

(e) 16QAM-64QAM (f) 16QAM-64QAM

Figure 4.8: Theoretical (solid) and simulated (○) outage probability and throughput performance of a coded cooperation system consisting of two attempts ($J_{\mathrm{MAX}} = 2$) using incremental encoding and different modulation couples over a block fading channel.

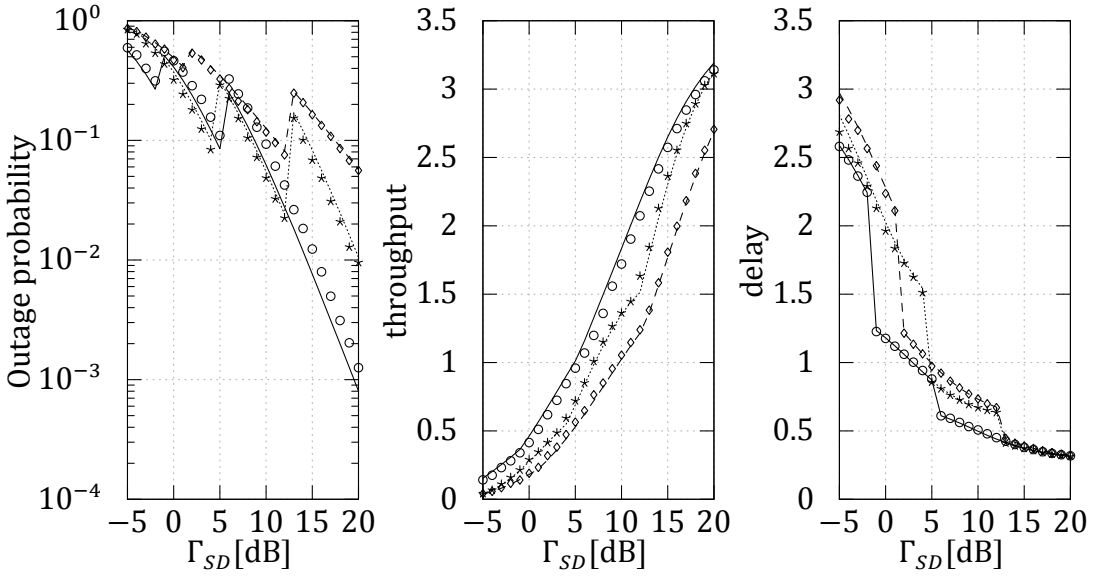

Figure 4.9: Theoretical (solid: cooperative incremental, dotted: cooperative repetition, dashed: non-cooperative) and simulated (○: cooperative with incremental forwarding, ⋆: cooperative with repetition forwarding, ◇: non-cooperative with repetition transmissions) outage probability, throughput and normalised average delay performance of an adaptive coded cooperation system consisting of three attempts ($J_{\mathrm{MAX}} = 3$) over a slow fading channel.

and the 16QAM mode. The cooperative system is capable of using different modulation mode couples for the transmissions of the source and relay stations. These modulation mode couples are the BPSK-QPSK pair, the QPSK-16QAM pair and the 16QAM-64QAM pair.

Assume a block fading scenario, where the instantaneous link qualities γ_{SD}, γ_{SR} and γ_{RD} change in every attempt and are independent from previous values. Assume also that the source station and the relay know the mean SNRs quantities Γ_{SD} and Γ_{RD} of the source-destination and relay-destination links, while the destination knows the instantaneous quantities γ_{SD} and γ_{RD}.

Consider an adaptive system where modulation adaptation is used for maximising the network throughput. Such adaptive scheme may be obtained in a cooperative scenario by letting the source and relay stations choosing the modulation mode couple which offers the highest throughput, obtained using to (4.38), for given values of Γ_{SD} Γ_{SR}, and Γ_{RD}. Similarly, consider a non-cooperative adaptive scheme that maximises the throughput value obtained using the non-cooperative performance analysis formulation of [65], which is a particular case of the analysis presented in this chapter. Finally, consider an adaptive scheme that transmits three

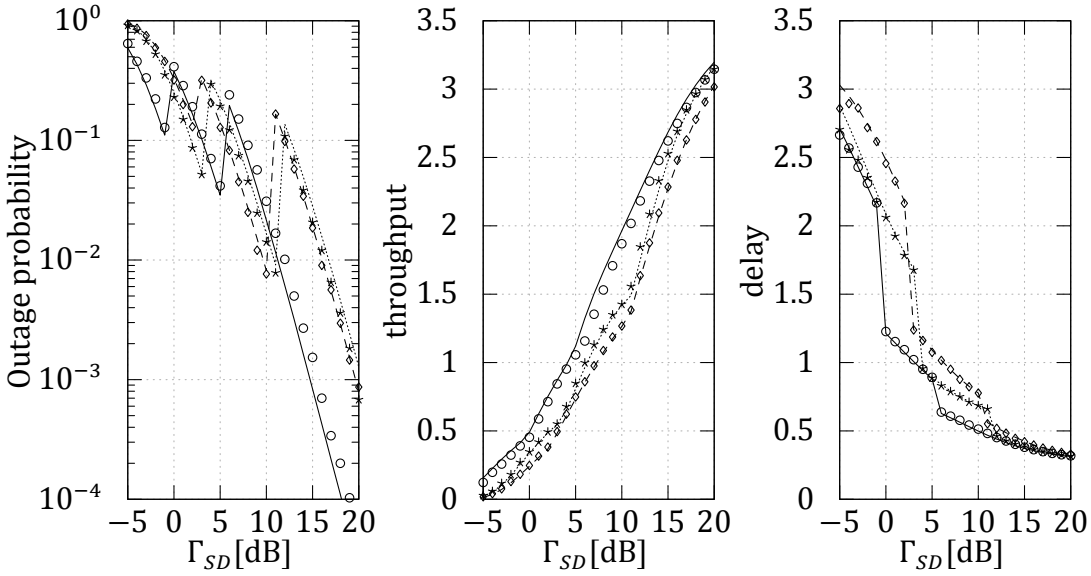

Figure 4.10: Theoretical (solid: cooperative incremental, dotted: cooperative repetition, dashed: non-cooperative) and simulated (○: cooperative with incremental forwarding, ⋆: cooperative with repetition forwarding, ◇: non-cooperative with repetition transmissions) outage probability, throughput and normalised average delay performance of an adaptive coded cooperation system consisting of three attempts ($J_{\mathrm{MAX}} = 3$) over a block fading channel.

attempts using either repetition or incremental forwarding.

The presented adaptive algorithm has to be considered as an example to validate the theoretical framework since it uses only three modulation modes and does not consider different coding rates. However, the results may be easily extended to select the best modulation mode pair-coding rate couple from a predetermined set by choosing the couple that offers the highest throughput calculated according to (4.38).

Results for the considered adaptive scheme without cooperation and with cooperation are shown in Figures 4.9 and 4.10 for slow and block faded regimes, respectively. More explicitly, Figures 4.9 and 4.10 compare the theoretical performance of the repetition non-cooperative and cooperative schemes and of an incremental cooperative scheme transmitting the maximum number of previously punctured bits in each attempt (i.e. attaining the lowest code rate at the destination for each attempt).

Results confirm previous studies showing that cooperation may be used for increasing the network performance, even in the block faded scenario, where all the considered schemes have the same diversity gain. Finally, the analysis confirms

and quantifies that among cooperative coded techniques the one offering the best performance is the incremental forwarding. In particular, the incremental scheme uses a more efficient channel code, and attains a lower coding rate at the destination, hence compensating the fact that some bits are received less times than using a repetition scheme.

Figures 4.9 and 4.10 also compare the theoretical outage, throughput and delay values with the actual simulated performance. One can see that the performance of the turbo coded system is very close to the analytic prediction, proving that the theory is capable of capturing the performance of carefully designed schemes and that such schemes exist.

4.4 Conclusions

This chapter analysed the limiting performance of coded cooperation schemes over a faded channel. The analytic framework is not limited to a particular encoding and decoding scheme, rather it is accurate for every efficient distributed encoding technique. Furthermore, the estimator takes into account the general case where many transmission attempts are sent by the source and relay stations, possibly using different modulation modes and incorporating different encoded bits. It was shown that the limiting performance may be seen as a benchmark tool for assessing whether a particular code scheme is efficient.

The following chapter will be focused on the design of turbo code schemes that approach the limiting performance, such as the benchmark system used through this chapter for validation purposes.

5

Design of efficient distributed turbo code schemes

The previous chapter analysed the limiting performance of a HARQ system for a cooperative channel. This chapter addresses the problem of designing schemes that are capable of approaching the limiting performance. More particularly, the chapter considers the design problem of finding sets of puncturing patterns for turbo codes for composing HARQ systems that perform close to the limiting performance. The chapter addresses both the problem of assessing the performance of a particular scheme and that of selecting well performing schemes from all the possible distributed coding systems relying on punctured turbo codes.[1]

5.1 Introduction

The previous chapter shown that the limiting performance of a coded cooperation scheme over a fading channel may be approached by efficient codes, though it dispensed with the design of such coding schemes. This chapter considers such design problem, and proposes a novel algorithm based on genetic optimisation techniques for contriving punctured turbo code systems that are suited for cooperative scenarios.

Punctured turbo codes [79] are selected among different candidate coding techniques, namely over Low Density Parity Check (LDPC) codes [68, 69] and rateless codes [80], since they are capable of obtaining a capacity approaching performance for many coding rates and for different attempts using a single decoding engine. Particularly, rate compatible LDPC codes have a waterfall performance loss com-

[1] The content of this chapter is based on F. Babich, A. Crismani and R.G. Maunder, ``EXIT chart aided design of periodically punctured turbo codes'', Electronics Letters, vol. 46, no 14, June 2010, and on F. Babich and A. Crismani, ``Cooperative coding schemes: design and performance evaluation'', IEEE Transactions on Wireless Communications, vol. 11, pp. 222–235, Jan. 2012.

pared to turbo codes under heavy puncturing. A performance at 1 dB from capacity at a rate of 0.9 transmitting more than 10^5 bits and using a mother code of rate 0.5 is reported in [81]. Rateless codes are better suited to erasure channels, where it is possible to design a single code capable of approaching the capacity for every erasure probability. However, rateless codes are not able to approach the capacity of different symmetric channels without changing the encoding and decoding engine [82].

Among turbo codes, non-systematic codes, where the information bits are spread over different attempts, are selected in order to obtain balanced schemes whose performance does not depend on the particular quality of different transmissions. The literature on punctured turbo codes aimed to optimise their error floor performance [83, 84], due to the computational difficulties found when directly addressing the waterfall behaviour [85]. Conversely, the design procedure presented in this chapter directly targets the waterfall performance by proposing a novel Genetic Algorithm (GA) for designing non-systematic punctured turbo code schemes for the source's and relay's attempts of a coded cooperation algorithm. The GA relies on a novel tri-dimensional (3D) EXIT chart technique for predicting the decoding behaviour of non-systematic periodically punctured turbo codes and allows one to contrive code schemes consisting of attempts optimised for the waterfall region for both the source and the relay. The chapter shows that the codes designed by the 3D EXIT chart aided GA closely approach the analytically estimated limiting performance and outperform previously proposed systematic and complementary schemes.

5.2 Hybrid automatic repeat and request systems using punctured turbo codes

The chapter considers the same coded cooperation system studied in the previous chapter. Namely, the scenario under study consists of an HARQ system where successive attempts are transmitted either by a source station or by a relay. Furthermore, this chapter considers coded cooperation systems that rely on punctured turbo codes for encoding the information bits in each attempt. More particularly, assume that the B encoded bits that are sent in each transmission attempt are obtained by puncturing the encoded bits produced by a mother code fed with U information bits. The mother code is a parallel concatenation of two convolutional encoders having the generator polynomial $(1\ \ 5)_8$ and the feedback polynomial $(1\ \ 3)_8$ that are separated by a random interleaver π with length equal to the information bit sequence size. Among turbo coded systems, the parallel concatenation architecture is chosen since it was shown to perform exceptionally well at

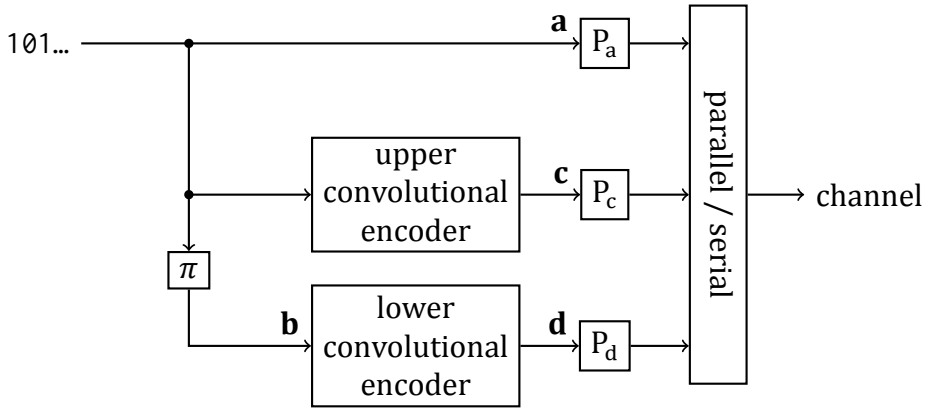

Figure 5.1: Encoder structure of the punctured turbo code under consideration.

low SNRs [86], where cooperative communications and ARQ techniques operate. Conversely, serial concatenations are best suited to applications requiring a lower error floor [87].

The encoder's structure is shown in Figure 5.1, where **a**, **c** and **d** represent the information bits sequence, the parity bits sequence produced by the upper convolutional encoder and the parity bits sequence produced by the lower convolutional encoder, respectively. The sequences of bits **a**, **c** and **d** are punctured by puncturers P_a, P_c and P_d, respectively, and the B bits that are preserved after the puncturing operation are sent on the channel.

The decoder for a single attempt operates on the LLR sequences $\tilde{\mathbf{a}}_c$, $\tilde{\mathbf{c}}_c$ and $\tilde{\mathbf{d}}_c$, pertaining to the sequences **a**, **c** and **d**, respectively. The zero value is used to represent the LLR value of punctured bits in the sequences $\tilde{\mathbf{a}}_c$, $\tilde{\mathbf{c}}_c$ and $\tilde{\mathbf{d}}_c$. The operation of adding the zero values in the positions of punctured bits is denoted by P_a^{-1}, P_c^{-1} and P_d^{-1}, respectively for the sequences $\tilde{\mathbf{a}}_c$, $\tilde{\mathbf{c}}_c$ and $\tilde{\mathbf{d}}_c$. The joint decoding of multiple attempts collects the LLRs received in each transmission and adds the LLRs pertaining to the same bit for obtaining the sequences $\tilde{\mathbf{a}}_c$, $\tilde{\mathbf{c}}_c$ and $\tilde{\mathbf{d}}_c$.

The turbo decoder operates in an iterative fashion [7], where the two Soft-Input Soft-Output (SISO) decoders, based on the Bahl-Cocke-Jelinek-Raviv (BCJR) algorithm [88] that is used for obtaining the maximum a-posteriori probability of the bits fed to the two RSC in the encoder, exchange their information until convergence is reached or a maximum number of iterations is performed. In particular, the upper SISO decoder uses the sequences of LLRs $\tilde{\mathbf{a}}_c$ and $\tilde{\mathbf{c}}_c$ and a sequence of a-priori LLRs $\tilde{\mathbf{a}}_a$ for the bits **a** for producing a sequence of extrinsic LLRs $\tilde{\mathbf{a}}_e$. The extrinsic LLRs $\tilde{\mathbf{a}}_e$ are interleaved and fed as a-priori information to the lower SISO decoder. The lower decoder, in turn, uses such a-priori information, together with the sequence $\tilde{\mathbf{b}}_c$ that is obtained by interleaving the sequence of LLRs $\tilde{\mathbf{a}}_c$ and the sequence $\tilde{\mathbf{d}}_c$, for producing a new sequence of extrinsic LLRs $\tilde{\mathbf{b}}_e$, which is interleaved

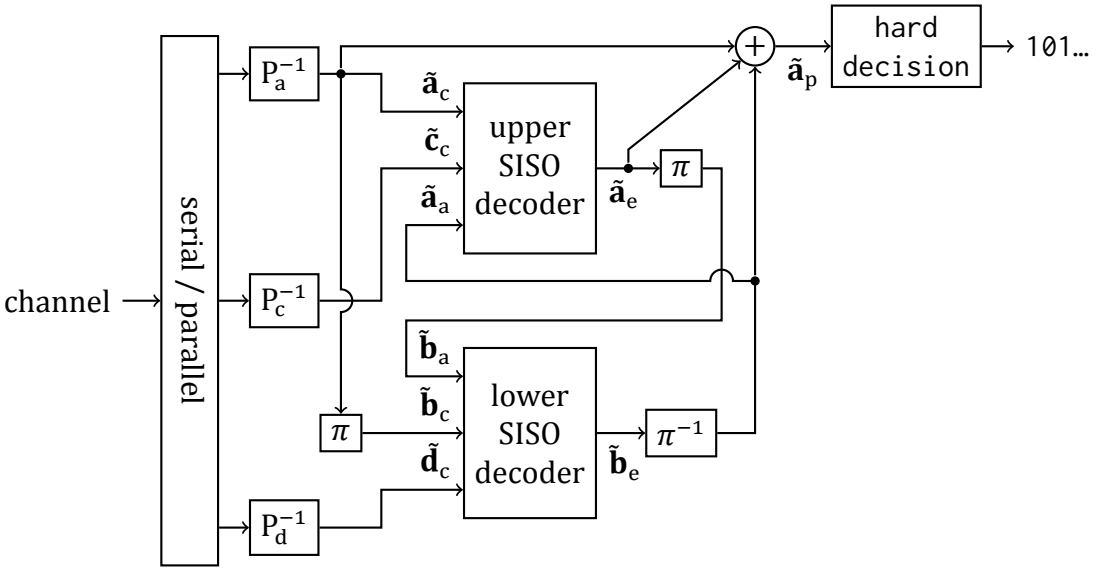

Figure 5.2: Decoder structure of the punctured turbo code under consideration.

and fed back to the upper decoder as a-priori information, continuing the iterative process. The decoder structure is shown in Figure 5.2, where $\tilde{\mathbf{a}}_p$ represents the sequence of a-posteriori LLRs that is produced at the end of the iterative process and is used for estimating the transmitted bits. A reader that is interested in the turbo decoding principle may find further details in [7, 89].

The HARQ system under study is obtained by using different puncturing schemes for each attempt, in order to operate with a lower code rate. Assume to adopt a periodic puncturing scheme for the k-th attempt. More explicitly, the information and parity bit sequences generated by the mother code are partitioned in sub-blocks of length equal to the puncturing period T. The sets $\mathcal{U}_a^k$, $\mathcal{U}_c^k$ and $\mathcal{U}_d^k$ specify the positions of unpunctured bits transmitted at the k-th attempt for each sub-block of sequences **a**, **c** and **d**, respectively. Similarly the punctured bit positions are enumerated by the sets $\mathcal{P}_a^k$, $\mathcal{P}_c^k$ and $\mathcal{P}_d^k$. The coding rate of the k-th attempt is given by:

$$R_{c_k} = \frac{P}{|\mathcal{U}_a^k| + |\mathcal{U}_c^k| + |\mathcal{U}_d^k|} = \frac{U}{B}. \tag{5.1}$$

Denote the sets containing the positions of information bits, upper and lower parities that have been transmitted at least once within the first k attempts by $\mathcal{T}_a^k = \bigcup_{h=1}^{k} \mathcal{U}_a^h$, $\mathcal{T}_c^k = \bigcup_{h=1}^{k} \mathcal{U}_c^h$ and $\mathcal{T}_d^k = \bigcup_{h=1}^{k} \mathcal{U}_d^h$, respectively. The code rate at the destination after receiving the first k attempts is equal to:

$$R_{c_k}^{D} = \frac{P}{|\mathcal{T}_a^k| + |\mathcal{T}_c^k| + |\mathcal{T}_d^k|}. \tag{5.2}$$

Finally, assume to adopt the same coding rate $R_{c_k} = R_c \ \forall k \in [1, J_{\text{MAX}}]$ for each attempt, where J_{MAX} is the maximum number of attempts of the cooperative scheme. Again, this chapter provides results for a set of coding rates chosen for exemplifying the design procedure, namely the coding rates of $R_c = \frac{4}{5}$, $R_c = \frac{8}{9}$ and $R_c = \frac{16}{17}$. Similar results are obtained for different coding rates.

5.3 The influence of the puncturing patterns on the performance of the turbo coded system

As introduced in the previous section, the distributed coded scheme under consideration is completely characterised by specifying the positions of punctured bits for all the attempts that compose the HARQ system. It is then expected that the system performance significantly depends on the particular set of puncturers under use. This section briefly analyses the performance of the classic systematic incremental puncturing solutions and details why they are not suited for cooperative scenarios. The following sections will address the problems identified in this section, proposing methods for evaluating the performance of a generic non-systematic punctured turbo code and for obtaining puncturing sets that perform close to the network figure values predicted by using the SPB estimator of Chapter 4.

Consider classic incremental HARQ schemes used for non-cooperative scenario, where the first attempt, transmitted by the source station, preserves all the information bits and some parity bits, while later attempts transmit either only parity bits or a wide set of parity bits complemented by few information bits. The quality required on the relay-destination link for achieving a target error ratio at the destination for a given value of SNR γ_{SD} on the source-destination link in a system that follows this puncturing rule is compared with the performance predicted using the SPB in Figure 5.3 for different values of code rate used for each attempt. The specific puncturing schemes used are listed in Table 5.1. Such puncturing schemes will be referred in the following of this thesis as systematic schemes, given that a systematic code that transmits all the information bits is used in the first attempt.

One can see from Figure 5.3 that the simulated performance of the system approaches the theoretical analysis when the quality of the source-destination link is high, while a severe performance downgrade occurs for low values of γ_{SD}, where the system operates at the target error rate only for values of γ_{RD} that are significantly higher than the ones predicted by the SPB.

Such downgrade may be explained by looking carefully at the distribution of information and parity bits across the transmission attempts of the scheme under consideration. Particularly, it was shown in [90] that information bits are critical for the waterfall performance of turbo codes. Looking carefully at the classic HARQ

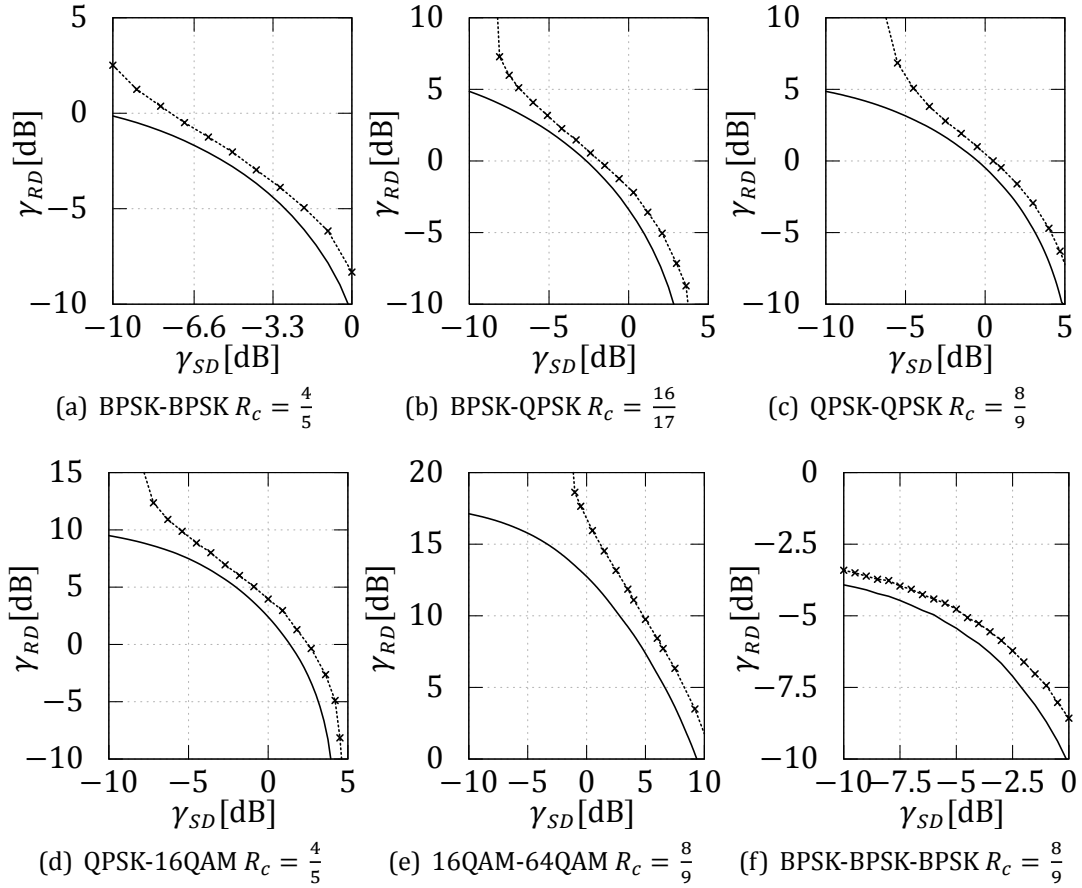

(a) BPSK-BPSK $R_c = \frac{4}{5}$ (b) BPSK-QPSK $R_c = \frac{16}{17}$ (c) QPSK-QPSK $R_c = \frac{8}{9}$

(d) QPSK-16QAM $R_c = \frac{4}{5}$ (e) 16QAM-64QAM $R_c = \frac{8}{9}$ (f) BPSK-BPSK-BPSK $R_c = \frac{8}{9}$

Figure 5.3: Comparison between the SPB limit (solid) and the actual simulated performance of a systematic incremental system (dashed ×) using different combinations of modulation modes for the source-destination and relay-destination links.

scheme one may note that when transmitting two attempts only, all the information bits are sent by the source station, while the relay forwards parity bits. Hence, the information bits are received with low quality when γ_{SD} is low, and since their quality is of paramount importance for the decoding performance in the waterfall region the system requires a much higher value of γ_{RD}, which ultimately means that the system requires having very reliable parity bits for compensating the low quality of the more important information bits in order to achieve the target error ratio.

One may note that the performance downgrade does not affect the system transmitting three attempts. This is because the third attempt, which is transmitted by the relay, contains some information bits. Hence, there are information bits received from the relay, and therefore with high quality, and the decoder is capable of

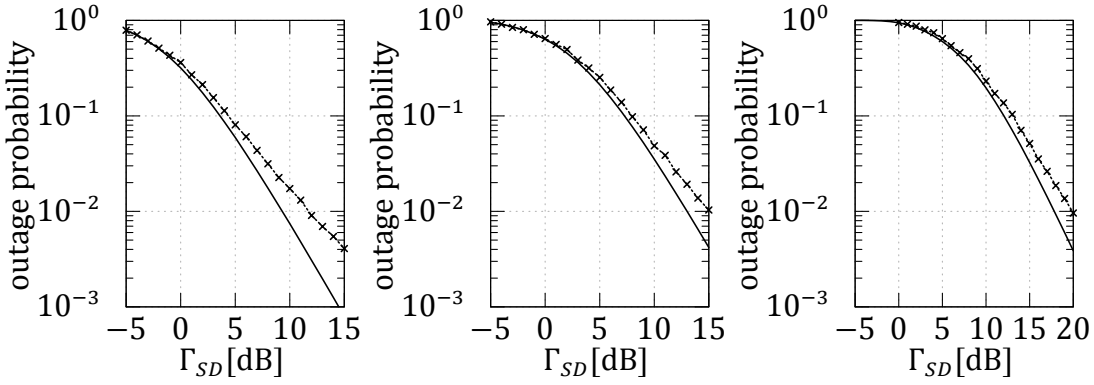

(a) BPSK-QPSK (b) QPSK-16QAM (c) 16QAM-64QAM

Figure 5.4: Comparison between the simulated outage probability (dashed ×) of a systematic incremental system consisting of two attempts ($J_{\mathrm{MAX}} = 2$) using and the performance predicted using the SPB (solid) in a slow fading regime.

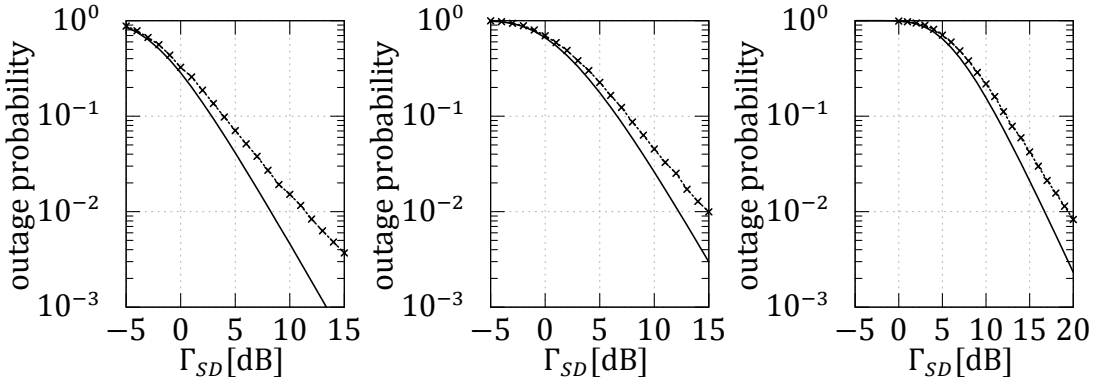

(a) BPSK-QPSK (b) QPSK-16QAM (c) 16QAM-64QAM

Figure 5.5: Comparison between the simulated outage probability (dashed ×) of a systematic incremental system consisting of two attempts ($J_{\mathrm{MAX}} = 2$) using and the performance predicted using the SPB (solid) in a block fading regime.

correctly decoding the transmitted signal at channel qualities close to the limiting performance predicted using the SPB.

The performance downgrade translates to the system performance and particularly to the outage probability. Figures 5.4 and 5.5 compare the simulated outage performance of the classic HARQ scheme with the SPB analysis for slow and block faded regimes, respectively. One can see again that the simulated performance does not follow the theoretical analysis, and it exhibits a floor behaviour when the value

Γ_{SD} increases.

One can finally conclude that the performance of an HARQ scheme based on punctured turbo codes significantly depends on the particular set of puncturers used. Particularly, the classic incremental schemes used for non-cooperative scenarios, where the quality of different attempts is likely to be similar, are not suited for cooperative systems, where different transmissions are characterised by quality values that may differ significantly, given that the transmissions are carried out by different stations.

5.4 Design of balanced turbo coded HARQ system for cooperative scenarios

The previous paragraph shown that a careful design of the puncturing sets composing a distributed turbo coded system is needed for approaching the performance predicted using the SPB. More explicitly, unbalanced systems, where different attempts contain different quantities of information and parity bits and hence have different decoding performance, cannot operate close to the predicted values.

It is then of interest to design balanced HARQ systems, where each attempt has the same decoding performance. Particularly, balanced schemes allow the destination to decode the received information independently of the quality of each attempt, and hence avoid transmitting the attempts that contribute the most to the decoding performance on links having a very low SNR, as may happen in unbalanced schemes. Balanced turbo coded HARQ schemes necessarily use non-systematic puncturers for each attempt, given that the information bits must be spread across all the transmissions since they significantly contribute to the decoding performance of the single attempt.

The design procedure for contriving balanced non-systematic punctured schemes for cooperative scenarios consists of two steps. Firstly, one needs to evaluate the performance of single non-systematic turbo codes, in order to compare different punctured solutions. Secondly, one needs to explore the search space composed by all possible non-systematic punctured turbo codes and select solutions that optimise the performance of the whole HARQ system.

This section details these design steps, where a novel tri-dimensional EXIT chart analysis is used for assessing the waterfall performance of a non-systematic punctured turbo code and a genetic algorithm based optimisation technique is adopted for selecting HARQ schemes that are capable of performing close to the analytic prediction.

5.4.1 Analysis of periodically punctured non-systematic turbo codes using tri-dimensional EXIT charts

Coding schemes suited for cooperative scenarios should be optimised to provide a satisfying waterfall behaviour, noting that cooperation operates in this region. This goal is opposed to previous literature works that optimised the error floor performance of punctured turbo codes [83, 84]. The performance of a turbo code in the waterfall region may be quantified by identifying the decoding threshold that characterises the scheme. The decoding threshold is defined as the lowest SNR value that allows the decoding engine to achieve a vanishingly low BER, and it may be estimated by using EXIT charts. In particular, EXIT charts have been proved to be an effective tool for predicting the waterfall performance of iteratively decoded schemes without relying on BER simulations [72, 91].

An EXIT chart depicts the iterative mutual information exchange between a parallel concatenation of two SISO decoders. In particular, the a-priori information I_A provided to the upper decoder by the lower decoder is quantified by the mutual information $I(\mathbf{a}; \tilde{\mathbf{a}}_\mathrm{a})$ between the systematic bit sequence $\mathbf{a}$ and the a-priori LLR sequence $\tilde{\mathbf{a}}_\mathrm{a}$ of Figure 5.2. In response, the upper decoder generates the extrinsic LLR sequence $\tilde{\mathbf{a}}_\mathrm{e}$, whose mutual information I_E is obtained as $I(\mathbf{a}; \tilde{\mathbf{a}}_\mathrm{e})$. The relation F_upper between the value of mutual information I_A of the a-priori LLR sequence and the value of mutual information I_E of the extrinsic LLR sequence produced by the upper decoder is referred to as the EXIT function, or EXIT curve, of the upper decoder. Hence, one may write:

$$I_E = I(\mathbf{a}; \tilde{\mathbf{a}}_\mathrm{e}) = F_\mathrm{upper}[I(\mathbf{a}; \tilde{\mathbf{a}}_\mathrm{a})] = F_\mathrm{upper}(I_A). \tag{5.3}$$

The extrinsic LLR sequence $\tilde{\mathbf{a}}_\mathrm{e}$ generated by the upper decoder is provided to the lower decoder as a-priori information. The lower decoder produces in turn an updated sequence of LLRs $\tilde{\mathbf{a}}_\mathrm{a}$, that is fed back to the upper decoder as a-priori information in an iterative fashion, as detailed in the previous section and pictured in Figure 5.2. Similarly to the upper decoder, the operation of the lower decoder may be characterised by an EXIT function. Particularly, one may write:

$$I_A = I(\mathbf{a}; \tilde{\mathbf{a}}_\mathrm{a}) = F_\mathrm{lower}[I(\mathbf{a}; \tilde{\mathbf{a}}_\mathrm{e})] = F_\mathrm{lower}(I_E). \tag{5.4}$$

An EXIT chart jointly plots the two EXIT functions of the concatenated decoders. The concatenated scheme is capable of attaining an infinitesimally low BER, when the two EXIT curves do not intersect, allowing the stair-case-shaped decoding trajectory to reach the (1, 1) point of perfect decoding convergence.

Consider the transmission of a single attempt of the HARQ system using the BPSK modulation mode over an AWGN channel having SNR equal to γ. Figure 5.6 plots the EXIT chart of the code used in the first attempt of the classic systematic

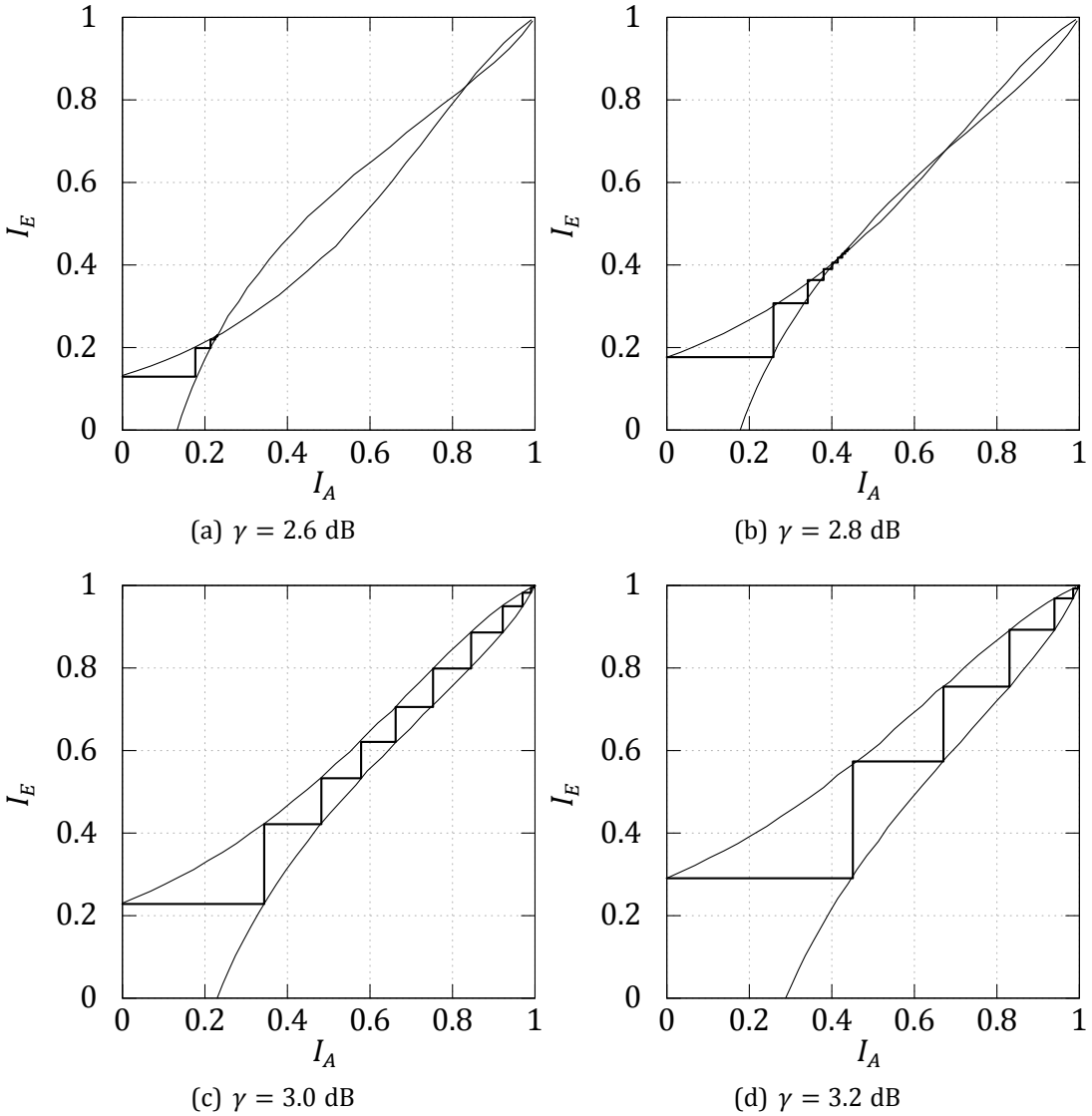

(a) $\gamma = 2.6$ dB (b) $\gamma = 2.8$ dB

(c) $\gamma = 3.0$ dB (d) $\gamma = 3.2$ dB

Figure 5.6: Classic EXIT charts of a periodically punctured systematic turbo code for different values of SNR.

incremental scheme having a rate of $R_c = \frac{8}{9}$ for different SNR values. The complete listing of punctured and unpunctured bits is given in Table 5.1.

It can be seen that the EXIT chart shows an open tunnel at an SNR value of about 2.9 dB, which is referred to as the decoding threshold of the scheme. Hence, the turbo code scheme is capable of attaining a vanishingly low BER for SNR values that are higher than 2.9 dB, as validated by BER simulations shown in Figure 5.7. Figure 5.6 also plots the actual stair-shaped decoding trajectory, showing that the

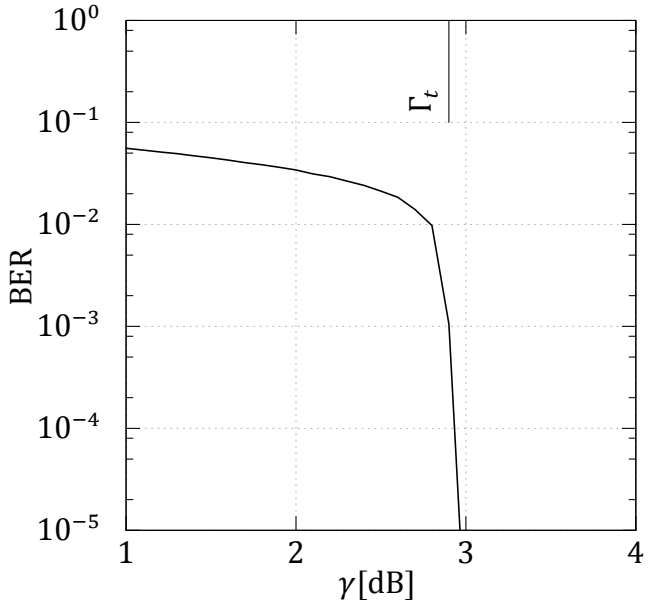

Figure 5.7: BER versus SNR curve of a periodically punctured systematic turbo code.

real decoding procedure is closely predicted by the EXIT chart analysis.

The same EXIT chart analysis is shown in Figure 5.8 for a non-systematic periodically punctured code of rate $R_c = \frac{8}{9}$, where only 8 information bits are preserved from the 16 information bits collected in each puncturing period. The listing of the particular puncturing scheme used may be found in 5.1, where the code is labeled as ``Genetic Algorithm aided designed''. It can be seen that the EXIT chart analysis fails to model the performance of the coded scheme. Particularly, the actual decoding trajectory is not predicted by the two EXIT curves, and it can be seen that the actual decoder is capable of reaching the $(1, 1)$ point of perfect convergence even when the two EXIT curves do intersect. Hence, one may conclude that a classic EXIT chart cannot be used for analysing the convergence behaviour of non-systematic periodically punctured turbo codes. It is then necessary to modify the EXIT chart analysis for accounting for the effect of periodic puncturing.

The mismatch between the EXIT chart and the actual performance originates from a reduction in the amount of extrinsic information for the neighbouring extrinsic LLRs in the sequence $\tilde{\mathbf{a}}_{\mathrm{e}}$. This reduction is produced by the puncturing of bits in the sequence $\mathbf{a}$. The effect is exacerbated if consecutive systematic bits in the sequence $\mathbf{a}$ are punctured, which happens consistently for periodic puncturing.

Hence, when periodic puncturing is employed, the extrinsic LLRs in the sequence $\tilde{\mathbf{a}}_{\mathrm{e}}$ can be divided into two categories, those in the vicinity of punctured

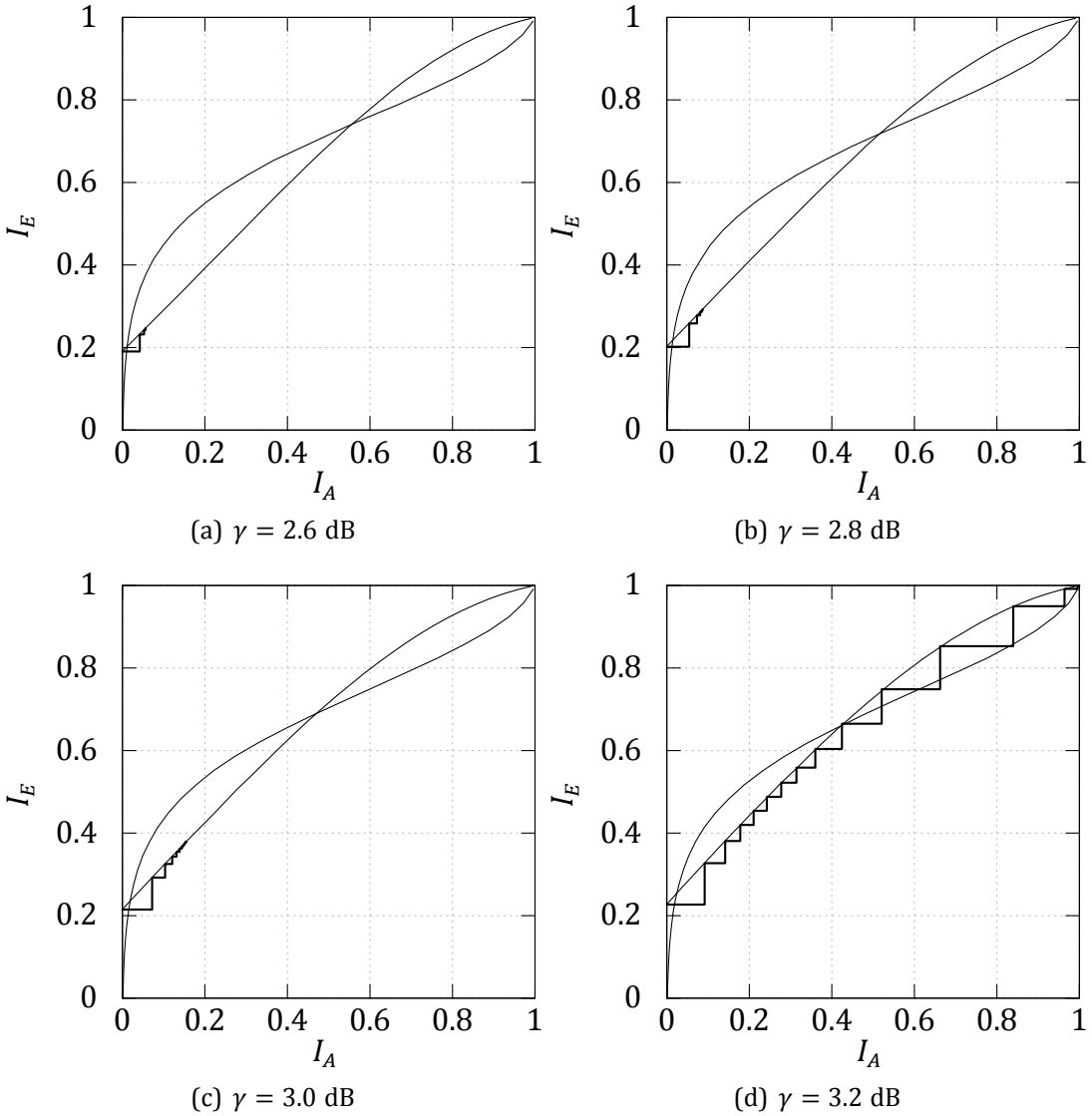

(a) $\gamma = 2.6$ dB (b) $\gamma = 2.8$ dB

(c) $\gamma = 3.0$ dB (d) $\gamma = 3.2$ dB

Figure 5.8: Classic EXIT charts of a periodically punctured non-systematic turbo code for different values of SNR.

bits and those not in the vicinity of punctured bits. Since the former category has a higher mutual information than the latter one, there is an *uneven* distribution of information within $\tilde{\mathbf{a}}_\mathrm{e}$. However, the classical EXIT chart analysis models the extrinsic LLR sequence $\tilde{\mathbf{a}}_\mathrm{e}$ using a single mutual information value of $I(\mathbf{a}; \tilde{\mathbf{a}}_\mathrm{e})$ and hence with an *even* distribution of information. Since the lower decoder is sensitive to the distribution of information in the extrinsic sequence $\tilde{\mathbf{a}}_\mathrm{e}$, the mutual information $I(\mathbf{a}; \tilde{\mathbf{a}}_\mathrm{a})$ of the a-priori sequence of LLRs $\tilde{\mathbf{a}}_\mathrm{a}$ provided by it is not correctly

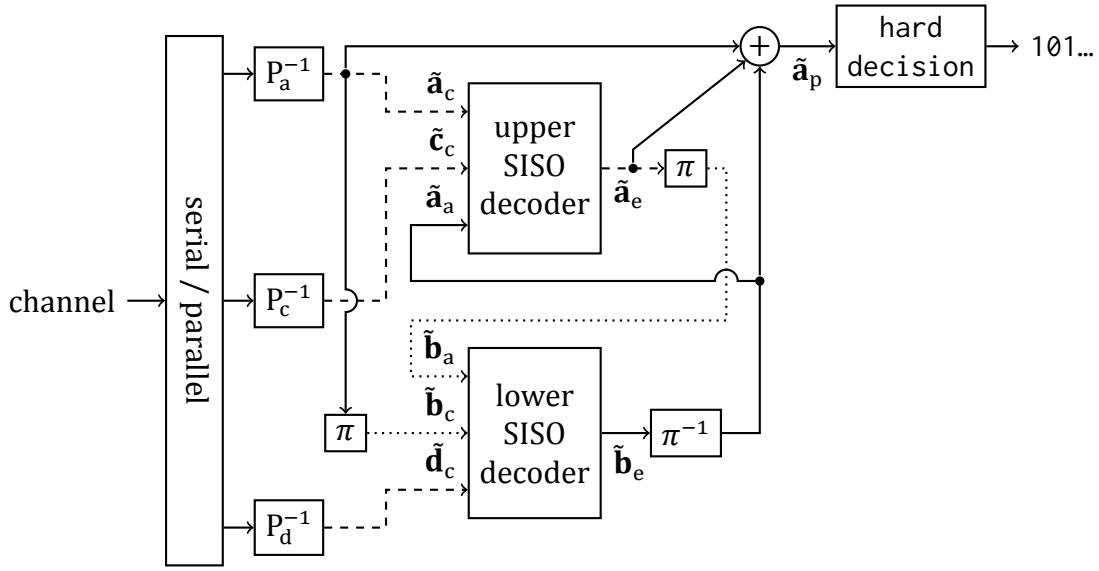

Figure 5.9: Decoder structure of the punctured turbo code with emphasis on the content of mutual information of the LLR sequences (solid lines: *even* mutual information content, dashed lines: periodic *uneven* mutual information content, dotted lines: random *uneven* mutual information content).

predicted.

Note also that the classic EXIT chart analysis is able to correctly obtain the upper decoder's EXIT function. This is because the interleaver π randomises the periodic uneven distribution of information within the LLR sequences $\tilde{\mathbf{a}}_e$ and $\tilde{\mathbf{a}}_c$ before they are provided to the lower decoder, as shown in Figure 5.9, which explicitly pictures LLR sequences having *even* or *uneven* distributions of mutual information. As a result, the LLR sequence $\tilde{\mathbf{a}}_a$ provided by the lower decoder has an even distribution of information, which is correctly modelled in the classic EXIT chart analysis.

In order to correctly model the behaviour of periodically punctured codes, the classical EXIT chart analysis is modified for taking into account the *uneven* distribution of mutual information in the LLR sequence $\tilde{\mathbf{a}}_e$. Particularly, a tri-dimensional EXIT chart analysis is proposed, where the artificial LLR sequence $\tilde{\mathbf{a}}_e$ is divided into two categories.

The first category $\tilde{\mathbf{a}}_e^p$ corresponds to the punctured bits $\mathbf{a}^p$ of the sequence $\mathbf{a}$, while the second category $\tilde{\mathbf{a}}_e^u$ corresponds to the unpunctured bits $\mathbf{a}^u$. The two categories of LLRs $\tilde{\mathbf{a}}_e^p$ and $\tilde{\mathbf{a}}_e^u$ that are fed to the lower decoder as a priori information are generated separately and have distinct mutual information values of $I_E^p = I(\mathbf{a}^p; \tilde{\mathbf{a}}_e^p)$ and $I_E^u = I(\mathbf{a}^u; \tilde{\mathbf{a}}_e^u)$, respectively. Such distinction allows separately accounting for the contributions of punctured and unpunctured bits. Particularly,

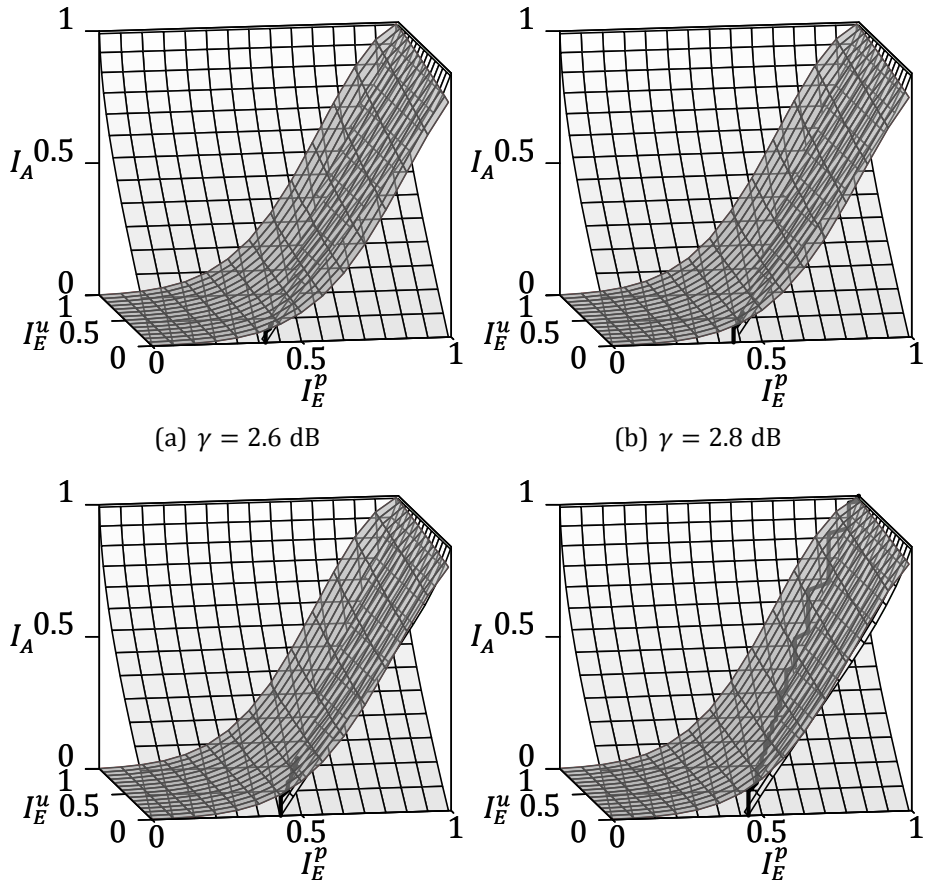

(a) $\gamma = 2.6$ dB (b) $\gamma = 2.8$ dB

(c) $\gamma = 3.0$ dB (d) $\gamma = 3.2$ dB

Figure 5.10: Tri-dimensional EXIT charts of a periodically punctured non-systematic turbo code for different values of SNR.

the behaviour of the lower encoder is now characterised by the EXIT function:

$$I_A = I(\mathbf{a}; \tilde{\mathbf{a}}_{\mathrm{a}}) = F_{\mathrm{lower}}[I(\mathbf{a}; \tilde{\mathbf{a}}_{\mathrm{e}}^{\mathrm{p}}), I(\mathbf{a}; \tilde{\mathbf{a}}_{\mathrm{e}}^{\mathrm{u}})] = F_{\mathrm{lower}}(I_E^p, I_E^u), \tag{5.5}$$

which represents a surface in the tri-dimensional space. Conversely, the behaviour of the upper decoder is characterised by two EXIT functions, one for the punctured bits and one for the unpunctured bits, that are obtained as:

$$I_E^p = I(\mathbf{a}^p; \tilde{\mathbf{a}}_{\mathrm{e}}^{\mathrm{p}}) = F_{\mathrm{upper}}^p[I(\mathbf{a}; \tilde{\mathbf{a}}_{\mathrm{a}})] = F_{\mathrm{upper}}^p(I_A) \tag{5.6}$$

$$I_E^u = I(\mathbf{a}^u; \tilde{\mathbf{a}}_{\mathrm{e}}^{\mathrm{u}}) = F_{\mathrm{upper}}^u[I(\mathbf{a}; \tilde{\mathbf{a}}_{\mathrm{a}})] = F_{\mathrm{upper}}^u(I_A) \tag{5.7}$$

The proposed tri-dimensional EXIT chart analysis jointly plots the EXIT curves F_{lower}, F_{upper}^p and F_{upper}^u. The analysis is exemplified for the non-systematic code under consideration in Figure 5.10, which pictures the tri-dimensional EXIT chart

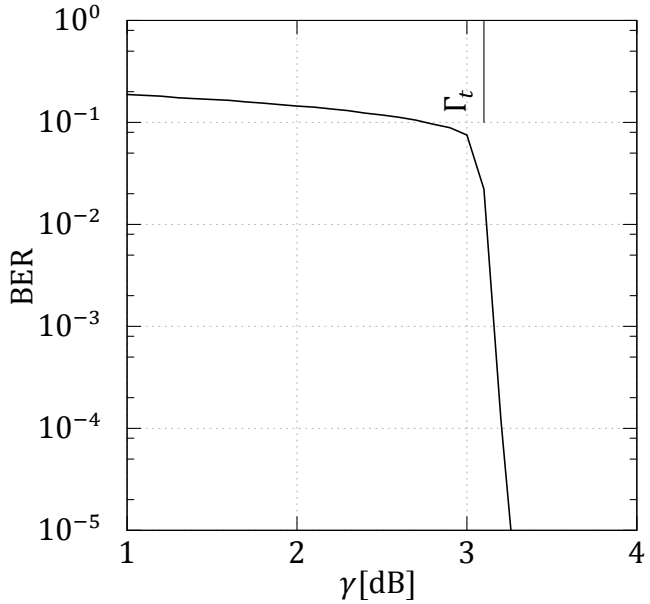

Figure 5.11: BER versus SNR curve of a periodically punctured non-systematic turbo code.

for different values of SNR. It can be seen that the proposed tri-dimensional approach allows one to correctly model the behaviour of the non-systematic scheme, while the classic EXIT chart analysis fails. The decoding threshold for the considered scheme is equal to 3.1 dB, as can be seen from the open tunnel appearing in Figure 5.10. Such threshold is validated by BER simulations shown in Figure 5.11, which again confirm the accuracy of the proposed EXIT chart method.

For visualisation purposes and for facilitating the user at identifying an open tunnel, the tri-dimensional EXIT chart of a non-systematic code may be projected into a bi-dimensional space. Particularly, the bi-dimensional projection may be obtained by weighting the contributions of punctured and unpunctured bits with real quantities w_p and w_u, representing respectively the fractions of punctured and unpunctured information bits. The upper decoder is characterised by the single EXIT function $F_{\text{upper}}^{\text{projected}}(I_A)$ obtained as:

$$\begin{aligned} I_E = I(\mathbf{a}; \tilde{\mathbf{a}}_{\text{e}}) &= w_p \cdot F_{\text{upper}}^{\text{p}}[I(\mathbf{a}; \tilde{\mathbf{a}}_{\text{a}})] + w_u \cdot F_{\text{upper}}^{\text{u}}[I(\mathbf{a}; \tilde{\mathbf{a}}_{\text{a}})] \\ &= w_p \cdot F_{\text{upper}}^{\text{p}}(I_A) + w_u \cdot F_{\text{upper}}^{\text{u}}(I_A) \\ &= F_{\text{upper}}^{\text{projected}}(I_A). \end{aligned} \tag{5.8}$$

The lower decoder may also be characterised by a single EXIT function that depends only on the value I_E. Particularly, one may model its behaviour by defining the EXIT

curve $F_{\text{lower}}^{\text{projected}}(w_p \cdot I_E^p + w_u \cdot I_E^u)$ as:

$$\begin{aligned} I(I_A) = I(I(\mathbf{a}; \tilde{\mathbf{a}}_{\text{a}})) &= F_{\text{lower}}^{\text{projected}}[w_p \cdot I(\mathbf{a}^p; \tilde{\mathbf{a}}_{\text{e}}^{\text{p}}) + w_u \cdot I(\mathbf{a}^u; \tilde{\mathbf{a}}_{\text{e}}^{\text{u}})] \\ &= F_{\text{lower}}^{\text{projected}}(w_p \cdot I_E^p + w_u \cdot I_E^u), \end{aligned} \tag{5.9}$$

for the values of I_E^p, I_E^u and I_A at which $F_{\text{upper}}^{\text{p}}(I_A)$ and $F_{\text{upper}}^{\text{u}}(I_A)$ intersect, i.e. for the values that contribute at matching the actual decoding trajectory.

The projections on the bi-dimensional space of the tri-dimensional EXIT charts pictured in Figure 5.10 are shown in Figure 5.12. It can be seen again that the proposed analysis allows one to correctly model the decoding behaviour and to obtain the decoding threshold value that characterises the coding scheme. Hence, opposed to the classic EXIT chart analysis, the proposed tri-dimensional approach may be used for evaluating the decoding behaviour of periodically punctured schemes in the waterfall region.

5.4.2 Genetic aided design of periodically punctured codes suited for HARQ systems

The previous sections shown that a balanced HARQ system consisting of non-systematic punctured coding schemes is required for approaching the system limiting performance and proposed an analytic method based on tri-dimensional EXIT charts for assessing the performance of the single attempts composing such HARQ system. Hence, the previous sections identified a suited HARQ structure and proposed a tool for evaluating how well one particular HARQ scheme performs. The next design step consists in finding balanced HARQ schemes that are capable of approaching the limiting performance predicted using the SPB.

Particularly, the design problem consists in finding HARQ schemes where the single attempts have the same performance in the waterfall region, this performance is as close as possible to the limiting one obtained by using the SPB and, finally, the coding rate at the destination when combining the received attempts is as low as possible. It has to be noted that, opposed to previous literature works that optimised the error floor performance of punctured turbo codes [83, 84], the waterfall performance is considered, since cooperative scenarios operate with low SNRs.

The design problem is addressed by proposing a novel code design technique, based on a genetic optimisation algorithm, that allows finding efficient puncturing schemes for the source's and relay's transmissions. More explicitly, a GA aided design tool is constructed for obtaining non-systematic punctured codes that combined at the destination provide a low code rate and whose performance in the waterfall region is capable of approaching the limiting one predicted by the SPB.

The choice of a GA is based on previous literature works where genetic optimisation techniques have been used as heuristic tools for selecting suitable coding

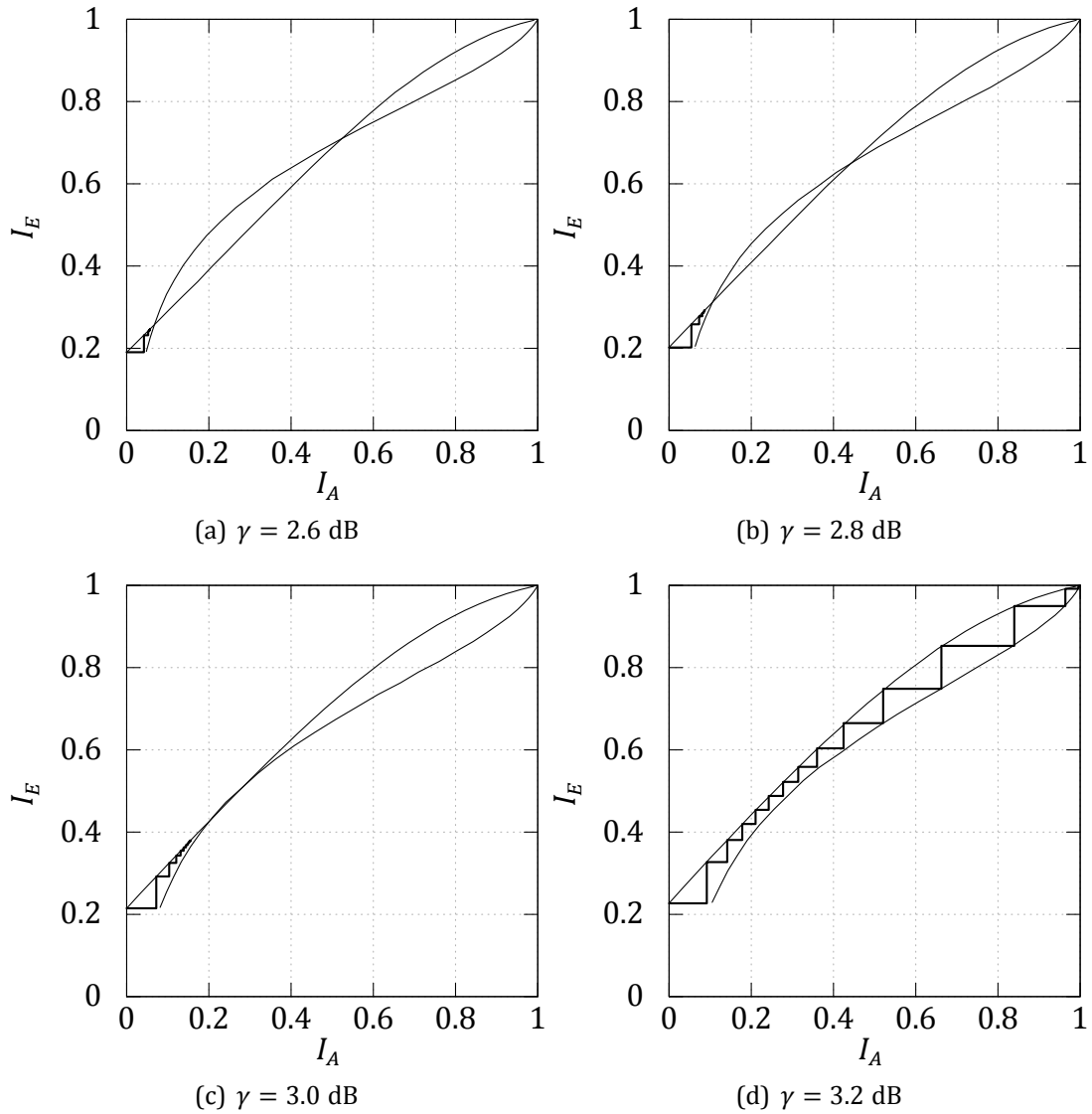

(a) $\gamma = 2.6$ dB (b) $\gamma = 2.8$ dB

(c) $\gamma = 3.0$ dB (d) $\gamma = 3.2$ dB

Figure 5.12: Bi-dimensional projections of tri-dimensional EXIT charts of a periodically punctured non-systematic turbo code for different values of SNR.

schemes [92]. This section shows that the GA allows efficiently exploring the set of possible punctured codes, opposed to performing an exhaustive search as proposed for turbo trellis coded modulation schemes in [93], which may be unfeasible for the considered design problem [85].

The GA operates in steps. The i-th step contrives codes for the i-th transmission attempt. More explicitly, the i-th step operates on a search list $\mathbf{C}$ formed by

candidate coding schemes. The generic code scheme C is composed by i puncturing patterns $\{C_j\}_{j=1}^{i}$, one for each attempt.

At each step, the GA tries to obtain codes that achieve the best waterfall performance for the target attempt. In order to select the schemes offering the best waterfall performance, the GA compares candidate codes in terms of their decoding thresholds. The decoding thresholds $\Gamma_{\text{EXIT}}(C_i)$ are predicted using the tri-dimensional EXIT chart analysis presented in the previous section, assuming to transmit a BPSK modulated signal over an AWGN channel. In particular, given that non-systematic codes are considered for the single attempt and that the classic EXIT chart analysis cannot correctly model the behaviour of such codes, the proposed tri-dimensional EXIT charts are of paramount importance for the GA as they allow selecting the best code candidates with a reduced computational cost than BER plots. More explicitly, the tri-dimensional EXIT chart analysis provides the means for comparing the waterfall performance of candidate codes that are considered during the GA operations in an efficient way.

The novel GA not only allows designing code schemes with satisfying waterfall performance for each attempt, but also prioritises code schemes that repeat less bits, in order to achieve a low coding rate at the destination. Particularly, the proposed cost function for the i-th step decreases for schemes formed by punctured codes performing closer to the channel capacity and takes into account the coding rate at the destination after receiving all the i attempts. Hence, the GA allows one to contrive coding schemes which repeat the least number of bits while guaranteeing a satisfying waterfall performance for each attempt.

The cost function for the i-th step is expressed as:

$$\Omega(C) = \sum_{j=1}^{i} \left(\Gamma_{\text{EXIT}}(C_j) - \Gamma_c\right) + \beta {R_c}_i^D, \tag{5.10}$$

where Γ_c is the SNR providing a channel capacity equal to the code rate R_c of the single attempt. The real valued quantity β is used to weight the contribution of performing near the channel capacity or achieving a lower code rate at the destination. More details on the influence of the parameters that control the behaviour of the GA will be provided in the following of the section.

In each step, the GA operates in stages. Particularly, at each stage the GA generates 10 mutations. Each mutation derives from a randomly chosen code scheme $C^* \in \mathbf{C}$. Among the 10 mutated codes, a new code scheme C' is appended to the search list only if its cost function $\Omega(C')$ is lower than the one of the originating code scheme, $\Omega(C^*)$. When 20 codes are already in the search list, C' substitutes the scheme with the highest cost function. The search loop for the particular step stops when a code scheme with a target cost function is found or when a maximum number of iterations without improvements is reached.

A mutated code scheme C' is generated by performing a set of Q operations on the i-th puncturing pattern C_i^*, where $P_Q\{Q\} = 2^{-Q}$. A decreasing probability is chosen to facilitate the convergence of the GA, however many operations are permitted to explore the search-space sufficiently densely. The operations applied for mutating a puncturing pattern are the following:

1. move an element from $\mathcal{U}_x^i$ to $\mathcal{P}_x^i$, and, viceversa, move an element from $\mathcal{P}_x^i$ to $\mathcal{U}_x^i$, where $x \in \{a, c, d\}$;

2. move an element from $\mathcal{U}_c^i$ to $\mathcal{P}_c^i$, and, viceversa, move an element from $\mathcal{P}_d^i$ to $\mathcal{U}_d^i$;

3. move an element from $\mathcal{P}_c^i$ to $\mathcal{U}_c^i$, and, viceversa, move an element from $\mathcal{U}_d^i$ to $\mathcal{P}_d^i$;

In order to facilitate the convergence to a low code rate at the destination, the candidate bits to be moved between sets when mutating a code scheme are not selected randomly.

Denote with $x \in \{a, c, d\}$ either the sequence containing systematic bits, upper parities or lower parities. For achieving a lower code rate at the destination, bits that have already been transmitted many times are more likely to be selected when choosing the bit to be punctured (i.e. when moving a bit from the set $\mathcal{U}_x^i$ of unpunctured bits to the set $\mathcal{P}_x^i$ of punctured bits). Viceversa, bits that have been transmitted less times are better candidates when choosing the bit that has to be unpunctured (i.e. when moving a bit from the set $\mathcal{P}_x^i$ of punctured bits to the set $\mathcal{U}_x^i$ of unpunctured bits).

More explicitly, denote with $\mathcal{R}^j(\mathcal{U}_x^i)$ the set enumerating the positions of bits of $\mathcal{U}_x^i$ that have been transmitted j times within the first i attempts. Similarly, $\mathcal{R}^j(\mathcal{P}_x^i)$ enumerates punctured bits. The probability $P\{\mathcal{R}^j(\mathcal{U}_x^i)\}$ of puncturing one of the bits from the set $\mathcal{U}_x^i$ that have been transmitted j times within the first i attempts is proportional to α^j. Hence, bits transmitted more times are preferred. Conversely, the probability $P\{\mathcal{R}^j(\mathcal{P}_x^i)\}$ of unpuncturing one of the bits in the set $\mathcal{P}_x^i$ that has been transmitted j times is proportional to α^{-j} and prioritises less transmitted bits.

It may be noted that all the operations preserve the coding rate, while some of them change the code's structure, in the sense that different numbers of upper and lower parity bits are transmitted after applying operations 2) and 3). Conversely, the number of transmitted information bits is fixed and the mutations only change the positions of unpunctured information bits. This is to prevent the GA from transmitting many information bits in the first step. In particular, codes which preserve many information bits exhibit a better waterfall performance, however they lead to repeated bits in the following attempts and do not facilitate the design of balanced schemes.

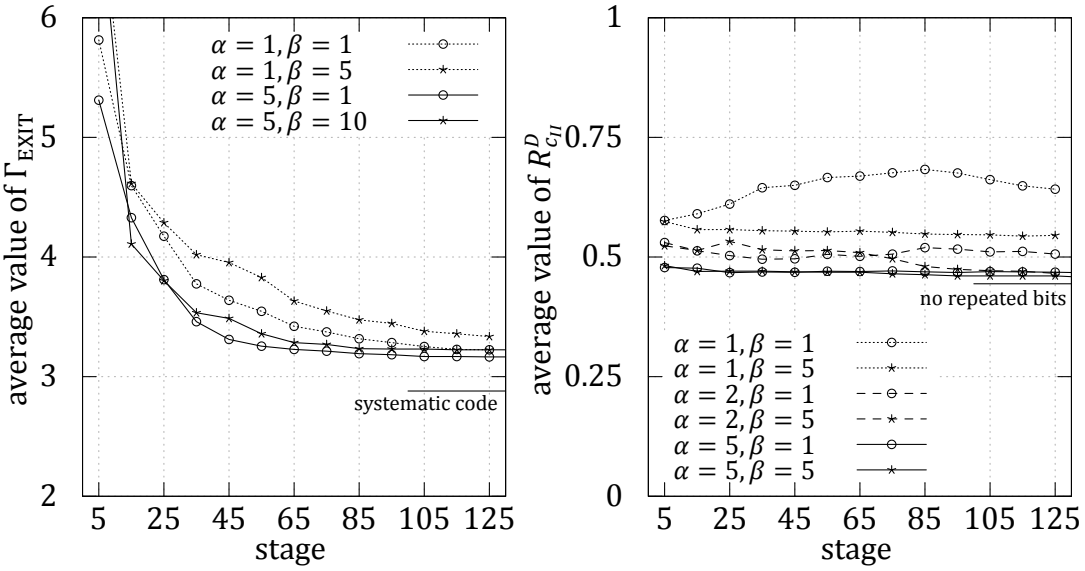

(a) average decoding threshold (b) average coding rate

Figure 5.13: Average decoding threshold and average coding rate at the destination at different stages when running the second step of the proposed GA.

Figure 5.13 shows the average decoding threshold and the coding rate at the destination at different stages of the second step of the proposed GA with different values of α and β.

It can be seen that prioritising the choice of bits to be punctured and unpunctured by using an higher value of α effectively reduces the coding rate at the destination. More explicitly, when the bits to be punctured and unpunctured are chosen randomly (i.e. using $\alpha = 1$), the candidate code schemes repeat many bits and the GA does not converge to a low rate solution. Conversely, a value $\alpha = 5$ allows one to obtain schemes that do not repeat any bit after only few GA stages.

The value of β is used to weight the contribution of the coding rate with respect to the decoding threshold on the cost function calculation. A lower β means that codes performing nearer to the channel capacity are preferred over codes having a lower rate at the destination.

This behaviour is confirmed by Figure 5.13, that shows that running the GA with lower values of β allows obtaining codes with satisfying waterfall behaviours after fewer steps. The results presented in the following of the section have been obtained using the values $\alpha = 5$ and $\beta = 5$, which provide a good compromise between the coding rate convergence and the decoding threshold performance.

The best code schemes generated by the GA for different coding rates of the single attempt are listed in Tables 5.1, 5.2 and 5.3 along with the 3D EXIT chart

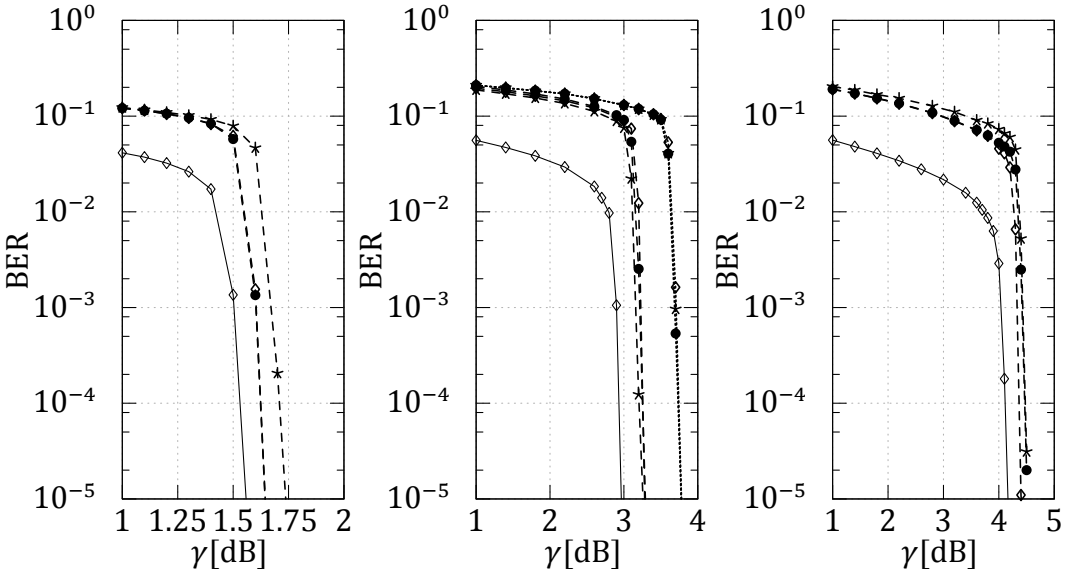

(a) $R_c = \frac{4}{5}$ (b) $R_c = \frac{8}{9}$ (c) $R_c = \frac{16}{17}$

Figure 5.14: BER versus SNR curves for the codes composing the GA designed (dashed) and the reviewed schemes (solid: systematic, dotted: scheme of [70]). The curves are shown for the codes composing the three single attempts of the HARQ scheme (first attempt: $\diamond$, second attempt: $\bullet$, third attempt: $\star$).

predicted decoding thresholds for each attempt.

Note that the presented GA aided design procedure is optimised for obtaining incremental schemes that rely on successive transmissions. Particularly, even though the schemes obtained are robust to erasures, since each attempt is invertible, they are not symmetric, in the sense that the decoding performance after receiving the first and the second attempt is different than the decoding performance achieved combining the first and the third attempts, or the second and the third attempts. This behaviour results from the particular structure of the GA, which optimises the performance of codes relying on the transmission of the whole attempt sequence, and does not account for erasures. Though the design problem of finding code schemes that satisfy the requirements listed in this chapter and, additionally, are symmetric is of interest, it is left for future works.

Finally, Tables 5.1, 5.2 and 5.3 also show the patterns of systematic incremental schemes and of the complementary scheme of [70] for a scenario where $R_c = \frac{8}{9}$.

Consider now the particular case of $R_c = \frac{8}{9}$. It can be seen that each attempt of the GA aided designed code scheme performs within 0.3 dB from the systematic punctured code, that offers the best waterfall performance. The predicted per-

Scheme	Puncturing patterns	Γ_{EXIT}	Coding rate at D
GA designed code	$\mathcal{U}_a^{\text{I}}$: {1 3 5 9 10 14 15 16} $\mathcal{U}_c^{\text{I}}$: {3 4 5 7 8 9 10} $\mathcal{U}_d^{\text{I}}$: {6 8 10}	3.17dB	$R_{c_1}^{D} = 0.889$
	$\mathcal{U}_a^{\text{II}}$: {2 4 6 7 8 11 12 13} $\mathcal{U}_c^{\text{II}}$: {2 11 12 13 14 15 16} $\mathcal{U}_d^{\text{II}}$: {1 2 16}	3.14dB	$R_{c_2}^{D} = 0.444$
	$\mathcal{U}_a^{\text{III}}$: {1 3 6 7 8 10 15 16} $\mathcal{U}_c^{\text{III}}$: {1 5 6 7 9 10 11} $\mathcal{U}_d^{\text{III}}$: {9 13 15}	3.12dB	$R_{c_3}^{D} = 0.39$
Code of [70]	$\mathcal{U}_a^{\text{I}}$: {3 4 5 6 9 10 11 13 15 16} $\mathcal{U}_c^{\text{I}}$: {1 2 7 8 13 14} $\mathcal{U}_d^{\text{I}}$: {1 2}	3.67dB	$R_{c_1}^{D} = 0.889$
	$\mathcal{U}_a^{\text{II}}$: {1 2 5 6 7 8 11 12 13 15} $\mathcal{U}_c^{\text{II}}$: {3 4 9 10 15 16} $\mathcal{U}_d^{\text{II}}$: {6 7}	3.65dB	$R_{c_2}^{D} = 0.516$
	$\mathcal{U}_a^{\text{III}}$: {1 3 4 7 8 9 10 13 14 15} $\mathcal{U}_c^{\text{III}}$: {1 2 5 6 11 12} $\mathcal{U}_d^{\text{III}}$: {11 12}	3.67dB	$R_{c_3}^{D} = 0.42$
Systematic code	$\mathcal{U}_a^{\text{I}}$: {1 ...16} $\mathcal{U}_c^{\text{I}}$: {9} $\mathcal{U}_d^{\text{I}}$: {1}	2.88dB	$R_{c_1}^{D} = 0.889$
	$\mathcal{U}_a^{\text{II}}$: ∅ $\mathcal{U}_c^{\text{II}}$: {1 3 4 5 7 11 13 15} $\mathcal{U}_d^{\text{II}}$: {2 4 6 8 9 10 12 13 14 16}	non invertible	$R_{c_2}^{D} = 0.444$
	$\mathcal{U}_a^{\text{III}}$: {1 5 9 10 12 13} $\mathcal{U}_c^{\text{III}}$: {2 6 8 10 12 14 16} $\mathcal{U}_d^{\text{III}}$: {3 5 7 11 15}	4.95dB	$R_{c_3}^{D} = 0.333$

Table 5.1: GA aided designed and reviewed coding schemes for a code rate of the single attempt equal to $R_c = \frac{8}{9}$.

formance of the codes shown in Table 5.1 is validated by BER curves shown in Figure 5.14.

It can be seen that the codes employed in each attempt of the scheme designed using the GA have a satisfying waterfall behaviour, while the codes composing the complementary scheme of [70] show a noticeably performance downgrade and require additional 0.5 dB to achieve a low BER. The scheme of [70] also transmits

Scheme	Puncturing patterns	Γ_{EXIT}	Coding rate at D
GA designed code	$\mathcal{U}_a^{\text{I}}$: {1 2 3 4 8} $\mathcal{U}_c^{\text{I}}$: {2 3 4} $\mathcal{U}_d^{\text{I}}$: {2 3}	1.57dB	$R_{c_1}^{D} = 0.8$
	$\mathcal{U}_a^{\text{II}}$: {1 5 6 7 8} $\mathcal{U}_c^{\text{II}}$: {1 7 8} $\mathcal{U}_d^{\text{II}}$: {7 8}	1.57dB	$R_{c_2}^{D} = 0.444$
	$\mathcal{U}_a^{\text{III}}$: {2 3 4 5 6} $\mathcal{U}_c^{\text{III}}$: {1 5 6} $\mathcal{U}_d^{\text{III}}$: {1 5}	1.64dB	$R_{c_3}^{D} = 0.364$
Systematic code	$\mathcal{U}_a^{\text{I}}$: {1 ...8} $\mathcal{U}_c^{\text{I}}$: {5} $\mathcal{U}_d^{\text{I}}$: {1}	1.57dB	$R_{c_1}^{D} = 0.8$
	$\mathcal{U}_a^{\text{II}}$: ∅ $\mathcal{U}_c^{\text{II}}$: {1 2 3 4 7} $\mathcal{U}_d^{\text{II}}$: {1 3 5 6 8 }	non invertible	$R_{c_2}^{D} = 0.4$
	$\mathcal{U}_a^{\text{III}}$: {1 4 7} $\mathcal{U}_c^{\text{III}}$: {1 5 6 8} $\mathcal{U}_d^{\text{III}}$: {2 4 7}	2.66dB	$R_{c_3}^{D} = 0.333$

Table 5.2: GA aided designed and systematic schemes for a code rate of the single attempt equal to $R_c = \frac{4}{5}$.

more information bits and hence suffers from a higher coding rate at the destination.

Finally, the performance of the second and third attempts of the systematic incremental scheme is not shown since only parities or few information bits are sent and hence the codes are either not invertible or exhibit a poor waterfall behaviour.

Similar considerations apply to schemes designed using the GA for coding rates of $R_c = \frac{4}{5}$ and $R_c = \frac{16}{17}$. It can be seen again that the performance of the GA designed codes is close to the optimal one of the correspondent systematic solutions.

To evaluate the computational complexity of the proposed GA, the number of candidate codes examined before obtaining a satisfactory scheme is compared with the number of possible punctured code configurations. Consider again the example case of $R_c = \frac{8}{9}$. The first step of the GA was stopped after around 200 stages, i.e. after evaluating around 2000 codes. An average decoding threshold of 3.23 dB was obtained. In comparison, the number N_{codes} of possible punctured schemes transmitting $e = 18$ encoded bits per puncturing period, where $u = 8$ are information

Scheme	Puncturing patterns	Γ_{EXIT}	Coding rate at D
GA designed code	$\mathcal{U}_a^{\text{I}}$: {1 2 3 5 6 7 8 9 10 14 15 16 21 23 26 29} $\mathcal{U}_c^{\text{I}}$: {3 5 6 9 12 15 16 19 20 21 23 24 26 27 28 29} $\mathcal{U}_d^{\text{I}}$: {2 23}	4.29dB	$R_{c_1}^{D} = 0.941$
	$\mathcal{U}_a^{\text{II}}$: {4 11 12 13 17 18 19 20 22 24 25 27 28 30 31 32} $\mathcal{U}_c^{\text{II}}$: {1 2 4 7 8 10 11 13 14 17 18 22 25 30 31 32} $\mathcal{U}_d^{\text{II}}$: {11 31}	4.35dB	$R_{c_2}^{D} = 0.47$
	$\mathcal{U}_a^{\text{III}}$: {3 4 6 9 10 12 15 16 17 21 22 24 25 26 27 30} $\mathcal{U}_c^{\text{III}}$: {5 6 9 10 11 15 16 18 21 23 26 27 28 31 32} $\mathcal{U}_d^{\text{III}}$: {5 7 15}	4.36dB	$R_{c_3}^{D} = 0.45$
Systematic code	$\mathcal{U}_a^{\text{I}}$: {1 ...32} $\mathcal{U}_c^{\text{I}}$: {17} $\mathcal{U}_d^{\text{I}}$: {1}	4.29dB	$R_{c_1}^{D} = 0.941$
	$\mathcal{U}_a^{\text{II}}$: ∅ $\mathcal{U}_c^{\text{II}}$: {1 2 3 5 6 8 11 12 15 18 20 22 23 25 28 29 32} $\mathcal{U}_d^{\text{II}}$: {2 3 4 7 9 10 13 14 16 19 21 22 24 26 27 30 31}	non invertible	$R_{c_2}^{D} = 0.47$
	$\mathcal{U}_a^{\text{III}}$: {6 17 27} $\mathcal{U}_c^{\text{III}}$: {2 4 7 9 10 13 14 16 19 21 24 26 27 30 31} $\mathcal{U}_d^{\text{III}}$: {3 5 6 8 11 12 15 17 18 20 22 23 25 28 29 32}	non invertible	$R_{c_3}^{D} = 0.33$

Table 5.3: GA aided designed and systematic schemes for a code rate of the single attempt equal to $R_c = \frac{16}{17}$.

bits, is:

$$N_{\text{codes}} = \binom{P}{u} \cdot \sum_{p_1=1}^{e-u-1} \binom{P}{p_1} \cdot \binom{P}{e-u-p_1} \simeq 8 \cdot 10^{11} \tag{5.11}$$

Hence, the GA reduces the number of EXIT chart simulations of a 10^8 factor compared to a deterministic full search.

Figure 5.13 also shows that running only 50 stages of the proposed GA allows one to contrive code schemes having no repeated bits in the first two attempts (i.e. obtaining a coding rate of $R_{c_2}^{D} = 0.444$) that perform within 0.7 dB from the channel capacity, achieved at $\Gamma_c = 2.51$ dB, and within 0.3 dB from the optimal systematic code. Hence, the GA is capable of obtaining satisfactory code schemes requiring a reasonable computational cost, opposed to the unfeasible full search required by a deterministic approach.

To further quantify how remarkable the results given by the GA are, the obtained codes are compared with the best ones obtained adopting a random search. Random searches are low complexity algorithms that have been used to obtain satisfying individuals from large search spaces [94].

After simulating 5000 schemes consisting of one attempt, none obtained a better decoding threshold than the one of the GA aided designed code. In particular, only 2 and 21 schemes performed, respectively, within 0.15 dB and 0.5 dB from the GA aided code.

Finally, 5000 codes formed by two attempts were randomly selected and their performance compared to the GA aided designed one. Again none performed better than the one designed by the proposed GA. Adding more, only 12 codes, representing the 0.24% of the searched schemes, had the same coding rate and decoding thresholds within 0.5 dB from the ones of the GA aided designed scheme.

Hence, the GA outperformed the random search, even considering that the latter required an higher computational complexity, since it evaluated a number of codes 2.5 and 10 times higher than the first and second steps of the GA, respectively.

To further elaborate on the computational complexity, simulating a stage of the proposed GA requires around 15 minutes when run on a 2.5 GHz Intel i5 CPU. Hence, the proposed GA is not suited for real time operations. Note that this is not a limitation, since the aim of the GA of designing capacity-approaching punctured codes is well fulfilled by an off-line operation.

Note also that the complexity of the search algorithm is of paramount importance due to the high number of possible solutions. More explicitly, it would be unfeasible to perform an exhaustive search to derive the optimum punctured scheme in a reasonable amount of time, particularly when the puncturing period increases.

Finally, it can be shown that the genetic aided designed codes are capable of performing close to the theoretical system limit obtained using the SPB. Particularly, the simulated curves that were shown in Chapter 4 were obtained using the code having rate of $R_c = \frac{8}{9}$ and designed using the GA, that is listed in Table 5.1. It was shown that such code approached the limiting performance, and the results are shown again for clarity purposes in Figures 5.15 and 5.16, where the actual performance of the HARQ system transmitting three attempts and using the GA aided designed code is recorded over slow and block fading scenarios, respectively.

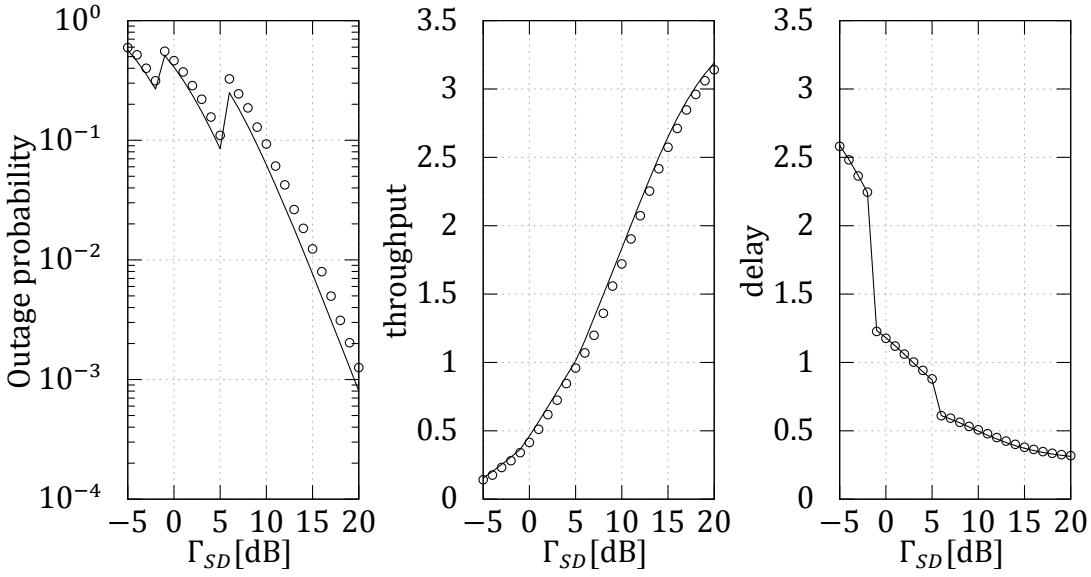

Figure 5.15: Comparison between the simulated performance of the HARQ system transmitting three attempts and based on the GA aided designed code of rate $R_c = \frac{8}{9}$ (○) and the theoretical values predicted using the SPB (solid) in a slow faded regime.

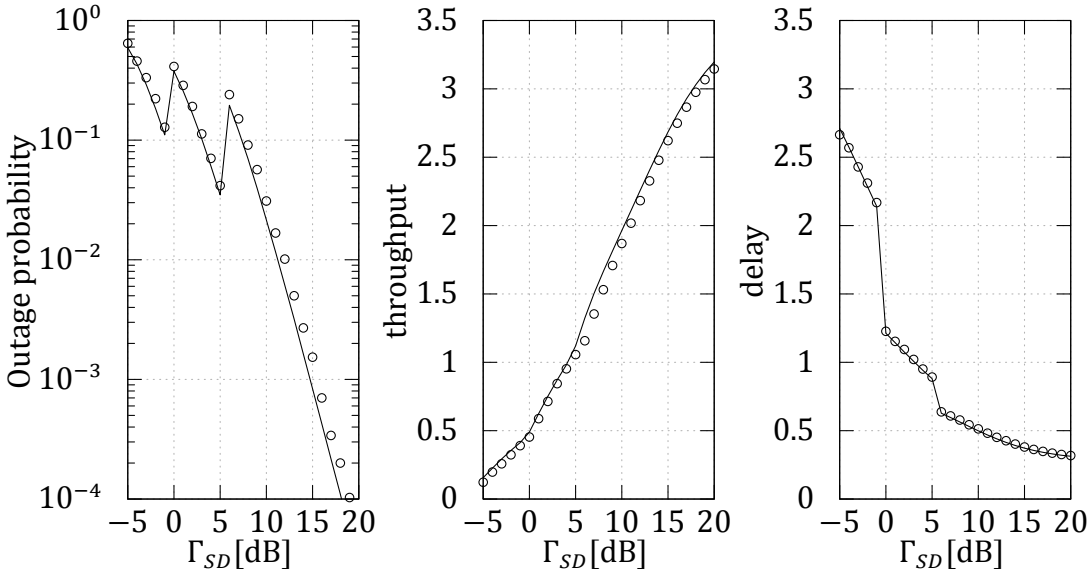

Figure 5.16: Comparison between the simulated performance of the HARQ system transmitting three attempts and based on the GA aided designed code of rate $R_c = \frac{8}{9}$ (○) and the theoretical values predicted using the SPB (solid) in a block faded regime.

Again, one can note that the proposed code scheme closely parallels the limiting performance of the system, showing that the GA aided code scheme design algorithm is capable of contriving efficient HARQ systems for the cooperative channel.

5.5 Conclusions

The chapter considered the design problem of finding practical distributed channel coding techniques that are capable of approaching the system limiting performance. The chapter proposed a novel genetic algorithm aided design approach for contriving punctured turbo codes for the transmissions of the source and relay stations. Furthermore, for selecting punctured codes that compose balanced schemes and provide remarkable waterfall performance, the chapter introduced a novel tri-dimensional EXIT chart analysis that correctly predicts the behaviour of non-systematic periodically punctured turbo codes. The chapter shown that the novel code design algorithm allows contriving distributed schemes that closely parallel the limiting performance predicted using the SPB.

6

Design and analysis of cooperative medium access control protocols

The cooperative approach is not limited to the physical layer, and it may be used as a base for designing cooperative MAC schemes where the transmission of a source station is aided by a relay. This chapter presents the design procedure of a novel cooperative MAC protocol. The novel protocol is designed using a cross-layer approach, where the PHY and MAC layer are jointly considered for the sake of exploiting the benefits of distributed channel coding at the MAC layer. The chapter also details a theoretical formulation for assessing the performance of the novel cross-layer protocol.[1]

6.1 Introduction

A cooperative design approach allows nodes equipped with a single antenna to share their information forming a virtual antenna array in order to exploit the spatial diversity provided by independently faded antenna elements. As shown in the previous chapters the literature on physical layer cooperative techniques is rich. Recently, a cooperative approach has been used for designing novel MAC protocols. Cooperative MAC schemes reduce the negative effects on the throughput of slow 802.11 stations [39, 40] by enabling faster multi-hop communications using relays with better channel conditions.

Cooperative MAC schemes may be found in [41, 42, 43, 45, 47, 50, 95]. The main limit of the above-mentioned references lies in adopting an ideal channel model

[1]The content of this chapter is based on F. Babich, A. Crismani and L. Hanzo, ``Cross-Layer solutions for cooperative medium access control protocols'', presented at the IEEE Vehicular Technology Conference, Taipei (Taiwan), May 2010, and on F. Babich and A. Crismani, ``Incremental and complementary coding techniques for cooperative medium access control protocols'', presented at the IEEE Vehicular Technology Conference, Budapest (Hungary), May 2011.

and over-simplified assumptions for the physical-layer. In particular, the theoretical analysis performed in [45, 95] considers a simplified adaptive regime, where data rates are fixed on each link and are based on the distance between stations, while outage is not taken into account. Furthermore, the works of [45, 95] fail to take into account the contribution of the signal gleaned by the destination from the source station and are not able to exploit the benefits offered by distributed physical-layer techniques. The cross-layer designed protocol of [42] considers a joint decoding at the destination of signals received from the source and the relay. However its benefits are not exploited by the adaptive regime algorithm and the analysis is based on idealised conditions which do not take into account channel coding.

This chapter investigates the effects of different channel coding schemes and provides adaptive regime rules to exploit their benefits at the MAC layer. A novel cooperative MAC protocol is designed extending the popular CoopMAC [42, 45] protocol in a cross-layer design fashion.

The novel protocol incorporates the benefits of PHY layer distributed coding by allowing the relay to forward different information than the one transmitted by the source station. Different forwarding coding schemes are investigated to address HARQ design issues, which are exacerbated in distributed scenarios.

The performance of the studied cooperative protocols are also analytically derived, extending the theory of [96, 97, 98] by introducing a more realistic channel model which accounts for fading impairments, adaptive modulation schemes, outage situations and channel coding. More explicitly, a finite state Markov chain models the backoff behaviour of a contending station while the ON-OFF approximation based on the SPB theory of Chapter 4 is used for assessing the performance of the selected channel code and modulation pair.

6.2 Extending the CoopMAC protocol for including distributed channel coding

As introduced and reviewed in Chapter 2, the CoopMAC protocol is a popular access scheme which extends the IEEE 802.11 DCF for enabling cooperative communications. The main drawback of the classic CoopMAC scheme is that the source and relay stations transmit the same information, while incremental schemes were shown to achieve a higher performance in previous chapters. Furthermore, in the CoopMAC protocol, the destination does not combine the signals gleaned from the source and relay stations, and rely only on the information received from the relay for decoding the frame. It is then of interest to extend the CoopMAC protocol in a cross-layer fashion using distributed channel coding techniques for improving the

decoding and ultimately the network performance.

6.2.1 The considered network scenario

Consider a normalised scenario, where $|\mathcal{N}|$ stations equally spaced on a circle with radius $R = 1$ transmit to an access point placed in the middle of the circle. The normalised scenario allows a fair comparison among different schemes, although the analysis may be easily extended to different topologies.

Assume that a station checks the channel conditions when it attempts a packet transmission. Block non-dispersive Rayleigh fading is considered, hence the instantaneous SNR of every frame's transmission between two stations ``$A$'' and ``B'' is given by:

$$\gamma_{AB} = h_{AB}\,\Gamma_{AB}, = h_{AB}\,\frac{\Gamma}{d^{\alpha}(a,b)}, \tag{6.1}$$

where h_{AB} is an exponentially distributed random variable with unity mean and variance, Γ_{AB} represents the average SNR characterising the AWGN, $\alpha = 3$ is the path-loss exponent, $d(a,b)$ is the distance between A and B and Γ is the average SNR at a distance equal to $d = R = 1$, i.e. the average SNR on the link between a station and the access point. Since block fading is assumed, the instantaneous SNR remains constant over a packet transmission, while it changes during the access period and when a station finishes its backoff the channel state is independent from previous values.

This chapter assumes that the source station has a perfect knowledge of the channel conditions of every link in the network. Even though this assumption is strong, it allows one to assess the limiting performance of the considered protocols. The performance of cooperative MAC protocols relying on imperfect channel knowledge is analysed in the next chapter.

6.2.2 The proposed adaptive regime for incremental encoding aided protocols

Assume to extend the CoopMAC protocol by allowing the relay station to forward different bits than the ones transmitted by the source station, in order to operate with a lower coding rate at the destination.

Particularly, consider a scenario where the relay decodes the information transmitted from the source station, re-encodes it using an incremental scheme and forwards it to the destination. The destination in turn combines the information gleaned from both the source and the relay stations performing a joint decoding. Furthermore, assume that the distributed encoding technique used is efficient, in

the sense that it operates near the limiting performance of the cooperative channel. The consequences of the coding scheme selection are thoroughly investigated in the following of the chapter.

Previous chapters shown that performing a joint decoding at the destination yields an improved error performance. Such performance increase may be exploited for selecting higher order modulation modes and for compensating the higher SNR required in order to meet a target error performance at the destination. Hence, incremental schemes may be used for enabling more aggressive adaptive strategies, obtaining faster transmissions whilst maintaining a target decoding performance. Particularly, the cross-layer protocol proposed exploits the benefits of the joint decoding at the destination, which decreases the SNR required on the relay-destination link for a successful transmission, by introducing a novel adaptive algorithm at the relay station.

The adaptive scheme selects the transmission mode from a finite set containing K available modulation modes. Opposed to recently published works mentioned in Chapter 2, where the transmission rates are decided using distances between stations or simulations of the used channel codes, the proposed adaptive regime is based on the SPB and on an ON-OFF approximation of the channel code, as detailed in Chapter 4. Relying on the SPB allows obtaining a limiting performance and avoids tying the protocol to a particular channel coding scheme.

Consider at first the transmission of the source station. This transmission may be either adapted to the SNR of the source-destination link, in the case of a direct communication, or to the SNR of the source-relay link in the case where cooperation is invoked. In both situations, the SPB is used for assessing the switching threshold $\gamma_t|^i_{\text{dB}}$ that allows selecting the i-th transmission rate $\mathcal{R}^i$, which derives from using a specific modulation mode $\mathcal{M}^i$.

Particularly, the threshold $\gamma_t|^i_{\text{dB}}$ is obtained as the SNR value, augmented by an offset $\psi|_{\text{dB}}$, that satisfies Equation (4.7) with an equal operator. If the actual SNR on the link is higher than $\gamma_t|^i_{\text{dB}}$, then the i-th modulation mode may be used for transmitting the information. The offset value $\psi|_{\text{dB}}$ accounts for the performance gap that separates the actual behaviour of the used channel code and the limiting block error ratio value derived using the SPB. Furthermore, an additional offset $\xi|_{\text{dB}} = 0.5$ dB is considered for selecting the modulation mode between the source station and possible relays in order to avoid the error propagation phenomenon of decode-and-forward and coded cooperation schemes.

The switching thresholds for the six considered modulation modes are shown in Table 6.1. A coding rate of $R_c = \frac{8}{9}$, a packet length of $P = 9000$ bits and a target BLER of $P_B = 10^{-1}$ are considered in the following of the paper as an example and without any loss of generality, given that the analysis, the protocol design procedure and the considerations presented apply to any coding rate and number of

transmission rate $\mathcal{R}$	modulation mode $\mathcal{M}$	switching threshold $\gamma_t\|_{\text{dB}}$
1 Mbps	BPSK	2.8 dB
2 Mbps	QPSK	5.6 dB
3 Mbps	8-PSK	10.2 dB
4 Mbps	16QAM	12.1 dB
5 Mbps	4-12-16APSK	14.9 dB
6 Mbps	64QAM	17.7 dB

Table 6.1: Used modulations and corresponding rates and thresholds for $\psi|_{\text{dB}} = 0$ dB, $B = 9000$ bits, $R_c = \frac{8}{9}$ and $P_B = 10^{-1}$.

encoded bits. Furthermore, the analysis may be easily extended to incorporate code rate adaptation by considering different rate-modulation pairs among the available transmission modes and by denoting with $\gamma_t|^j_{\text{dB}}$ the switching threshold for the j-th code rate-modulation mode pair.

The SPB is also used for the novel adaptive algorithm at the relay. More explicitly, when adopting a joint decoding of the signal transmitted by the source and relay stations, the switching thresholds used for selecting the modulation on the relay-destination link depend on both the modulation $\mathcal{M}^j$ chosen on the source-relay link and on the value γ_{SD}.

The novel thresholds $\gamma_{t_R}^l|\mathcal{M}^j, \gamma_{SD}$ are calculated according to the SPB analysis presented in Chapter 4, and particularly are obtained as the SNR value on the relay-destination link required for satisfying Equation (4.27) with an equal operator. Again, the thresholds γ_{t_R} include the offset $\psi|_{\text{dB}}$ for accounting for the gap between the limiting error performance and the actual behaviour of the used channel code.

6.2.3 The selection of used transmission mode

The source station decides whether to transmit directly to the destination or to invoke cooperation before initiating its communication, in a proactive fashion. The decision is based on a transmission duration minimisation criterion.

More particularly, the source station selects the transmission mode and the relay that provide the most prompt transmission for the given channel conditions γ_{SD}, $\left\{\gamma_{SR}^h\right\}_{h\in\mathcal{H}}$ and $\left\{\gamma_{R_hD}\right\}_{h\in\mathcal{H}}$, where $\mathcal{H}$ is the set that enumerates all available relay stations. Assume to use the i-th transmission mode $\mathcal{M}^i$ on the source-destination link and denote the duration of the direct transmission using the mode $\mathcal{M}^i$ with T_i^{dir}. Similarly, consider a particular relay $h \in \mathcal{H}$ and assume to transmit using the modulation modes $\mathcal{M}^j$ and $\mathcal{M}^l$, respectively on the source-relay and relay-destination links. Denote the duration of the cooperative communication through the relay h using the modulation modes $\mathcal{M}^j$ and $\mathcal{M}^l$ with $T_{j,l}^{r_h}$.

The duration of the direct transmission depends on the modulation mode $\mathcal{M}^i$ and may be obtained as:

$$T_i^{\text{dir}} = T_{\text{RTS}} + T_{\text{CTS}} + \frac{H_{\text{PHY}}}{\mathcal{R}^1} + \frac{H_{\text{MAC}} + \mathcal{E}[P]}{\mathcal{R}^i} + T_{\text{ACK}} + 3 \text{ SIFS} + \text{DIFS}. \tag{6.2}$$

Similarly, the duration of the cooperative transmission depends on the modulation modes $\mathcal{M}^j$ and $\mathcal{M}^l$ and may be calculated as: and

$$\begin{aligned} T_{j,l}^{r_h} =& T_{\text{RTS}} + T_{\text{HTS}} + T_{\text{CTS}} + 2\,\frac{H_{\text{PHY}}}{\mathcal{R}^1} + \frac{H_{\text{MAC}} + \mathcal{E}[P]}{\mathcal{R}^j} + \frac{H_{\text{MAC}} + \mathcal{E}[P]}{\mathcal{R}^l} + \\ & T_{\text{ACK}} + 5 \text{ SIFS} + \text{DIFS}. \end{aligned} \tag{6.3}$$

Denote the duration of a direct communication using the available transmission mode that provides the most prompt transmission with T^{dir}. A mode $\mathcal{M}^i$ is said to be available on the source-destination link if its enabling threshold γ_t^i is lower than the actual value of γ_{SD}. The duration T^{dir} may be obtained as:

$$T^{\text{dir}} = \text{argmin}\{T_i^{\text{dir}}\} \quad \text{subject to } i : \gamma_t^i \leq \gamma_{SD}. \tag{6.4}$$

Similarly, consider the h-th available relay and denote the duration of the cooperative communication using the available modulation modes that provides the most prompt transmission with T^{r_h}. Such duration may be obtained as:

$$T^{r_h} = \text{argmin}\{T_{j,l}^{r_h}\} \quad \text{subject to } j, l : (\gamma_t^j \leq \gamma_{SR}) \wedge (\gamma_{t_R^l} | \mathcal{M}^j, \gamma_{SD} \leq \gamma_{RD}). \tag{6.5}$$

Finally, the source station decides to cooperate if a relay provides a transmission having a smaller duration than the direct on, i.e. cooperation is invoked if:

$$T^{r_{h^*}} < T^{\text{dir}}, \tag{6.6}$$

where h^* indicates the relay in $\mathcal{H}$ that provides the most prompt transmission, obtained as.:

$$h^* = \underset{h \in \mathcal{H}}{\text{argmin}}\{T^{r_h}\}. \tag{6.7}$$

The transmission durations are related to the transmission rates derived using the SPB and hence are likely to provide successful communications. Conversely, when no transmission modes are available, the transmission is likely to be unsuccessful. Hence, the source station believes to be in an outage situation when the instantaneous SNRs on the source-destination link and on either the source-relay or the relay-destination link for each relay are lower than the threshold enabling the BPSK mode. When the source station is in outage, it defers the packet transmission procedure to a later time and resumes its backoff procedure, as if the packet collided or was unsuccessfully received.

6.3 Analytic formulation of the network performance

For avoiding time consuming simulations, it is interesting to model the network performance of the proposed protocol and to obtain an analytic formulation for the throughput, the outage probability and the delay values. The analytic approach is detailed in the following of the section.

The theoretical analysis is divided into three parts. The mean duration for a successful transmission and the probability that a station defers the transmission to a later time due to outage are derived in the first part for the DCF and for cooperative schemes. The second part models the backoff process of a contending station using a bi-dimensional Markov chain. The Markov model for the backoff process of a station is obtained extending the results of [96, 97, 98] by accounting for outage situations and coded adaptive modulation schemes. Finally, the mean saturation throughput and the average packet delay are obtained by accounting for all the diverse events that may occur during a single network slot.

6.3.1 Average successful transmission duration and outage probability

Consider at first the legacy DCF access scheme used in the IEEE 802.11 standard protocol. The DCF is a non-cooperative protocol and it only allows direct transmissions from the source station to the destination.

As detailed in the previous section, the duration of the direct communication depends on the particular modulation mode adopted, since it defines the transmission rate. The probability of choosing the i-th modulation mode for a direct communication may be obtained as:

$$\begin{aligned} P\{\mathcal{M}^i\} &= P\{\gamma_t^i < \gamma_{SD} < \gamma_t^{i+1}\} \\ &= \exp\left(-\frac{\gamma_t^i}{\Gamma_{SD}}\right) - \exp\left(-\frac{\gamma_t^{i+1}}{\Gamma_{SD}}\right), \end{aligned} \tag{6.8}$$

where $\mathcal{M}^0$ represents an outage situation, $\gamma_t^0 = 0$ and $\gamma_t^{K+1} = +\infty$. From the previous definition, one can also obtain the probability of outage for the DCF scheme as:

$$P_{\text{out}}^{\text{dir}} = P\{\gamma_{SD} < \gamma_t^1\} = P\{\mathcal{M}^0\}. \tag{6.9}$$

As previously detailed, each modulation mode $\mathcal{M}^i$ ($i \in [1, K]$) corresponds to a transmission duration T_i^{dir} calculated according to (6.2). From this consideration follows that the average duration $\overline{T_S}$ of a successful transmission from the source

station to the destination is:

$$\overline{T_S} = \mathcal{E}[T^{\text{dir}}] = \frac{\sum_{i=1}^{K} T_i^{\text{dir}} P\{\mathcal{M}^i\}}{1 - P_{\text{out}^{\text{dir}}}}, \tag{6.10}$$

where, in order to consider only successfully received packets, the expected value operator takes into account only transmissions which do not experience outage situations.

Consider now the cross-layer cooperative MAC scheme relying on the modified adaptive regime at the relay introduced in the previous section. The considerations made for a direct communication using the DCF protocol still apply to the cooperative scheme, when source to destination transmissions take place. It is however interesting to consider a transmission that relies on cooperation.

The transmission duration in a cooperative scenario depends on the modulation modes chosen on the source-relay and relay-destination links. In turn, such modulation mode couple depends on the particular channel quality of the source-destination link, given that a joint decoding procedure is used at the destination. Particularly, given a value of SNR on the source-destination link γ_{SD}, the probability $P\{\mathcal{M}^j, \mathcal{M}^l|\gamma_{SD}\}$ that the couple $(\mathcal{M}^j, \mathcal{M}^l)$ is chosen for the source-relay and relay-destination transmissions, respectively, using the h-th relay may be calculated as:

$$\begin{aligned} P\{\mathcal{M}^j, \mathcal{M}^l|\gamma_{SD}\} =& P\{\mathcal{M}^l|\mathcal{M}^j, \gamma_{SD}\} P\{\mathcal{M}^j\} \\ =& \left[\exp\left(\frac{\gamma_{t_R}^{\ l}|\mathcal{M}^j, \gamma_{SD}}{\Gamma_{R_hD}}\right) - \exp\left(\frac{\gamma_{t_R}^{\ l+i}|\mathcal{M}^j, \gamma_{SD}}{\Gamma_{R_hD}}\right)\right] \times \\ & \left[\exp\left(\frac{\xi\ \gamma_t^j}{\Gamma_{SR_h}}\right) - \exp\left(\frac{\xi\ \gamma_t^{j+1}}{\Gamma_{SR_h}}\right)\right], \end{aligned} \tag{6.11}$$

where again choosing the modulation mode $\mathcal{M}^0$ on a link means that the link is in outage.

More explicitly, a cooperative link is in outage if at least one between the source-relay link or the relay-destination link is in outage. Hence, the outage probability $P_{\text{out}}^{R_h}$ for the h-th relay may be obtained as:

$$P_{\text{out}}^{R_h}|\gamma_{SD} = \sum_{j=0}^{K} P\{\mathcal{M}^j, \mathcal{M}^0|\gamma_{SD}\} + \sum_{l=1}^{K} P\{\mathcal{M}^0, \mathcal{M}^l|\gamma_{SD}\}. \tag{6.12}$$

The overall transmission is in outage when the direct link is in outage, i.e. when the value γ_{SD} is lower than the threshold that enables the BPSK modulation mode, and all the relay aided links are in outage, given the particular value of γ_{SD}. More

particularly, the outage probability of the cooperative system P_{out} may be calculated as:

$$P_{\text{out}} = \int_0^{\frac{\gamma_t^1}{\Gamma_{SD}}} \prod_{h \in \mathcal{H}} (P_{\text{out}}^{R_h} | \gamma_{SD}) f_{\gamma_{SD}}(\gamma_{SD}) \mathrm{d}\gamma_{SD}, \tag{6.13}$$

where $f_X(x)$ denotes the probability density distribution of a continuous random variable X. Denote also the cumulative distribution function of a random variable X with $F_X(x)$.

As previously described, each modulation mode couple $(\mathcal{M}^j, \mathcal{M}^l)$ $(j, l \in [1, K])$ corresponds to a transmission duration $T_{j,l}^{r_h}$ when invoking the help of the h-th relay. The duration is calculated according to (6.3).

Given that each modulation mode couple, and in turn each value for the transmission duration, is selected with probability $P\{\mathcal{M}^j, \mathcal{M}^l | \gamma_{SD}\}$, one may calculate the probability $F_{T^{r_h}}(x)$ that the duration is less than a value x by summing the probabilities of modulation modes that provide transmissions having durations smaller than x. Similarly, one may calculate the probability $F_{T^{\text{dir}}}(x)$ that the direct communication lasts less than x by summing the probabilities of selecting modulation modes for the source-destination link that provide transmission having durations that are less than x.

Recall now that, being $Z = \min(X, Y)$, where X and Y are independent random variables, one has:

$$F_Z(Z) = 1 - (1 - F_X(x)) - (1 - F_Y(y)). \tag{6.14}$$

As detailed in the previous section, the transmission mode selection rule operates following a duration minimisation criterion. Particularly, the duration T of the transmission made by a source station may be obtained as the minimum between the duration of a direct transmission and the duration of each relay-aided communication, i.e.:

$$T = \min(T^{\text{dir}}, T^{r_1}, \ldots, T^{r_{|\mathcal{H}|}}). \tag{6.15}$$

It follows from the previous equation that the probability $F_T(x) = P\{T \leq x\}$ that an ongoing transmission lasts less than x may be evaluated as:

$$F^T(x) = 1 - \int_0^{+\infty} \left(1 - F_{T^{\text{dir}}}(x)\right) \prod_{h \in \mathcal{H}} \left(1 - F_{T^{r_h}}(x)\right) f_{\gamma_{SD}}(\gamma_{SD}) \mathrm{d}\gamma_{SD}, \tag{6.16}$$

Finally, the average duration of a successful communication $\overline{T_S}$ may be obtained as:

$$\overline{T_S} = \mathcal{E}\left[\frac{T}{1 - P_{\text{out}}}\right], \tag{6.17}$$

where again only transmissions that do not experience outage are considered.

6.3.2 Markov chain based model for the backoff procedure of a cooperative station

The average duration of a communication models the behaviour of a station when it already accessed the channel and hence it is ready for transmitting its information. For reaching such a state, a station has to undergo through a backoff procedure for reducing the changes of colliding with another station that wants to transmit its packet. The backoff procedure of the single station is analysed in the following of the section.

Consider a discrete time scenario, where t and $t+1$ mark the beginning of consecutive time slots. Let $b(t)$ and $s(t)$ be the stochastic processes representing the backoff counter and the backoff state of a contending station. References [96, 97, 98] model the joint stochastic process $\{s(t), b(t)\}$ with a finite state Markov chain, assuming that the probability p_c that a transmitted packet collides does not depend on the backoff state. In the proposed protocol, however, a transmission may also fail because of an outage situation.

The analytic results of [96, 97, 98] may be extended in order to account for outage by noting that a transmission attempt fails either when a station estimates an outage situation or due to a packet collision, when the station is not in outage. Hence, the probability p_F that an attempt fails may be expressed as:

$$p_F = P_{\text{out}} + (1 - P_{\text{out}})p_c, \tag{6.18}$$

where P_{out} is the outage probability derived in the previous part.

The finite state Markov chain modelling the backoff process of a station is shown in Figure 6.1. The quantities included in Figure 6.1 are the following: m is the maximum retry limit, i.e. the maximum number of times a single packet is retransmitted after its previous transmissions failed; m' is the maximum backoff stage, i.e. the maximum number of times that the contention window is doubled, W_0 is the minimum contention window and, finally, W_i is the contention window in the state $s(t) = i$ and is equal to:

$$W_i = \begin{cases} 2^i W_0 & \text{if } i \leq m' \\ 2^{m'} W_0 & \text{if } m' < i \leq m \end{cases}. \tag{6.19}$$

Denote the transition probability $P\{s(t+1) = i, b(t+1) = k | s(t) = h, b(t) = l\}$ with $P\{i, k|h, l\}$. The only non-zero probabilities that characterise the Markov chain are:

$$\begin{cases} P\{i, k|i, k+1\} = 1 & k \in [0, W_i - 2], \quad i \in [0, m] \\ P\{0, k|i, 0\} = (1 - p_F)/W_0 & k \in [0, W_0 - 1], \quad i \in [0, m-1] \\ P\{i, k|i-1, 0\} = p_F/W_i & k \in [0, W_i - 1], \quad i \in [1, m] \\ P\{0, k|m, 0\} = 1/W_0 & k \in [0, W_0 - 1] \end{cases}. \tag{6.22}$$

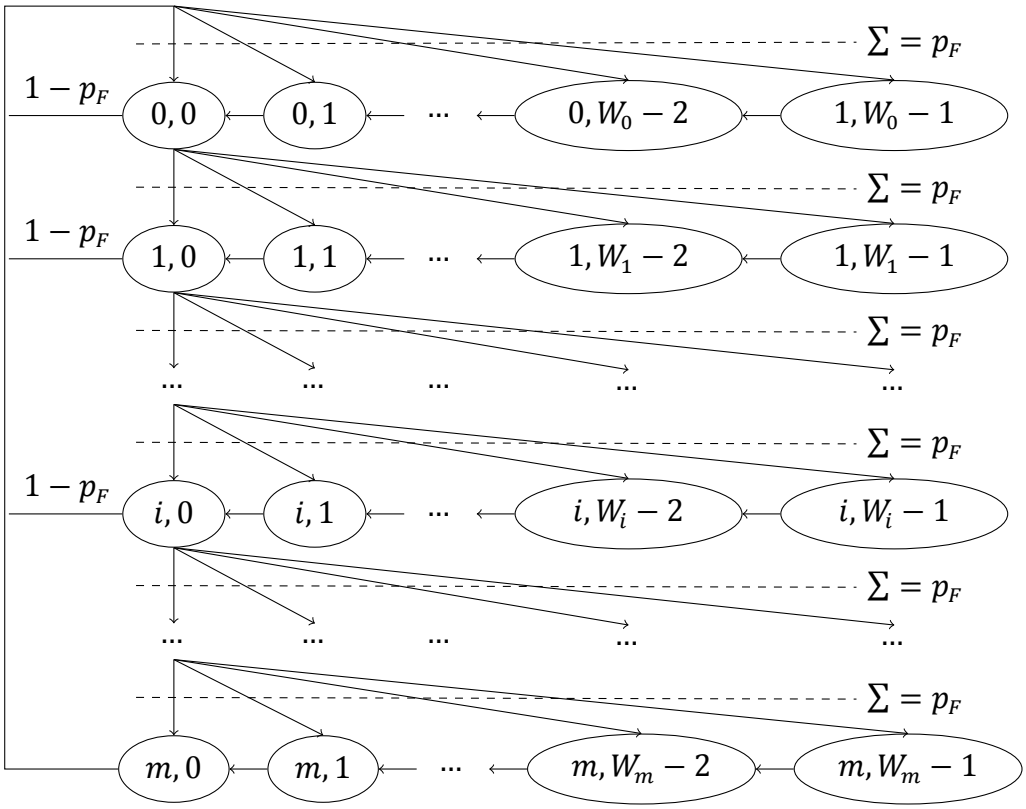

Figure 6.1: Markov chain used to model the backoff process of a contending station.

Consider now the evolution over time of the Markov chain. Particularly, let $b_{i,k}$ denote the stationary chain distribution, i.e.:

$$b_{i,k} = \lim_{t \to \infty} P\{s(t) = i, b(t) = k\}. \tag{6.23}$$

Noting that $b_{i,0} = p_F \cdot b_{i-1,0}$ one can obtain:

$$b_{i,0} = p_F^i \cdot b_{0,0}. \tag{6.24}$$

Then, the stationary probability for a generic state may be evaluated as:

$$b_{i,k} = \frac{W_i - k}{W_i} \begin{cases} (1 - p_F) \sum_{j=0}^{m-1} b_{j,0} + b_{m,0} & i = 0 \\ p_F \, b_{i-1,0} & i \in [1, m] \end{cases}. \tag{6.25}$$

and substituting the expression for $b_{i,0}$ one has:

$$b_{i,k} = \frac{W_i - k}{W_i} \, p_F^i \, b_{0,0}. \tag{6.26}$$

Finally, the stationary distribution is obtained imposing:

$$\sum_{i=0}^{m}\sum_{k=0}^{W_i} b_{i,k} = 1. \tag{6.27}$$

Opposed to [96, 97, 98], where the source station tries to send a packet when its backoff counter reaches zero, the proposed cross-layer protocol avoids transmitting if the station is in outage. Hence, a transmission occurs only if the source station has at least an available way of transmitting to the destination, either using a direct communication or invoking cooperation. From this follows that the probability τ that a chosen station transmits in a random time slot may be evaluated as:

$$\tau = (1 - P_{\text{out}}) \sum_{i=0}^{m} b_{i,0} = \frac{1 - p_F^{m+1}}{1 - p_F}(1 - P_{\text{out}})\, b_{0,0}. \tag{6.28}$$

A collision occurs when more than one station is transmitting in the considered time slot, which happens with probability:

$$p_c = 1 - (1 - \tau)^{|\mathcal{N}|-1}. \tag{6.29}$$

Equations (6.18), (6.28), and (6.29) represent a non-linear system which may be numerically solved to obtain the values τ, p_c and p_F for a given number $|\mathcal{N}|$ of contending stations.

6.3.3 Saturation throughput and average packet delay

The backoff model of a station characterises the behaviour of the single node composing the network. For obtaining the throughput and delay values it it necessary to analyse how the single stations interact together and influence the events that may happen in a time slot. Such analysis is detailed in the following part, completing the theoretical model for the network performance of the cross-layer cooperative protocol proposed in the previous section.

Consider a single time slot of duration σ. The probability p_{tr} that at least one station is transmitting in the particular considered slot is:

$$p_{\text{tr}} = 1 - (1 - \tau)^{|\mathcal{N}|}. \tag{6.30}$$

Recalling that a packet that is transmitted will be successfully received if there are no other active communications in the same slot, the probability p_S that a transmitted packet is correctly received by the destination in the time slot is given by:

$$p_S = \frac{|\mathcal{N}|\tau(1 - \tau)^{|\mathcal{N}|-1}}{p_{\text{tr}}}, \tag{6.31}$$

From the previous considerations it follows that a randomly chosen time slot is empty with probability $(1 - p_{\text{tr}})$, hosts a successful transmission with probability $p_{\text{tr}}p_S$ or contains a collision with probability $p_{\text{tr}}(1 - p_S)$. From the previous slot characterisation, and following the steps of [96], the average time between two consecutive backoff decrements E_s may be calculated as:

$$E_s = (1 - p_{\text{tr}})\sigma + p_{\text{tr}}p_S\overline{T_S} + p_{\text{tr}}(1 - p_S)T_{\text{coll}}, \tag{6.32}$$

where $\overline{T_S}$ is the average duration of a successful transmission for the considered access scheme, which was derived in the first step of the analysis, and T_{coll} is the time wasted when colliding, obtained as:

$$T_{\text{coll}} = T_{\text{RTS}} + \texttt{timeout}. \tag{6.33}$$

Denoting with $p_D = p_F^{m+1}$ the probability that a packet is dropped and recalling that the backoff counter in the state $s(t) = i$ is uniformly distributed between 0 and $W_i - 1$, the mean number of time slots required to successfully transmit a packet E_{sn} is [98]:

$$\begin{aligned} E_{\text{sn}} &= \sum_{i=0}^{m} \frac{W_i - 1}{2} \frac{p_F^i - p_D}{1 - p_D} \\ &= \frac{p_D[W + m + 1 - W\,2^{m'}\,(m - m' + 2)]}{2(1 - p_D)} + \frac{W[1 - (2p_F)^{m'+1}]}{2(1 - p_D)(1 - 2p_F)} + \\ &\quad \frac{W\,2^{m'}(p_F^{m'+1} - p_D) + p_D - 1}{2(1 - Pd)(1 - p_F)}. \end{aligned} \tag{6.34}$$

Finally, the mean saturation throughput $\mathcal{S}$ and the average delay $\mathcal{D}$ may be evaluated as [96, 98]:

$$\mathcal{S} = \frac{p_S\,p_{\text{tr}}\,\mathcal{E}[P]}{E_s}, \tag{6.35}$$

and

$$\mathcal{D} = E_{\text{sn}}\,E_s. \tag{6.36}$$

6.4 Network performance of the proposed cooperative protocol

This section presents simulated results for the performance of the proposed cross-layer designed cooperative MAC protocol. The simulated results are compared with the performance obtained using the CoopMAC protocol as well as with the

Parameter	Value
SIFS duration	10 μs
DIFS duration	50 μs
RTS duration	352 μs
HTS, CTS, ACK durations	304 μs
H_{PHY}	192 bits
H_{MAC}	272 bits
W_0	32
m, m'	5
Packet length P	9000 bits
Slot time σ	20 μs

Table 6.2: 802.11 Parameters used in MAC protocols simulations.

non-cooperative IEEE 802.11 standard DCF algorithm. Furthermore, the performance values are also compared with the analytic values obtained following the steps shown in the previous section. Monte-Carlo simulations have been performed using a discrete-time custom made simulator written in the C++ programming language with the aid of IT++ libraries [99].

Table 6.2 provides a summary of the parameters used in the simulations. Furthermore, different distributed coding techniques are used at the PHY layer of the cross-layer designed MAC protocol for assessing the influence of the channel coding scheme on the network performance.

Figure 6.2 compares the theoretical saturation throughput, the mean packet delay and the outage performance for the DCF, the CoopMAC and the proposed MAC protocols. The first two attempts of the genetic algorithm aided designed HARQ scheme having a rate of $R_c = \frac{8}{9}$ and listed in Table 5.1 of Chapter 5 are used for the transmissions of the source and relay stations, respectively. Finally, a value $\psi|_{\text{dB}} = 0.8\,\text{dB}$ is used for repetitive schemes and a less aggressive value $\psi|_{\text{dB}} = 1.3\,\text{dB}$ is used for the cross-layer scheme that relies on distributed coding. Furthermore, the additional offset $\xi|_{\text{dB}}$ used for determining the thresholds of source to relay transmissions is set to $\xi = 0.5\,\text{dB}$. The influence of the threshold values will be analysed in the following of the section.

It can be seen from Figure 6.2 that the novel scheme offers the highest saturation throughput as well as the lowest outage probability among the studied algorithms. It also helps reducing the delay compared to the CoopMAC protocol and it achieves the lowest delay value when the average channel quality Γ is equal to 10 dB. Hence, results confirm that the proposed cross-layer design, which benefits from using distributed channel coding techniques, is capable of providing an enhanced network performance.

For assessing the influence of distributed channel encoding techniques, Fig-

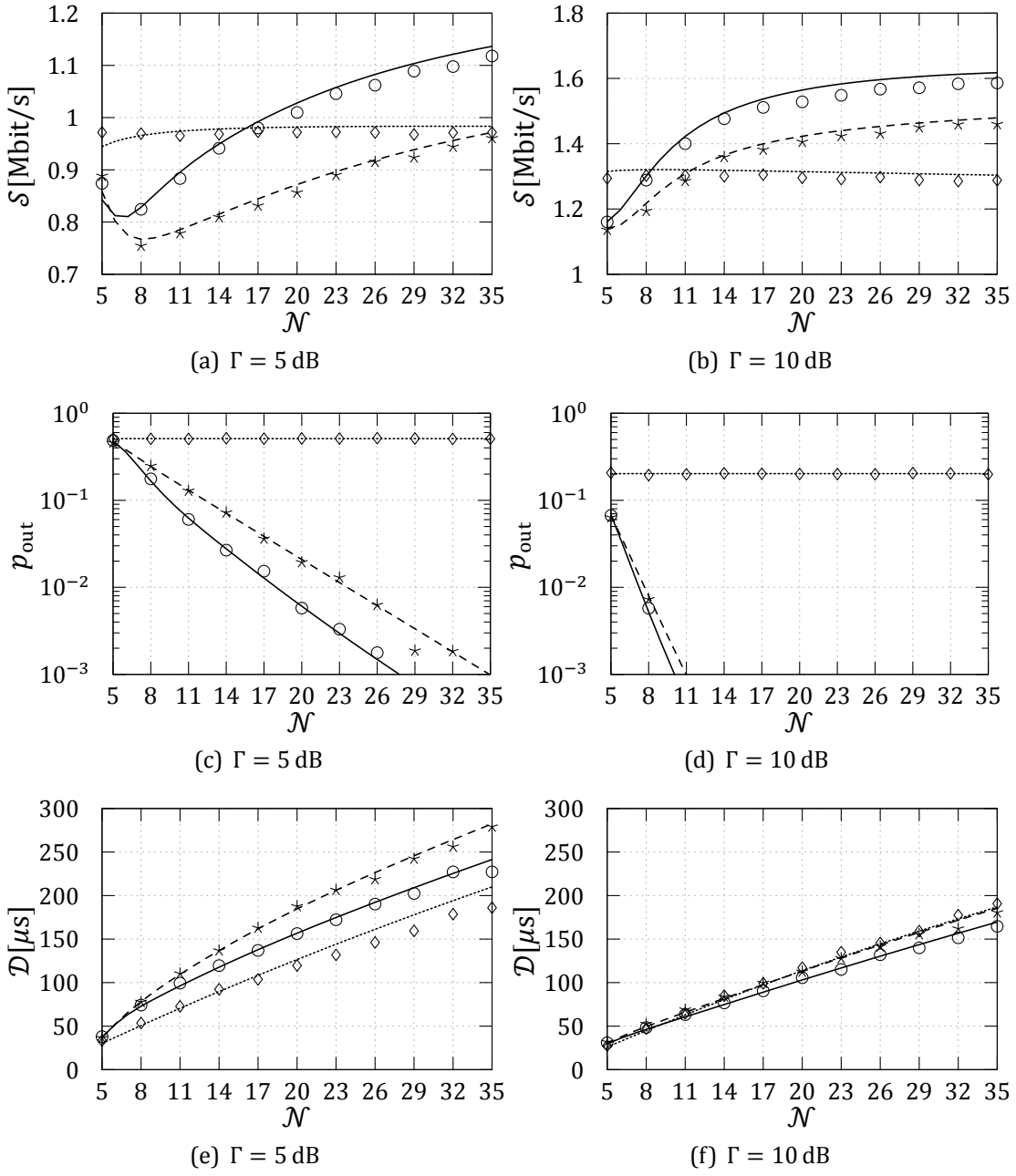

(a) $\Gamma = 5$ dB (b) $\Gamma = 10$ dB

(c) $\Gamma = 5$ dB (d) $\Gamma = 10$ dB

(e) $\Gamma = 5$ dB (f) $\Gamma = 10$ dB

Figure 6.2: Theoretical (solid: cross-layer protocol, dashed: CoopMAC, dotted: DCF) and simulated (○: cross-layer protocol, ⋆: CoopMAC, ⋄: DCF) saturation throughput, outage and average delay performance of the MAC schemes under study.

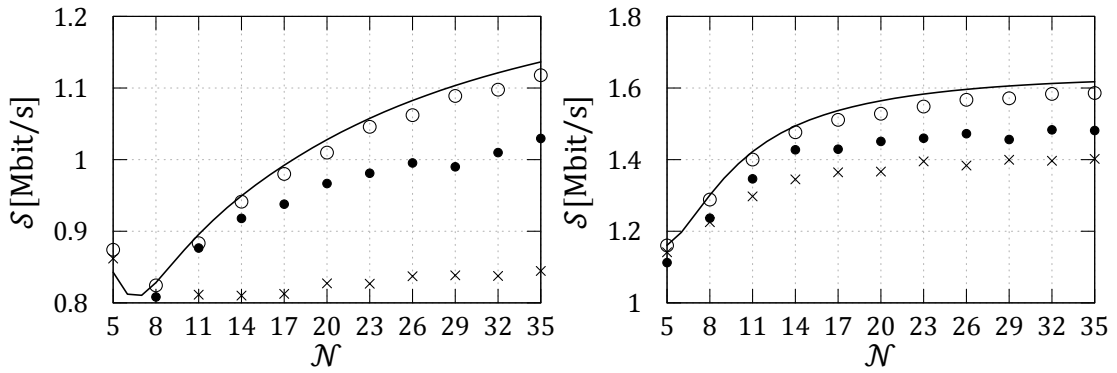

(a) $\Gamma = 5\,\mathrm{dB}$ (b) $\Gamma = 10\,\mathrm{dB}$

Figure 6.3: Theoretical (solid) and simulated (○: genetic aided protocol, ×: systematic incremental, •: complementary scheme of [70]) saturation throughput performance of the cross-layer MAC scheme using different distributed channel coding techniques.

ure 6.3 shows the throughput performance of the cross-layer MAC using different puncturing schemes for the source and relay transmissions. Particularly, the benchmarked schemes are the genetic aided scheme, the systematic incremental scheme and the complementary scheme of [70] listed in Table 5.1.

It can be seen that the only scheme that is capable of performing near the analytic values obtained following the steps shown in the previous section is the one that relies on the genetic algorithm aided designed channel code. Conversely the performance of the other forwarding schemes is not closely predicted by the theoretical analysis.

In particular, when using the systematic technique, the transmission of the relay station contains only parity bits and hence does not perform close to the SPB, used as a base for the theoretical analysis. Noting that a cooperative transmission takes place when the source-destination link is severely corrupted by fading, the decoding performance at the destination mainly depends on the bits received from the relay. Consequently, the ON-OFF model does not correctly predict the decoding performance of the systematic incremental scheme, where the relay station transmission achieves a low error ratio only for SNR values that are much higher than the one calculated with the SPB. More explicitly, higher switching thresholds should be considered at the relay for the incremental scheme.

Conversely, when using the balanced complementary scheme of [70], the transmissions of the source and relay stations have the same decoding performance. However, the codes defined by the puncturing patterns used in such scheme are not optimised for the waterfall performance and do not closely parallel the SPB, as shown in Chapter 5. Hence the scheme is less suited for cooperative scenarios,

where the best performance is achieved by codes with the lowest convergence SNR. Furthermore, since the ON-OFF model assumes that the decoding thresholds of the channel code are closely predicted by the SPB, the theoretical analysis fails to match the performance of the complementary scheme. More explicitly, a higher offset should be added to the switching thresholds employed by both the source and the relay stations for considering the gap between the channel code performance and the SPB.

Finally, note that only the switching thresholds to be used at the relay station are mispredicted using the systematic incremental scheme. Hence, the throughput downgrade regards only cooperative communications and is more severe when many stations are connected to the network and thus the use of a relay is facilitated. Conversely, also the thresholds to be used at the source station are not correctly predicted when using the scheme of [70]. Hence, this scheme experiences many decoding errors also in direct transmissions, which reduce the throughput even for a small number of connected nodes, when cooperation is less likely to be invoked.

The effect of the offset ψ on the throughput is shown in Figures 6.4 and 6.5 for the cross-layer and the CoopMAC schemes, respectively. A small offset leads to many transmission errors and to a throughput downgrade, since the switching thresholds are too close to the SPB and do not account for the convergence SNRs gap characterising the used code. Increasing ψ reduces the number of decoding errors, since the analytically derived thresholds better approximate the code's behaviour. As a results, the ON-OFF model, which assumes that transmissions are always successful, closely predicts the network performance. However, an unnecessary high value for ψ leads to a throughput decrease since the channel code's decoding thresholds are overestimated.

It can be seen that the offset value that maximises the actual performance of the proposed cross-layer protocol satisfies $\psi|_{\text{dB}} \in [1.2 \text{ dB}, 1.4 \text{ dB}]$, while for the CoopMAC protocol one finds that the offset should be either 0.6 dB or 0.8dB, respectively for $\Gamma = 5$ dB or $\Gamma = 10$ dB. These results justify the adoption of the particular values of $\psi|_{\text{dB}}$ used in the chapter.

6.5 Successive relaying aided cross-layer protocol

The cooperative MAC scheme considered in the previous parts rely on a three-terminal scenario, where a single relay aids the communication between a source station and a destination. In such a scenario, a significant *multiplexing loss* is incurred compared to direct transmissions due to the half duplex constraint of stations.

To mitigate this time loss, a successive relaying aided extension of the proposed cross-layer MAC protocol is presented in the following. The successive relaying ex-

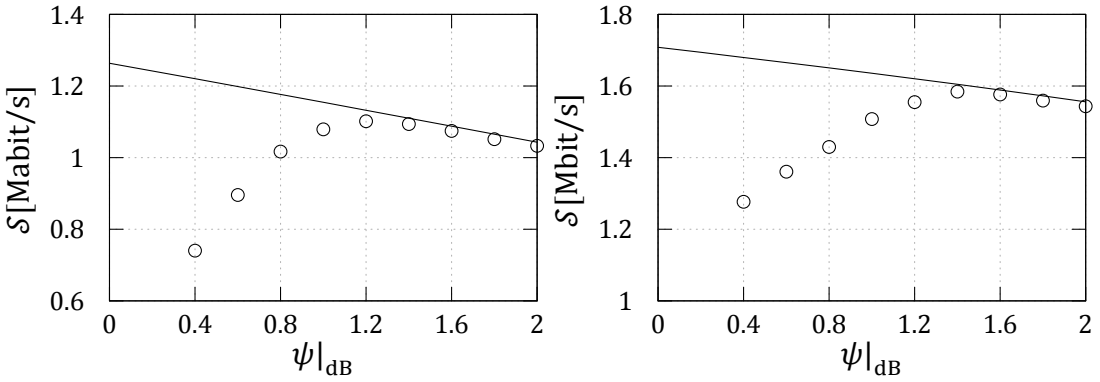

(a) $\Gamma = 5\,\mathrm{dB}$ (b) $\Gamma = 10\,\mathrm{dB}$

Figure 6.4: Theoretical (solid) and simulated (○) saturation throughput performance of the cross-layer MAC scheme for different values of $\psi|_{\mathrm{dB}}$.

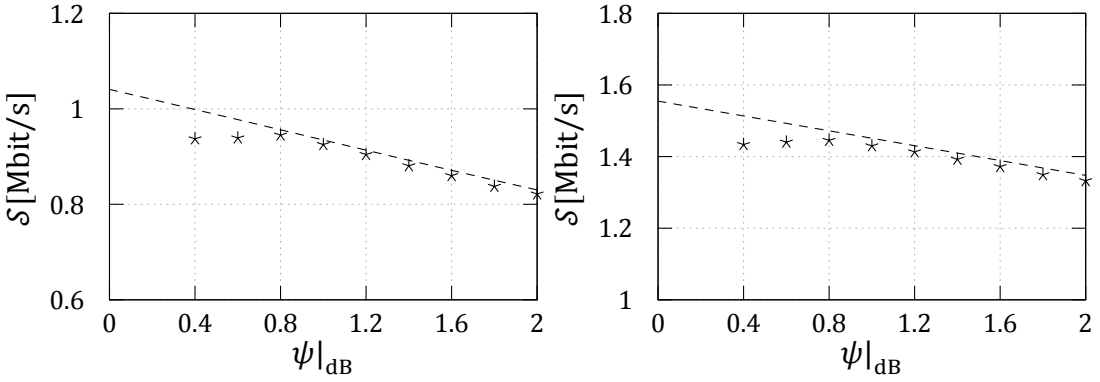

(a) $\Gamma = 5\,\mathrm{dB}$ (b) $\Gamma = 10\,\mathrm{dB}$

Figure 6.5: Theoretical (dashed) and simulated (⋆) saturation throughput performance of the CoopMAC scheme for different values of $\psi|_{\mathrm{dB}}$.

tension is based on the works of [100, 101]. In order to support successive relaying, two relays are needed and the corresponding packet transmission sequence is detailed in the following.

Assume to divide the packet to be transmitted into F segments, denoted by $\{\mathcal{F}_m\}_{f=1}^{F}$. The source station encodes each of the F segments separately and transmits them in F consecutive phases. The complete transmission scheme takes place in $(F+1)$ consecutive phases and ensues as follows:

- in the first phase the source station transmits $\mathcal{F}_1$; the first relay and the destination listen to the source's transmission, while the second relay remains idle;
- in the second phase the source station transmits $\mathcal{F}_2$ and the first relay re-

encodes and forwards $\mathcal{F}_1$; the second relay receives $\mathcal{F}_2$ from the source station and the destination receives $\mathcal{F}_2$ from the source station as well as $\mathcal{F}_1$ from the first relay;

- in the third phase the source station transmits $\mathcal{F}_3$ and the second relay re-encodes and forwards $\mathcal{F}_2$; the first relay receives $\mathcal{F}_3$ from the source station and the destination receives $\mathcal{F}_3$ from the source station as well as $\mathcal{F}_2$ from the second relay;
- this process continues in this way up to phase F;
- in phase $(F + 1)$ both the source station and the first relay (or the second relay) remain silent, while the second relay (or the first relay) re-encodes and forwards $\mathcal{F}_M$.

Note that segments forwarded by the relay stations may contain the same information as the ones transmitted by the source station, as in repetition schemes, or may include new information, using incremental encoding techniques.

Using the above-described successive relaying technique the *multiplexing loss* is reduced to the value of $\frac{F+1}{F}$, which approaches unity, if F is sufficiently high.

In order to use the above-mentioned successive relaying scheme the source has to address in its RTS message the two highest-SNR relays stored in its `CoopTable`. For supporting feedback from each relay, an additional HTS message is introduced, where the two HTS frames are issued by both the relays in order to confirm that they are willing to cooperate. The ensuing frame exchange of the successive transmission regime is shown in Figure 6.6.

In order to decode the signal arriving from both the relay and the source during the same phase, the destination has to perform Successive Interference Cancellation (SIC). Given that defining a suited SIC algorithm is beyond the scope of this work, perfect interference cancellation is assumed. A suited choice for the SIC algorithm may be the low-complexity scheme of [101, 102]. In order to mitigate the interference between the relays, it is assumed that they also employ a SIC algorithm to recover the source frames.

To decide whether to invoke cooperation or not, the source station evaluates the expected transmission duration of a direct transmission, of a classic cooperative communication adopting the fastest relay, as well as of a successive transmission using the fastest pair of relays. The time durations of direct and relay-aided communications are calculated according to (6.2) and (6.3). The time required for a successive relaying aided transmission using the relays h_1 and h_2 and adopting for both the source-relays and relays-destination links the fastest available modulation

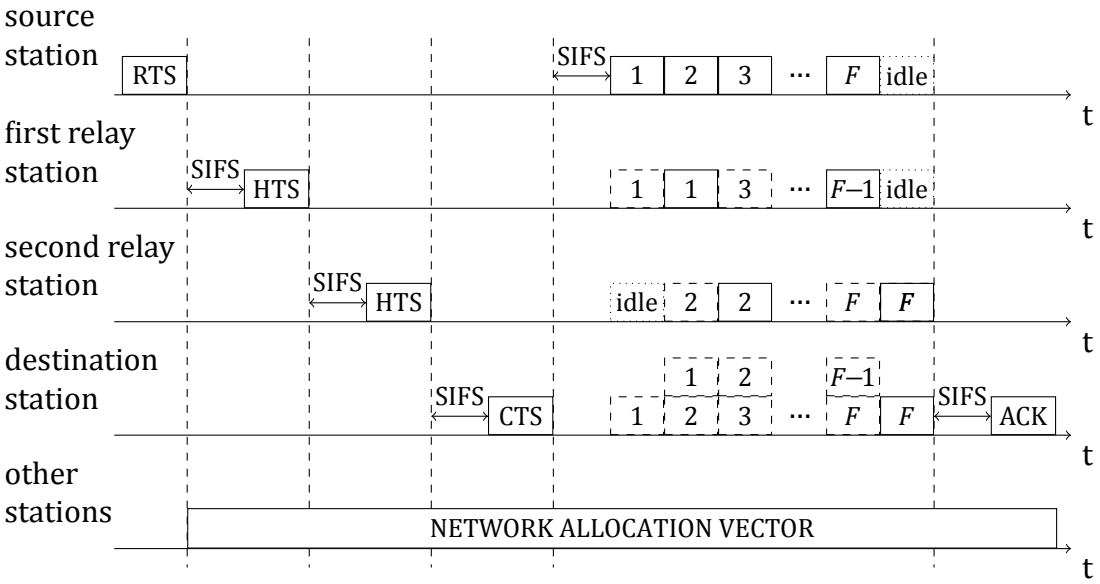

Figure 6.6: Frames exchange in successive relaying aided cooperation; numbers indicate the indexes of the packet segments, solid boxes represent transmitted packet segments, while dashed boxes represent received ones.

modes, that correspond respectively to the rates $\mathcal{R}^{SR_{h_1}}, \mathcal{R}^{SR_{h_2}}, \mathcal{R}^{R_{h_1}D}, \mathcal{R}^{R_{h_2}D}$, is:

$$T^{r_{h_1},r_{h_2}} = T_{\text{RTS}} + 2\,T_{\text{HTS}} + T_{\text{CTS}} + \frac{H_{\text{PHY}}}{\mathcal{R}^1} + \left\lceil \frac{M+1}{2M} \right\rceil \frac{H_{\text{MAC}} + \mathcal{E}[P]}{\min(\mathcal{R}^{SR_{h_1}}, \mathcal{R}^{R_{h_2}D})} + \left\lceil \frac{M+1}{2M} \right\rceil \frac{H_{\text{MAC}} + \mathcal{E}[P]}{\min(\mathcal{R}^{SR_{h_2}}, \mathcal{R}^{R_{h_1}D})} + T_{\text{ACK}} + 6\ \text{SIFS} + \text{DIFS}. \quad (6.37)$$

The two relays that minimise the time duration of the successive relaying procedure are chosen by the source station as candidate relays. Finally, the specific scheme which provides the fastest transmission at the highest average rate is activated.

The throughput of the successive relaying assisted protocol using incremental forwarding and relying on the genetic algorithm aided designed incremental turbo code is compared in Figure 6.7 with the performance of the single relay cross-layer system and with the performance of the CoopMAC protocol. It can be seen that successive relaying provides an additional performance increase compared to simply adopting distributed coding techniques in a single relay aided system.

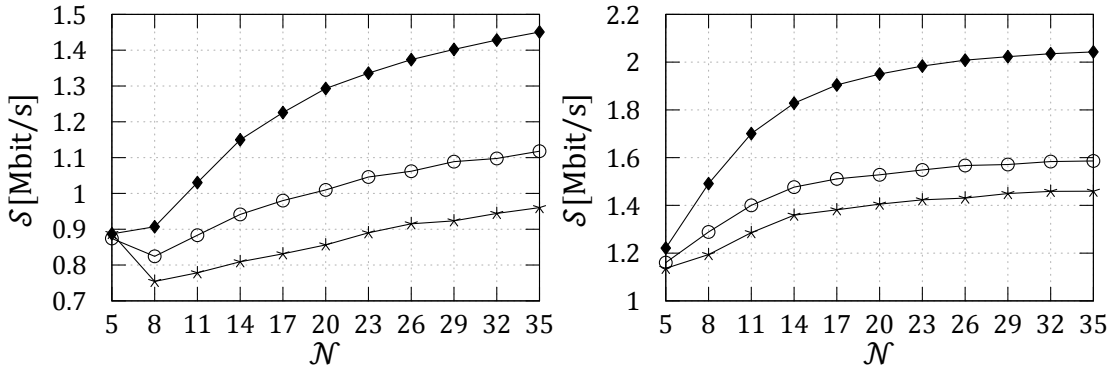

(a) $\Gamma = 5\,\mathrm{dB}$ (b) $\Gamma = 10\,\mathrm{dB}$

Figure 6.7: Simulated saturation throughput performance of different cooperative MAC protocols (○: single relay cross-layer scheme, ⋆: CoopMAC scheme, ♦: successive relaying cross-layer scheme).

6.6 Conclusions

This chapter presented a novel cross-layer designed cooperative MAC protocol based on the popular CoopMAC scheme. It was shown that a cross-layer approach allows contriving protocols that achieve a higher network performance, since they benefit from distributed channel coding techniques at the PHY layer. Furthermore, the chapter proposed a successive relaying aided scheme, which further enhances the performance of the cross-layer MAC by invoking the cooperation of two relays for mitigating the *multiplexing loss* incurred in the single relay scenario. Summarising, the chapter shown that a cross-layer design approach should be considered when designing MAC protocol schemes, since it provides benefits that enhance the network performance.

7

MEDIUM ACCESS CONTROL PROTOCOLS RELYING ON IMPERFECT KNOWLEDGE

The previous chapter shown that adopting a cross-layer approach for the design procedure of proactive MAC protocols allows contriving schemes than enhance the network performance, since they benefit from the distributed channel coding at the PHY layer. However, the performance of such schemes was analysed under the assumption that the source station knew the instantaneous channel qualities of each link composing the network. Such assumption is very limiting in faded scenarios, where the channel quality of a link fluctuates over time. This chapter studies the performance of both proactive and reactive MAC schemes when the relay selection algorithm adopted by the source station relies on imperfect channel quality estimates. Furthermore, novel relay selection algorithms based on Markov techniques for predicting the actual channel qualities from the imperfect estimates are proposed and are shown to mitigate the downgrade incurred when the source station has to rely on outdated and corrupted information.[1]

7.1 INTRODUCTION

The majority of cooperative MAC protocols found in the literature rely on idealised simplifying assumptions for the physical layer. In particular, [41, 45, 47, 52] assume that either the source station or some of the relays benefit from instantaneous and perfect CSI.

Partially Observable Markov Decision Process (POMDP) techniques have been used for improving the performance of non-cooperative schemes, when the sys-

[1]The content of this chapter is based on F. Babich, A. Crismani and L. Hanzo, ``Relay selection schemes relying on adaptive modulation and imperfect channel knowledge for cooperative networks'', presented at the IEEE International Conference on Communications, Ottawa (Canada), June 2012.

tem's state is characterised by a certain degree of uncertainty [103, 104].

A cooperative system using realistic imperfect CSI knowledge was considered in [55], where the different relays employed a POMDP for selecting the cooperative partner, though a transmission technique dispensing with adaptive modulation or channel coding was assumed. Similarly, a POMDP based approach was used in [58] for assessing the performance of a cooperative sensor network. Again, the authors of [58] also dispensed with adaptive modulation systems and with detailing the cooperative MAC protocol's procedures. As a further advance, a Markov formulation was used in [105] for modelling the time instants of a cooperative communication system, where the relay selection problem was treated as a ``multi-armed bandit problem''.

This chapter models and compares the performance of both proactive and reactive relay selection algorithms using realistic outdated and imperfect CSI knowledge. Furthermore, novel POMDP based relay selection algorithms are conceived for mitigating the performance degradation introduced by the channel uncertainty. A sophisticated physical layer is considered, which includes adaptive modulation and incremental encoding. The SPB is used for assessing the attainable performance of efficient codes, as detailed in the previous chapters. The chapter shows that the performance of a relay selection scheme employed for a cooperative MAC protocol is sensitive to the quality of the CSI knowledge. It is also shown that MDP based techniques allow one to mitigate the impairments imposed by the imperfect CSI, hence effectively increasing the network performance.

7.2 Performance of cooperative MAC protocols relying on imperfect information

Consider a cooperative MAC protocol where the relay selection algorithm is performed at the source station. Such choice is opposed to other solutions were contention between relays is used for enabling cooperation at the MAC layer [41, 52].

The particular choice where the source station selects the relay invoked for cooperation is motivated by noting that it avoids time-consuming backoff procedures and collisions at relay stations and at the same time it reduces the power consumption of relay stations in reactive schemes, where the candidate partners have to decode the message of the source station even if they will not be the preferred helper.

Particularly, this chapter consider a scenario where the relay station is chosen by the source station based on imperfect channel estimates that might be outdated. Furthermore, since the scope of the chapter is to compare the performance of diverse relay selection techniques, rather than to analyse a particular MAC scheme, the MAC overhead involved in setting up cooperation (e.g. the RTS/HTS/CTS frame

exchange considered in the previous chapter) is not taken into account.

Similarly to the previous chapter, consider a scenario having a source station, $|\mathcal{H}|$ relay stations $\{R_h\}_{h\in\mathcal{H}}$ and a destination station. Denote the distance between stations ``$A$'' and ``B'' normalised to the distance between the source station and the destination station by $d(A,B)$.

Time is discrete and divided into slots. Consider the n-th time slot t_n. Denote the instantaneous SNR of the source-destination link by $\gamma_{SD}^{t_n}$. Similarly, denote the instantaneous SNRs of the link between the source station and the h-th relay-station and of the link between the h-th relay station and the destination by $\gamma_{SR_h}^{t_n}$ and $\gamma_{R_hD}^{t_n}$, respectively.

Assume that the SNRs pertaining to different time slots are identically distributed and denote their average quantities on the corresponding links by:

$$\begin{aligned}\Gamma_{SD} &= \mathcal{E}[\gamma_{SD}^{(\cdot)}],\\ \Gamma_{SR_h} &= \mathcal{E}[\gamma_{SR_h}^{(\cdot)}] = \Gamma_{SD}/d^2(S,R_h),\\ \Gamma_{R_hD} &= \mathcal{E}[\gamma_{R_hD}^{(\cdot)}] = \Gamma_{SD}/d^2(R_h,D).\end{aligned}$$

Assuming Rayleigh fading, $\gamma_{SD}^{(\cdot)}$, $\{\gamma_{SR_h}^{(\cdot)}\}_{h\in\mathcal{H}}$ and $\{\gamma_{R_hD}^{(\cdot)}\}_{h\in\mathcal{H}}$ are exponentially distributed with means equal to Γ_{SD}, $\{\Gamma_{SR_h}\}_{h\in\mathcal{H}}$ and $\{\Gamma_{R_hD}\}_{h\in\mathcal{H}}$, respectively.

The values of SNRs on the same link in two time slots t_n and $t_{n+\tau}$ are correlated according to:

$$\mathcal{E}(\gamma_{(\cdot)}^{t_n},\gamma_{(\cdot)}^{t_{n+\tau}}) = J_0^2(2\pi f_d\tau), \tag{7.1}$$

where J_0 is the zero-order unmodified Bessel function of the first kind and f_d is the Doppler frequency. The channel qualities of the different links are independent.

Again, similarly to Chapter 6, consider an adaptive scenario, where $\{\mathcal{R}^i\}_{k=1}^K$ are the K available transmission rates corresponding to K different transmission modes. This chapter considers the BPSK, QPSK, 16-QAM and 64-QAM modulation modes, that provide rates of $1, 2, 4, 6$ Mbits/s, respectively. Denote the switching threshold used by the source station to select the i-th transmission mode by γ_t^i. The adaptive mode switching thresholds are analytically derived by using the SPB, as already adopted for the cross-layer designed cooperative MAC protocol of Chapter 6 and discussed in Chapter 4.

Finally, note that the destination station combines the signal received from the source station and from the activated relay station, performing a joint decoding. Hence, as deeply detailed in previous chapters, the new success threshold $\gamma_{t_R}^{\,j}$ of the j-th mode on the relay to destination link depends both on the mode $\mathcal{R}^i$ used by the source station and on the SNR value γ_{SD} of the source-destination link.

The purpose of this chapter is to assess the performance of different relay selection schemes, rather than analysing the influence of the channel coding technique adopted. Hence the chapter does not consider a particular distributed cod-

ing scheme, rather it is assumes that both the codes used by the source station and by the relay station are near-capacity schemes and hence the SPB-based predicted performance is accurate. Note however, that both the design procedure for contriving efficient distributed coding techniques of Chapter 5 and the considerations about using diverse schemes of Chapter 6 apply to the considered scenario.

Assume now that the SNR values are quantised by the station and opt for the SNR quantisation thresholds of $(\mathcal{Q}_0 = 0) < (\mathcal{Q}_k = \gamma_t^k) < (\mathcal{Q}_{K+1} = \infty)$. The fading envelope at a time instant t_n is quantised to the value c_k $(0 \leq k \leq K)$ if it satisfies $\mathcal{Q}_k \leq \gamma_{(\cdot)}^{t_n} < \mathcal{Q}_{k+1}$. Finally, denote the SNR value obtained after quantising the quantity $\gamma_{(\cdot)}^{t_n}$ by $\hat{\gamma}_{(\cdot)}^{t_n}$.

This chapter also considers the case where the channel state information values obtained by the source station are not only outdated, but may be corrupted by noise. More particularly, the source station observes potentially corrupted estimates $\tilde{\gamma}_{(\cdot)}$ of the quantised SNR values $\hat{\gamma}_{(\cdot)}$.

Denote the probabilities of under-estimating and over-estimating the SNR value by σ_1 and σ_2, respectively. The probability of observing a channel SNR value $\tilde{\gamma}_{(\cdot)}$, when the link quality is $\hat{\gamma}_{(\cdot)}$ is given by:

$$P\left(\tilde{\gamma}_{(\cdot)}^{t_n} = c_i | \hat{\gamma}_{(\cdot)}^{t_n} = c_j\right) = \begin{cases} \sigma_1 & i = j - 1 \\ 1 - \sigma_1 & i = j = K \\ \sigma_2 & i = j + 1 \\ 1 - \sigma_2 & i = j = 0 \\ 1 - \sigma_1 - \sigma_2 & 0 < i = j < K \\ 0 & \text{otherwise.} \end{cases} \tag{7.2}$$

The relay selection algorithms studied in the following follow a time minimisation criterion, similarly to the one presented in the previous chapter.

7.2.1 Proactive relay selection scheme

In a proactive relay selection scheme the source station chooses the relay station providing the highest-rate transmission, and hence the most prompt communication.

Consider the n-th time slot and the h-th relay. Assume that the source station knows the corrupted and outdated channel state information values $\tilde{\gamma}_{SD}^{t_{n-\tau}}$, $\{\tilde{\gamma}_{SR_h}^{t_{n-\tau}}\}_{h=1}^{|\mathcal{H}|}$ and $\{\tilde{\gamma}_{R_hD}^{t_{n-\tau}}\}_{h=1}^{|\mathcal{H}|}$. Denote the highest-rate transmission mode available on the source-relay link by:

$$\mathcal{R}_{SH_h}^* = \max\left\{\mathcal{R}^j \in [\mathcal{R}^1, \cdots, \mathcal{R}^K] : \gamma_t^j < \tilde{\gamma}_{SR_h}^{t_{n-\tau}}\right\}, \tag{7.3}$$

and the highest-rate transmission mode available on the relay-destination link by:

$$\mathcal{R}_{H_hD}^* = \max\left\{\mathcal{R}^j \in [\mathcal{R}^1, \cdots, \mathcal{R}^K] : \gamma_{t_R}^j | \tilde{\gamma}_{SD}^{t_{n-\tau}}, \mathcal{R}_{SH_h}^* < \tilde{\gamma}_{R_hD}^{t_{n-\tau}}\right\}. \tag{7.4}$$

The relay station that achieves the highest transmission rate is selected according to:

$$\texttt{choose relay } h^* = \underset{h\in\mathcal{H}}{\operatorname{argmax}}\left\{\left(\frac{1}{\mathcal{R}^*_{SH_h}}+\frac{1}{\mathcal{R}^*_{H_hD}}\right)^{-1}\right\}. \tag{7.5}$$

Finally, cooperation is activated if one has:

$$\left(\frac{1}{\mathcal{R}^*_{SH_{h^*}}}+\frac{1}{\mathcal{R}^*_{H_{h^*}D}}\right)^{-1} > \mathcal{R}^*_{SD}, \tag{7.6}$$

where $\mathcal{R}^*_{SD}$ is the highest attainable rate on the source-destination link and is obtained as:

$$\mathcal{R}^*_{SD} = \max\{\mathcal{R}^j \in [\mathcal{R}^1, \cdots, \mathcal{R}^K] : \gamma_t^j < \tilde{\gamma}_{SD}^{t_{n-\tau}}\}. \tag{7.7}$$

If Equation 7.6 is not satisfied, a direct communication provides a higher-rate and hence is to be preferred.

Note that, since the CSI known at the source station is not the instantaneous one, the specific transmission mode activated may result in an unsuccessful decoding at the destination, especially when the CSI fluctuates rapidly.

Particularly, consider a direct communication and assume that the source station chooses the i-th transmission mode based on the SNR value $\tilde{\gamma}_{SD}^{t_{n-\tau}}$. The transmission is unsuccessful if we have $\gamma_{SD}^{t_n} < \gamma_t^i$. Similarly, if the source station opts for choosing the h-th relay station and the transmission modes $\mathcal{R}^j$ and $\mathcal{R}^l$ on the source-relay and relay-destination links, respectively, the cooperative transmission is unsuccessful if $\gamma_{SR_h}^{t_n} < \gamma_t^j \vee \gamma_{R_hD}^{t_n} < \gamma_{t_R}^l | \gamma_{SD}^{t_n}, \mathcal{R}^j$.

7.2.2 Reactive relay selection scheme

In reactive schemes, the source station opts for the specific relay station that provides the most prompt retransmission to the destination, given that it should be able to decode the source station's signal. More explicitly, the source station transmits a packet to the destination choosing the highest attainable rate $\mathcal{R}^*_{SD}$, obtained as:

$$\mathcal{R}^*_{SD} = \max\{\mathcal{R}^j \in [\mathcal{R}^1, \cdots, \mathcal{R}^K] : \gamma_t^j < \tilde{\gamma}_{SD}^{t_{n-\tau}}\}. \tag{7.8}$$

Assume to denote the index of the rate $\mathcal{R}^*_{SD}$ used for the direct communication by i. If the direct transmission at rate $\mathcal{R}^*_{SD}$ fails, the source station considers as candidate partners all the relay stations capable of decoding the direct transmission. Hence, the h-th relay station is a candidate partner if:

$$\tilde{\gamma}_{SR_h}^{t_{n-\tau}} \geq \gamma_t^i. \tag{7.9}$$

Denote the set containing the candidate relay stations at the time slot t_n by $\tilde{\mathcal{H}} \subset \mathcal{H}$. Furthermore, denote the highest-rate attainable on the relay-destination link for a candidate relay $h \in \tilde{\mathcal{H}}$ by $\mathcal{R}^*_{H_hD}$, which may be obtained as:

$$\mathcal{R}^*_{H_hD} = \max\left\{\mathcal{R}^j \in [\mathcal{R}^1, \cdots, \mathcal{R}^K] : \gamma^j_{t_{RD}} | \tilde{\gamma}^{t_{n-\tau}}_{SD}, \mathcal{R}^*_{SD} < \tilde{\gamma}^{t_{n-\tau}}_{R_hD}\right\}. \tag{7.10}$$

The relay station selection algorithm chooses the highest-rate relay station from the candidate partners and proceeds according to:

$$\texttt{choose relay} \quad h^* = \underset{h\in\tilde{\mathcal{H}}}{\operatorname{argmax}}\left\{\mathcal{R}^*_{H_hD}\right\}. \tag{7.11}$$

Naturally, transmission errors are imposed by the imperfect CSI knowledge. Assume again that the source station chooses to transmit at a rate of $\mathcal{R}^*_{SD} = \mathcal{R}^i$ and invokes cooperation by relying on the h-th relay using a rate of $\mathcal{R}^*_{H_hD} = \mathcal{R}^j$, in the case of failure of the source-destination link.

The direct transmission fails if one has $\gamma^{t_n}_{SD} < \gamma^i_t$, and hence cooperation is invoked. Then, the relay station's transmission may also fail if $\gamma^{t_n}_{R_hD} < \gamma^j_{t_R} | \gamma^{t_n}_{SD}, \mathcal{R}^i$, in which case the packet has to be retransmitted.

7.3 Partially observable Markov decision processes aided relay selection schemes

The previous section identified how to model the relay selection algorithm and how to quantify the error events when the source station relies on imperfect channel knowledge.

This section proposes novel relay selection algorithms that are capable of mitigating the degradation introduced by the imperfect channel knowledge by predicting the actual channel state information from the delayed and corrupted estimates.

Estimation is achieved using POMDPs. The section briefly reviews POMDPs techniques and then details how the relay selection algorithm for cooperative scenarios may be formulated using a POMDP aided approach and how the source station might benefit from using POMDPs for selecting the transmission mode.

7.3.1 Partially observable Markov decision processes

Markov Decision Processes (MDP) provide a mathematical framework for modelling decisions when the underlying system evolves according to a Markov probability law.

A MDP may be represented by a tuple (S, A, T, r). The set S enumerates the possible states of the system. Different actions obeying $a(s^{t_n}_i) \in A$ may be chosen when

the system is in a state $s_i^{t_n} \in S$ at the time instant t_n. The law $T(s_i^{t_n}, a, s_j^{t_{n+1}}), T : S \times A \times S \rightarrow \mathbb{R}$ represents the probability that the system moves from the state $s_i^{t_n}$ to the state $s_j^{t_{n+1}}$ upon taking action a. Finally, an immediate reward $r(s_i^{t_n}, a), r : S \times A \rightarrow \mathbb{R}$ is earned upon choosing action a when in the state $s_i^{t_n}$.

A stationary policy $\pi : S \rightarrow A$ is a function that selects an action based on the current state of the system. The optimisation problem aims to maximise the discounted reward [103]:

$$J(\pi, s_i) = \mathcal{E}_\pi^{s_i}\left[\sum_{k=0}^{\infty} \psi^k r(s_i^k, a_\pi(s_i^k))\right], \tag{7.12}$$

where ψ is the discount factor.

Define the expected reward earned by choosing the policy π when commencing from state s_i by $V(\pi, s_i)$. The Bellman equation of [106] may be used to find the optimal expected reward as:

$$V^*(s_i) = \max_{a \in A}\left[r(s_i, a) + \psi \sum_{s_j \in S} T(s_i, a, s_j) V^*(s_j)\right]. \tag{7.13}$$

The policy that achieves $V^*(s_i)$ is the optimal policy $\pi^*(s_i)$ to be adopted when in state s_i, and may be expressed as:

$$\pi^*(s_i) = \operatorname*{argmax}_{a \in A}\left[r(s_i, a) + \psi \sum_{s_j \in S} T(s_i, a, s_j) V^*(s_j)\right]. \tag{7.14}$$

MDPs require a perfect knowledge of the current state. When the state is not perfectly known, the decision process may be aided by using POMDPs, which rely on observations of the system gleaned after performing an action.

Denote the set enumerating all the possible observations by O. The law $\Omega(s_i^{t_n})$, $\Omega : S \times A \rightarrow \Pi(O)$, where Π is a probability distribution, represents the probability of observing $o_j(t_n) \in O$ upon taking action a when the system is in the state $s_i^{t_n}$.

Denote the probability of being in a state $s_i^{t_n}$ by $b(s_i^{t_n})$, which is referred to as the state belief, and the vector enumerating the belief of every possible state by $\mathbf{b}(t_n)$. A stationary policy selects an action based on the probabilities $\mathbf{b}(t_n)$ of the different states.

Diverse algorithms have been proposed for finding the optimal policy of a POMDP [107]. However, these algorithms are typically suitable for problems associated with a small number of states.

When aiming for finding sub-optimal policies that guarantee satisfying a given performance in more complex problems, typically heuristic algorithms have been

proposed. The so-called Q-MDP [107] heuristic is used for solving the POMDP based relay selection problem in this work, since it achieves better results compared to other heuristics, such as the Most Likely State [108] and Action Voting [109] heuristics.

7.3.2 POMDP AIDED FORMULATION OF RELAY SELECTION SCHEMES

Consider the u-th link of the cooperative network. The evolution of the quantised fading process on a specific link may be modelled using a Finite State Markov Chain (FSMC), where transitions are governed by the first order Markov law:

$$P(\hat{\gamma}_{(\cdot)}^{t_{n+1}} = c_j | \hat{\gamma}_{(\cdot)}^{t_n} = c_i) = t_u^{i,j}. \tag{7.15}$$

The transition process may be described by a matrix $T_u = [t_u^{i,j}]$. The values $t_u^{i,j}$ depend both on the Doppler spread as well as on the average SNR and may be obtained for a Rayleigh fading process as detailed in [110]. The link is in state $s_i^{t_n}$ at a time t_n, if $\hat{\gamma}_{(\cdot)}^{t_n} = c_i$. The $(K+1)$ legitimate states on the u-th link are enumerated by the set S_u.

The cooperative system may be modelled by using $(1 + 2|\mathcal{H}|)$ FSMCs. The states of the cooperative network are obtained by enumerating all the combinations between the single states of each of the $(1 + 2|\mathcal{H}|)$ FSMCs. Denote the set enumerating all the states of the cooperative system by $\mathbf{S} = S_1 \times S_2 \times \ldots \times S_{1+2|\mathcal{H}|}$ and the state at time t_n by $\mathbf{s}^{t_n}$. The transition matrix $\mathbf{T}$ may be obtained as:

$$\mathbf{T}(\mathbf{s}^{t_n}, \mathbf{s}^{t_{n+1}}) = \prod_{u=1}^{1+2|\mathcal{H}|} t_u^{s_i^{t_n}, s_j^{t_{n+1}}}. \tag{7.18}$$

The set of actions differs between the proactive as well as the reactive scheme and characterises the behaviour of the source station.

In proactive systems the source station may opt for remaining silent, transmitting directly or transmitting with the aid of cooperation. In the case of a direct communication the action further divides into K actions corresponding to the K transmission modes. In the case of a cooperative session, the action further divides into K^2 actions given by the combination of the two transmission modes used on the source-relay and relay-destination links. Hence, $(1 + K + |\mathcal{H}|K^2)$ actions are considered.

The reward is zero if the source station remains silent. In the case of a direct transmission, the reward is:

$$r(\hat{\gamma}_{SD}^{t_n} = c_v, a = R_k) = \begin{cases} R_k & c_v \geq \gamma_t^k \\ 0 & \text{otherwise.} \end{cases} \tag{7.19}$$

In the case that the h-th relay station is chosen for a cooperative communication, the reward is obtained as:

$$r\left([\hat{\gamma}_{SD}^{t_n} = c_v, \hat{\gamma}_{SR_h}^{t_n} = c_w, \hat{\gamma}_{R_hD}^{t_n} = c_z], a = \{\mathcal{R}^j, \mathcal{R}^l\}\right) = \\ = \begin{cases} \left(\frac{1}{\mathcal{R}^j} + \frac{1}{\mathcal{R}^l}\right)^{-1} & c_w \geq \gamma_t^j \wedge c_z \geq \gamma_{t_R}^l | c_v, \mathcal{R}^j \\ 0 & \text{otherwise} \end{cases} \tag{7.20}$$

In reactive systems, the source station can choose to remain silent or to transmit at any time instant. In the case of opting for transmission the action divides into $|\mathcal{H}| \times K^2$ further actions corresponding to the transmission modes selected on the source-destination and relay-destination links for each relay station.

The reward is zero if the source-station remains silent and is calculated according to Equation (7.21) if the source station transmits, where the value $\alpha = 0.1$ is used to prioritise the activation of the highest-rate relay station in the case where the direct communication might fail.

$$r\left([\hat{\gamma}_{SD}^{t_n} = c_v, \hat{\gamma}_{SR_h}^{t_n} = c_w, \hat{\gamma}_{R_hD}^{t_n} = c_z], a = \{\mathcal{R}^i, \mathcal{R}^l\}\right) = \\ = \begin{cases} \left(\frac{1}{\mathcal{R}^i} + \frac{1}{\mathcal{R}^l}\right)^{-1} & c_v < \gamma_t^i \wedge c_w \geq \gamma_t^i \wedge c_w \geq \gamma_{t_R}^l | c_z, \mathcal{R}^i \\ \mathcal{R}^i + \alpha\mathcal{R}^l & c_v \geq \gamma_t^i \wedge c_w \geq \gamma_t^i \wedge c_z \geq \gamma_{t_R}^l | c_v, \mathcal{R}^i \\ \mathcal{R}^i & c_v \geq \gamma_t^i \wedge (c_w < \gamma_t^i \vee c_z < \gamma_{t_R}^l | c_v, \mathcal{R}^i) \\ 0 & \text{otherwise} \end{cases} \tag{7.21}$$

Finally, similarly to acting relying only on imperfect channel state information, the communication using the selected transmission mode may fail. Particularly, the same error events enumerated for non POMDP aided schemes characterise the success of a communication using a particular transmission mode.

Assume that in a slot t_n the source station observes an outdated and imperfect SNR estimate on each network link. More explicitly, consider one of the $(1 + 2|\mathcal{H}|)$ FSMCs modelling the network and assume that an observation $o_j(t_{n-\tau}) = \tilde{\gamma}_{(\cdot)}^{t_{n-\tau}}$ of the state $s_i^{t_{n-\tau}}$ is obtained at the time instant t_n. The probability $P(o_j(t_{n-\tau})|s_i^{t_{n-\tau}})$ of observing a state j while the system was in the state i is obtained using (7.2).

Since observations pertain to the past, an approach similar to that of [103] is used for updating the belief, namely by introducing the initial belief b and the updated belief $\tilde{b}$ concepts. The initial belief at time $t_{n-\tau}$ is obtained from the updated belief at time $t_{n-\tau-1}$ as:

$$b(s_i^{t_{n-\tau}}) = P\{s_i^{t_{n-\tau}}\} = \sum_{j=0}^{K} P\left\{s_i^{t_{n-\tau}} | s_j^{t_{n-\tau-1}}\right\} \tilde{b}(s_j^{t_{n-\tau-1}}). \tag{7.22}$$

The updated belief $\tilde{b}(s_i^{t_{n-\tau}}) = P\{s_i^{t_{n-\tau}}|o_j(t_{n-\tau})\}$ represents the probability of being in a particular state at the time $t_{n-\tau}$ after obtaining an observation $o_j(t_{n-\tau})$

and is obtained as:

$$\tilde{b}(s_i^{t_{n-\tau}}) = \frac{P\{o_j(t_{n-\tau})|s_i^{t_{n-\tau}}\}b(s_i^{t_{n-\tau}})}{P\{o_j(t_{n-\tau})\}}. \tag{7.23}$$

The updated belief of the cooperative network $\tilde{b}(\mathbf{s}^{t_{n-\tau}})$ may be obtained as the product of the believes $\tilde{b}(s^{t_{n-\tau}})$ of the single links. Finally, the outdated belief is projected into the actual time slot and the current belief is calculated as $b(\mathbf{s}^{t_n}) = P\{\mathbf{s}^{t_n}\} = \tilde{b}(\mathbf{s}^{t_{n-\tau}}) \cdot \mathbf{T}^{\tau}$.

Once one obtains the current belief, the Q-MDP heuristic may be used for finding the transmission policy π.

7.4 Network performance results

This section compares the simulated performance of POMDP aided relay selection schemes with their non-POMDP aided counterparts.

Figure 7.1 shows the throughput and the outage probability of both non-cooperative and cooperative systems using a single relay station that is located halfway between the source station and the destination. A perfect but outdated CSI is considered. It can be seen that the performance rapidly degrades, when the normalised delay increases (subsequent attempts become less correlated), due to the errors introduced by the outdated CSI. The degradation is much more severe for proactive protocols, where an aggressive adaptive regime is used for improving the throughput. By contrast, reactive schemes are less sensitive to the outdated CSI, and hence they are better suited for scenarios where the CSI uncertainty is high. One may also observe that the POMDP framework efficiently improves the attainable network performance.

Figure 7.2 compares the throughput of cooperative systems subjected to imperfect SNR knowledge. Two relay stations are considered, both located at the same distance from the source station and the destination, respectively. It can be seen again that the POMDP aided relay selection techniques are the ones offering the best throughput and that the reactive scheme is less sensitive than the proactive one to the SNR uncertainty. Furthermore, the reactive scheme benefits less from employing POMDP based decisions than the proactive one.

Figure 7.3 compares the throughput of the schemes under investigation in a normalised scenario, where the relay stations are placed randomly between the source station and the destination. A different number of candidate relay stations selected from the set of 10 available ones is considered for the non-POMDP aided schemes and their performance is compared. A scheme always uses the specific relays closest to the source station. By contrast, the POMDP schemes rely on only

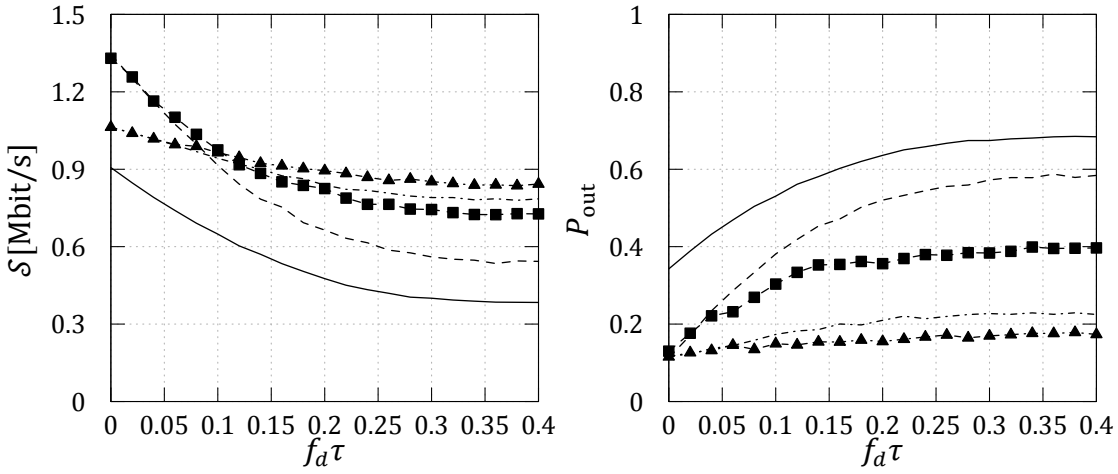

(a) (b)

Figure 7.1: Throughput and outage performance of the non-cooperative (solid) the proactive (dashed), the POMDP aided proactive (dashed, ■), the reactive (dash-dotted) and the POMDP aided reactive (dash-dotted, ▲) relay selection schemes using outdated CSI estimates for $\Gamma_{SD} = 10$ dB.

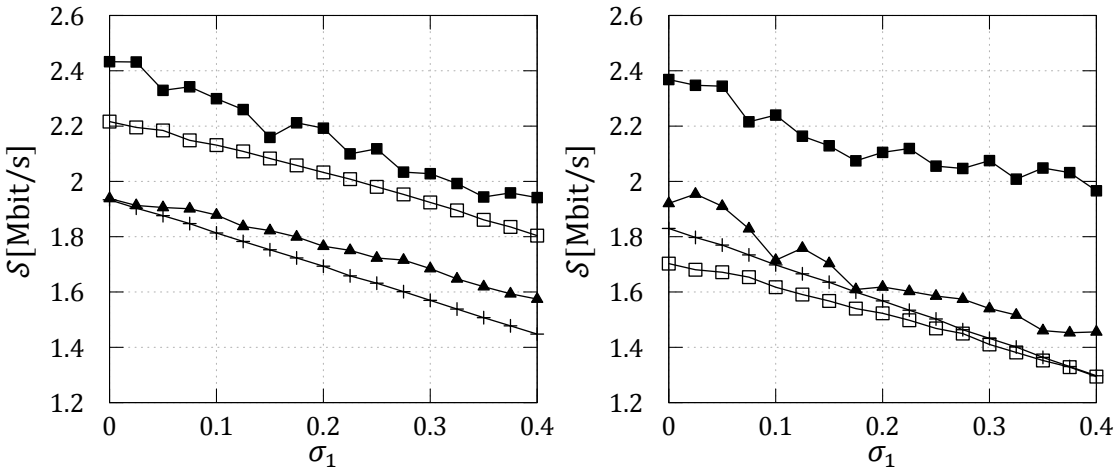

(a) $\sigma_2 = 0.1$ (b) $\sigma_2 = 0.3$

Figure 7.2: Throughput performance of the proactive (□), the POMDP aided proactive (■), the reactive (+) and the POMDP aided reactive (▲) relay selection schemes using corrupted CSI estimates for $\Gamma_{SD} = 10$ dB.

two relay stations, since the number of states of the underlying POMDP problem grows exponentially with the number of helpers.

Again, one can see that the POMDP aided relay selection schemes attain the highest performance. Furthermore, it is interesting to note that the attainable per-

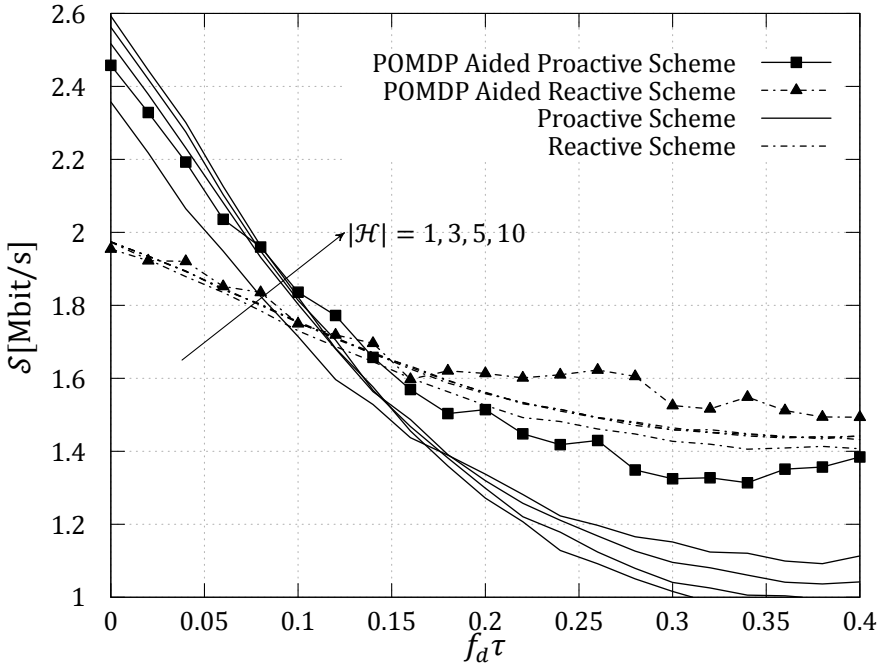

Figure 7.3: Throughput performance of the proactive, the POMDP aided proactive, the reactive and the POMDP aided reactive relay selection schemes using corrupted CSI estimates for $\Gamma_{SD} = 10$ dB.

formance hinges on the relay station link SNRs of those closest to the source station. More specifically, the performance of the schemes using the two relay stations closest to the source station approaches that of the schemes using all the ten relay stations. Finally, the POMDP aided schemes using only two relay stations clearly outperform the schemes where the decision is only based on the outdated CSI and not assisted by the Markov framework, even if all the ten relay stations are available for cooperation.

The erratic fluctuation of the throughput curves of the POMDP based solutions is caused by the quantised model adopted for the faded channel and by the finite set of actions. Particularly, since the policy chosen by the POMDP aided schemes remains the same for a set of under-estimation probabilities, the throughput curve exhibits an oscillating behaviour across the entire probability domain.

7.5 Conclusions

This chapter investigated the performance of reactive and proactive relay selection schemes when the CSI is not perfectly known at the source stations. It was shown that reactive schemes are less sensitive to the CSI inaccuracy, while proact-

ive schemes exhibit a better performance when the CSI is accurate.

Novel relay selection selection schemes, using a POMDP aided framework, were proposed for predicting the CSI and hence for mitigating the errors introduced by imperfect CSI. It was shown that the POMDP aided schemes clearly outperform their non-POMDP based counterparts. More specifically, proactive schemes exhibit a significant performance improvement when POMDP aided relay selection is considered. Even though reactive schemes exhibit less substantial improvements, the POMDP approach may still be used for increasing the attainable performance.

8

Design of smart antenna aided medium access control protocols

The previous chapters shown that a cooperative approach may be used for increasing the performance of a wireless network. However, in the cooperative network only one station may be active at a single time, since multiple simultaneous transmissions fail because of collisions due to mutual interference. Smart antenna systems may be used for mitigating the interference received from undesired sources, and hence may provide a tool for enabling multiple communications in a wireless network. This chapter presents the design steps for enabling multiple communications in a wireless network where nodes are equipped with smart antennas.[1]

8.1 Introduction

The previous chapters shown that a cooperative approach may be adopted increasing the performance of wireless networks. Particularly, in cooperative networks stations equipped with a single antenna adapt their transmission strategy to the instantaneous channel conditions of links composing the network and select the fastest route to the destination, accounting for the joint decoding algorithm employed by the destination itself.

Another approach for increasing the performance of wireless networks is to equip stations with multiple antenna elements and exploit beamforming techniques for reducing interference hence allowing hosting multiple communications at a single time. Note that such approach is opposed to MIMO solutions, such as

[1]The content of this chapter is based on F. Babich, M. Comisso, A. Crismani and A. Dorni ``On the design of MAC protocols for multi-packet communication in IEEE 802.11 heterogeneous networks using adaptive antenna arrays'', submitted to the IEEE Transactions on Mobile Computing and on F. Babich, M. Comisso, A. Crismani and A. Dorni ``Multi-Packet communication in 802.11 networks by spatial reuse: from theory to protocol'', submitted to the IEEE International Conference on Communications, 2013.

the one used in the 802.11n extension [36], which use multi-antenna systems for increasing the data rate of the single link, but maintain the access limited to just one user at a time.

The use of beamforming techniques for increasing the capacity of wireless networks has been theoretically investigated in several research papers [111, 112, 113, 114, 115]. In particular, the limiting network performance when nodes are equipped with smart antenna systems is analysed in [111], which shows that the scalability limitations of ad-hoc networks may be alleviated by using directional communications. This result is confirmed by [112], which additionally reveals that the throughput can be kept constant by asymptotically decreasing the antenna beamwidth according to the inverse of the square root of the number of nodes. In a mobile environment, the analysis of [113] shows that fading, statistically decreasing the interference power, can increase the capacity of ad-hoc networks adopting spatial reuse.

Three protocols for multi-hop networks are proposed in [114], where the authors analyse the degrees of freedom that are available when multi-antenna nodes operate in a network context. Further corroborations of the results of [111, 112] are provided in [115], which proves that not only the antenna beamwidth, but also the side lobe level has an impact on the throughput scaling of an ad-hoc network.

The wide diffusion of the IEEE 802.11 family of standards has further focused the research interests on the introduction of smart antennas on IEEE 802.11 stations. In this field the research efforts are currently focused on two main topics: the simultaneous reception of many packets by a unique destination, also known as Multi-Packet Reception (MPR), and the concurrent communication between different node pairs, defined as Multi-Packet Communication (MPC).

In MPR scenarios the objective is allowing a destination to simultaneously receive multiple packets from different sources. Hence, the access must be synchronised, since all allowed transmissions must begin at the same instant [116, 117].

By contrast, in MPC scenarios the aim is hosting multiple communications between different node pairs. Hence, the access can be asynchronous, since each source may start its transmission independently of the instants chosen by the other sources [118, 119].

In [116] the authors explore the impact of MPR on the throughput of a random access network, discussing the problems related to the collision model when multiple users may be simultaneously active.

The characteristics of the propagation environment in the presence of directional communications are considered in [120], where the authors propose a realistic cross-layer model of the IEEE 802.11 DCF in the presence of path-loss, shadowing, and Rayleigh fading. A mathematical framework for analysing the IEEE 802.11 DCF in the presence of a directional virtual carrier sensing mechanism is presented

in [121]. The influence of the channel-antenna characteristics on the throughput and the delay of an IEEE 802.11 network using MPR is analysed in [117] using a Markov chain approach.

An asynchronous access for carrier sensing multiple access (CSMA) networks is numerically explored in [118], where a cross-layer redesign of the MAC layer is proposed. A completely asynchronous scenario is analysed in [119], where a theoretical model for evaluating the throughput of an IEEE 802.11 multi-packet network is presented.

The influence of the Signal to Interference plus Noise Ratio (SINR) on the capture probability of an MPR receiver having successive interference cancellation capabilities is investigated in the analysis presented in [122], which can be extended to account for an heterogeneous scenario where each user may be characterised by a different capture threshold and a different power statistic.

The conditions required for fully exploiting a smart antenna system in a wireless network are investigated in [123], where the author identifies a fundamental issue of distributed scenarios: the preservation of the active nodes' distribution at the beginning of a source-destination communication cannot be maintained for the entire duration of that communication.

Despite the limitation outlined in [123], several wireless networks have to operate in ad-hoc mode due to the lack of a coordinating infrastructure. Hence, together with solutions for centralised networks [124, 125], several MAC layer modifications using advanced antenna systems and enabling MPR have been proposed for distributed networks [126, 127, 128].

In particular, extensions for exploiting adaptive arrays in slotted Aloha and IEEE 802.11 networks are proposed in [126], while [129] improves the RTS/CTS access and the virtual carrier sensing mechanism of the DCF for increasing the channel utilisation when nodes are equipped with smart antenna systems. A multi-hop RTS approach is presented in [130], where the proposed design is inspired by the typical problems related to the adoption of directional antennas in IEEE 802.11 networks, including deafness and hidden terminal, and the obtained results reveal that the throughput depends on the topology and on the traffic patterns.

A receiver initiated approach is proposed in [131], where MPR is enabled by combining spatial multiplexing with a modified handshake mechanism. In [132] multiple simultaneous communications are enabled using directional antennas and adopting a circular directional RTS transmission in order to disseminate information concerning the availability of the different antenna beams. A cooperative scheme, in which the handshake mechanism is modified to support the interference suppression capabilities of each node, is described in [127]. Both space-division and time-division multiplexing are adopted in [124], which presents a MAC layer extension for IEEE 802.11 networks where the access points are equipped with ad-

vanced antenna systems.

The concept of directional virtual carrier sensing, introduced in [128], is exploited for allowing the DCF to support MPC and interoperability between directional and omnidirectional antennas. An asynchronous IEEE 802.11 MPR scheme based on the use of space-time coding is presented in [125], where the impact of hidden terminals on the network throughput is investigated.

Even though the above-cited schemes are able to provide considerable throughput improvements, the majority of them are designed assuming homogeneous scenarios, where all nodes have the same antenna system, namely the same number of antennas and the same processing technique.

Moreover, some of these schemes introduce tones [126], new fields in the RTS and CTS frames [129], or even modify the IEEE 802.11 handshake by adding further control frames [127, 130, 131, 132], thus potentially inhibiting the communications of the legacy nodes that share the same frequency channel and may not be aware of the additional access rules.

These design choices may lead to backward compatibility problems, which are taken into account in [124], where a centralised-synchronous MPR scenario is assumed, and in [125], where the proposed MPR extension considers a centralised-asynchronous network. Mixed networks including legacy and non-legacy nodes are addressed in [128], though it dispenses with analysing a completely heterogeneous scenario.

Motivated from the analysis of [119], which proves that in a distributed IEEE 802.11 network an asynchronous access can provide a higher throughput than a synchronous one, hence making MPC more suitable for a completely distributed environment, and from the limitations of the reviewed research works, this chapter considers the design of multi-packet communication aided MAC schemes that are backward compatible with the IEEE 802.11 standard and are suited for heterogeneous networks.

The chapter proposes two schemes, namely the Threshold Access MPC (TAMPC) and the Signal to interference ratio access MPC (SAMPC) and shows that the novel protocols provide an increased network performance.

8.2 Heterogeneous and asynchronous network scenario

Consider a distributed IEEE 802.11 network including a set $\mathcal{N}$ of $|\mathcal{N}|$ nodes, where the generic node $n \in \mathcal{N}$ has an antenna system composed by $N_n (\geq 1)$ radiating elements. Such scenario is heterogeneous in the sense that different stations have different antenna capabilities. Furthermore, the network performance of different

nodes is also influenced by their relative positions within the network. In fact, two nodes with identical antenna systems may anyway experience significant differences in their ability to communicate, since the capability of suppressing an interferer depends on the reciprocal position of the nodes. This implies that a network in which each node has a different position with respect to the others is in practice heterogeneous, even if it consists of nodes with identical antenna systems.

The set of node $\mathcal{N}$ can be partitioned in two subsets: the subset $\mathcal{N}^{\mathrm{l}}$ that contains the $|\mathcal{N}^{\mathrm{l}}|$ IEEE 802.11 legacy nodes having $N_n = 1$, and the subset $\mathcal{N}^{\mathrm{nl}}$ that contains the $|\mathcal{N}^{\mathrm{nl}}| = |\mathcal{N}| - |\mathcal{N}^{\mathrm{l}}|$ non-legacy nodes having $N_n > 1$.

During the reception of a packet each non-legacy node equipped with a smart antenna system may generate a radiation pattern $G(\phi)$ that has the main lobe steered towards the desired direction and a certain number of nulls placed towards the interferers [133], being ϕ the azimuth angle. The radiation pattern $G(\phi)$ may be characterised by an average gain G_n^{av} and a null gain $G_n^{\mathrm{null}}(<< 1)$ values, which depend on the beamforming algorithm, the geometry, and the number of elements of the array [117].

In the homogeneous scenario considered, the ability of a node n of correctly receiving a packet in an interfered environment may be modelled by considering the number of communications $\mathcal{L}$ that can be sustained by the network [117], and the number of ongoing transmissions $L_t(< \mathcal{L})$ that allows a contending node to asynchronously transmit its packet without destroying the communications of the other nodes [119].

Given that nodes in an heterogeneous network are equipped with different antenna systems, each of them may be characterised by its particular value of L_{t_n}, and, differently from the homogeneous case, a single node cannot infer the thresholds of the other nodes from the knowledge of its value of L_{t_n}. In particular, if the node n is an IEEE 802.11 legacy station, then $L_{t_n} = 0$, since a node with a unique omnidirectional antenna can correctly receive a packet only if there are no other ongoing transmissions within its communication range. By contrast, if n is a non-legacy node, then L_{t_n} is related to the channel-antenna characteristics and to the network topology [114, 117].

The above-described scenario suggests two possible MAC layer approaches for introducing multi-packet communication in an IEEE 802.11 distributed network: a first approach is based on the ``resumptive'' parameter L_{t_n}, while a second approach may be based on a detailed estimation of the instantaneous Signal to Interference Ratio (SIR) value.

The former approach has the advantage of summarising the channel-antenna characteristics in a single value that may be calculated offline and included in the set of MAC layer parameters that characterise the access behaviour of a station, similarly to the minimum contention window or the maximum backoff stage. In fact,

the value L_{t_n} may be approximately evaluated assuming an homogeneous scenario, in which all n nodes have N antennas, and relying on the analysis presented in [117, 119]. Hence, the former approach requires a small computational complexity at each node, however it relies on an averaged quantity.

By contrast, the latter approach relies on a real-time local estimation of the instantaneous SIR. Such estimation accounts for the single-node antenna parameters and the relative position of the node within the network. Since the second solution requires real time computing, it imposes higher complexity on transmitting nodes, but at the same time it may guarantee an access behaviour that matches more closely the real traffic evolution.

Finally, note that the node behaviour in IEEE 802.11 is asynchronous, given that each station transit at the beginning of a time slot that is chosen independently of other stations' decisions [116, 117, 118, 119, 120, 121, 122, 123, 124, 126, 127, 128, 129, 130, 131, 132, 134, 135].

While in a synchronous-homogeneous scenario a collision event leads to the loss of all involved packets, since the transmissions are perfectly superimposed because of the synchronisation (all bits are corrupted), in all the other three possible cases (homogeneous-asynchronous, heterogeneous-synchronous, heterogeneous-asynchronous), the collision may determine the loss of only a subset of the involved packets. In fact, different packets, even of the same length, may be differently corrupted because they span different time slots, and/or different nodes may have different interference mitigation capabilities. This implies that in the heterogeneous-asynchronous network under consideration the consequences of a collision must be evaluated locally, since they depend on the individual characteristics of the involved nodes and on the evolution of each SIR.

8.3 Design requirements and strategy for IEEE 802.11 MPC aided networks

Independently of the adopted approach, a commercially attractive extension for the 802.11 DCF using adaptive arrays should fulfil three main requirements.

First, the adopted policy should preferably be asynchronous, given that in a distributed IEEE 802.11 network, MPC can provide a higher throughput than a synchronous approach [119].

For achieving the highest degree of benefit from the adaptive array system equipped on nodes that operate in this context, a reliable criterion for the channel access should target two main objectives [123]: the acquisition of information on active nodes, and the preservation of the conditions present at the beginning of the transmission for the entire duration of the transmission itself (since the generated

pattern $G(\phi)$ cannot be changed during reception).

While the first target can be reached in a distributed scenario by monitoring the channel activity and relying on information contained in control packets, the second goal cannot be completely achieved, due to the absence of centralised control and to the asynchrony of the scenario [123]. Hence, for enabling MPC in distributed environments a MAC protocol should provide ways for source stations to infer the distribution of interferers at the beginning of transmission and means for evaluating the possible evolution of such distribution.

The second fundamental requirement for introducing MPC in future IEEE 802.11 networks is achieving backward compatibility of the developed MAC layer extensions. In particular, MPC solutions ought to guarantee the possibility of communicating to single-antenna legacy nodes, and hence they should strive for avoiding modifications to the IEEE 802.11 MAC layer, which may be perceived as in contrast with the access rules adopted by these stations.

The third fundamental requirement for a protocol enabling MPC in distributed networks concerns the heterogeneity of the scenario. Since IEEE 802.11 networks are often extended by adding new routers and the continue progresses in antenna miniaturisation allows accommodating an increasing number of antennas on a device [136], the scenario of the near future may involve devices of different ``generations'', characterised by increasing antenna capabilities. Hence, heterogeneity may represent a plausible aspect of forthcoming networks, where the MAC protocol should prevent nodes equipped with more powerful antenna systems from acquiring all the resources at the expense of nodes equipped with less powerful antenna systems.

These three requirements suggest some design choices for extending the IEEE 802.11 DCF in order to allow multiple communications at a single time.

First, the RTS/CTS access seems preferable to the basic access, since the former helps disseminating information on active communications and hence is used by almost all MAC protocols proposed for supporting MPC in asynchronous networks [124, 127, 128, 129, 130, 131, 132, 134, 135].

The second choice consists in adopting two non-overlapping frequency channels, where the first channel can be used by both the legacy and the non-legacy nodes and is referred to as the Common Channel (CC), while the second one can be used only by the non-legacy nodes and is referred to as the Multiple Communications Channel (MCC). Just one communication at a time is allowed on the CC, while multiple simultaneous communications are allowed on the MCC. A legacy node can monitor only the CC, while a non-legacy node can perform an omnidirectional sensing of both channels.

The main reason for using two separate channels is that it allows adding novel fields to the control packets. These new fields contain information required by sta-

tions for exploiting their antenna systems. Non standard frames cannot be used in a channel that is shared with legacy nodes, since they are unable to understand the modified format. Besides, in the standard RTS/CTS frames there are no bits available for including novel information, since all fields are used for standard operations [124].

Finally, omnidirectional transmissions are used on both channels and non-legacy nodes use their interference mitigation capabilities only during reception. This choice may appear to limit the achievable performance, since it reduces spatial reuse. However, such decision increases robustness against hidden terminal and deafness problems [130] and simplifies the procedure for sensing active transmissions [127]. In particular, the latter aspect is relevant when a node, being involved in a communication on the MCC, has lost some RTS/CTS exchanges and, once its communication is completed, tries to update its knowledge of the medium occupation.

8.4 The proposed MPC aided protocols for wireless networks

This part details the design of the proposed extensions for allowing hosting multiple communications during a single slot of an IEEE 802.11 network. The design goal is to contrive access schemes where nodes are capable of adapting their access behaviour to the particular instantaneous distribution of interferers, in order to transmit their packets if they do not interrupt other ongoing communications.

8.4.1 Recognition between non-legacy stations

In an heterogeneous network, non-legacy nodes should be able to infer whether their intended partner is a non-legacy node itself or not, in order to adapt their access procedure to the interference mitigation capabilities of the destination, Furthermore, non-legacy stations should also be capable of estimating the antenna capabilities of other stations that are transmitting and receiving a packet. Hence, the first novel feature to be designed for contriving an MPC extension for the IEEE 802.11 MAC layer is a mechanism of reciprocal recognition of non-legacy nodes. Furthermore, for backward compatibility purposes, such recognition mechanism cannot modify the legacy communication rules.

The proposed recognition scheme relies on the use of the `More Data` field included in RTS/CTS control frames. Such field, consisting of a unique bit, must be set equal to zero in distributed networks and can be ignored by legacy nodes during the contention period, since it has meaning only for centralised operations [34, p.

37]. The reciprocal recognition between non-legacy nodes rely on this field, which is set to one and read during the contention period by stations having advanced antenna capabilities.

In particular, when a generic non-legacy source n has a packet for a destination $D(n)$ of unknown antenna characteristics, n can communicate to $D(n)$ its multi-antenna capabilities by setting to one the `More Data` field of the transmitted RTS packet and can also infer the (possible) multi-antenna capabilities of $D(n)$ by reading the `More Data` field of the received CTS. If n and/or $D(n)$ are legacy nodes, they will not read the `More Data` field and the communication will follow the standard IEEE 802.11 operations.

The adopted mechanism of recognition is used both for the access scheme that relies on the parameter ``L_t'' and for the access scheme that accounts for the SIR evolution of ongoing transmissions. These two access solutions are presented in the following of the section.

8.4.2 Threshold access multi-packet communication protocol

The TAMPC protocol relies on the threshold L_{t_n}, which summarises the channel-antenna characteristics of a node n [117, 119], for determining the access behaviour of a station. Such behaviour is described in the following by considering the communication between a generic non-legacy source n and its non-legacy destination $D(n)$.

8.4.2.1 Operations in the CC: single communication

The communication between n and $D(n)$ begins with a common RTS/CTS exchange on the CC channel. Once the RTS/CTS exchange and the recognition process are completed, n transmits a modified DATA packet, that includes the original data, the threshold L_{t_n} and a preamble. This preamble is used by the smart antenna system equipped on $D(n)$ for estimating the Direction Of Arrival (DOA) of the source station and to synthesise the receiving radiation pattern using the adopted beamforming algorithm [133]. Similarly, once the DATA reception is completed, the destination $D(n)$ transmits the ACK packet by adding its threshold $L_{t_{D(n)}}$ and the preamble.

After this first RTS/CTS/DATA/ACK handshake the nodes n and $D(n)$ have acquired their reciprocal characteristics. These characteristics are stored into a table, referred to as the Neighbouring Characteristic Table (NCT), which has one entry for each neighbour with whom data has been previously exchanged.

More precisely, the generic entry m of the NCT_n of node n contains the IDentifier (ID) of m (ID_m), the corresponding threshold L_{t_m}, the estimated DOA $\phi_{n,m}$, and the NAV relative to m (NAV_m). Observe that the modifications made to the DATA and ACK frames are not seen by legacy nodes, since they set their NAVs and turn off their

radio for the time specified in the duration field of the sensed RTS (or CTS) frame once the RTS/CTS exchange between n and $D(n)$ completes.

8.4.2.2 Operations in the MCC: multiple communications

Consider now the case where a non-legacy source n has a packet for an already recognised non-legacy destination $D(n)$, whose ID is hence already present in NCT_n. In this case the non-legacy pair is allowed communicating on the MCC.

As in the IEEE 802.11 DCF, n generates a backoff and monitors the medium using its antenna array to estimate the l_n DOAs $\phi_{n,1}$, ..., $\phi_{n,m}$, ..., ϕ_{n,l_n} of signal received from active transmitters. Such estimation may include RTS, CTS, DATA, and ACK transmissions, because the scenario is asynchronous.

Noting that an array with $N_n \geq 2$ elements may allow estimating up to N_n active transmissions, the estimation of active DOAs can be considered reliable only when $l_n \leq N_n - 1$. In fact, the case where the source station estimates $l_n = N_n$ cannot be considered reliable, since it represents every situation where the actual value l of the number of transmissions that are active in the MCC is equal or greater than N_n. Hence, if $l_n = N_n$, the MCC is considered busy and n freezes its backoff counter.

Conversely, if $l_n < N_n$, n examines the NCT_n for each $m = 1, \dots, l_n$ for verifying if the entry relative to $\phi_{n,m}$ is complete, lacks information on ID_m, L_{t_m}, or has a NAV_m equal to zero. If each entry is complete, n continues monitoring the channel, while, if an entry m is not complete, n receives the packet incoming from $\phi_{n,m}$ by running its beamforming algorithm using $\phi_{n,m}$ as the desired direction and all the other estimated DOAs as undesired directions. If this packet is relative to a communication between a source k and a destination $D(k)$, the contained information is used by n to update its NCT_n.

Precisely, the control packets sent on the MCC (RTS_{MCC} and CTS_{MCC}) are modified versions of the standard RTS/CTS packets, and contain the IDs, the thresholds, and the NAVs relative to k and $D(k)$. The novel control frames also contain the preamble for allowing the required antenna processing operations. Observe that the structure of the frames can be freely modified on the MCC channel, since only not legacy operates on it.

If the sensed packet has n as its destination ($D(k) = n$) or involves the destination of n ($k = D(n)$ or $D(k) = D(n)$), n freezes its backoff counter. Otherwise, n updates the current threshold as:

$$L_{t_n}^{\text{cur}} = \min_{m \in \mathcal{C} \cup \{n, D(n)\}} (L_{t_m}), \tag{8.1}$$

where $\mathcal{C} = \{p \in \mathcal{N}^{\text{nl}} | \text{NAV}_p > 0\}$ is the set of the non-legacy nodes currently involved in a communication on the MCC (i.e. having a NAV greater than zero in NCT_n). If $l_n \leq L_{t_n}^{\text{cur}}$, all nodes can sustain the current traffic load and hence the

backoff counter can be decreased, since the potential communication between n and $D(n)$ would not destroy the ongoing communications. Otherwise, the backoff is frozen.

This monitoring operation continues until the backoff counter reaches the zero value and the source n sends its RTS_{MCC} frame. When the destination $D(n)$ receives the RTS_{MCC} frame, it replies with its CTS_{MCC} after a SIFS time, and the rest of the handshake (DATA/ACK) is completed by using the receiving patterns synthesised using the preambles contained in the control frames.

8.4.3 SIR access multi-packet communication protocol

The SIR access multi-packet communication protocol (SAMPC) enables MPC by relying on the instantaneous SIR of ongoing communications for accessing the channel. The instantaneous SIR is more adherent to the real network behaviour and is able to account in detail and in real-time for the antenna pattern, the topology, and the traffic information. Furthermore, the SAMPC protocol relies on efficient channel coding techniques at the PHY layer, which are used for recovering occasionally collided slots.

8.4.3.1 Operations in the CC: single communication

Once station n finishes the recognition phase with $D(n)$, it sends a modified DATA packet that contains the antenna parameters N_n, G_n^{av} (average gain), G_n^{null} (average gain in a null), and a preamble that allows $D(n)$ to estimate the relative DOA $\phi_{D(n),n}$ and to synthesise the receiving pattern $G_{D(n)}(\phi)$ using its beamforming algorithm [133].

Remembering that the transmission gain is equal to unity (omnidirectional transmission), the power received by $D(n)$ from n can be expressed using the Friis transmission equation as [117]:

$$P^{\text{r}}_{D(n),n} = \frac{P^{\text{t}} \cdot 1 \cdot G_{D(n)}(\phi_{D(n),n})\tilde{h}_{\alpha}}{d^{\alpha}(D(n),n)}, \tag{8.2}$$

where P^{t}=100 mW is the legacy transmission power, $\tilde{h}_{\alpha}$ is a constant depending on the height of the antennas with respect to the floor and on the estimated path-loss exponent α [137], and $d(D(n),n)$ is the distance between $D(n)$ and n. Hence, the distance $d(D(n),n)$ can be calculated at $D(n)$ by inverting (8.2), obtaining:

$$d(D(n),n) = \left(\frac{P^{\text{t}} G_{D(n)}(\phi_{D(n),n})\tilde{h}_{\alpha}}{P^{\text{r}}_{D(n),n}}\right)^{\frac{1}{\alpha}}. \tag{8.3}$$

Similarly, the ACK of $D(n)$ includes $N_{D(n)}$, $G^{\text{av}}_{D(n)}$, $G^{\text{null}}_{D(n)}$, and the preamble, hence allowing n to estimate $\phi_{n,D(n)}$ and $d(n,D(n))$. Observe that, since a unique omni-directional transmission is allowed on the CC, also a non-legacy node $k \neq n, D(n)$, sensing the DATA/ACK exchange between n and $D(n)$, may acquire the exchanged parameters and estimate $\phi_{k,n}$, $\phi_{k,D(n)}$, $d(k,n)$, and $d(k,D(n))$. Besides, since the positions of n, $D(n)$ and k form a triangle, k can use these estimations to evaluate on its own the relative distance between n and $D(n)$ as:

$$d(n,D(n))=\sqrt{d^2(k,n)+d^2(k,D(n))-2d(k,n)d(k,D(n))\cos[\phi_{k,n}-\phi_{k,D(n)}]}. \quad (8.4)$$

Finally, together with the above-mentioned values, k also stores the values of NAV_n and $\text{NAV}_{D(n)}$ into its NCT_k, which has, similarly to the TAMPC protocol, one entry for each sensed node m, but now contains N_m, G^{av}_m, G^{null}_m, NAV_m, $\phi_{m,p}$, and all the $d(m,p)$ values estimated using (8.4) for nodes p that are already present in NCT_k.

8.4.3.2 Operations in the MCC: multiple communications

Similarly to the TAMPC protocol, when a transmission on the MCC is sensed, the generic node n estimates the current DOAs and checks in the NCT_n if one DOA corresponds to a NAV equal to zero. Such condition implies that a new communication m-$D(m)$ has started. Hence, n runs its beamforming algorithm to receive the RTS_{MCC} and CTS_{MCC} frames, which, differently from the TAMPC protocol, now contain $N_{m/D(m)}$, $G^{\text{av}}_{m/D(m)}$, $G^{\text{null}}_{m/D(m)}$, and the code rates $R_c^{D(m)}$ and R_c^m adopted for the corresponding DATA and ACK transmissions, respectively. These antenna parameters are included again in the $\text{RTS}_{\text{MCC}}/\text{CTS}_{\text{MCC}}$ frames for allowing a node that missed the first DATA/ACK exchange in the CC between m and $D(m)$, being involved in a communication on the MCC, to receive them.

After the $\text{RTS}_{\text{MCC}}/\text{CTS}_{\text{MCC}}$ exchange, n first derives the instant of beginning of the corresponding DATA reception $t_{D(m)}$ and that of the relative ACK reception $t_m = t_{D(m)} + T_{\text{DATA}} + \text{SIFS}$, where T_{DATA} is the duration of the DATA frame. Secondly, for each of the two nodes $q \in \{m, D(m)\}$, n stores the ordered set:

$$\mathcal{I}^0_{n,q} = \{p \in \mathcal{N}^{\text{nl}} : \text{NAV}_p > 0; p \neq q, D(q); P^{\text{r}}_{q,1} \leq \ldots \leq P^{\text{r}}_{q,p} \leq \ldots \leq P^{\text{r}}_{q,l_n}\}, \quad (8.5)$$

of the l_n estimated currently active interferers of q in the q-th entry of the NCT_n.

The set $\mathcal{I}^0_{n,q}$ in (8.5) is generated by n by taking the position of q as reference, since each $P^{\text{r}}_{q,p}$ can be calculated from the $d(q,p)$ value obtained when sensing the CC. This set accounts for the fact that in an asynchronous scenario the interference configuration cannot be preserved [123]. Hence, if n intends to perform a reliable SIR estimation for a node q, the initial interference configuration experienced by q must be stored.

Since adaptive arrays aim to maximise the SIR [133], n can reasonably assume that, for a node q, the $N_q - 2$ available nulls are used to suppress the strongest interferers in $\mathcal{I}_{n,q}^0$, while the other interferers are received with the average gain G_q^{av} [117]. Hence, $\mathcal{I}_{i,q}^0$ can be partitioned in two subsets: $\mathcal{I}_{n,q}^{0^{\mathrm{null}}}$, containing the $N_q - 2$ suppressed interferers, and $\mathcal{I}_{n,q}^{0^{\mathrm{av}}}$, containing the not suppressed ones.

The information stored can be used by a non-legacy source n, having a packet for a recognised non-legacy destination $D(n)$, to assess whether to the decrease the backoff counter or not according to the SIR estimated not only for the pair n-$D(n)$, but also for all pairs active on the MCC.

More particularly, n considers the set $\mathcal{C} = \{p \in \mathcal{N}^{\mathrm{nl}} : \mathrm{NAV}_p > 0\}$ containing the nodes currently involved in a communication on the MCC. For each $q \in \mathcal{C}$, n evaluates the set $\mathcal{I}_{n,q}^{\mathrm{nul}} = \mathcal{C} \cap \mathcal{I}_{n,q}^{0^{\mathrm{null}}}$, containing the still active interferers suppressed by q, and the set $\mathcal{I}_{n,q}^{\mathrm{av}} = (\mathcal{C} - \mathcal{I}_{n,q}^{\mathrm{null}}) \cup \{n, D(n)\}$, containing the still active interferers of q that are not nulled together with n and $D(n)$. For $q \in \{n, D(n)\}$, n just partitions $\mathcal{C}$ into the subsets $\mathcal{I}_{n,q}^{\mathrm{null}}$, containing the $N_q - 2$ interferers that may be nulled, and $\mathcal{I}_{n,q}^{\mathrm{av}}$, containing the others.

Besides, for each $q \in \mathcal{C} \cup \{n, D(n)\}$, n defines the function:

$$f_{n,q}(t) = \begin{cases} 1 & t_q \le t \le t_q + T_{\mathrm{ACK}}, q \in \mathcal{N}^{\mathrm{src}} \cup \{n\} \text{ or} \\ & t_q \le t \le t_q + T_{\mathrm{DATA}}, q \in \mathcal{N}^{\mathrm{dst}} \cup \{D(n)\}, \\ 0 & \text{elsewhere} \end{cases} \tag{8.6}$$

where T_{ACK} is the duration of the ACK frame, $\mathcal{N}^{\mathrm{src}} (\subset \mathcal{C})$ is the subset of the active sources, and $\mathcal{N}^{\mathrm{dst}} (\subset \mathcal{C})$ is the subset of the active destinations.

The function (8.6) describes the activity of the node q as a function of the time t. For $q \in \mathcal{C}$, t_q is stored in the q-th entry of the NCT_n, while, for $q \in \{n, D(n)\}$, t_q is the current time. Moreover, by setting a counter for each $q \in \mathcal{N}^{\mathrm{nl}}$, n can estimate the probability of activity $\eta_{n,q}$ as the ratio between the number of packets sent by q and the overall packets sensed on the MCC. Finally, n can estimate the time evolution of the interference experienced by each node $q \in \mathcal{C} \cup \{n, D(n)\}$ as:

$$\mathrm{I}_{n,q}(t) = G_q^{\mathrm{null}} \sum_{p \in \mathcal{I}_{n,q}^{\mathrm{null}}} f_{n,p}(t) P_{q,p}^{\mathrm{r}} + G_q^{\mathrm{av}} \sum_{p \in \mathcal{I}_{n,q}^{\mathrm{av}}} f_{n,p}(t) P_{q,p}^{\mathrm{r}} + G_q^{\mathrm{av}} \sum_{p \in \mathcal{N}^{\mathrm{nl}} - \{q\}} \eta_{n,p} P_{q,p}^{\mathrm{r}}. \tag{8.7}$$

The first two terms in (8.7) are deterministic and account for the time evolution of the active interferers, while the third term estimates the probability that each non-legacy node becomes an interferer. Observe that the set $\mathcal{N}^{\mathrm{nl}} - \{q\}$ in the third term includes also the currently active nodes, because a node that has completed its transmission may begin another one.

From (8.7), the SIR for the node q can be derived as:

$$\mathrm{SIR}_{n,q}(t) = \frac{1}{\mathrm{I}_{n,q}(t)} \cdot \begin{cases} P_{q,D(q)}^{\mathrm{r}} & q \in \mathcal{N}^{\mathrm{src}} \cup \{n\} \\ P_{S(q),q}^{\mathrm{r}} & q \in \mathcal{N}^{\mathrm{dst}} \cup \{D(n)\} \end{cases}, \tag{8.8}$$

where $S(q)$ is the source of the packet having q as destination.

Once all SIRs are available, the success of a frame exchange may be evaluated by using the SPB aided framework presented in Chapter 4. Particularly, the equivalent rate $r_{\text{eq}}^{n,q}(t)$, is estimated using the SIR value at each time instant, and its average value is compared to the selected code rate R_c^n. More formally, the averaged equivalent rate, which is referred to as the sustainable rate, is obtained as:

$$r_{\text{sus}}^{n,q} = \begin{cases} \dfrac{1}{T_{\text{ACK}}} \displaystyle\int_0^{T_{\text{ACK}}} r_{\text{eq}}^{n,q}(t)\mathrm{d}t & q \in \mathcal{N}^{\text{src}} \cup \{n\} \\ \dfrac{1}{T_{\text{DATA}}} \displaystyle\int_0^{T_{\text{DATA}}} r_{\text{eq}}^{n,q}(t)\mathrm{d}t & q \in \mathcal{N}^{\text{dst}} \cup \{D(n)\} \end{cases} . \tag{8.9}$$

A received packet may be assumed successful if the adopted code rate R_c satisfies $R_c \leq r_{\text{sus}}^{n,q}$. Hence, defining as $\mathcal{R}_c$ the set of the available code rates, the two conditions:

$$\begin{cases} \exists (R_c^n, R_c^{D(n)}) \in \mathcal{R}_c \times \mathcal{R}_c : R_c^n \leq r_{\text{sus}}^{n,D(n)}, R_c^{D(n)} \leq r_{\text{sus}}^{D(n),n} \\ R_c \leq r_{\text{sus}}^{n,q}, q \in \mathcal{C} \end{cases} , \tag{8.10}$$

may be used by n as the criterion for decreasing its backoff counter.

These conditions require that, if the potential communication n-$D(n)$ becomes active, this communication and the currently active ones can be all successful. Observe from (8.10) that the SAMPC scheme considers the potential effect of the concurrent transmissions not only on the DATA receptions, but also on the ACK receptions, which are often neglected but can have a considerable impact on the result of the communication attempt.

Summarising, the SAMPC protocol adopts an advanced collision avoidance policy based on an accurate estimation of the instantaneous SIR and of the code behaviour, in order to allow each node to evaluate the effect of the interference on its potential communication and on all the active ones, taking into account both the DATA and the ACK receptions.

Similarly to the TAMPC scheme, the SAMPC algorithm acquires information on the current medium occupation, thus matching the first condition outlined in [123] for exploiting adaptive arrays. Additionally, the SAMPC protocol estimates the evolution of the interference, in order to compensate for the impossibility of preserving the interference configuration in a distributed scenario [123].

8.5 Results

The proposed MAC protocols have been implemented in a C++ simulation platform developed adopting the IT++ libraries for signal processing and communications [99].

Common parameters	
Preamble	128 bits
Slot time	20 μs
DOA estimation algorithm	MUSIC [133]
DIFS duration	50 μs
Beamforming algorithm	Constrained Least Mean Square (LMS) [133]
SIFS duration	10 μs
Path-loss exponent α	3
Maximum backoff stage	4
Retry limit	4
RTS	160 bits
CTS	112 bits
DATA header	240 bits
Average payload	6960 bits
ACK	112 bits
Data rate	12 Mbits/s
Control rate	2 Mbits/s
Modulation	QPSK
TAMPC parameters	
$L_{t_{n/D(n)}}$	4 bits
RTS_{MCC}	RTS + L_{t_n} + preamble
CTS_{MCC}	CTS + $L_{t_{D(n)}}$ + preamble
SAMPC parameters	
$N_{i/\text{d}(i)}$	4 bits
$G^{\text{n/a}}_{i/\text{d}(i)}$	8 bits
$R_{i/\text{d}(i)}$	2 bits
RTS_{MCC}	RTS + N_n + G_n^{null} + G_n^{av} + R_c^n + $R_c^{D(n)}$ + preamble
CTS_{MCC}	CTS + $N_{D(n)}$ + $G_{D(n)}^{\text{null}}$ + $G_{D(n)}^{\text{av}}$ + R_c^n + $R_c^{D(n)}$ + preamble

Table 8.1: Adopted parameters and algorithms.

The selected algorithms and parameters are reported in Table 8.1, where the payload is assumed geometrically distributed with an average length equal to 870 bytes (6960 bits) [135]. For each simulation, 60 seconds of network activity are recorded. To simplify the comparison between the two presented schemes, a fixed code rate R_c^n ($n \in \mathcal{N}$) equal to 2/3 is assumed for the ACK frames in all the simulations, while the value of the code rate $R_c^{D(n)}$ ($n \in \mathcal{N}$) for the DATA frames, which is still maintained fixed during a particular simulation, will be specified for each examined scenario. Efficient codes are also used at the PHY of the TAMPC protocol, where, however, they simply replace the convolutional codes typically used by IEEE

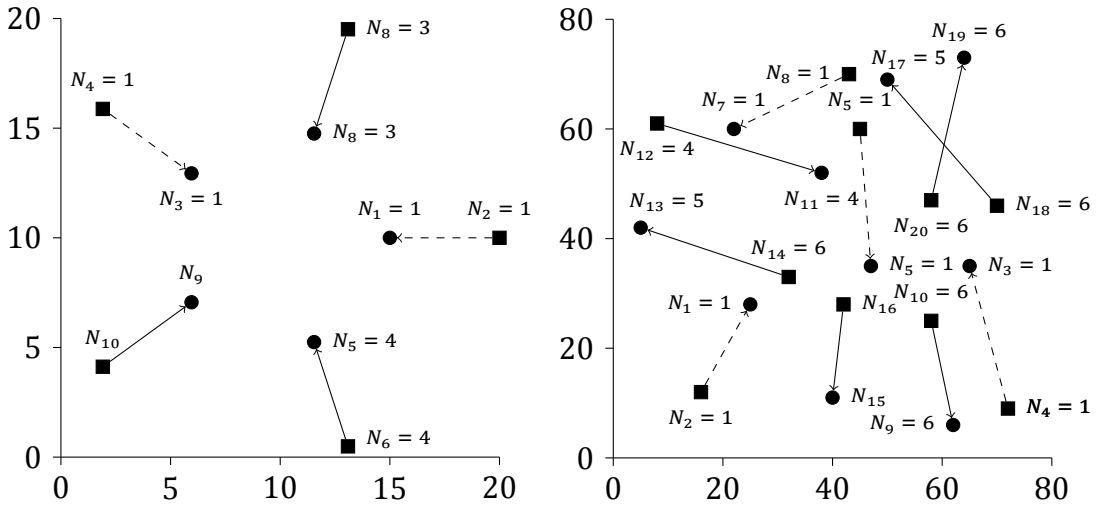

(a) Heterogeneous concentric topology (b) Heterogeneous random topology

802.11 stations, but are not involved in the backoff counter process as in the SAMPC protocol. Besides, the threshold adopted by the generic non-legacy node n for the TAMPC scheme is assumed to be equal to the number of degrees of freedom of its antenna system, thus $L_{t_n} = N_n - 1$ for $n \in \mathcal{N}^{\text{nl}}$ [135].

The adopted performance figures are the throughput and the Jain's fairness index. In particular, the throughput is expressed in terms of the average number of packets that may be successfully hosted in a slot time at the net of the adopted code rate. In other words, the sum of the throughput of all network nodes directly provides the number of simultaneous communications that can be hosted in a slot.

The presented results are divided into two parts. The first part reports the performance of the TAMPC and SAMPC schemes in heterogeneous scenarios involving both legacy and non-legacy nodes equipped with different antenna systems, and asymmetric network topologies. The second part compares the protocols' behaviour to the analytic model proposed in [119] for scenarios characterised by a symmetric topology.

8.5.1 Protocols' performance

The first set of results is obtained considering a minimum contention window equal to 32 and a code rate $R_c^{D(n)} = 8/9\,(n \in \mathcal{N})$ in the presence of a Poisson packet arrival process of mean μ.

The adopted topologies with the corresponding N_n values are shown in Figures 8.1(a) and 8.1(b). Precisely, the ring topology in Figure 8.1(a) consists of two legacy pairs and three non-legacy pairs, while the random one in Figure 8.1(b) con-

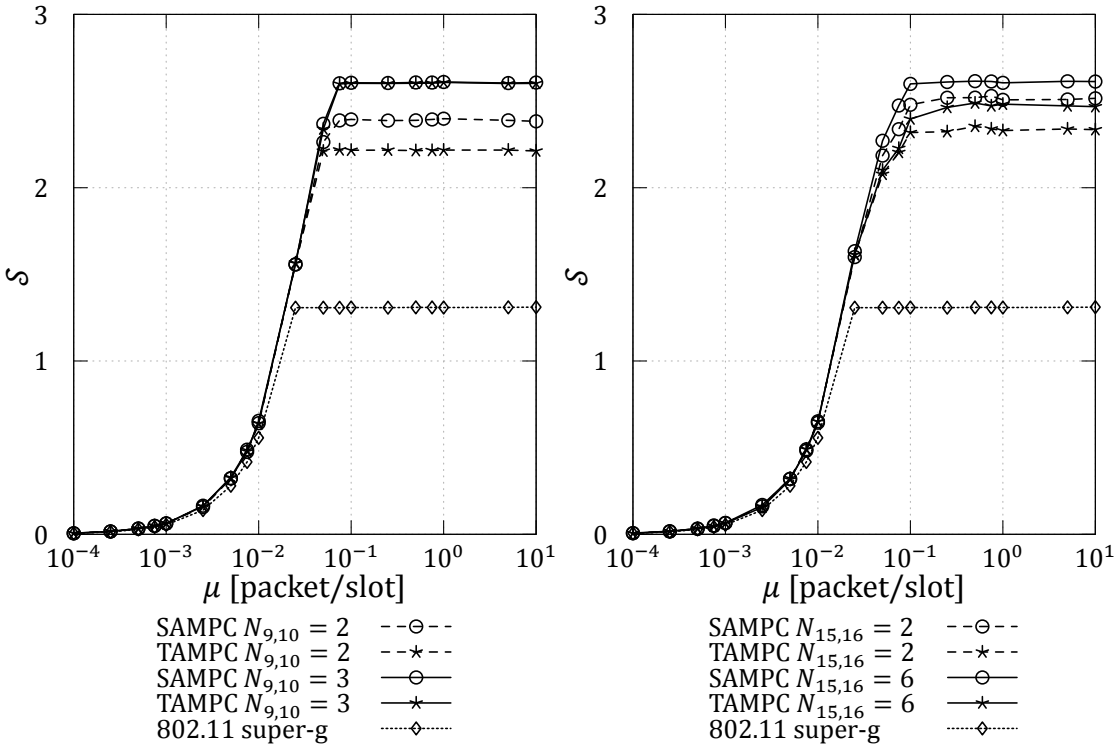

(c) Topology of Figure 8.1(a)

(d) Topology of Figure 8.1(b)

Figure 8.1: Network throughput as a function of the average arrival rate.

sists of four legacy pairs and six non-legacy pairs. The number of antennas of the pair $9-10$ in the ring topology and of the pair $15-16$ in the random topology is not specified, since it will be used to put into evidence the different performance of the developed schemes.

Figures 8.1(c) and 8.1(d) report the aggregate throughput, given by the sum of the throughput in the CC and in the MCC. In particular, Figure 8.1(c) refers to the topology of Figure 8.1(a) considering the cases $N_{9,10} = 3$ and $N_{9,10} = 2$, while Figure 8.1(d) refers to the topology in Figure 8.1(b) considering the cases $N_{15,16} = 6$ and $N_{15,16} = 2$. The figures also show the throughput obtained using the IEEE 802.11 super-g extension [138], where the adoption of two frequency channels at 12 Mbits/s is assumed for the sake of providing a fair comparison with the proposed schemes.

The curves show that both the TAMPC and SAMPC protocols provide a higher performance with respect to the super-g extension, allowing the coexistence of a number of simultaneous communications ranging from two to three for all the considered scenarios.

With reference to Figure 8.1(c), a direct comparison between the two proposed

Pair	TAMPC	SAMPC	TAMPC	SAMPC
	$N_{9,10} = 3$		$N_{9,10} = 2$	
1-2	0.38	0.38	0.38	0.38
3-4	0.38	0.38	0.38	0.38
5-6	0.62	0.62	0.50	0.62
7-8	0.62	0.62	0.49	0.62
9-10	0.60	0.61	0.47	0.39
Fairness (CC)	1.00	1.00	1.00	1.00
Fairness (MCC)	1.00	1.00	1.00	0.96

Table 8.2: Single-node saturation throughput (in packets/slot) for topology of Figure 8.1(a).

schemes reveals that, when $N_{9,10} = 3$, their performance is substantially identical, while, when $N_{9,10} = 2$, the SAMPC scheme provides a higher throughput than the TAMPC protocol.

The different behaviour of the two solutions can be explained in detail considering the single-node saturation throughput reported in Table 8.2. In the case $N_{9,10} = 3$, the minimum threshold among all nodes operating in the MCC is $L_{t_n} = N_n - 1 = 3 - 1 = 2$ ($n \in \mathcal{N}^{\mathrm{nl}}$). As described previously, using the TAMPC protocol the backoff counter is decreased when two conditions are satisfied: the number of estimated active sources l_n is lower or equal to $L_{t_n} = L_t = 2$ and $l_n \leq N_n - 1 = 2$ for $n \in \mathcal{N}^{\mathrm{nl}}$. This implies that when two communications are active, a further one can be established and hence three transmissions may be simultaneously performed on the MCC. Considering also the CC, a total of four concurrent transmissions may be sustained by the network. Observe that the adoption of a large minimum contention window, which has been selected equal to 32, and the presence of the channel encoder, determine throughput values lower than four, as it can be shown in Figure 8.1(c) for $N_{9,10} = 3$. However, independently of these aspects, in the case $N_{9,10} = 3$ the proposed protocols guarantee the same throughput and a fair access to the network nodes.

By contrast, in the case $N_{9,10} = 2$, the SAMPC protocol provides a higher throughput, while the TAMPC scheme maintains a better fairness. This result can be explained by analysing the access of the nodes operating on the MCC, namely the pairs $5-6$, $7-8$, and $9-10$, for the two developed schemes. For $N_{9,10} = 2$, the thresholds become $L_{t_{5\div8}} = 2$ and $L_{t_{9\div10}} = 1$. Adopting both protocols, when the pairs $5-6$ and $7-8$ (having three antennas) are active, the source 10 (having just two antennas) freezes its backoff counter because it cannot estimate more than one active transmitter.

A different behaviour appears for the two schemes in another configuration of transmitters. When adopting the TAMPC protocol, and in the case where one of the

Pair	TAMPC	SAMPC	TAMPC	SAMPC
	$N_{15,16} = 6$		$N_{15,16} = 2$	
1-2	0.22	0.22	0.22	0.22
3-4	0.20	0.20	0.20	0.20
5-6	0.19	0.19	0.19	0.19
7-8	0.21	0.21	0.21	0.21
9-10	0.60	0.54	0.56	0.58
11-12	0.03	0.08	0.02	0.05
13-14	0.03	0.14	0.37	0.40
15-16	0.60	0.46	0.09	0.05
17-18	0.15	0.34	0.07	0.35
19-20	0.23	0.24	0.42	0.27
Fairness (CC)	1.00	1.00	1.00	1.00
Fairness (MCC)	0.56	0.76	0.60	0.69

Table 8.3: Single-node saturation throughput (in packets/slot) for topology of Figure 8.1(b).

two pairs with three antennas ($5-6$ or $7-8$) and the unique pair with two antennas ($9-10$) are active, the source of the other pair with three antennas (8 or 6) freezes its backoff counter to protect the communication of the pair $9-10$, according to the criterion on the minimum threshold of (8.1). This implies a fair reduction of the single-node throughput. Conversely, adopting the SAMPC scheme in the same configuration of transmitters, the source 8 or 6 does not freeze its backoff counter, since it estimates that the communication involving the pair $9-10$ may remain successful in the presence of the other two communications. This implies that the pairs with three antennas acquire more resources, leading to a higher throughput at the expense of a slight fairness reduction.

The curves in Figure 8.1(d) confirm the higher performance of the proposed protocols with respect to the IEEE 802.11 super-g extension for the random topology in Figure 8.1(b). Besides, the results in Table 8.3 show that in this case the SAMPC scheme outperforms the TAMPC one for the two considered scenarios ($N_{15,16} = 6$ and $N_{15,16} = 2$) both in terms of throughput and fairness.

In both the proposed protocols each node tries to protect not only its own communication but also those of the other active nodes. The TAMPC protocol reaches this objective by accounting for the load threshold sustainable by the active node with the less powerful antenna system, without considering the characteristics of the topology. The SAMPC protocol adopts a more advanced protection mechanism based on a SIR estimation, and hence is able to account for a larger number of network elements, including not only the number of antennas, but also the antenna gains and the relative positions between the nodes. The values in Table 8.3 confirm

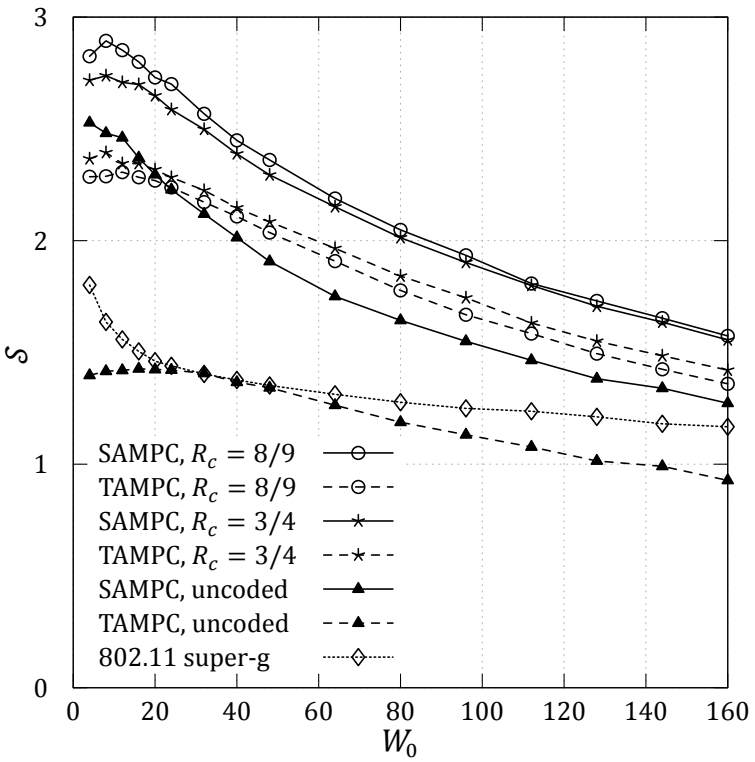

Figure 8.2: Protocols' performance in saturated conditions (average values for 50 randomly generated topologies).

that the adoption of this more reliable process of estimation of the network conditions provides considerable benefits to the global performance of the network. This result suggests the usefulness of the SAMPC protocol for random topologies, which represent a more realistic scenario for the commonly deployed wireless networks.

To further investigate this issue, a third set of simulations is carried out by considering 50 random topologies, each having $n = 20$ non-legacy nodes, namely 10 pairs operating in the MCC once the process of recognition is completed. All nodes are equipped with an antenna array having $N_n = 5$ ($n \in \mathcal{N}^{\text{nl}} \equiv \mathcal{N}$) elements. Observe that, while the previously simulated scenarios in Figures 8.1(c) and 8.1(d) were heterogeneous both in terms on nodes and topologies, in this case the scenario is heterogeneous only because of the spatial distribution of the nodes, since all stations have identical antenna systems.

Figure 8.2 reports the average network throughput in saturated traffic conditions as a function of the minimum contention window for different values of the code rate $R_{\text{d}(i)}$. One can observe that Figure 8.2 confirms that the SAMPC protocol provides a higher throughput when compared to the TAMPC scheme. In particular, for the TAMPC protocol, the rate $3/4$ leads to a higher throughput, while, for the

SAMPC protocol, the best performance is obtained using a rate of 8/9. Furthermore, a direct comparison between the uncoded scenario ($R_c^{D(n)} = 1$) and the coded ones reveals that a certain channel coding is necessary to maintain an acceptable performance. However, the required redundancy can be maintained low, since even a high code rate, such as 8/9, provides a satisfactory performance that is close to the one achievable using the lower rate of 3/4.

In general, the results presented for heterogeneous scenarios show that the capability of an antenna system alone does not represent an absolute element for the single-node performance, which is also influenced by its position within the network. Therefore, the adoption of a rigid threshold on the number of communications for establishing the success or failure of the transmission attempts in an MPC scenario might sometimes result in a partial under-utilisation of the network resources.

This second part of the results aims to compare the protocols' performance to the analysis presented in [119]. Simulations are carried out assuming saturated traffic conditions and maintaining the settings reported in Table 8.1. Since the model developed in [119] holds for an homogeneous network, the comparison between theoretical and numerical results is performed adopting a symmetric topology in which $|\mathcal{N}| = 20$ identical non-legacy nodes are placed on two concentric rings, where the sources lie in the outer ring, having a radius equal to 20 m, and the destinations lie in the inner ring, having a radius equal to 10 m. Each node has $N_n = 5\ (n \in \mathcal{N}^{\mathrm{nl}} \equiv \mathcal{N})$ antennas and, for each DATA frame, a fixed code rate $R_c^{D(n)} = 8/9\ (n \in \mathcal{N})$ is used. Since only non-legacy nodes are involved, the CC is used just for the process of recognition and the rest of the traffic is delivered using the MCC.

Figure 8.3 shows the network throughput as a function of the minimum contention window obtained using the TAMPC and the SAMPC protocols, the IEEE 802.11 super-g extension, and the analysis of [119].

Since the theory of [119] considers an access based on a threshold on the number of allowed communications, the comparison with the theory is more meaningful when it involves the TAMPC protocol. In particular, the analysis in [119] and the TAMPC scheme are compared for the two thresholds $L_{t_n} = L_t = 3\ (n \in \mathcal{N})$ and $L_{t_n} = L_t = 5\ (n \in \mathcal{N})$. One can immediately observe that the analytic and the numerical throughput values of the TAMPC protocol are very close for a large part of the considered range of minimum contention windows.

More precisely, the theoretical and simulated curves almost overlap when the minimum contention window is high, while differences appear when it becomes low, mainly for the case $L_t = 5$. These differences are due to the fact that the studied scenario, even if symmetric and composed by identical nodes, is not perfectly homogeneous. In fact, in the simulation, the result of a reception in the presence

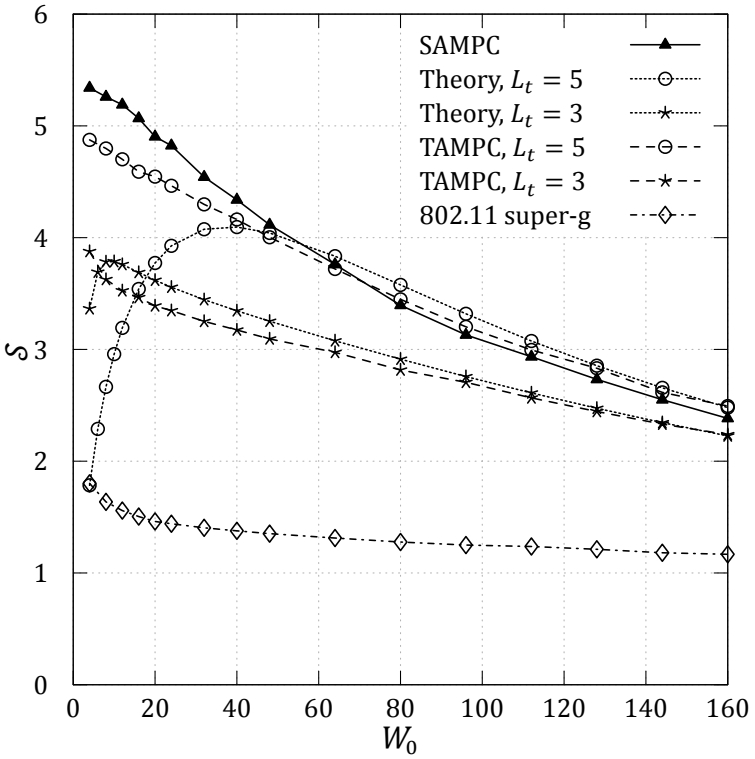

Figure 8.3: Network throughput in saturated conditions as a function of minimum contention window for a concentric topology.

of a certain number of simultaneous transmissions does not depend only on the number of transmitters itself, but also on which transmitters are active. Thus, different configurations of the same number of active sources can be present, some of which may lead to unsuccessful receptions, while others may lead to successful receptions. The analysis, instead, assuming an homogeneous scenario, considers all possible configurations of a given number of transmitters as identical and hence leading to the same result.

A direct comparison between Figure 8.2 and Figure 8.3 shows that the performance improvement achievable by the proposed protocols with respect to the IEEE 802.11 super-g extension considerably increases in the symmetric scenario. The same comparison reveals that the concentric topology provides, for the TAMPC and the SAMPC schemes, an average throughput that is almost doubled compared to the case where the nodes are located at random positions. The strong impact of the topology on the achievable performance becomes more evident when noting that the results in Figure 8.2 and Figure 8.3 refer only to different topologies, since both networks are characterised by the same number of identical nodes, the same single-node antenna characteristics, and the same code rate. Hence, one may conclude

that the location of stations in the network plays a significant role in determining the network performance.

8.6 Conclusions

This chapter outlined the design requirements for enabling multi-packet communication in IEEE 802.11 networks by using advanced antenna systems. Two novel protocols where stations are capable of adapting their access procedure on the instantaneous network conditions were proposed and their performance analysed.

The results proved that the developed schemes outperform the legacy IEEE 802.11 MAC layer with the super-g PHY layer extension. In particular, the SIR-based access adopted by the SAMPC scheme can guarantee higher throughput and fairness values than the threshold-based access adopted by the TAMPC protocol, at the cost of an increased complexity. Furthermore, a comparison between the throughput of the TAMPC scheme and that obtained from the theory has shown that the selection of the load threshold has a significant impact on the final performance.

9
Conclusions

This thesis considered the analysis and the design of high throughput wireless networks. Particularly, it was shown that the performance of a wireless network may be increased by relying on cooperative communications and on advanced antenna techniques. Such techniques, which benefit from adaptive strategies where the stations change their transmission policy according to the physical layer and network characteristics, were shown to be an effective way to provide faster communications and to increase the number of simultaneous ongoing transmissions, ultimately yielding a better performance.

Particularly, the thesis discussed the problem of identifying the performance of a distributed channel coding technique, proposing a novel estimator that was shown to be an accurate benchmark tool for comparing different coding schemes. Such benchmark was also used for contriving practical physical layer cooperative schemes that are capable of approaching the limiting performance for a wide range of channel conditions and transmission policies. The thesis also discussed the analytic tools required for designing such schemes. Summarising, this work confirmed and enriched results obtained by previous studies, evidencing that cooperation may be an effective physical layer technique for increasing the decoding performance at the destination in faded scenarios.

The promised performance increase at the physical layer motivated the use of a cross-layer approach for designing medium access control procedures that benefit from advanced distributed coding techniques for increasing the network performance. This thesis discussed the design of cooperative medium access control schemes that rely on efficient distributed encoders. Particularly, the thesis discussed the influence of the adaptive algorithm used by stations in the network for identifying their transmission strategy, and it shown that a carefully designed adaptive regime, which accounts for the benefit provided by the advanced physical layer, provides a significant performance increase. Finally, the thesis investigated the performance of cooperative adaptive systems at the MAC layer when stations rely on imperfect channel estimates, which represents a more realistic scenario compared to the idealised case of knowing the instantaneous channel conditions

without errors. As a summary, this work shown that cooperation may be used also at the MAC layer for providing an enhanced network behaviour, and characterised the influence of using different encoding schemes on the network performance in different network scenarios.

Finally, the thesis considered the design of access protocols for wireless networks where stations are equipped with multiple radiating elements. It was shown that an advanced antenna system may be used for increasing the number of ongoing communications by reducing the interference produced by undesired sources and ultimately increasing the network performance without sacrificing the backward compatibility with legacy nodes that equip an omnidirectional antenna.

Future works may consider further enhancements to the design of cooperative MAC protocols. It would be of particular interest to develop schemes that fully exploit the benefit offered by Markov frameworks for increasing the network performance in scenarios where the information on other nodes is partial, corrupted or delayed. It would be also of interest to study cooperative MAC schemes that rely on advanced antenna systems at the PHY layer. Such schemes may reduce interference between stations, allowing multiple nodes to cooperate without corrupting other ongoing transmissions. Finally, it would be interesting to obtain further analytic results for the performance of networks where stations rely on adaptive physical layer techniques, including a mixture of cooperation and beamforming.

List of publications

Journal papers

- F. Babich, A. Crismani and R.G. Maunder, ``EXIT chart aided design of periodically punctured turbo codes'', Electronics Letters, vol. 46, no 14, June 2010
- F. Babich and A. Crismani, ``Cooperative coding schemes: design and performance evaluation'', IEEE Transactions on Wireless Communications, vol. 11, pp. 222–235, Jan. 2012.
- F. Babich, A. Crismani, M. Driusso and L. Hanzo, ``Design criteria and genetic algorithm aided optimization of three-stage-concatenated space-time shift keying systems'', IEEE Signal Procesing Letters, vol. 19, no 8, August 2012.
- F. Babich, M. Comisso, A. Crismani and A. Dorni ``On the design of MAC protocols for multi-packet communication in IEEE 802.11 heterogeneous networks using adaptive antenna arrays'', submitted to the IEEE Transactions on Mobile Computing.

Conference proceedings

- F. Babich, A. Crismani and L. Hanzo, ``Cross-Layer solutions for cooperative medium access control protocols'', IEEE Vehicular Technology Conference, Taipei (Taiwan), May 2010.
- F. Babich and A. Crismani, ``Incremental and complementary coding techniques for cooperative medium access control protocols'', IEEE Vehicular Technology Conference, Budapest (Hungary), May 2011.
- F. Babich, A. Crismani and L. Hanzo, ``Relay selection schemes relying on adaptive modulation and imperfect channel knowledge for cooperative networks'', IEEE International Conference on Communications, Ottawa (Canada), June 2012.
- F. Babich, M. Comisso, A. Crismani and A. Dorni ``Multi-Packet communication in 802.11 networks by spatial reuse: from theory to protocol'', accepted at the IEEE International Conference on Communications, 2013.

National workshops

- F. Babich, M. Comisso, A. Crismani and A. Dorni, ``Asynchronous 802.11 networks: USRP implementation and multi-antenna heterogeneous scenarios'', in Workshop Reti.it, Bormio (Italy), January 2013.

Bibliography

[1] G. Stüber, ``Principles of mobile communication,'' 1996.

[2] E. Biglieri, J. Proakis, and S. Shamai, ``Fading channels: information-theoretic and communications aspects,'' *IEEE Transactions on Information Theory*, vol. 44, no. 6, pp. 2619--2692, October 1998.

[3] T. Ue, S. Sampei, N. Morinaga, and K. Hamaguchi, ``Symbol rate and modulation level-controlled adaptive modulation TDMA TDD system for high-bit-rate wireless data transmission,'' *IEEE Transactions on Vehicular Technology*, vol. 47, no. 4, pp. 1134--1147, November 1998.

[4] F. Babich, ``Considerations on adaptive techniques for time-division multiplexing radio systems,'' *IEEE Transactions on Vehicular Technology*, vol. 48, no. 6, pp. 1862--1873, November 1999.

[5] S. Alamouti and S. Kallel, ``Adaptive trellis-coded multiple-phase-shift keying for Rayleigh fading channels,'' *IEEE Transactions on Communications*, vol. 42, no. 6, pp. 2305--2314, June 1994.

[6] L. Hanzo and J. Woodard, ``An intelligent multimode voice communications system for indoor communications,'' *IEEE Transactions on Vehicular Technology*, vol. 44, no. 4, pp. 735--748, November 1995.

[7] C. Berrou, A. Glavieux, and P. Thitimajshima, ``Near Shannon limit error correcting coding and decoding: Turbo-codes (1),'' in *IEEE International Conference on Communications*, vol. 2, May 1993, pp. 1064--1070.

[8] L. Ye and A. Burr, ``Adaptive modulation and code rate for turbo coded OFDM transmissions,'' in *IEEE Vehicular Technology Conference, Spring*, April 2007, pp. 2702--2706.

[9] R. Liu, J. Luo, and P. Spasojevic, ``Adaptive transmission with variable-rate turbo bit-interleaved coded modulation,'' *IEEE Transactions on Wireless Communications*, vol. 6, no. 11, pp. 3926--3936, November 2007.

[10] Z. Jiancun, S. Wentao, L. Hanwen, and X. Youyun, ``Pragmatic approach to adaptive turbo coded modulation,'' *Journal of Systems Engineering and Electronics*, vol. 14, no. 4, pp. 20--24, December 2003.

[11] Y. Xiao and M. Lee, ``Adaptive LDPC decoding for multipath channels,'' in *IEEE International Conference on Signal Processing*, vol. 1, November 2006.

[12] Y. Zhang, D. Yuan, and H. Zhang, ``Adaptive LDPC for Rayleigh fading channel,'' in *ISCC International Symposium on Computers and Communications*, vol. 2, June 2004, pp. 651--656--2.

[13] Z. He, R. Sebastien, and P. Fortier, ``Adaptive LDPC codes for MIMO transceiver with adaptive spectral efficiency,'' in *Biennial Symposium on Communications*, June 2008, pp. 120--123.

[14] Z. He and S. Roy, ``High-speed design of adaptive LDPC codes for wireless networks,'' in *Joint International IEEE Northeast Workshop on Circuits and Systems and TAISA Conference*, June 2008, pp. 249--252.

[15] Y. Zhang, ``Approaching V-BLAST capacity with adaptive modulation and LDPC encoding,'' *IEEE Transactions on Communications*, vol. 55, no. 12, pp. 2261--2269, December 2007.

[16] S. Alamouti, ``A simple transmit diversity technique for wireless communications,'' *IEEE Journal on Selected Areas in Communications*, vol. 16, no. 8, pp. 1451 --1458, October 1998.

[17] V. Tarokh, H. Jafarkhani, and A. Calderbank, ``Space-time block codes from orthogonal designs,'' *Information Theory, IEEE Transactions on*, vol. 45, no. 5, pp. 1456 --1467, July 1999.

[18] T. Hunter and A. Nosratinia, ``Cooperation diversity through coding,'' in *IEEE International Symposium on Information Theory*, 2002, p. 220.

[19] M. Janani, A. Hedayat, T. Hunter, and A. Nosratinia, ``Coded cooperation in wireless communications: space-time transmission and iterative decoding,'' *Signal Processing, IEEE Transactions on*, vol. 52, no. 2, pp. 362--371, February 2004.

[20] T. Hunter and A. Nosratinia, ``Diversity through coded cooperation,'' *IEEE Transactions on Wireless Communications*, vol. 5, no. 2, pp. 283--289, 2006.

[21] J. Laneman and G. Wornell, ``Distributed space-time-coded protocols for exploiting cooperative diversity in wireless networks,'' *Information Theory, IEEE Transactions on*, vol. 49, no. 10, pp. 2415--2425, October 2003.

[22] L. Hanzo, O. Alamri, M. El-Hajjar, and N. Wu, *Near-capacity multi-functional MIMO systems: sphere-packing, iterative detection and cooperation*. Wiley-Blackwell, 2009.

[23] B. Hassibi and B. Hochwald, ``High-rate codes that are linear in space and time,'' *Information Theory, IEEE Transactions on*, vol. 48, no. 7, pp. 1804 --1824, July 2002.

[24] M. Valenti and B. Zhao, ``Distributed turbo codes: towards the capacity of the relay channel,'' in *IEEE Vehicular Technology Conference, Fall*, vol. 1, October 2003, pp. 322--326.

[25] M. Butt, R. Riaz, S. X. Ng, and L. Hanzo, ``Distributed self-concatenated codes for low-complexity power-efficient cooperative communication,'' in *IEEE Vehicular Technology Conference, Fall*, September 2009, pp. 1--5.

[26] S. Benedetto, D. Divsalar, G. Montorsi, and F. Pollara, ``Self-concatenated trellis coded modulation with self-iterative decoding,'' in *IEEE Global Telecommunications Conference*, vol. 1, November 1998, pp. 585 --591.

[27] L. Kong, S. X. Ng, R. Maunder, and L. Hanzo, ``Irregular distributed space-time code design for near-capacity cooperative communications,'' in *IEEE Vehicular Technology Conference, Fall*, September 2009, pp. 1--6.

[28] H. Wen, L. Zhou, and Z. Zhang, ``Cooperative coding using parallel concatenated LDPC codes,'' in *IEEE Information Theory Workshop*, October 2006, pp. 395 --398.

[29] D. Duyck, M. Moeneclaey, M. Azmi, J. Yuan, and J. Boutros, ``Universal LDPC codes for cooperative communications,'' in *International Symposium on Turbo Codes and Iterative Information Processing*, September 2010, pp. 73 --77.

[30] G. de Oliveira Brante, A. Uchoa, and R. Souza, ``Cooperative coded partial retransmission scheme using Type-I HARQ and LDPC codes,'' in *IEEE International Symposium on Personal Indoor and Mobile Radio Communications*, September 2010, pp. 123 --128.

[31] M. Wu, P. Weitkemper, D. Wubben, and K.-D. Kammeyer, ``Comparison of distributed LDPC coding schemes for decode-and-forward relay channels,'' in *International ITG Workshop on Smart Antennas*, February 2010, pp. 127 --134.

[32] M. Azmi, J. Li, J. Yuan, and R. Malaney, ``Design of distributed multi-edge type LDPC codes for two-way relay channels,'' in *IEEE International Conference on Communications*, June 2011, pp. 1 --5.

[33] N. Qiu, X. Peng, Y. Lu, and S. Goto, ``Distributed punctured LDPC coding scheme using novel shuffled decoding for MIMO relay channels,'' in *European Signal Processing Conference*, August 2012, pp. 1404 --1408.

[34] ``IEEE Standard for Wireless LAN Medium Access Control (MAC) and PHYsical Layer (PHY) Specifications, organization=IEEE Standard 802.11,'' November 1997.

[35] ``IEEE Standard for Wireless LAN Medium Access Control (MAC) and PHYsical Layer (PHY) Specifications: Amendment 4: Further Higher Data Rate Extension in the 2.4 GHz Band,'' IEEE Standard 802.11g, June 2003.

[36] ``IEEE Standard for Wireless LAN Medium Access Control (MAC) and PHYsical Layer (PHY) Specifications: Amendment 5: Enhancements for Higher Throughput,'' IEEE Standard 802.11n, October 2009.

[37] ``IEEE Standard for Wireless LAN Medium Access Control (MAC) and PHYsical Layer (PHY) Specifications: Amendment 8: Medium Access Control (MAC) Quality of Service Enhancements,'' IEEE Standard 802.11e, November 2005.

[38] ``IEEE Standard for Wireless LAN Medium Access Control (MAC) and PHYsical Layer (PHY) Specifications: Amendment 6: Medium Access Control (MAC) Security Enhancements,'' IEEE Standard 802.11i, July 2004.

[39] M. Heusse, F. Rousseau, G. Berger-Sabbatel, and A. Duda, ``Performance anomaly of 802.11b,'' in *IEEE International Conference on Computer Communications*, vol. 2, no. 30, March 2003, pp. 836--843.

[40] B. Sadeghi, V. Kanodia, A. Sabharwal, and E. Knightly, ``Opportunistic media access for multirate ad hoc networks,'' in *Proceedings of the 8th annual International Conference on Mobile Computing and Networking*, 2002, pp. 24--35.

[41] H. Shan, W. Zhuang, and Z. Wang, ``Distributed cooperative MAC for multihop wireless networks,'' *IEEE Communications Magazine*, vol. 47, no. 2, pp. 126--133, February 2009.

[42] P. Liu, Z. Tao, Z. Lin, E. Erkip, and S. Panwar, ``Cooperative wireless communications: a cross-layer approach,'' *IEEE Wireless Communications*, vol. 13, no. 4, pp. 84--92, August 2006.

[43] H. Zhu and G. Cao, ``rDCF: A relay-enabled medium access control protocol for wireless ad hoc networks,'' *IEEE Transactions on Mobile Computing*, vol. 5, no. 9, pp. 1201--1214, March 2006.

[44] C.-T. Chou, J. Yang, and D. Wang, ``Cooperative MAC protocol with automatic relay selection in distributed wireless networks,'' in *IEEE International Conference on Pervasive Computing and Communications Workshops*, March 2007, pp. 526--531.

[45] P. Liu, Z. Tao, S. Narayanan, T. Korakis, and S. Panwar, ``CoopMAC: a cooperative MAC for wireless LANs,'' *IEEE Journal on Selected Areas in Communications*, vol. 25, no. 2, pp. 340--354, February 2007.

[46] Y. Yuan, B. Zheng, W. Lin, and C. Dai, ``An opportunistic cooperative MAC protocol based on cross-layer design,'' in *International Symposium on Intelligent Signal Processing and Communication Systems*, December 2007, pp. 714--717.

[47] S. Sayed, Y. Yang, and H. Hu, ``CARD: cooperative access with relay's data for multi-rate wireless local area networks,'' in *IEEE International Conference on Communications*, June 2009, pp. 1--6.

[48] S. S. N, C.-T. Chou, and M. Ghosh, ``Cooperative communication MAC (CMAC) - a new MAC protocol for next generation wireless LANs,'' in *International Conference on Wireless Networks, Communications and Mobile Computing*, vol. 1, June 2005, pp. 1 -- 6.

[49] M. Dianati, X. Ling, K. Naik, and X. Shen, ``A node-cooperative ARQ scheme for wireless ad hoc networks,'' *Vehicular Technology, IEEE Transactions on*, vol. 55, no. 3, pp. 1032--1044, May 2006.

[50] L. Yi and J. Hong, ``A New cooperative communication MAC strategy for wireless ad hoc networks,'' *IEEE-ACIS International Conference on Computer and Information Science*, pp. 569--574, 2007.

[51] D. Chen, H. Ji, and X. Li, ``An energy-efficient distributed relay selection and power allocation optimization scheme over wireless cooperative networks,'' in *IEEE International Conference on Communications*, June 2011, pp. 1--5.

[52] J. Alonso-Zarate, E. Stavrou, A. Stamou, P. Angelidis, L. Alonso, and C. Verikoukis, ``Energy-efficiency evaluation of a medium access control protocol for cooperative ARQ,'' in *IEEE International Conference on Communications*, June 2011, pp. 1--5.

[53] N. Marchenko, E. Yanmaz, H. Adam, and C. Bettstetter, ``Selecting a spatially efficient cooperative relay,'' in *IEEE Global Telecommunications Conference*, December 2009, pp. 1 --7.

[54] N. Marchenko, C. Bettstetter, and E. Yanmaz, ``On radio resource allocation in proactive cooperative relaying,'' in *IEEE International Conference on Communications Workshops*, June 2009, pp. 1--5.

[55] G. Shirazi, P.-Y. Kong, and C.-K. Tham, ``A cooperative retransmission scheme in wireless networks with imperfect channel state information,'' in *IEEE Wireless Communications and Networking Conference*, April 2009, pp. 1--6.

[56] N. Marchenko and C. Bettstetter, ``Impact of relay selection overhead in cooperative diversity protocols,'' in *IEEE Vehicular Technology Conference, Fall*, September 2011, pp. 1--4.

[57] E. Gilbert, ``Capacity of a burst-noise channel,'' *Bell System Technical Journal*, vol. 39, no. 9, pp. 1253--1265, 1960.

[58] H. Li, N. Jaggi, and B. Sikdar, ``Relay scheduling for cooperative communications in sensor networks with energy harvesting,'' *IEEE Transactions on Wireless Communications*, vol. 10, no. 9, pp. 2918--2928, september 2011.

[59] B. Zhao and M. Valenti, ``Practical relay networks: a generalization of hybrid-ARQ,'' *IEEE Journal on Selected Areas in Communications*, vol. 23, no. 1, pp. 7--18, January 2005.

[60] G. Kramer, M. Gastpar, and P. Gupta, ``Capacity theorems for wireless relay channels,'' in *Conference on Communication Control and Computing*, vol. 41, no. 2, 2003, pp. 1074--1083.

[61] ------, ``Cooperative strategies and capacity theorems for relay networks,'' *IEEE Transactions on Information Theory*, vol. 51, no. 9, pp. 3037--3063, September 2005.

[62] B. Wang, J. Zhang, and A. Host-Madsen, ``On the capacity of MIMO relay channels,'' *IEEE Transactions on Information Theory*, vol. 51, no. 1, pp. 29--43, January 2005.

[63] M.-A. Badiu, M. Varga, and V. Bota, ``Link performance prediction methods for cooperative relaying in wireless networks,'' in *7th International Symposium on Wireless Communication Systems*, September 2010, pp. 556--560.

[64] R. Gallager, *Information Theory and Reliable Communication*. John Wiley & Sons, Inc., 1968.

[65] F. Babich, ``On the performance of efficient coding techniques over fading channels,'' *IEEE Transactions on Wireless Communications*, vol. 3, no. 1, pp. 290--299, January 2004.

[66] ------, ``Design of adaptive systems for the fading channel adopting efficient coded modulations,'' in *IEEE International Conference on Communications*, vol. 3, June 2006, pp. 1433--1438.

[67] A. Viterbi and J. Omura, *Principles of digital communication and coding*. McGraw-Hill, Inc. New York, NY, USA, 1979.

[68] R. Gallager, *Low-density parity-check codes*. MIT press Cambridge, MA, 1963.

[69] T. Richardson and R. Urbanke, ``The capacity of low-density parity-check codes under message-passing decoding,'' *IEEE Transactions on Information Theory*, vol. 47, no. 2, pp. 599--618, February 2001.

[70] F. Babich, ``Cooperative systems for the fading channel with adaptive modulation and incremental encoding,'' in *IEEE Global Telecommunications Conference*, December 2010, pp. 1--5.

[71] M. Valenti, ``An information-theoretic approach to accelerated simulation of hybrid-ARQ systems,'' in *IEEE International Communication Conference*, June 2011, pp. 1--6.

[72] S. ten Brink, ``Convergence behavior of iteratively decoded parallel concatenated codes,'' *IEEE Transactions on Communications*, vol. 49, no. 10, pp. 1727--1737, October 2001.

[73] S. ten Brink, G. Kramer, and A. Ashikhmin, ``Design of low-density parity-check codes for modulation and detection,'' *IEEE Transactions on Communications*, vol. 52, no. 4, pp. 670--678, April 2004.

[74] M. Benjillali, L. Szczecinski, and S. Aissa, ``Probability Density Functions of Logarithmic Likelihood Ratios in Rectangular QAM,'' in *23rd Biennial Symposium on Communications*, May 2006, pp. 283--286.

[75] A. Martinez, A. Guillen i Fabregas, and G. Caire, ``Error probability analysis of bit-interleaved coded modulation,'' *IEEE Transactions on Information Theory*, vol. 52, no. 1, pp. 262--271, January 2006.

[76] S. Kallel and D. Haccoun, ``Generalized type II hybrid ARQ scheme using punctured convolutional coding,'' *IEEE Transactions on Communications*, vol. 38, no. 11, pp. 1938--1946, November 1990.

[77] S. Kallel, ``Complementary punctured convolutional (CPC) codes and their applications,'' *IEEE Transactions on Communications*, vol. 43, no. 6, pp. 2005--2009, June 1995.

[78] F. Babich, O. Kelly, and G. Lombardi, ``Generalized Markov modeling for flat fading,'' *IEEE Transactions on Communications*, vol. 48, no. 4, pp. 547--551, April 2000.

[79] F. Babich, G. Montorsi, and F. Vatta, ``Some notes on rate-compatible punctured turbo codes (RCPTC) design,'' *IEEE Transactions on Communications*, vol. 52, no. 5, pp. 681--684, May 2004.

[80] A. Shokrollahi, ``Raptor codes,'' *IEEE Transactions on Information Theory*, vol. 52, no. 6, pp. 2551--2567, June 2006.

[81] J. Ha and S. McLaughlin, ``Optimal puncturing of irregular low-density parity-check codes,'' in *IEEE International Conference on Communications*, vol. 5, May 2003, pp. 3110--3114.

[82] O. Etesami, M. Molkaraie, and A. Shokrollahi, ``Raptor codes on symmetric channels,'' in *International Symposium on Information Theory*, June 2004, p. 38.

[83] A. Graell i Amat, F. Brännström, and L. Rasmussen, ``On the design of rate-compatible serially concatenated convolutional codes,'' *European Transactions on Telecommunications*, vol. 18, no. 5, pp. 519--527, 2007.

[84] A. Graell i Amat, G. Montorsi, and F. Vatta, ``Design and performance analysis of a new class of rate compatible serially concatenated convolutional codes,'' *IEEE Transactions on Communications*, vol. 57, no. 8, pp. 2280--2289, August 2009.

[85] F. Brännström, A. Graell i Amat, and L. Rasmussen, ``A general structure for rate-compatible concatenated codes,'' *IEEE Communications Letters*, vol. 11, no. 5, pp. 437--439, May 2007.

[86] N. Chandran and M. Valenti, ``Hybrid ARQ using serial concatenated convolutional codes over fading channels,'' in *IEEE Vehicular Technology Conference, Spring*, vol. 2, May 2001, pp. 1410--1414.

[87] S. Benedetto, D. Divsalar, G. Montorsi, and F. Pollara, ``Serial concatenation of interleaved codes: performance analysis, design, and iterative decoding,'' *IEEE Transactions on Information Theory*, vol. 44, no. 3, pp. 909--926, May 1998.

[88] L. Bahl, J. Cocke, F. Jelinek, and J. Raviv, ``Optimal decoding of linear codes for minimizing symbol error rate (Corresp.),'' *IEEE Transactions on Information Theory*, vol. 20, no. 2, pp. 284--287, mar 1974.

[89] L. Hanzo, T. Liew, and B. Yeap, *Turbo coding, turbo equalisation and space-time coding for transmission over fading channels*. John Wiley & Sons, Inc., 2002.

[90] D. Divsalar, S. Dolinar, and F. Pollara, ``Iterative turbo decoder analysis based on density evolution,'' *IEEE Journal on Selected Areas in Communications*, vol. 19, no. 5, pp. 891--907, may 2001.

[91] S. ten Brink, ``Convergence of iterative decoding,'' *Electronics Letters*, vol. 35, no. 10, pp. 806--808, 1999.

[92] R. Maunder and L. Hanzo, ``Genetic algorithm aided design of Component codes for irregular variable length coding,'' *IEEE Transactions on Communications*, vol. 57, no. 5, pp. 1290--1297, May 2009.

[93] S. X. Ng, O. Alamri, Y. Li, J. Kliewer, and L. Hanzo, ``Near-capacity turbo trellis coded modulation design based on EXIT charts and union bounds,'' *IEEE Transactions on Communications*, vol. 56, no. 12, pp. 2030--2039, December 2008.

[94] S. Sugiura, S. Chen, and L. Hanzo, ``Coherent and differential space-time shift keying: a dispersion matrix approach,'' *IEEE Transactions on Communications*, vol. 58, no. 11, pp. 3219--3230, November 2010.

[95] S. Sayed, Y. Yang, and H. Hu, ``Throughput analysis of cooperative access with relay's data protocol for unsaturated WLANs,'' in *International Conference on Wireless Communications and Mobile Computing*, June 2009, pp. 790--794.

[96] G. Bianchi, ``Performance analysis of the IEEE 802.11 distributed coordination function,'' *IEEE Journal on Selected Areas in Communications*, vol. 18, no. 3, pp. 535--547, March 2000.

[97] H. Wu, Y. Peng, K. Long, and S. Cheng, ``A simple model of IEEE 802.11 wireless LAN,'' in *International Conferences on Info-tech and Info-net*, vol. 2, October 2001, pp. 514--519.

[98] P. Chatzimisios, A. Boucouvalas, and V. Vitsas, ``IEEE 802.11 packet delay - a finite retry limit analysis,'' in *IEEE Global Telecommunications Conference*, vol. 2, December 2003, pp. 950--954.

[99] ``IT++ 4.2.0.'' [Online]. Available: http://sourceforge.net/projects/itpp/files/itpp/4.2.0/

[100] Y. Fan, C. Wang, J. Thompson, and H. Poor, ``Recovering multiplexing loss through successive relaying using repetition coding,'' *IEEE Transactions on Wireless Communications*, vol. 6, no. 12, pp. 4484--4493, December 2007.

[101] L. Kong, S. X. Ng, R. Maunder, and L. Hanzo, ``Successive relaying aided near-capacity irregular distributed space-time coding,'' in *IEEE Global Telecommunications Conference*, November 2009, pp. 5589--5593.

[102] L. Kong, S. X. Ng, and L. Hanzo, ``Near-capacity three-stage downlink iteratively decoded generalized layered space-time coding with low complexity,'' in *IEEE Global Telecommunications Conference*, November 2008, pp. 1--6.

[103] A. Karmokar, D. Djonin, and V. Bhargava, ``POMDP-based coding rate adaptation for type-I hybrid ARQ systems over fading channels with memory,'' *IEEE Transactions on Wireless Communications*, vol. 5, no. 12, pp. 3512--3523, December 2006.

[104] A. T. Hoang and M. Motani, ``Cross-layer adaptive transmission with incomplete system state information,'' *IEEE Transactions on Communications*, vol. 56, no. 11, pp. 1961--1971, November 2008.

[105] Y. Wei, F. R. Yu, and M. Song, ``Distributed optimal relay selection in wireless cooperative networks with finite-state markov channels,'' *IEEE Transactions on Vehicular Technology*, vol. 59, no. 5, pp. 2149--2158, June 2010.

[106] R. Bellman, *Dynamic Programming*. Princeton University Press, 1957.

[107] M. Littman, A. Cassandra, and L. Kaelbling, ``Learning policies for partially observable environments: scaling up,'' in *Proceedings of the Twelfth International Conference on Machine Learning*, 1995, pp. 362--370.

[108] I. Nourbakhsh, R. Powers, and S. Birchfield, ``DERVISH: an office-navigating robot,'' *AI magazine*, vol. 16, no. 2, p. 53, 1995.

[109] R. Simmons and S. Koenig, ``Probabilistic robot navigation in partially observable environments,'' in *International Joint Conference on Artificial Intelligence*, vol. 14, 1995, pp. 1080--1087.

[110] H. S. Wang and N. Moayeri, ``Finite-state Markov channel - a useful model for radio communication channels,'' *IEEE Transactions on Vehicular Technology*, vol. 44, no. 1, pp. 163--171, February 1995.

[111] A. Spyropoulos and C. Raghavendra, ``Asympotic capacity bounds for ad-hoc networks revisited: the directional and smart antenna cases,'' in *IEEE Global Telecommunications Conference*, vol. 3, December 2003, pp. 1216--1220.

[112] S. Yi, Y. Pei, and S. Kalyanaraman, ``On the capacity improvement of ad hoc wireless networks using directional antennas,'' in *ACM International Symposium on Mobile Ad Hoc Networking & Computing*, June 2003, pp. 108--116.

[113] S. Toumpis and A. Goldsmith, ``Capacity regions for wireless ad hoc networks,'' *IEEE Transactions on Wireless Communications*, vol. 2, no. 4, pp. 736--748, July 2003.

[114] B. Hamdaoui and K. Shin, ``Throughput behavior in multi-hop multiantenna wireless networks,'' *IEEE Transactions on Mobile Computing*, vol. 8, no. 11, pp. 1480--1494, November 2009.

[115] P. Li, C. Zhang, and Y. Fang, ``The capacity of wireless ad hoc networks using directional antennas,'' *IEEE Transactions on Mobile Computing*, vol. 10, no. 10, pp. 1374--1387, October 2011.

[116] L. Tong, Q. Zhao, and G. Mergen, ``Multipacket reception in random access wireless networks: from signal processing to optimal medium access control,'' *IEEE Communications Magazine*, vol. 39, no. 11, pp. 108--112, November 2001.

[117] F. Babich and M. Comisso, ``Throughput and delay analysis of 802.11-based wireless networks using smart and directional antennas,'' *IEEE Transactions on Communications*, vol. 57, no. 5, pp. 1413--1423, May 2009.

[118] D. Chan and T. Berger, ``Performance and cross-layer design of CSMA for wireless networks with multipacket reception,'' in *IEEE Asilomar Conference on Signals, Systems and Computers*, vol. 2, November 2004, pp. 1917--1921.

[119] F. Babich and M. Comisso, ``Theoretical analysis of asynchronous multipacket reception in 802.11 networks,'' *IEEE Transactions on Communications*, vol. 58, no. 6, pp. 1782--1794, June 2010.

[120] L.-C. Wang, S.-Y. Huang, and A. Chen, ``On the throughput performance of CSMA-based wireless local area network with directional antennas and capture effect: a cross-layer analytical approach,'' in *IEEE Wireless Communications and Networking Conference*, vol. 3, March 2004, pp. 1879--1884.

[121] M. Carvalho and J. Garcia-Luna-Aceves, ``Modeling wireless ad hoc networks with directional antennas,'' in *IEEE International Conference on Computer Communications*, April 2006, pp. 1--12.

[122] A. Zanella and M. Zorzi, ``Theoretical analysis of the capture probability in wireless systems with multiple packet reception capabilities,'' *IEEE Transactions on Communications*, vol. 60, no. 4, pp. 1058--1071, April 2012.

[123] J. Stine, ``Exploiting smart antennas in wireless mesh networks using contention access,'' *IEEE, Wireless Communications*, vol. 13, no. 2, pp. 38--49, April 2006.

[124] G. Bianchi, D. Messina, L. Scalia, and I. Tinnirello, ``A space-division time-division multiple access scheme for high throughput provisioning in WLANs,'' in *IEEE International Conference on Communications*, vol. 4, May 2005, pp. 2728--2733.

[125] S. Barghi, H. Jafarkhani, and H. Yousefi'zadeh, ``MIMO-assisted MPR-aware MAC design for asynchronous WLANs,'' *IEEE-ACM Transactions on Networking*, vol. 19, no. 6, pp. 1652--1665, December 2011.

[126] H. Singh and S. Singh, ``Smart-802.11b MAC protocol for use with smart antennas,'' in *IEEE International Conference on Communications*, vol. 6, June 2004, pp. 3684--3688.

[127] N. Fahmy and T. Todd, ``A selective CSMA protocol with cooperative nulling for ad hoc networks with smart antennas,'' in *IEEE Wireless Communications and Networking Conference*, vol. 1, March 2004, pp. 387--392.

[128] M. Takai, J. Martin, R. Bagrodia, and A. Ren, ``Directional virtual carrier sensing for directional antennas in mobile ad hoc networks,'' in *ACM International Symposium on Mobile Ad Hoc Networking & Computing*, 2002, pp. 183--193.

[129] J. Yang, J. Li, and M. Sheng, ``MAC protocol for mobile ad hoc network with smart antennas,'' *Electronics Letters*, vol. 39, no. 6, pp. 555--557, March 2003.

[130] R. Choudhury, X. Yang, R. Ramanathan, and N. Vaidya, ``On designing MAC protocols for wireless networks using directional antennas,'' *IEEE Transactions on Mobile Computing*, vol. 5, no. 5, pp. 477--491, May 2006.

[131] D. Lal, R. Toshniwal, R. Radhakrishnan, D. Agrawal, and J. Caffery, J., ``A novel MAC layer protocol for space division multiple access in wireless ad hoc networks,'' in *IEEE International Conference on Computer Communications and Networks*, October 2002, pp. 614--619.

[132] T. Korakis, G. Jakllari, and L. Tassiulas, ``CDR-MAC: a protocol for full exploitation of directional antennas in ad hoc wireless networks,'' *IEEE Transactions on Mobile Computing*, vol. 7, no. 2, pp. 145--155, February 2008.

[133] L. Godara, ``Application of antenna arrays to mobile communications, part II: beam-forming and direction-of-arrival considerations,'' *Proceedings of the IEEE*, vol. 85, no. 8, pp. 1195--1245, August 1997.

[134] K. Sundaresan, R. Sivakumar, M. Ingram, and T.-Y. Chang, ``Medium access control in ad hoc networks with MIMO links: optimization considerations and algorithms,'' *IEEE Transactions on Mobile Computing*, vol. 3, no. 4, pp. 350--365, October 2004.

[135] F. Babich, M. Comisso, and A. Dorni, ``A PHY Design for asynchronous multi-packet reception in 802.11 heterogeneous networks,'' in *IEEE Vehicular Technology Conference, Spring*, May 2011, pp. 1--5.

[136] A. Skrivervik, J.-F. Zurcher, O. Staub, and J. Mosig, ``PCS antenna design: the challenge of miniaturization,'' *IEEE Antennas and Propagation Magazine*, vol. 43, no. 4, pp. 12--27, August 2001.

[137] S. Srinivasa and M. Haenggi, ``Path loss exponent estimation in large wireless networks,'' in *Information Theory and Applications Workshop*, February 2009, pp. 124--129.

[138] ``TL-WN660G: Super G and eXtended Range 108M Wireless mini PCI Adapter.'' [Online]. Available: http://www.mantronic.com/Products/Networking/tl-wn660g.htm

Authors index

M

N

O

P

Q

R

S

T

U

V

W

X

Y

Z